Domain-wall brane models of an infinite extra dimension

Damien P. George

Submitted in total fulfilment
of the requirements of the degree of
Doctor of Philosophy

March 2009

School of Physics
The University of Melbourne

Produced on archival quality paper

Abstract

In this thesis we consider aspects related to the construction and phenomenology of domain-wall brane models of a single, infinite, extra spatial dimension. We discuss how gravity, gauge- and matter-fields become four-dimensional at low energies due to the dynamical formation of a topological defect known as a brane. These ideas are amongst the leading candidates for extensions to the standard models of particle physics and cosmology.

We first examine a toy model where a pair of scalar fields, charged under a $\mathrm{U}(1) \otimes \mathrm{U}(1)$ gauge symmetry, form a background domain-wall configuration. This analysis demonstrates the general ideas of domain-wall formation and stability, dimensional reduction and semi-confinement of gauge fields. Gravity is incorporated into this toy model, in the form of a regularised version of the Randall-Sundrum warped metric.

For the case of a single real scalar field, we show in detail how a domain wall can be obtained, and determine its relationship to the fundamental brane in the infinitely thin wall limit. Explicit expressions for the modes of such a domain wall are found, as well as the modes associated with coupled fermions and scalars. The symmetric modified Pöschl-Teller potential arises in this context, and the analysis elucidates the reduction of a five-dimensional field to a tower of four-dimensional modes.

Adding gravity to the model alters the spectrum of four-dimensional modes trapped to the wall. What were once discrete modes become resonances within a continuum, and low-energy modes are coupled to these continuum bulk modes. We show explicitly how this comes about, and use a toy model to demonstrate that this coupling can be made small enough to avoid experimental constraints.

The Dvali-Shifman mechanism for gauge field localisation is introduced, and we use it, along with the previously discussed techniques for constructing domain walls, to write down an SU(5) grand unified, single generation

version of the standard model. Fermion mass relations and Higgs induced proton decay are significantly improved from usual SU(5) models due to an inherent split fermion set-up. An extension of the gauge group to E_6 is considered, naturally including the clash-of-symmetries mechanism, and it is shown that the field content can be simplified.

Cosmological implications of domain-wall branes are investigated, and we attempt to reproduce an effective four-dimensional Friedmann, Lemaître, Robertson-Walker metric for brane-localised matter. We find that for a domain wall of finite thickness it is not possible to define a common spacetime for all localised species of matter. As a consequence, different species experience a different effective four-dimensional scale factor, an unusual effect that is suppressed when the domain wall is made sufficiently thin.

We conclude that domain-wall brane models of an infinite extra dimension are viable extensions of the standard models of particle physics and cosmology. These models provide a rich set of phenomenology, and allow new ways to tackle existing theoretical problems.

Acknowledgements

Available only in printed version.

Contents

List of Figures

List of acronyms

BBN	Big-Bang nucleosynthesis
CoS	clash of symmetries
CKM	Cabibbo-Kobayashi-Maskawa
DS	Dvali-Shifman
DW	domain wall
FLRW	Friedmann, Lemaître, Robertson-Walker
GUT	grand unified theory
GR	general relativity
KK	Kaluza-Klein
PMNS	Pontecorvo-Maki-Nakagawa-Sakata
QCD	quantum chromodynamics
QED	quantum electrodynamics
QFT	quantum field theory
RS	Randall-Sundrum
SM	standard model of particle physics
VEV	vacuum expectation value

Chapter 1

Introduction

Exploiting the philosophy of special relativity — that space and time should be considered part of the single entity known as spacetime — was on Gunnar Nordström's agenda when, in 1912, he attempted to write down a relativistic generalisation of Newton's law of gravitation [1]. The idea was simple: Newtonian gravity is modelled by the Poisson equation $\nabla^2\phi = 4\pi G\rho$, and a relativistic version could be found by replacing the Laplace operator ∇^2 with the d'Alembert operator $\Box = \partial_t^2 - \nabla^2$. This gives the Lorentz invariant equation

$$\Box\phi = -4\pi G\rho\,. \tag{1.1}$$

In such a model, the gravitational field is described by the potential ϕ, and so this constitutes a *scalar* theory of gravity. The strength of the force is dictated by Newton's constant G, and ρ describes the distribution of matter density. This is not a good theory of relativistic gravity. Among its many problems is its linearity: it does not capture the self interaction of the gravitational field. Nordström went on to improve his theory, but it remained a scalar theory of gravity,[1] and it was Albert Einstein who, in 1916, wrote down the correct *tensor* formulation known as general relativity (GR).

In 1914, during the final stages of the development of GR by Einstein, Nordström was already thinking about the idea which dwells in the mind of

[1] Nordström's next attempt, in 1913, was $\phi\Box\phi = -4\pi GT$, where T is the trace of the matter stress-energy tensor. A year later, Einstein and Fokker noticed that this improved scalar theory could be described by the metric $g_{\mu\nu} = \phi^2\eta_{\mu\nu}$, and the associated equation of motion relates the Ricci scalar R to the stress-energy: $R = 24\pi GT$.

almost every theoretical physicist: *unification*. Nordström was captivated by the elegance of Maxwell's equations and their formulation in the framework of special relativity. Here, the electric- and magnetic-field three-vectors, $\vec{E}$ and $\vec{B}$ respectively, were combined into a six component anti-symmetric tensor. In modern notation we would write this tensor as

$$F_{\mu\nu} = \partial_\mu A_\nu - \partial_\nu A_\mu \,, \tag{1.2}$$

where μ and ν index (t, x, y, z) (also labelled (0,1,2,3) respectively) and A_μ is the electromagnetic vector potential. The symbol ∂_μ denotes a derivative with respect to the coordinate x^μ. Nordström next assumed that equation (1.1) was the correct description of gravity, and so at each point in space the gravitational field is described by a four-vector, corresponding to the time and three-spatial derivatives of ϕ. Now it seemed natural to Nordström to combine the six components of electromagnetism with the four components of his scalar gravity theory, and, on purely theoretical grounds, he wrote down a ten-component analogue of electromagnetism [2, 3, 4].

The key insight that Nordström had was the following: a ten component anti-symmetric tensor arises naturally from the anti-symmetric derivatives of a five-vector, so he upgraded the four-vector potential A_μ to the five-vector A_M. Here, the index M runs over the original four coordinates of our universe, in addition to a new, fifth coordinate w; a coordinate which Nordström interpreted as an extra spatial dimension. The fifth component of A_M then plays the role of the scalar gravity potential, $A_w = -\phi/\sqrt{4\pi G}$, and the fifth component of the electromagnetic source vector J_M is proportional to the matter density, $J_w = \rho\sqrt{4\pi G}/\mu_0$. This five-dimensional theory reproduces electromagnetism and scalar gravity on one condition: the w derivative of all five of the components of A_M must vanish. Nordström interpreted this mathematical fact as the physical requirement that fields in our universe must be perpendicular to w, and thus the extra dimension is distinguished in some way from the usual four. In his conclusion he writes [2]:

> It is shown that a unifying treatment of the electromagnetic and gravitational fields is possible if one considers the four dimensional spacetime-world to be a surface in a five dimensional world.

Today, 95 years later, although they take on a more sophisticated form, we are still concerned with the ideas of unification, extra dimensions and the modern name given to a four-dimensional surface in a higher dimensional spacetime: a brane world. All these topics are dealt with in depth throughout the course of this thesis, and many of Nordström's pioneering ideas are present. The central idea that we explore is that of a *domain-wall brane*. Here, the supposed brane world on which our universe resides forms dynamically as a junction that divides an infinite, or at least cosmologically sized, five-dimensional bulk into two pieces, or two domains. Such domain-wall theories are among many of the modern ways to model the hypothetical existence of an extra spatial dimension. It is intriguing to see that such a hypothesis can be made realistic, and that future experiments may discover these hidden extra dimensions.

For the remainder of this chapter we shall discuss the relevant ideas and theories that have developed, in a more or less chronological order, since Nordström's attempt at a unified brane-world theory. Any modern theory of fundamental physics is built upon these tried and tested theories of the past, and domain-wall brane models are no exception. At the end of this introductory chapter we give a detailed overview of the structure of the rest of the thesis, and, in the chapters that follow, our model is presented in detail. We start with the basics of domain-wall brane formation, stability and the way in which such branes can trap matter and force fields, including gravity. We write down a version of the standard model of particle physics confined to a domain wall, and discuss ideas about grand unification. Cosmological aspects are also worked through in detail. By the end of the thesis we will have developed a working version of a domain-wall model of an infinite extra dimension.

1.1 Kaluza and Klein

Although Nordström's idea of unifying gravity with electromagnetism was lost amidst the great success of GR, it was re-invented, it seems independently, by Theodor Kaluza in 1921 [5]. Struck by the similarity of the field equations of electromagnetism and GR, Kaluza guessed that the field strength tensor of the former, $F_{\mu\nu}$, was related in some way to the lowered

connection coefficients of the latter,[2]

$$\Gamma_{\mu\nu\lambda} = g_{\mu\sigma}\Gamma^{\sigma}_{\nu\lambda} = \tfrac{1}{2}(\partial_\lambda g_{\mu\nu} + \partial_\nu g_{\mu\lambda} - \partial_\mu g_{\nu\lambda})\,. \tag{1.3}$$

Here $g_{\mu\nu}$ is the tensor metric of GR and describes the curvature of spacetime, and the resulting force due to gravity, in a similar way that A_μ describes the electromagnetic force. So that there would be enough degrees of freedom for both A_μ and $g_{\mu\nu}$ to originate from a common object, Kaluza introduced, as Nordström did, the fifth dimension. Recall that Nordström upgraded the vector potential A_μ to A_M and identified gravity as the extra scalar component associated with the extra dimension. Kaluza's theory worked the other way around: he extended the metric of GR to a fifteen component tensor, g_{MN}, with the intention of allocating A_μ to the new positions of this five-dimensional metric.

Because there was no evidence of such an extra spatial dimension, Kaluza assumed the "cylinder condition": that extra dimensional derivatives of all quantities vanished, or, at the least, were higher order and very small. In light of this condition, Kaluza was able to write $\Gamma_{\mu\nu5} = \frac{1}{2}(\partial_\nu g_{\mu5} - \partial_\mu g_{\nu5})$ and so made the identification $A_\mu = \frac{1}{2}\alpha g_{\mu5}$. Here, the constant α is chosen to get the correct coupling between gravity and electromagnetism. In this way, the four-dimensional gravitational metric $g_{\mu\nu}$ and the electromagnetic potential A_μ are both embedded in the five-dimensional metric g_{MN}. These objects have ten, four and fifteen independent components, respectively, so there remains an extra scalar degree of freedom: $\psi = \frac{1}{2}g_{55}$. This field is now known as the dilaton, and plays an important role in string theory, but, at the time, Kaluza did not understand its significance and did not attempt to ascribe it a physical meaning.[3]

The crucial part of Kaluza's work was his demonstration that the *dynamics* of his five-dimensional theory are equivalent to the combined dynamics of GR and electromagnetism. In the linear approximation, i.e. that the five-dimensional metric is nearly Minkowski space, Kaluza was able to prove this dynamical equivalence: he derived Maxwell's and Einstein's equations along with an equation of motion for the scalar field ψ. This is Kaluza's theory, and his main interest in it lay in the formality of the mathematics. He made

[2] In this thesis, repeated indices are to be summed over.

[3] We now know that for consistency of the five-dimensional dynamics, the dilaton field cannot be set to zero if the electromagnetic field strength is to be non-zero.

no specific geometric interpretation of the extra dimension, although he did correctly mention that electric charge is to be understood as momentum in this extra dimension. One of Kaluza's concerns was that his theory did not have anything to say about quantum mechanics, which was under intense development around this time. These two issues, of a physical interpretation of the extra dimension and of quantum mechanics, were on Oskar Klein's agenda, and would also receive much attention years later during the development of string theory.

Independently to Kaluza, in 1924, Oskar Klein began thinking seriously about a fifth dimension.[4] As with Nordström and Kaluza, Klein was also captured by the elegant similarity of the equations of gravity and electromagnetism, and he reproduced Kaluza's theory, first in the linear approximation and later for the general non-linear case. Klein also had the idea of using an extra dimension in connection with wave (quantum) mechanics, and thought that quantisation may arise from periodicity of the extra dimension. Klein put together a manuscript describing these ideas of unification, an extra dimension and quantum mechanics, and showed it to Wolfgang Pauli, who then informed him of Kaluza's previous work. Klein was disappointed that his ideas were not original, but published his work anyway [8], as he himself says: "the paper I then wrote in a spirit of resignation" [9]. Although not the first to unify electromagnetism and GR, Klein's paper did demonstrate that Kaluza's theory worked correctly in the general non-linear regime, and, importantly, gave a physical realisation of the extra dimension.

Klein was imagining that the extra dimension was real and was closed upon itself to form a tiny circle, an image that came from his conviction that quantum mechanics could be derived from the periodicity of this dimension. In particular, Klein related the strength of the electric charge to the momentum in the extra dimension, and hypothesised that this momentum was quantised according to the de Broglie wavelengths that could fit around the circular extra dimension. The longest allowed wavelength, being the size of the extra dimension, would correspond to the smallest allowed electric charge: the charge on an electron. Using this relation, Klein derived the size of the extra dimension to be $l = 0.8 \times 10^{-30}$ cm (see his paper [10]). Klein commented that, because this extra dimension is so small, the physics

[4] For a more detailed historical overview of Klein's contributions to physics, see Chapter 7 of [6], and also [7] for a personal account by Klein himself.

that has been observed so far is an *averaged version* of true five-dimensional physics. The acceptance of the extra dimension as something real, a prediction of its size, and the idea of averaging out the five-dimensional behaviour of physical objects are the main contributions of Klein to what is now known collectively as Kaluza-Klein theory.

As evident from the independent work of Nordström, Kaluza and Klein, extra dimensions have their roots in the unification of electromagnetism and gravity. But, as experiments were showing, there were other fundamental phenomena in nature, aside from these two forces, that required an explanation. After decades of research — of which an overview is given in the next section — the standard model of particle physics would emerge as the accepted model of the sub-atomic world. Focus would then return to extra dimensions, and, as we shall discuss, they could be used as a tool for more than just unification.

1.2 The standard model of particle physics

In 1926, Erwin Schrödinger wrote down his famous equation [11] describing the evolution of the wave-function of a quantum state. This wave-function was subsequently interpreted by Max Born as the probability amplitude, which, after taking the modulus squared, yields a probability density. Development of this quantum mechanics continued for over twenty years, spurred by its great success in explaining atomic properties and related phenomena. Among the driving features of this program were the incorporation of special relativity, and the description of a particle as a quantum excitation of a field. This led to the construction of the language of quantum field theory (QFT) [12, 13], which is the basis of almost all modern particle physics models, and is our best way of modelling the quantum nature of the world. Using this language, we will now proceed to explain the main ingredients of the standard model of particle physics, give an outline of this model, discuss some of its shortcomings, and also take a look at one of the more promising avenues beyond it.

1.2.1 Gauge theories

The expression of Maxwell's equations of electromagnetism in the new language of QFT was worked out in the 1940s by Richard Feynman, Freeman

Dyson, Julian Schwinger and Sin-Itiro Tomonaga. This theory is known as quantum electrodynamics (QED) and it is a beautifully precise description, including all known quantum behaviour, of not only the electromagnetic field, but also the way in which electrons and positrons (or any charged particle) interact with the field and with each other. This theory can be written as the action

$$\mathcal{S}_{\text{QED}} = \int d^4x \left[-\frac{1}{4} F^{\mu\nu} F_{\mu\nu} + \overline{\psi} \left(i\gamma^\mu \partial_\mu - e\gamma^\mu A_\mu - m \right) \psi \right] , \tag{1.4}$$

where A_μ is, as previously, the electromagnetic field with $F_{\mu\nu}$ defined by equation (1.2), $F^{\mu\nu} = \eta^{\mu\sigma}\eta^{\nu\lambda}F_{\sigma\lambda}$, and $\eta_{\alpha\beta} = \text{diag}(+1, -1, -1, -1)$ is the Minkowski metric. The electron and positron are described by the field $\psi(x^\mu)$ which transforms as a four-component Dirac spinor whose adjoint is $\overline{\psi} = \psi^\dagger \gamma^0$, and the associated γ^μ are defined by the relation $\{\gamma^\mu, \gamma^\nu\} \equiv \gamma^\mu\gamma^\nu + \gamma^\nu\gamma^\mu = 2\eta^{\mu\nu}$. The constant e is the charge of the electron and describes the strength with which it couples to the electromagnetic field, and m is the mass of the electron. Of course, the action of QED can only be understood in the full context of QFT, where there exists a definite prescription for quantisation of the fields along with a way to calculate physical observables that can be connected with experiments in the real world.

In modern terminology, QED is a U(1) Abelian gauge theory; the action (1.4) is invariant, or symmetric, under local U(1) phase transformations. To understand this, first consider the more restricted symmetry of *global* phase transformations, where $\psi \to \psi' = e^{i\alpha}\psi$ and α is an arbitrary real constant. Due to the pairing of $\overline{\psi}$ and ψ in all the terms in equation (1.4), such a transformation leaves this action unchanged. Thus, the model of QED predicts equivalent physics, irrespective of the choice we make for the global phase of ψ. Notice that under such a global transformation, the gauge field A_μ plays no role. This gauge field is present in the model because the U(1) of QED is actually a *local* symmetry: the choice we make for the phase at one point in spacetime does not restrict our choice at any other point, and so α is a function of spacetime, $\alpha = \alpha(x^\mu)$. Although this may seem to provide a large amount of arbitrariness for the definition of the phase, the model of QED makes physical sense — the action remains invariant — precisely because the gauge field undergoes the simultaneous transformation

$A_\mu \to A'_\mu = A_\mu + \frac{1}{e}\partial_\mu \alpha$. The presence of A_μ, and its associated gauge transformation, is thus necessary to ensure local U(1) gauge invariance. This idea is known as a *gauge symmetry* and is one of the most important constructions in modern physics; we will revisit the idea frequently in this thesis.

The theory of QED marked the beginning of our modern understanding of the sub-atomic world and provided, at the time, the starting point for a more complete theory. Early modifications included the addition of the proton and the description of beta decay, the process where a proton decays into a neutron, emitting an electron and anti-neutrino. Around the early 1930s, the details of this process were becoming clear, and Enrico Fermi wrote down his model of beta decay in 1934. The essence of Fermi's model was a single interaction term coupling the proton, neutron, electron and neutrino. The term contained a constant factor G_F which described the strength of the force, and was determined from experiment to be quite small leading to the eventual naming of this force as the weak force. Due to the dimensionality of G_F, Fermi's model was not renormalisable[5] and so did not fit well in language of QFT, where, at the time, renormalisability was considered a requirement. Thus, while Fermi's interaction term described the weak force with good precision at the available energies, the model was lacking a more complete understanding.

There was also the emerging problem of the strong force, named for its role in holding protons and neutrons together to form an atomic nucleus. Due to its strength, the nature of this force remained hidden for decades, and was only partially manifest by a shorted lived particle known as the pion.[6] The pion acts between protons and neutrons similar to the way a photon acts between oppositely charged particles: it mediates an attractive force. Chen Ning Yang and Robert Mills tried to account for such a force in 1954 [14], after noticing that, if one ignored electric charge, the proton and neutron seemed indistinguishable, a property known as isospin symmetry. They hypothesised that the interchange of these two nucleons was a symmetry of nature (ignoring electric charge), just as the phase transformation of QED is a symmetry. They strengthened this analogy with QED by assuming

[5] We will not provide an overview or any details of the renormalisation process in this thesis.

[6] The existence of a pion-like particle was predicted in 1935 by Hideki Yukawa, and later observed in 1947. In the realm of the strong force, the pion is a relatively light particle, due to the up and down quarks having small masses.

that the isospin interchange symmetry was a local symmetry — that what one defines as the proton or neutron at one point does not determine the definition at another point — and introduced a new gauge field, in analogy to the photon, to consistently counteract such an interchange.

In making such a bold hypothesis regarding local isospin symmetry, Yang and Mills invented non-Abelian gauge theory and wrote down an SU(2) version of QED. As a theory of the strong interaction, their model was flawed, as the gauge bosons (the force carriers) could not be identified with pions since their spins did not match. Furthermore, the bosons seemed to be massless and therefore ruled out due to lack of observation in any experiment. For these reasons, the theory was initially dismissed, but, after the discovery of the Higgs mechanism and asymptotic freedom, would later find application to both the weak and strong forces. Now known as Yang-Mills theory, it is the generalisation of QED to more complicated gauge groups, and has paved the way for using these other groups in model building, as will be evident in this thesis.

1.2.2 Symmetry breaking and the electroweak force

More experimental data on the strong force was needed before any real progress could occur beyond the idea of Yang and Mills. In the meantime, the weak force was proving to be a more tractable problem, and, in 1960, Sheldon Glashow managed to combine this force with the electromagnetic force [15], by assuming that the weak force is mediated by massive unstable gauge bosons. In this context the Fermi interaction is split into two separate, simpler interactions, mediated by a massive gauge boson. At the time it seemed as though the weak force experimental data could be explained with two such charged gauge bosons, but Glashow's theory required a third neutral gauge boson for theoretical reasons. In his model, these three gauge bosons were unified with the photon, but the issue of such different masses between the four remained unresolved, and the model was unable to give experimental predictions for these masses or for the couplings. In 1964, Abdus Salam and John Ward pushed further this idea of unifying the electromagnetic and weak forces [16], but a more complete theory would require Goldstone's theorem and the Higgs mechanism.

In 1961, Jeffrey Goldstone made a conjecture [17]: if a continuous symmetry is broken by the vacuum, a massless spin zero particle must exist.

While attempting to construct a model of the strong interaction, and account for the light pion, Yoichiro Nambu (and Giovanni Jona-Lasinio) also came across such massless particles arising in the context of a broken symmetry [18, 19]. A proof of the conjecture was provided in 1962 by Goldstone, Salam and Steven Weinberg [20], and the theory is now known as Goldstone's theorem. In the theorem, the continuous symmetry is a global symmetry; for example a global U(1), where the phase is changed at all points in space-time by the same angle. A symmetry can be broken in two distinct ways: either explicitly or dynamically. Explicit symmetry breaking occurs when a model would have a symmetry if certain terms, or interactions, were absent. These terms are said to explicitly break the symmetry. For the U(1) example, this type of breaking would occur if one of the terms in the action depended upon the phase, which can be realised, for example, by not pairing a field with its complex conjugate. Explicitly broken symmetries are a useful concept when the symmetry breaking term is not a dominant term; there may be an energy regime where certain terms in a model dominate and together contain a symmetry.

Dynamical symmetry breaking (also known as spontaneous symmetry breaking) is a more sophisticated phenomenon than its explicit counterpart, and occurs when a model contains a true symmetry, but the *solutions* to the equations of motion do not. Such symmetry breaking is abundant; for example, most theories possess translation invariance, or a translation symmetry, which can be dynamically broken simply by creating a particle at a particular location. Such a particle, which is just one of many solutions to the equations of motion of the theory, sets a special spot in space, and renders this instance of the theory translation non-invariant. But a crucial feature of such a particle is that, if it has non-zero momentum, it will change its location *at no energy cost*. This brings us to the central idea of Goldstone's theorem: if a symmetry is dynamically broken by the vacuum solution, for example because the vacuum chooses a particular phase, then a massless particle, knows as a Nambu-Goldstone boson, exists to account for the fact that the original theory is phase invariant. In other words, the vacuum wants to be at a particular phase, yet the theory dictates that the vacuum cannot distinguish among phases, so a Nambu-Goldstone boson is induced to transform the vacuum from one phase to another at no energy cost. The general term used to refer to the phase, or state, that the vacuum

is in is the vacuum expectation value, or VEV. Symmetry breaking plays a very important role in this thesis, where domain-wall brane solutions dynamically break the translation invariance of the models we consider. In some cases a domain wall dynamically breaks a gauge symmetry, which, as we now discuss, has very interesting consequences.

Between 1964 and 1965 Peter Higgs worked out an interesting and extremely useful loophole in Goldstone's theorem. He demonstrated [21] that the proof of Goldstone's theorem fails if the broken vacuum is gauged; that is, if the vacuum dynamically breaks a local gauge symmetry. Furthermore, Higgs later showed [22] that some of the gauge fields associated with the dynamically broken symmetry acquire a mass. The massless Nambu-Goldstone bosons of the broken symmetry are no longer present because their degrees of freedom are "eaten" by the gauge fields, whose mass is a result of their inherited longitudinal degree of freedom.This is an important discovery: previously, the only way to construct a massive gauge field was to explicitly break the symmetry in the model from the outset (recall the problems Glashow had with his model of the weak interaction). Higgs was well aware of the applications of his result, and suggested that this may be a way to get massive vector bosons for the weak interaction, while keeping the photon massless. In a subsequent paper [23], Higgs detailed the calculation of what is now called the Higgs mechanism, and which has become a major tool in particle physics model building. The name "Higgs field" is also often used to refer to a scalar field which is responsible for breaking a gauge symmetry in a model. As mentioned previously, some of the domain walls in this thesis are designed to play the role of a Higgs field.

With the establishment of the Higgs mechanism, Glashow's preliminary model of electromagnetic and weak interactions could be completed. It is now called the electroweak model, and the leptonic sector of this model, containing the electron and neutrino, was written down in 1967 by Weinberg [24], and also independently by Salam [25]. The weak force is chiral and biases interactions towards the left-handed projection of fermions. In our notation we define $\gamma^5 = i\gamma^0\gamma^1\gamma^2\gamma^3$ and the left-handed projection of ψ is $\psi_L = \frac{1}{2}(1-\gamma^5)\psi$, while the right-handed projection is $\psi_R = \frac{1}{2}(1+\gamma^5)\psi$. The electroweak theory has two local gauge symmetries: $\mathrm{U}(1)_Y$ is the Abelian hypercharge symmetry with associated gauge field B_μ, and $\mathrm{SU}(2)_L$ is the non-Abelian left-handed symmetry with the set of three fields W^a_μ $(a = 1, 2, 3)$

in the adjoint representation.[7] The electron field e, the electron neutrino ν_e and the Higgs doublet Φ make up the rest of the theory. The left-handed projections of the fermions are put in a doublet representation of $\mathrm{SU}(2)_L$, so we have

$$l_L = \begin{pmatrix} (\nu_e)_L \\ e_L \end{pmatrix} \qquad \text{and} \qquad \Phi = \begin{pmatrix} \phi^0 \\ \phi^- \end{pmatrix}, \tag{1.5}$$

where ϕ^0 and ϕ^- are the complex scalar field components of the Higgs field.

In slightly modified notation, Weinberg's model of leptons and the electroweak interaction is given by the action

$$\begin{aligned} \mathcal{S}_{\mathrm{EW}} = \int d^4x \Big[& -\frac{1}{4}\mathcal{B}^{\mu\nu}\mathcal{B}_{\mu\nu} - \frac{1}{4}\mathcal{W}^{a\,\mu\nu}\mathcal{W}^a_{\mu\nu} \\ & + \overline{l}_L\gamma^\mu(i\partial_\mu - \frac{g}{2}B_\mu + \frac{g'}{2}W^a_\mu\sigma^a)l_L + \overline{e}_R\gamma^\mu(i\partial_\mu - gB_\mu)e_R \\ & + |(\partial_\mu + \frac{g}{2}B_\mu + \frac{g'}{2}W^a_\mu\sigma^a)\Phi|^2 - \lambda\left(|\Phi|^2 - v^2\right)^2 \\ & + G_e(\overline{l}_L\Phi e_R + \overline{e}_R\Phi^\dagger l_L)\Big], \end{aligned} \tag{1.6}$$

where the gauge field tensors are $\mathcal{B}_{\mu\nu} = \partial_\mu B_\nu - \partial_\nu B_\mu$ and $\mathcal{W}^a_{\mu\nu} = \partial_\mu W^a_\nu - \partial_\nu W^a_\mu + g' f^{abc} W^b_\mu W^c_\nu$, the structure constants, f^{abc}, of $\mathrm{SU}(2)_L$ are defined by $[\sigma^a, \sigma^b] \equiv \sigma^a\sigma^b - \sigma^b\sigma^a = 2if^{abc}\sigma^c$, and σ^a are the Pauli matrices.[8] The parameters g and g' correspond to the $\mathrm{U}(1)_Y$ and $\mathrm{SU}(2)_L$ coupling respectively. The Higgs potential, which determines the vacuum state and induced dynamical symmetry breaking, is controlled by λ and v. The final parameter is G_e, whose size dictates the mass of the electron. The different signs and factors of $\frac{1}{2}$ multiplying g are a consequence of the different hypercharges of each field, which are: $Y(l_L) = -1$, $Y(e_R) = -2$, $Y(\Phi) = 1$. Weinberg showed that this model contained electromagnetism, with a massless photon, as well as a plausible theory of the weak interaction mediated by the heavy gauge bosons W^+_μ, W^-_μ and Z_μ.[9] Bounds on the masses of the W and Z particles were given, along with predictions for the coupling of the

[7] In the current context, a representation of a group, or of a symmetry, is a composite object whose elements are individual fields which rotate amongst themselves in a way that exemplifies, or represents, the symmetry at hand.

[8] See Section A.1 for the explicit forms of the Pauli matrices.

[9] The photon is the linear combination $A_\mu = \cos(\theta_W)B_\mu + \sin(\theta_W)W^3_\mu$ and the heavy weak gauge bosons are defined by $Z_\mu = -\sin(\theta_W)B_\mu + \cos(\theta_W)W^3_\mu$ and $W^\pm_\mu = (W^1_\mu \pm iW^2_\mu)/\sqrt{2}$. The angle θ_W is called the Weinberg angle, or weak mixing angle.

fermions to Z. This model accounts for a significant part of the standard model of particle physics; the missing ingredients are the hadrons and the strong force.

1.2.3 Quarks, gluons and strings

Aside from the electroweak force, experiments designed to elucidate the nature of the strong force, and the internal structure of hadrons, were yielding almost too much data. A huge spectrum of strongly interacting particles were being seen, the pion being the just the tip of the iceberg, and there was the growing feeling that these particles were not fundamental. It was believed that the particle spectrum was the consequence of an underlying dynamics, of which there were two competing theories. One theory was the eightfold way, introduced in 1961 by Murray Gell-Mann [26]. The hadrons seemed to divide into two main groups called the mesons and the baryons, and the eightfold way was a combinatorial mechanism which Gell-Mann used to further classify individual mesons and baryons. In 1964, he introduced [27] the concept of a quark with fractional electric charge, and showed how combinations of three distinct quarks could reproduce the combinatorics of the eightfold way and account for the observed particle spectrum. The two main problems with this model were that quarks, or fractionally charged particles, were not seen in nature, and the way in which quarks were bound together to form hadrons was not understood. Further work related to quarks, their formation of composite entities, and the so-called "colour" SU(3) symmetry was performed by Oscar Greenberg [28], and Moo-Young Han and Nambu [29].

The other model of the strong force was developed between 1968 and 1974. It was called the dual resonance model [30], and was instigated by Gabriele Veneziano who found an elegant way of mathematically expressing scattering amplitudes of strongly interacting particles. QFT can be used to describes theories with local, point-like interactions, and seemed to work well for QED and the electroweak force, but not for the strong force. It seemed that the strong force, and the plethora of strongly interacting particles, needed a different type of internal description — a non-local description — and the dual resonance model provided this, as it could be interpreted as a theory of vibrating strings. Instead of modelling a hadron (or any other particle) as a point-like object, the dual resonance model, later referred to

as string theory, modelled different particles by different vibrations of the same underlying string entity.

There were two distinct dual resonance models with different spectrums for the vibrations of the string.[10] The "Veneziano model" contained only bosonic vibration states, so could not model any of the hadrons (which are fermions), and also contained unphysical tachyonic states. Furthermore, this model was only consistent when spacetime had twenty-six dimensions, one being a time-like dimension and the other twenty-five being space-like. The second model, the so-called "dual pion model", had both bosonic and fermionic states; the accommodation of fermions making it more promising than the Veneziano model. Under certain conditions, it was also possible to eliminate tachyons by having an equal number of fermions and bosons at each given mass of the string vibration spectrum. Such a pairing is now known as supersymmetry, a global symmetry relating fermions and bosons, which when made a local symmetry yields supergravity.[11] Successors of the dual pion model are known as superstring theories and, for consistency, these theories need to be formulated in a ten-dimensional spacetime. For a model of the strong force these necessary extra dimensions were seen as a downfall, but they would later play a significant role in string theory when it became a candidate for a fundamental theory of nature, and the unwanted dimensions would be compactified away [33] as in the original proposal of Klein. As we discuss later, the discovery that branes could reside in these extra dimensions of string theory lead to a lot of the research which has motivated the topic of this thesis.

Returning to the traditional idea of utilising QFT and gauge fields to model the strong force, it was found that non-Abelian gauge theories possessed a special feature which rendered the original idea of Yang and Mills — to use a gauge field to mediate the strong force — much more plausible. This special feature is called asymptotic freedom and was discovered in 1973 by David Gross and Frank Wilczek [34], and by David Politzer [35]. They demonstrated that non-Abelian Yang-Mills gauge theories have vastly different properties to Abelian versions of the theory, and could be the correct way of describing the strong force. Asymptotic freedom refers to the phe-

[10] For a good technical overview see the report by Schwarz [31] and also Green, Schwarz and Witten [32] for an introduction to string theory.

[11] We do not make use of any technical details of supersymmetry in this thesis.

nomenon whereby the force due to a non-Abelian gauge field gets weaker for closer distances, and the force ultimately vanishes for asymptotically small distances. This is conceptually the opposite to an Abelian force, where the strength weakens at large distances. Two or more particles held together by a non-Abelian force are very difficult to separate, and such a composite entity had properties (such a Bjorken scaling) which mimicked the hadrons.

Building on the idea of asymptotic freedom, and on the previous theories of quarks and colour symmetry, Harald Fritzsch, Gell-Mann and Heinrich Leutwyler described a model [36] where the strong force is a manifestation of the non-Abelian group SU(3). Unlike the weak force and the broken $SU(2)_L$ symmetry, the local SU(3) gauge symmetry of the strong force is exact, and "phase rotations" of this group correspond to interchanging the three colours of the strong force. There are eight massless gauge bosons associated with SU(3); they are called "gluons" and come in combinations of the three colours. Each quark that is included in the theory will come in a triple of the three colours. The success of this model, now known as quantum chromodynamics (QCD), pushed aside the dual resonance model and is our current theory of the strong interaction.

1.2.4 The standard model

All of these pieces of work — QFT, QED, Yang-Mills theory, Goldstone's theorem and the Higgs mechanism, the electroweak model, asymptotic freedom, quarks and QCD — were shedding light on exactly how nature ticked underneath, and were ready to be put together in a complete model of subatomic, high-energy particle physics. All that was left to determine were the different types of particles that exist in nature. As we have seen from the electroweak model, the leptons consist of the electron and the neutrino, which do not interact with the strong force (they do not have colour). The coloured fermions are the quarks, of which there are the up quark u and the down quark d. These four fermions — e, ν_e, u and d — together make up the first generation of particles. There are a total of three generations, each subsequent generation being a copy of the previous, with the only distinguishing feature a larger mass. The second generation, listed here in the same order as the first generation, contains the muon, muon neutrino, charm quark and strange quark. The third generation, in order, contains the tau,

tau neutrino, top quark and bottom quark.[12]

The model that is the culmination of these decades of research is called the standard model of particle physics (SM). It is a unified description of the electromagnetic, weak and strong forces, and the dynamics and interactions of the three generations of fermions. It is a theory that has provided precise and correct predictions for the past 35 years or so of observations of low and high energy experiments. In the language of QFT and gauge symmetries, the gauge group of the standard model is

$$G_{\text{SM}} = \text{SU}(3)_C \otimes \text{SU}(2)_L \otimes \text{U}(1)_Y \,, \tag{1.7}$$

where $\text{SU}(3)_C$ is the group corresponding to the coloured strong force and $\text{SU}(2)_L \otimes \text{U}(1)_Y$ is the electroweak force. The first generation of fermions consists of the following fields and their associated quantum numbers:

$$\begin{gathered} q_L = \begin{pmatrix} u_L \\ d_L \end{pmatrix} \sim (\mathbf{3},\mathbf{2})_{1/3} \quad u_R \sim (\mathbf{3},\mathbf{1})_{4/3} \quad d_R \sim (\mathbf{3},\mathbf{1})_{-2/3} \\ l_L \sim (\mathbf{1},\mathbf{2})_{-1} \quad \nu_R \sim (\mathbf{1},\mathbf{1})_0 \quad e_R \sim (\mathbf{1},\mathbf{1})_{-2} \end{gathered} \tag{1.8}$$

The Higgs field, which gives mass to the fermions and the heavy weak gauge bosons, is

$$\Phi \sim (\mathbf{1},\mathbf{2})_1 \,, \tag{1.9}$$

and the symmetry breaking pattern to the electromagnetic group $\text{U}(1)_{\text{EM}}$ is

$$\text{SU}(3)_C \otimes \text{SU}(2)_L \otimes \text{U}(1)_Y \longrightarrow \text{SU}(3)_C \otimes \text{U}(1)_{\text{EM}} \,. \tag{1.10}$$

The lepton doublet l_L and Higgs doublet Φ have a composition as given by the equations in (1.5). The notation for the quantum numbers in (1.8) and (1.9) is the $\text{SU}(3)_C$ representation followed by the $\text{SU}(2)_L$ representation in parenthesis, and then the $\text{U}(1)_Y$ hypercharge Y as subscript. The electric charge Q corresponding to the group $\text{U}(1)_{\text{EM}}$ is related to the $\text{U}(1)_Y$ hypercharge Y and the $\text{SU}(2)_L$ isospin charge I_3 (which is 0 for a singlet and $\pm\frac{1}{2}$ for the upper/lower component of a doublet) by the Gell-Mann-Nishijima relation $Q = I_3 + \frac{1}{2}Y$. The second and third generations of fermions have

[12] The history of the experimental observation of the fermions is just as interesting as the history of the theoretical discoveries, but will not be discussed here. We will mention though that the last fermion to be discovered was the top quark in 1995.

equivalent quantum numbers to those of the first.

The action of the standard model is a more complete version of the electroweak action (1.6). We will not give the explicit form, but instead just mention that, in addition to the electroweak terms, there are kinetic terms for the gluon gauge fields and for the quarks as well as interaction terms between the quarks and the Higgs. In fact, the prescription for constructing the action is to write down *all* the renormalisable terms that can be made from the given particle content and which are consistent with the given symmetries. When incorporating three generations, a large number of such terms must be written down, but it is nevertheless a straightforward task. In this case, the notation is simplified by putting the three generations of each species in a three component vector and writing the Higgs-fermion couplings, such as G_e, as 3×3 matrices. The analysis that then follows leads to the Cabibbo-Kobayashi-Maskawa (CKM) matrix which describes the mixing of the three quarks, a phenomenon that has been observed in experiments.

In summary, the physical content of the standard model is as follows. There are eight massless gluons, three massive weak bosons and one massless photon, giving a total of *twelve gauge bosons*. There are three generations of fermions, each generation having two leptons, and two quarks with three colours each. This gives a total of *twenty-four fermions*. There is also *one scalar Higgs* particle.[13] As for the free, real parameters, there are three gauge coupling constants, three lepton masses, six quark masses, four real parameters in the CKM matrix and two parameters in the Higgs potential. This gives a total of *eighteen parameters*. Actually, there is one more parameter: the QCD vacuum angle θ_{QCD} which is typically taken to be zero.[14] And if one incorporates neutrino masses (see the next section), along with neutrino mixing and the Pontecorvo-Maki-Nakagawa-Sakata (PMNS) matrix, there will be at least seven additional parameters.

Today, any purported model of particle physics *must*, in some way or another, reproduce, or reduce to, the standard model. Such a condition severely constrains the way one goes about constructing extensions of the standard model. In particular, it has meant that a large portion of this thesis

[13] The Higgs doublet, made of the complex scalar fields ϕ^0 and ϕ^-, has four degrees of freedom, three of which are eaten by the W and Z bosons leaving a single physical Higgs field.

[14] Experiments have been done to measure the effect of θ_{QCD} but none have succeeded and instead given the bound $\theta_{\text{QCD}} \lesssim 10^{-11}$.

is devoted to studying mechanisms that are able to confine the separate pieces of the standard model to a domain-wall region. Using a combination of such mechanisms, we will eventually demonstrate how to construct a model very close to the standard model, but which is confined to a brane.

To finish our discussion of the standard model, we will point out some of its important shortcomings and also discuss the grand idea of grand unification.

1.2.5 Shortcomings of the standard model

Despite its great successes and sound mathematical footing, the standard model has some unresolved omissions, and also scope for theoretical improvement. Excluding gravity, the standard model should be a model of all particles and forces, but it lacks a description of neutrino masses and of dark matter. There is also no convincing mechanism for baryogenesis. To make any experimental predictions, the parameters of the standard model need to be set; they could theoretically take almost any value, and this could potentially be improved. There is also no profound reason for the particular set of fermions that nature contains,[15] or the fact that there are three generations. An even more difficult question, which is probably related more to the theory of gravity than particle physics, is why there seems to be only three spatial dimensions and one time dimension. More technical and possibly aesthetic problems with the standard model include the hierarchy problem and the allure of grand unification. We will elaborate on some of these issues here and in the following section.

Initially, neutrinos were thought to be massless particles because the energy they carry away from a reaction is almost all in the form of kinetic energy.[16] They are also very difficult to detect directly. Recent experiments which detect neutrinos from the sun, astrophysical sources, man-made nuclear reactors and accelerators, indicate that the three generations of neutrinos can morph into one another. The straightforward quantum mechanical explanation for this phenomenon, known as neutrino oscillations, assumes that the three neutrinos have slightly different masses, and over time dif-

[15] Actually, anomaly cancellation (ensuring that the quantum version of a classical theory retains the desired symmetries) does have something to say about the fermion content.

[16] In a relativistic context, the energy of a particle is split between its rest mass energy (a fixed quantity) and its kinetic energy, or momentum. Massless particles have all their energy in their momentum.

ferent masses evolve at different rates, transforming the neutrinos amongst themselves. Neutrino masses can be incorporated into the standard model using a range of different techniques. The leading candidate is the see-saw mechanism, which posits the existence of a right-handed neutrino, and generates a very light, along with a very heavy, neutrino state. We will not discuss neutrinos in any depth in this thesis, and, where we do work with them, we will make the approximation that they are massless.

There is also a lot of astrophysical evidence for a new form of matter, called dark matter, that interacts very weakly with the gauge bosons and fermions in the standard model. In the framework of QFT, dark matter can be added to the standard model by simply adding a new matter field or fields, and possibly gauge fields, that have very small couplings to the existing standard model fields. There is currently not enough experimental data to narrow down the plethora of ways in which dark matter can be implemented, and we do not consider it at all in this thesis. We also ignore the problem of baryogenesis, which is the name given to the mechanism that supposedly generated, in the early stages of the universe, the excess of matter compared to anti-matter.

The free parameters of the standard model include the gauge coupling constants, couplings between the Higgs and the fermions, and the Higgs potential parameters. These parameters are set by performing experiments, and once this is done they can be used to predict results of further, independent experiments. Reducing the number of parameters by finding a model that predicts a relation among two or more of them, or a model that derives them from fewer, more fundamental parameters, is the goal of many theoretical physicists. As we shall show in this thesis, our domain-wall brane models provide the framework for such a reduction in the number of parameters, which is typical of theories with extra dimensions. The issue of particle content, the reason for the seemingly random choice of quantum numbers in (1.8), and the choice of three generations, are theoretically similar to free parameters, and it is hoped that they too have a deeper explanation. In this thesis, as in many other models that have been developed, the quantum numbers find a partial meaning in the context of grand unification.

The hierarchy problem of the weak force is an aesthetic problem concerning the way the Higgs mechanism is implemented, and may point to a deep problem in our construction of the standard model. It is expected

that this model, a model of the sub-atomic world, should be able to make predictions at all available energy scales. Current experiments can reach energies of around 1 TeV,[17] and the standard model agrees very well with data produced at such energies. But it is believed that energies, and theoretical predictions, should go at least all the way up to the Planck scale, $M_{\text{Pl}} \sim 10^{19}$ GeV,[18] because this is the energy scale of gravity (more precisely, at this energy, gravity will compete with QFT effects). Due to the nature of QFT — where all processes can occur, even ones that violate energy conservation — the theoretically natural value for a dimensionful parameter is proportional the largest energy accessible in the theory. In the standard model, the only dimensionful parameter is the parameter which controls the magnitude with which the Higgs dynamically breaks the electroweak symmetry; this is v in equation (1.6). So if the standard model is to provide predictions up to Planck sized energies, the natural value of v should be of order the Planck scale. But such a value is at complete odds with experiment; correct predictions of weak processes requires v to be 174 GeV. This discrepancy between the natural value and the required value is known as the (electroweak) hierarchy problem. There are many models which attempt to resolve this hierarchy problem, and two particular ones that utilise extra dimensions will be discussed shortly.

In relation to questions about nature's particular choice of fermions, it is also interesting to wonder why the particular gauge group that describes interactions is (1.7), and not some other choice of group. This is a much more profound problem than most of the other issues with the standard model, and a greater understanding of the problem is undoubtedly found in the study of grand unification.

1.2.6 Grand unification

Perhaps the first attempt at a major improvement of the standard model was the further unification of the individual gauge groups. Since the electromagnetic and weak forces had common origins in the electroweak force, it seemed sensible to try and generalise such a theme and unite the electroweak

[17] Throughout this thesis we will make liberal use of both natural units, where the speed of light in vacuum is $c = 1$ and the reduced Planck constant $\hbar \equiv h/2\pi = 1$, as well as the SI prefixes G=10^9 and T=10^{12}. Conversion from electron-volts (eV) to SI units involves the equality 1 eV = 1.6×10^{-19} Joules, along with certain powers of c and $\hbar$.

[18] Defined by $M_{\text{Pl}}^2 = \hbar c^5/G$, where G is Newton's constant.

force with the strong force. This idea is called grand unification and a model that incorporates such an idea is called a grand unified theory or GUT. The first attempt at constructing a GUT was the SU(5) model proposed by Howard Georgi and Glashow in 1974 [37]. Here, the three gauge groups of the standard model are contained as sub-groups in the larger SU(5):

$$\mathrm{SU}(5) \supset \mathrm{SU}(3)_C \otimes \mathrm{SU}(2)_L \otimes \mathrm{U}(1)_Y \,. \tag{1.11}$$

In the context of local gauge symmetries and gauge bosons, the relation (1.11) implies that, of the 24 gauge bosons of SU(5), 12 of them are precisely those of the standard model. The other 12 gauge bosons, labelled X and Y, are an addition to the theory, carry a colour charge, isospin and hypercharge, and mediate interactions which mix the strong and electroweak forces.

One of the major drawbacks of unification is the complexity, and extra parameters, introduced in order to break the GUT group to the standard model; this is usually accomplished by using a dedicated Higgs field χ (in the 24 component adjoint for SU(5)) and associated symmetry breaking potential. The energy scale at which χ breaks the GUT symmetry is known as the GUT scale, denoted M_{GUT}, whose value varies for different grand unified models. It is typically around 10^{16} GeV, just below the Planck scale. At energies below M_{GUT} the SU(5) symmetry is broken by the vacuum state of χ, and the Higgs mechanism gives a mass of order M_{GUT} to the 12 additional gauge bosons X and Y,[19] with the standard model gauge group as the left over symmetry. Such complexity in the Higgs sector is counteracted by the reduction in the number of gauge group coupling constants; for the SU(5) model there is only one parameter, as opposed to the original three. Although, in order to obtain predictions for the three standard model couplings at low energies, one requires two values: the SU(5) coupling constant and M_{GUT}.

Unification of the gauge bosons is one part of a grand unified theory, the other being unification of the fermions. SU(5) is remarkable in that, not only is it the unique smallest group that contains the standard model,[20] it

[19] In order to give the X and Y gauge bosons a mass and keep the standard model gauge bosons massless, the Higgs field χ must break the GUT symmetry in a very particular way.

[20] In other words, any simple group H (which cannot be decomposed into a product of groups) that is not SU(5) but contains the standard model G_{SM}, also contains at least one additional group J, i.e. $H \supset G_{\mathrm{SM}} \otimes J$.

also admits precisely one generation of fermions in just two representations. These representations are the $\mathbf{5}^*$ and $\mathbf{10}$ and they contain the fermions as follows:

$$\psi_5 = \begin{pmatrix} d_1^c \\ d_2^c \\ d_3^c \\ e \\ \nu_e \end{pmatrix}_L , \qquad \psi_{10} = \frac{1}{\sqrt{2}} \begin{pmatrix} 0 & u_3^c & -u_2^c & -u_1 & -d_1 \\ -u_3^c & 0 & u_1^c & -u_2 & -d_2 \\ u_2^c & -u_1^c & 0 & -u_3 & -d_3 \\ u_1 & u_2 & u_3 & 0 & -e^c \\ d_1 & d_2 & d_3 & e^c & 0 \end{pmatrix}_L . \tag{1.12}$$

The charge conjugate field used here is defined by $\psi^c = \gamma^2 \psi^*$ and has opposite quantum numbers to ψ. We use subscript L on the vector and matrix to indicate that one needs to take the left-handed projection of all component fields. The three separate colours of the quarks are labelled with the subscripts 1, 2 and 3.

We shall elaborate on exactly what it means for ψ_5 and ψ_{10} to be composed of the individual fermion fields as expressed by (1.12). Consider ψ_5 which *a priori* is just a vector of five Dirac spinors. Under a general SU(5) rotation[21] all five of these spinors will transform into combinations of each other. If we restrict our rotations to, for example, the rotations corresponding to the $\mathrm{SU}(3)_C$ sub-group, then the three d^c's in ψ_5 transform only into combinations of themselves; they do not mix with the leptons e and ν_e. Thus the d_i^c are a triplet of $\mathrm{SU}(3)_C$ (and a singlet of $\mathrm{SU}(2)_L$) and can be called the down quark. Similarly, the e and the ν_e remain fixed under the restricted rotations corresponding to $\mathrm{SU}(3)_C$, so they are singlets of this group. In this manner, one can check all the quantum numbers of the components of ψ_5 and ψ_{10} by restricting SU(5) rotations to rotations of its sub-groups. This is the information that is expressed in (1.12). The fact that such an economical yet complete unification of the fermions can be done is quite remarkable, and is what draws physicists to the idea of grand unification. An effective way to visualise all the different fermions in the standard model, and gain insight as to why SU(5) unification works, is to plot the quantum numbers of (1.8) in a particular way, as we have done in Figure 1.1.

Apart from unifying the fermions into larger representations (although in SU(5) they are not completely unified; full unification would put ψ_5 and

[21] If $U \in \mathrm{SU}(5)$ then ψ_5 transforms as $\psi_5 \to \psi_5' = U^* \psi_5$. And $\psi_{10} \to \psi_{10}' = U \psi_{10} U^T$.

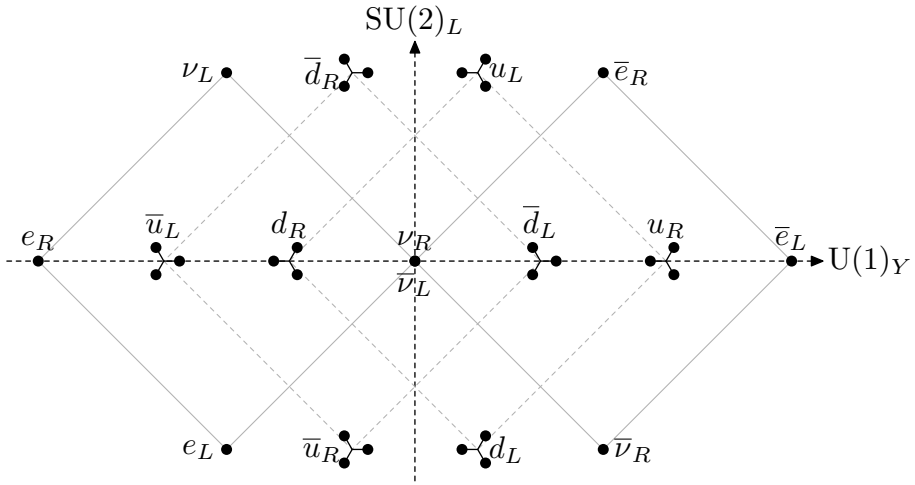

Figure 1.1: Weight diagram of the fermions of the standard model. The fermions are plotted according to their quantum numbers given by (1.8): Y is along the horizontal axis and I_3 (0 for an SU(2)$_L$ singlet, $\pm\frac{1}{2}$ for the upper/lower component of a doublet) is along the vertical axis. A single dot represents an SU(3)$_C$ singlet (a colour-neutral lepton), while three dots represent a triplet (a coloured quark).

ψ_{10} together), grand unification also explains charge quantisation: why the Y hypercharges in (1.8) take on their specific values. When there is a U(1) group that does not have its roots in a larger group, the hypercharge values corresponding to the U(1) are not restricted to any value. In the case of the standard model group (1.7), this is true for U(1)$_Y$, and one seeks an explanation as to why the electric charge of a down quark seems to be exactly one third of the electric charge of an electron (since electric charge is directly related to Y). In a GUT the hypercharges corresponding to all U(1) sub-groups are restricted: the sum of the hypercharges of all the individual components within each representation of the GUT group must be equal to zero. For example, in ψ_5 we have three down quarks and two leptons which give the sum $3 \times \frac{2}{3} + 2 \times -1 = 0$, and ψ_{10} yields $3 \times -\frac{4}{3} + 6 \times \frac{1}{3} + 1 \times 2 = 0$.

In the SU(5) scheme, along with the χ Higgs field which breaks the GUT symmetry to the standard model, another Higgs is needed for the usual electroweak breaking. Just as the lepton doublet l is put into the representation ψ_5, the Higgs doublet Φ (made of ϕ^- and ϕ^0) is contained in

a scalar multiplet that transforms as a $\mathbf{5}^*$:

$$\Phi_5 = \begin{pmatrix} \phi_1 \\ \phi_2 \\ \phi_3 \\ \phi^- \\ \phi^0 \end{pmatrix} . \tag{1.13}$$

The three extra fields ϕ_1, ϕ_2 and ϕ_3 are called coloured Higgs fields because they transform as a $\mathbf{3}^*$ of the $\mathrm{SU}(3)_C$ sub-group. The vacuum state of the ϕ^0 component is again responsible for breaking electroweak symmetry, and the full breaking pattern is

$$\mathrm{SU}(5) \xrightarrow{\chi} \mathrm{SU}(3)_C \otimes \mathrm{SU}(2)_L \otimes \mathrm{U}(1)_Y \tag{1.14a}$$

$$\xrightarrow{\Phi_5} \mathrm{SU}(3)_C \otimes \mathrm{U}(1)_{\mathrm{EM}} . \tag{1.14b}$$

Unfortunately, the SU(5) model that we have described is not a good description of nature. Since the down quark and electron have a common origin in ψ_5 they obtain identical masses, which obviously contradicts observation. One way to alleviate this problem is to introduce more Higgs fields, which end up complicating the model and reduce its predictive power. Another major issue is the prediction of more rapid proton decay than is observed. Both the heavy X and Y gauge bosons and the coloured Higgs fields induce proton decay, a feat achieved by mediating interactions that transform leptons into quarks, and vice versa. The most predominant reaction is $p \to \pi^0 e^+$, and it is difficult to reduce the rate of such processes without drastic modifications to the model.

There is also the problem of so-called gauge coupling unification. The three values corresponding to the strong and electroweak coupling constants of the standard model are predicted from the single coupling constant of the SU(5) group, and they do not agree with experiment. The precise values of these couplings, as well as the rate of proton decay, actually depend on the GUT scale of the model, which, when adjusted to higher energies, can help to bring the predicted values closer to the observed ones. In the simplest SU(5) model, it is not possible to raise the GUT scale high enough and major modifications — such as supersymmetry — are required to produce a viable theory where the three gauge coupling constants have a common

origin.

Nevertheless, the basic SU(5) scheme is at the core of many GUT based models, and is also the starting point for further grand unification. It is possible to completely unify the fermions by embedding SU(5) in SO(10) [38], and placing ψ_5, ψ_{10} and a new singlet neutrino (which can be used to generate neutrino masses) together in a sixteen component representation. One can go even further and embed SO(10) in E_6 and then embed E_6 in E_8. All such embeddings require an increasingly sophisticated Higgs mechanism to break the symmetries, although there are some tricks that can be used to keep the model as minimal as possible and reduce the number of free parameters. In this thesis we will discuss how extra dimensions can help alleviate some of the problems of grand unified theories, like proton decay, while keeping their complexity to a minimum. In particular we will present models based on SU(5) and E_6 and introduce the notion of clash of symmetries [39].

Aside from using SU(5), there are also other ways of embedding the standard model gauge group in larger groups, and the fermions in larger representations. One such model, due to Jogesh Pati and Salam [40], was conceived in 1974, just after the model of Georgi and Glashow, and is based on the symmetry group $SU(4)\otimes SU(2)_L\otimes SU(2)_R$.[22] The fermion electroweak doublets q and l are put in a $(\mathbf{4},\mathbf{2},\mathbf{1})$ representation, and the singlets d^c, u^c, e^c along with a singlet neutrino ν^c are put in a $(\overline{\mathbf{4}},\mathbf{1},\mathbf{2})$. As usual, the GUT symmetry of this set-up needs to be broken to the standard model, which can be implemented using Higgs fields, albeit at the cost of complexity.

These days grand unification plays a large part in many theories, including electroweak scale supersymmetry and its many variations, as well as technicolour, trinification, extra dimensions and superstring theory. Indeed, there are many paths, not just in the direction of GUTs, which can be taken to address the shortcomings of the standard model and enhance our understanding of the sub-atomic world. Our focus will now turn to the extra-dimension avenue, the modern ideas of brane worlds and domain walls, and the various ways of realising a brane world model as an extension of the standard model.

[22] Actually, Pati and Salam's main proposal was the unification group $SU(4)\otimes SU(4)_L\otimes SU(4)_R$. At the time only two generations of fermions were known to exist, so they made the L and R groups twice as big as they needed to be to accommodate the first two generations. Today, the Pati-Salam model is named after what they originally called the "economical" version of their main proposal.

1.3 The early years of brane world models

So far we have seen extra dimensions invoked in order to facilitate the unification of electromagnetism and general relativity, and they also appear as a necessary part of the various string theories. In these models, extra dimensions were generally considered an unwanted artifact — a mathematical necessity whose presence was tolerated for the sake of some grander physical idea. But by the 1980s, particle physics had come a long way, physicists were looking for directions beyond the standard model, and extra dimensions started to look more like a tool than a hindrance. Some basic ideas were fleshed out in the form of toy field theories where particles were trapped to a subspace in a higher dimensional background. Then the 1990s saw the revolution of superstring theory and its ten dimensions, the discovery of M-theory, and the realisation that strings were not alone in the extra dimensions, but that they lived in the presence of branes. This realisation spurred a new class of extra dimensional models that promised exciting solutions to old problems, and seemed to offer unlimited model building potential. In this section we will discuss some of the more notable and relevant discoveries that chart the way through these two decades of extra-dimensional renaissance.

1.3.1 Field theoretic domain walls

In the early 1960s, there was some independent interest in using extra dimensions as a purely mathematical tool to help determine representations of the Lorentz group in curved spacetime. The idea was to embed our curved four-dimensions in a *flat* higher dimensional spacetime, and use the known behaviour of particles in these flat dimensions to determine their effective behaviour as seen from the four-dimensional subspace [41, 42]. This idea of embedding our spacetime in something larger gained renewed interest in the 1980s when various people discovered ways to reduce the dimensionality of a model, and dynamically generate a subspace, by using certain fields as a trap.

One of the very early ideas, conceived in 1982, of using classical fields to produce a subspace and reduce the number of dimensions is due to Keiichi Akama [43]. In his model the higher-dimensional spacetime, or bulk, is six-dimensional Minkowski spacetime, and in it reside a charged Higgs field

and associated U(1) gauge field. Akama found particular solutions for the background configuration of these two coupled fields, a solution which takes the form of a vortex, an extended string-like topological defect,[23] similar to the Nielsen-Olesen solution [44]. Such a configuration reduces the dimensionality of spacetime by two: particles can be trapped inside the vortex and are only free to move in the three spatial directions running along the direction of the string (and they also retain their time degree of freedom). Akama showed that, at low energies, fields are suppressed outside the vortex solution and such a trapping is induced, and he also showed that the equations of general relativity hold in this four-dimensional subspace. Thus the universe that we observe, including the standard model and gravity, may be trapped inside a vortex living in six dimensions.

A year later, Valery Rubakov and Mikhail Shaposhnikov [45] independently discussed the idea that the ordinary particles that we observe may be trapped in a "well" which is very deep and narrow in extent in any extra dimensions (so that particles find it difficult to move in these dimensions), but which is flat along the usual three dimensions that we observe. As did Akama, Rubakov and Shaposhnikov suggested that the well might have dynamical origins, and presented a toy model whereby particles are trapped to a domain wall residing in a five-dimensional bulk; the dimensionality is therefore reduced by one. Their model is described by the five-dimensional action (disregard any previous meaning given to variables used here; they will be redefined)

$$\mathcal{S}_\phi = \int d^5x \left[\frac{1}{2} \partial^M \phi \, \partial_M \phi - V(\phi) \right] , \tag{1.15}$$

where ϕ is a real scalar field which will form the domain-wall structure. Our usual four dimensions will be labelled by x^μ and the extra dimension, by w. Note that gravity is not described, or taken into account, by this theory. The potential for the scalar field is

$$V(\phi) = \frac{\lambda}{4} \left(\phi^2 - v^2 \right)^2 , \tag{1.16}$$

where λ and v are free parameters of the model. As can be seen in Fig-

[23] These strings are extended composite objects arising from a configuration of the underlying fields. They are not to be confused with the fundamental strings of string theory!

ure 1.2a, there are two degenerate minima of $V(\phi)$ which occur at $\phi = \pm v$, which will be the preferred values for the ground, or vacuum, state of ϕ. As discussed previously, such vacuum solutions will dynamically break a symmetry of the original action (1.15); in this case the particular symmetry is a $\mathbb{Z}_2$ symmetry where $\phi \to \phi' = -\phi$.

So what value does ϕ actually take in a given instance of the theory? The answer depend on the particular boundary conditions that are imposed: ϕ could be $-v$ everywhere, $+v$ everywhere or, more interestingly, $-v$ in one particular region of spacetime and $+v$ in another. This latter scenario corresponds to a domain-wall configuration; the domain wall being the relatively small region that separates the $-v$ vacuum from the $+v$ vacuum. Mathematically, one can find this solution by looking at the classical equation of motion for ϕ:

$$\partial^M \partial_M \phi + \lambda \phi^3 - \lambda v^2 \phi = 0 \,. \tag{1.17}$$

A particular solution that depends only on the extra dimension w is

$$\phi_{\mathrm{DW}}(w) = v \tanh\left(v\sqrt{\lambda/2}\, w\right) \,, \tag{1.18}$$

which is the domain-wall (DW) solution, and is plotted in Figure 1.2b. Due to its pictorial representation, a domain wall is commonly referred to as a kink, and such solutions are part of the more general class of soliton solutions [46], which are stable field configurations that have an inherently extended nature and non-trivial topology.

Rubakov and Shaposhnikov analysed the perturbations of ϕ — the ability of ϕ to deform away from the solution (1.18) — and found the massless Nambu-Goldstone boson associated with zero-energy-cost translations of the kink. The details of this mode and the other modes of the kink will be discussed in detail in Chapter 3. For now it is enough to mention that, after averaging out the extra dimension (integrating over w in the action), such modes look like typical four-dimensional scalar fields confined to the domain wall. This trapping of scalar fields is a useful phenomenon, but one also needs to be able to trap fermions, and Rubakov and Shaposhnikov found that such a thing occurred rather naturally in their model. They took the original action (1.15) and added the action for a coupled, five-dimensional fermion:

$$\mathcal{S}_\Psi = \int d^5x\, \overline{\Psi}\left(i\Gamma^M \partial_M - h\phi\right)\Psi \,, \tag{1.19}$$

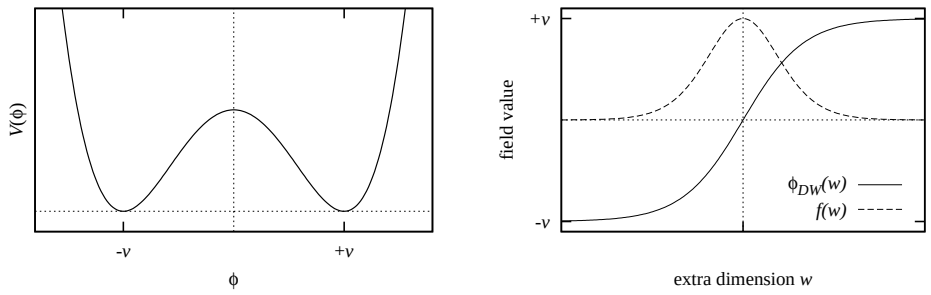

(a) (b)

Figure 1.2: (a) The quartic potential described by equation (1.16) used to induce a domain-wall configuration. (b) In solid is the domain-wall solution given by equation (1.18) that interpolates between the two degenerate vacua $-v$ and $+v$. A localised fermion profile, equation (1.22), is shown dashed; its vertical axis has arbitrary units.

where Ψ is a four-component Dirac spinor, $\Gamma^\mu = \gamma^\mu$, $\Gamma^5 = -i\gamma^5$ and h is the strength of the coupling between the kink and the fermion. To determine the behaviour of Ψ, one looks at the Dirac equation of motion in the background of the domain wall, which is

$$\left(i\Gamma^M \partial_M - h\phi_{\rm DW}\right)\Psi = 0\,. \tag{1.20}$$

This equation can be solved using separation of variables

$$\Psi(x^\mu, w) = f(w)\;\psi(x^\mu)\,, \tag{1.21}$$

where $\psi(x^\mu)$ is interpreted as a four-dimensional fermion and $f(w)$ is its extra dimensional profile. Because the standard model is constructed using massless, left-chiral fermions, one would like to assume these two properties for the form of ψ. A massless fermion obeys $i\gamma^\mu\partial_\mu\psi = 0$, and left-chirality can be imposed by $\gamma^5\psi = -\psi$. Rubakov and Shaposhnikov showed that there exists a solution for f compatible with these assumptions:

$$\begin{aligned} f(w) &= \exp\left(-h\int_0^w \phi_{\rm DW}(w')dw'\right) \\ &= \left[\cosh\left(v\sqrt{\lambda/2}\;w\right)\right]^{-h\sqrt{2/\lambda}}\,. \end{aligned} \tag{1.22}$$

The general form of f, shown in Figure 1.2b, is a smooth lump peaked

at the centre of the domain wall. The width of f can be controlled by the coupling h; a larger value of h gives a sharper peak. The physical interpretation of this solution is twofold. First, ψ has definite, fixed behaviour in the extra dimension and so looses its w degree of freedom, making it look like a true four-dimensional field. Second, the fact that f is centred on the kink solution means that the four-dimensional ψ is localised, or trapped, to the domain-wall region. This is exactly the kind of mechanism that is needed to construct a domain-wall confined standard model! Indeed, we make heavy use of this localisation mechanism, and its generalisations, throughout this thesis.

Rubakov and Shaposhnikov mention that one should expect the fermion confinement mechanism to generalise to other topological defects such as vortex and monopole traps, and they even speculate that expansion of our universe (more on this later) could find an explanation in the expansion of a closed vortex. They also highlight the fact the massless fermions would need to acquire a small mass if they are to be identified with the ones we observe, and that gravity would need to be incorporated. We present solutions to both of these issues in this thesis. As they point out, it is also very important to determine the lower limit on the domain-wall trapping strength, since one would expect to observe new physics above this energy.

Different approaches to trapping particles to a lower-dimensional subspace were investigated in the following years. In 1985, Matt Visser [47] had the general idea that a particular form of the gravitational metric could be arranged to break translation invariance in the extra dimension and prevent particles from escaping from a thin region. He presented a specific example where a five-dimensional U(1) gauge field coupled to gravity yielded a working gravitational trap. This idea was improved upon by Euan Squires [48] who found a simple, three-dimensional (down to two-dimensional) analytic realisation of Visser's idea, where the gravitational metric alone was able to trap a scalar field. An important ingredient of this model was the necessity of having a large cosmological constant in the bulk, something that will be present in many of the models we discuss. Another gravity-based model is due to Gary Gibbons and David Wiltshire [49] who found that electromagnetism and GR in a d-dimensional spacetime has a thick $(d-2)$-dimensional membrane (similar to a domain wall) as a natural solution. They showed that the electromagnetic field in their model was able to trap massless chi-

ral fermions to the membrane, and that Lorentz invariance was properly reproduced in this subspace, in contrast to Visser's model.

These early constructions of domain-wall configurations that could trap particles and produce a lower-dimensional subspace were only the beginnings of using extra dimensions as a theoretical tool. The original superstring models were about to be revived and they would provide a compelling and sophisticated framework for building extra-dimensional models.

1.3.2 Superstring theory and D-branes

In 1984, Michael Green and John Schwarz made a discovery [50] which started the first so-called string theory revolution. They considered a model with two components: supersymmetric Yang-Mills theory and $N = 1$ supergravity. Usually, such a theory is inconsistent (it does not have full anomaly cancellation), but Green and Schwarz showed that *if* the Yang-Mills gauge group is SO(32) or $\mathrm{E}_8 \otimes \mathrm{E}_8$, and *if* the supergravity is formulated in ten dimensions, then there is a chance to obtain consistency. The chance is in the fact that you need to choose some specific extra terms to add to the original action. Green and Schwarz determined what these extra terms had to be, and this would have been an interesting discovery in its own right had it not been for the remarkable thing they found: in the (type I) ten-dimensional superstring theory based on SO(32), these extra terms appear automatically! There seemed to be something inherent in the way superstrings were described that meant they produced a consistent theory. A similar phenomenon was suggested to occur with $\mathrm{E}_8 \otimes \mathrm{E}_8$ superstrings, which would later be shown to be true.

The discovery of this consistent superstring theory was an important breakthrough because it meant that physicists now had a single theory with all the ingredients necessary to describe our world: fermions and gauge bosons (from the supersymmetric Yang-Mills), a large enough gauge group (SO(32) or $\mathrm{E}_8 \otimes \mathrm{E}_8$) to contain the standard model gauge group, gravity (from supergravity), and, most importantly, it was quantum mechanically consistent. But there was still the problem of the six extra dimensions in the superstring spacetime that needed to be somehow hidden from the low-energy physics that we are familiar with. Of course, the original Kaluza-Klein idea that the extra dimensions are tiny and curled up — compactified — has a direct application here, and this is the most often used mech-

anism in string theory to hide most, if not all, of the extra dimensions. As we will see though, there is the possibility that some of the dimensions are much larger than the tiny 10^{-29} mm envisaged by Klein all those years ago.

An inherent feature of superstring theory is supersymmetry; this latter idea can also be applied directly to the standard model, where all the gauge bosons get new fermionic partners, and all the fermions get new bosonic partners. This particular form of supersymmetry is implemented at the electroweak scale and, among other attractions, provides a solution to the hierarchy problem. In an attempt to understand why electroweak supersymmetry occurs at such an energy scale, Ignatios Antoniadis suggested in 1990 [51] that this energy scale may be related to the internal compactification radius of an extra dimension of superstring theory. The electroweak scale is around about 1 TeV, so the extra dimension would need to have a corresponding length of about 10^{-16} mm. This number is huge compared with the traditional Kaluza-Klein compactification size, yet Antoniadis argued that such a size is possible, and that it yields very distinct experimental signatures in its spectrum of supersymmetric Kaluza-Klein particles.

Another important discovery of string theory was that of the Dirichlet-brane, or D-brane. Such objects were proposed in 1989 by Jin Dai, Robert Leigh and Joseph Polchinski [52] to be fundamental entities that lived and propagated in the string-theory spacetime. As the name suggests, a brane is a higher dimensional version of a string, and, while branes can be of any dimension that fits in the spacetime, it is useful to think of them as a malleable two-dimensional surface, or a sheet (denoted D2-brane). A Dirichlet boundary condition is a restriction on the value of some entity, and, in the case of Dirichlet-branes, the restriction applies to the ends of open strings which are forced to terminate on D-branes. In ten-dimensional superstring theory, the end points of an open strings have nine spatial degrees of freedom, and if they terminate on a D2-brane, they loose seven of these, but retain the two corresponding to movement on the surface of the D2-brane. This corresponds exactly to the phenomena of dimensional reduction and localisation! Further analysis of D-branes by Polchinski [53] in 1995 fuelled the second string theory revolution, and D-branes would become a fundamental building block of models based on string theory.

In that same year, 1995, M-theory was discovered by Edward Witten; see the paper by Petr Hořava and Witten [54]. The details of this myste-

rious theory were unknown, but the authors suggested that the 'M' stand for "membranes" since the theory was an eleven-dimensional extension of superstring theory. In fact, what they did know about M-theory was that, in different limits, it seemed to reduce to the five different superstring theories known at the time. Furthermore, they determined the low-energy limit of M-theory to be eleven-dimensional supergravity. Hořava and Witten later found more evidence for M-theory [55], and, in 1998, André Lukas, Burt Ovrut, Kellogg Stelle and Daniel Waldram found a way of interpreting this theory [56]. They were interested in the low-energy behaviour of the $E_8 \otimes E_8$ superstring, and proposed that one should take M-theory and eliminate six of the spatial dimensions by compactifying them in the usual Kaluza-Klein way (on a Calabi-Yau manifold). The leftover five-dimensional spacetime then admits a pair of D3-brane solutions which live at the two edges of the fifth spatial dimension, and they identified the spacetime of our universe as the volume inside the D3-branes. This construction uses the fact that strings are localised to D-branes, and provides a scenario, in the formalism of superstring theory, whereby our universe is confined to a brane.

We are now going to leave the details of eleven-dimensional M-theory and superstrings behind, but retain the generic ability to write down a model with branes and extra dimensions, and where particles are automatically confined to these branes. We will refer to such branes as *fundamental branes*, and remember that they have some deeper origin in string theory. The other kind of branes we will be working with are *domain-wall branes*. These are dynamically generated, field theoretic domain walls that play the role of a D-brane by confining other fields using some particular mechanism in the context of field theory. As discussed previously, Rubakov and Shaposhnikov found a way of confining fermions; we now discuss a mechanism which confines gauge fields.

1.3.3 The Dvali-Shifman mechanism

It turns out that confining gauge fields to a domain-wall brane requires much more sophisticated theoretical machinery than the mechanism which confines fermions. Consider the case of confining a U(1) gauge field (electromagnetism) to a wall. The straightforward approach might involve taking a five dimensional U(1) gauge field, and dynamically breaking the symmetry associated with this field in the region *outside* the domain wall; the region

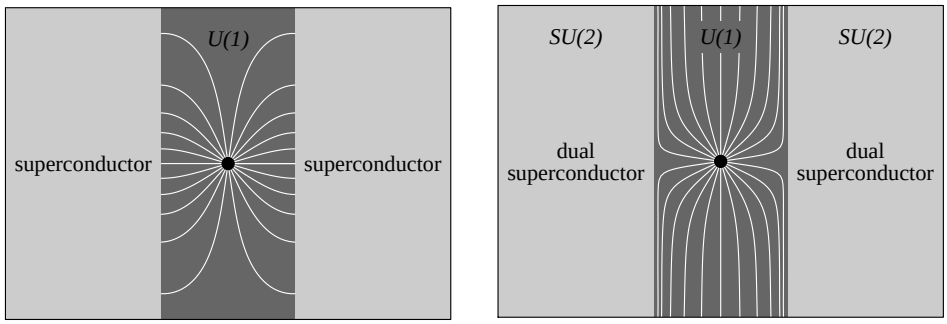

(a) (b)

Figure 1.3: In both of these figures, the bulk on the left and right is light gray, the centre region of the domain wall is dark gray, the black dot is an electric charge, and the white lines are electric field lines. (a) A naïve approach to confining a U(1) gauge field that fails. The symmetry is broken in the bulk by a Higgs, making this region a superconductor and forcing electric field lines to end here, effectively screening the charge. (b) A schematic representation of the Dvali-Shifman mechanism at work. The SU(2) symmetry is unbroken in the bulk and this region is in the confinement phase and acts as a dual superconductor, repelling electric field lines. For observers in the domain wall separated by a large enough distance, the electric field lines run parallel to the bulk and the dimensionality of the electric force is reduced by one.

where we want to suppress the gauge fields, to keep them localised to the wall. Such a symmetry breaking is easy enough to arrange: you just need a Higgs field with a vacuum state that changes as one moves along the extra dimension. In this set-up, the photons associated with the U(1) group acquire a mass in the bulk outside the domain wall — where the Higgs vacuum is arranged to be non-zero — and is massless inside the wall — where the Higgs vacuum goes to zero. One would imagine that an individual photon would prefer to remain massless (since this requires less energy) and so would stay localised in the region close to the wall.

Figure 1.3a depicts this situation with a single electric charge placed inside the wall. In the bulk, the non-zero Higgs vacuum creates a superconductor, and, just like ordinary conductors, the electric field lines corresponding to U(1) photons must end on this superconductor. Thus we get exactly the opposite effect to what we intended: electric charges are rendered invisible, or screened, because the photons disappear into the bulk!

In 1996, Gia Dvali and Mikhail Shifman found a way around this problem by making the bulk a dual superconductor instead of a normal superconductor [57]. They showed that in order to confine a U(1) gauge field, the

theory needs to begin with a five-dimensional $G = \mathrm{SU}(2)$ gauge field, along with two scalar fields. One of these scalar fields, ϕ, is a singlet of G (i.e. it is un-charged) and serves to form a domain wall, as per equation (1.18) and Figure 1.2b. The other scalar field, χ^a ($a = 1, 2, 3$), is a triplet (in the adjoint) of G and is used to break the gauge symmetry in a specific way. This theory is formulated in five-dimensions, and the action is

$$\mathcal{S} = \int d^5x \left[\frac{-1}{4} F^{aMN} F^a_{MN} + \frac{1}{2} \partial^M \phi \partial_M \phi - \frac{\lambda}{4} \left(\phi^2 - v^2 \right)^2 + \frac{1}{2} (D^M \chi^a)^\dagger D_M \chi^a - \frac{\lambda'}{2} \left(\chi^a \chi^a + \kappa^2 - v^2 + \phi^2 \right)^2 \right], \tag{1.23}$$

where F^a_{MN} is the field strength tensor corresponding to the SU(2) gauge group, and λ, λ', v and κ are real parameters which control the formation of the domain wall and the Higgs symmetry breaking profile.[24] The vacuum configuration of this model is as follows. The field ϕ obtains a kink profile and asymptotes to $\pm v$ on either side of the domain wall. Near the centre of the wall $\phi \sim 0$ and, if one chooses parameters such that $\kappa^2 - v^2 < 0$, χ becomes tachyonic, meaning that its vacuum state will be non-zero and the G gauge symmetry is dynamically broken *inside* the domain wall. Far from the wall $\phi \to \pm v$ and the vacuum state of χ will be zero. The extra dimensional profile, or solution, for χ is therefore a peak centred in the domain-wall region. (In fact, the configuration of ϕ and χ looks exactly like the two curves in Figure 1.2b, where χ has the shape of f.)

Figure 1.3b is a schematic representation of such a configuration of fields, and again we have shown the electric field lines for a charge placed in the wall. The bulk is a dual superconductor because G is a non-Abelian gauge group and has the property of asymptotic freedom. In contrast to a superconductor which repels magnetic field lines, a dual superconductor repels electric field lines and, from the point of view of a charge on the wall, gives the impression that photons are confined to the central wall region. Now in this region, χ dynamically breaks the symmetry $\mathrm{SU}(2) \to \mathrm{U}(1)$ and the non-Abelian nature of G is destroyed, leaving a massless photon-like gauge field associated with the remaining U(1) symmetry. It is possible to argue that the reason these photons do not leave the wall is because in the bulk they

[24] It is not possible in this simple model to have one scalar field play the role of the domain wall and the Higgs at the same time.

must be incorporated into an entity which is completely SU(2) symmetric; the lowest energy state of this form having a large mass corresponding to the mass gap of this non-Abelian group. On the domain wall, for distances r much larger than wall width, the electric field lines are parallel to the wall and the electric potential looks like it does in our four-dimensional universe: $U_{\text{elec}} \sim 1/r$.

This mechanism for gauge field confinement, the Dvali-Shifman (DS) mechanism, works with any non-Abelian SU(N) theory broken to any of its sub-groups.[25] One important feature of the DS mechanism is gauge universality: all charged fields couple to the corresponding gauge field with equal strength, irrespective of any details of the distribution of the fields in the extra dimension. This is a crucial feature because it guarantees, for example, that the up quark has exactly two-thirds the electric charge of the electron. This occurs in the DS mechanism because any part of a particle that is outside the domain wall is connected back by a tube of gauge-field flux lines. There is good discussion of this phenomenon in the 1998 paper by Nima Arkani-Hamed and Martin Schmaltz [58], and these authors also discuss the similarities between the DS mechanism and D-brane string confinement.[26]

The major drawback of the Dvali-Shifman mechanism is the reliance on non-perturbative field theory in order to get gauge field confinement (asymptotic freedom) in the bulk. As a consequence, it is difficult to perform a quantitative analysis of the bulk gauge sector. Nevertheless, the DS mechanism seems to provide a comprehensive solution to the problem of confining gauge fields to a field theoretic domain-wall brane. There does not seem to be any other satisfactory way to do this (see Chapter 2 for an attempt), and we use the DS mechanism in our brane-localised version of the standard model in Chapter 5, as well as in the extension to E_6 in Chapter 6.

We now move on to discuss models of extra dimensions based on the fundamental branes of string theory, as a prelude to the Randall-Sundrum set-up which provides a way to confine gravity.

[25] To use the DS mechanism in five-dimensions (or higher), one must assume non-Abelian gauge field confinement works, even though Yang-Mills theory is not renormalisable in dimensions higher than four. We will discuss this caveat in greater detail in Chapter 5.

[26] Another lucid discussion of these matters can be found in Dvali, Nielsen and Tetradis [59]. See also the paper by Dubovsky and Rubakov [60].

1.3.4 Low-energy string theory and brane worlds

Recall the electroweak hierarchy problem (Section 1.2.5): the natural size of the Higgs dimensionful parameter is the Planck scale (the largest energy the standard model is valid up to), yet such a value is not consistent with experiment. There is a deep assumption here: that our weak measurement of gravity is a direct probe of the highest available energies. It is quite possible that the scale of gravity, the four-dimensional Planck scale $M_{\rm Pl}$, is an illusion that is indirectly related to the true, or fundamental, Planck scale M_*, that is, the energy at which general relativity must be replaced by a quantum theory of gravity.

The idea that $M_{\rm Pl}$ and M_* could differ was realised in early 1998 in the model of Arkani-Hamed, Savas Dimopoulos and Dvali [61]; the ADD model. They proposed that the weak scale is actually the fundamental energy scale, so $M_* \sim 1$ TeV, and gravity, the Higgs mechanism and gauge field interactions unite at this scale. We observe gravity to be weak in our four-dimensional universe because of the presence of two (or more) extra compact dimensions which *dilute* the gravitational field. Note that there is no need to localise gravity to a subspace to ensure that we observe a four-dimensional gravitational force: it is enough that the extra dimensions are compactified (maybe even on a large scale) so that gravity can saturate the extra dimensions first, become diluted, and then propagate in the usual way in the remaining three spatial dimensions. In fact, this mechanism of reducing the strength of gravity only works *because* gravity has not been localised to a brane of some sort. Of course, at distances which are of comparable size to or, smaller than the extra dimensions, gravity is heavily modified from the usual case because at these distances you notice that gravity is not really four-dimensional at all.

In the ADD model, the apparent Planck scale is related to the fundamental Planck scale through the relation

$$M_{\rm Pl}^2 \sim M_*^{2+n} R^n \,, \tag{1.24}$$

where n is number of extra dimensions and R is their common radius. For the interesting case of two extra dimensions $n = 2$, we want $M_* \sim 1$ TeV to solve the hierarchy problem, and so the radius must be $R \sim 10^4$ eV$^{-1} \sim$ 1 mm. This is a huge distance for particle physics — recall that the length

corresponding to 1 TeV is 10^{-16} mm — and this distance explains (in this model at least) why the observed Planck scale is so much larger than M_*. The generic idea of the ADD proposal is that the hierarchy problem is solved by bringing down the fundamental Planck scale, making the natural value for the dimensionful Higgs parameter about 1 TeV, which is consistent with observation.

Arkani-Hamed et al. gave a particular realisation of their proposal where a vortex in six-dimensions was identified with our world, and the Pati-Salam gauge group was used to incorporate the standard model. While gravity could propagate in the bulk, the usual standard model fields had to be confined to the vortex, or else their Kaluza-Klein excitations would ruin the phenomenology of the model. They proposed that some new quantum theory took over above about 1 TeV, and, in a subsequent paper in collaboration with Antoniadis [62], outlined a way of embedding the ADD model in superstring theory. Here, gravity is a manifestation of closed strings in the bulk, and fermions and gauge fields are made from open strings ending on D3-branes. One of the most exciting features of this model is the prediction of stringy physics at energies that may be experimentally accessible in the near future. Such a possibility meant that a great deal of attention was given to the ADD model in the following years (see, for example, the phenomenological studies by Arkani-Hamed, Dimopoulos and Dvali [63], and Arkani-Hamed and Dimopoulos [64]), and some important problems were ironed out, like stabilising the large size of the extra dimensions with bulk scalar fields, and suppressing proton decay with split fermions.

Towards the end of 1998, Arkani-Hamed, Dimopoulos and John March-Russell tackled the problem of the stabilisation of the millimetre sized extra dimensions [65]. Since D-branes are dynamical entities, they are allowed to deform and travel in the extra dimension(s), and these radial oscillations can be modelled by a field, known as the radion. If the radion is left to behave as it naturally would, there is no reason for the separation of the D3-branes in the ADD model, and the radius of the extra dimension, to stay at the desired value. In this later paper of Arkani-Hamed et al., it was shown that a positive bulk cosmological constant could prevent the branes from moving apart: a cosmological constant induces a potential energy that scales with volume, so a smaller volume is preferred. To prevent a collapse, the authors suggested either placing many branes in the bulk that repelled one another

and supported the large size of the extra dimensions, or having a bulk field with a non-trivial vacuum configuration that could not, in a sense, unwind because of a conserved topological charge. The topic of stabilisation has received much attention since this work, see Section 1.5.2 for some of the details.

As discussed previously, the see-saw mechanism is the standard method used to generate small neutrino masses; it relies on the fundamental Planck scale being large. Despite this, small neutrino masses in the range 10^{-1} eV – 10^{-4} eV found natural explanations in the ADD model, as discovered by Arkani-Hamed, Dimopoulos, Dvali and March-Russell [66]. One method relied on the fact that any massless singlet fermions in the bulk could be interpreted as right-handed neutrinos, and, due to the large size of the bulk, would have a very small probability of interacting with brane localised left-handed neutrinos. This leads to an effective coupling between left- and right-handed neutrinos which is very small, and endows the neutrinos with a small Dirac mass. For Majorana neutrinos, one can arrange to break lepton-number on a brane which is far away from our brane, and have this breaking transmitted by messenger fields which are suppressed due to the large bulk. So large extra dimensions can not only dilute gravity, they can also dilute the couplings that lead to neutrino masses.

In early 1999, Arkani-Hamed and Schmaltz invented the split fermion mechanism [67] to solve the general problem, in the context of large extra dimensions, of unnaturally small couplings between fields. Usually, one obtains small couplings by imposing a symmetry which, if broken in the correct way, allow only small couplings for the terms that break the symmetry. Arkani-Hamed and Schmaltz's alternative idea was to use "higher dimensional geography", whereby different fermionic fields are localised at different locations in a large extra dimension. If the extra-dimensional profiles of these fermions (see for example f in Figure 1.2b) are sharply peaked and drop off exponentially, they only need to be separated by a small distance, of the order of a few multiples of the width of the profiles, to have a tiny overlap. This yields naturally small, effective four-dimensional couplings, which are computed from integrals over the extra dimension of the product of the profiles. The couplings can be controlled by arranging the locations of the fermions, using a five-dimensional Dirac mass term, and a good match to reality can be obtained by separating the quarks from the lep-

tons. In order to assure gauge universality, the profiles of the lowest energy gauge fields must be flat in the extra dimension. This split fermion mechanism finds broad application, including suppressing proton decay, producing the fermion mass hierarchy, and generating small neutrino masses. We will show that the mechanism finds a natural implementation in our model in Chapter 5.

In the year just following the introduction of the ADD model, Merab Gogberashvili proposed a model whereby the universe is a thin shell, a three-dimensional sphere, expanding in a five-dimensional spacetime [68, 69, 70, 71]. His model solved the electroweak hierarchy problem in a very similar way to the ADD model: the fundamental Planck scale is much smaller than the observed Planck scale, and is set by the thickness ϵ of the shell, which was determined to be $\epsilon \leq 0.1$ mm. The stability of these shells were analysed using general relativity, and they were found to be long lasting. Furthermore, gravity was found to trap matter to the shell and Newton's law was recovered for large distances. This shell-universe model is yet another example of how extra dimensions can be successfully incorporated into a realistic model of fundamental physics.

As is evident from the previous discussions, many old problems can be solved, or at least understood from a different point of view, by using extra dimensions. D-branes can confine the particles of the standard model to a subspace in these extra dimensions, and mechanisms such as split fermions can be invoked to construct models that agree with experiment, and provide natural explanations for certain properties of our world. So far we have seen realistic models with large (1 mm sized) extra dimensions. In this thesis we are going to construct models of an *infinitely* large extra dimension, which requires a mechanism that traps gravity to a domain wall, and we will discuss such a mechanism shortly. But for the moment we need to take a detour and introduce the basics of cosmology.

1.4 Basic cosmology

The many decades that saw the advancement of elementary particle physics and the construction of the standard model also saw significant development in the field of early universe cosmology. Physicists gained a broad understanding of the evolutionary time-line of our universe: from the initial big

bang, through inflation and phase transitions, baryogenesis and nucleosynthesis, all the way to the formation of large scale structures that we observe today. Here, we give a brief overview of the basic theory behind these ideas.

1.4.1 Expansion and the FLRW metric

Cosmological events are played out upon the stage of an expanding universe. The mathematics of this expansion are described by Einstein's equations of general relativity, and were determined very early on, between 1922 and 1937, by Alexander Friedmann [72, 73], Georges Lemaître [74, 75], Howard Robertson [76, 77, 78] and Arthur Walker [79] (FLRW). Two important observations about our universe are that, on the largest of scales, it looks spatially homogeneous (the same at all locations) and spatially isotropic (the same in all directions). Such observations can be modelled by the FLRW metric[27]

$$ds^2 \equiv g_{\mu\nu} dx^\mu dx^\nu = -dt^2 + a^2(t) \left(\frac{dr^2}{1 - kr^2} + r^2 d\theta^2 + r^2 \sin^2\theta d\phi^2 \right) , \quad (1.25)$$

where ds^2 measures spacetime distances, $g_{\mu\nu}$ is the metric of GR, and $x^\mu = (t, r, \theta, \phi)$ are the four-dimensional spacetime coordinates (the spatial part is in spherical coordinates). The function $a(t)$ is known as the scale factor and its evolution describes the expansion (or contraction) of spatial sections. The constant k describes the curvature of the spatial sections, and can take the values $+1$, 0 or -1 (after a suitable rescaling of r), which correspond respectively to positive-curvature (like the surface of a sphere), flat space, or negative-curvature (like the surface of a saddle).

A metric such as equation (1.25) is used to compute physical spacetime distances between some given coordinates x^μ. Having the scale factor $a(t)$ in the metric has the following consequence: two objects may remain stationary at the same coordinates (so their x^μ's are constant), yet the physical distance between them may be changing due to a changing $a(t)$! To find the behaviour of $a(t)$, and hence determine the evolution of the universe, one solves Einstein's equations:

$$G_{\mu\nu} = 8\pi G\, T_{\mu\nu} - g_{\mu\nu}\Lambda \, . \quad (1.26)$$

[27] Note that in this section on cosmology, we will be using $-+++$ for the metric signature, for consistency with Chapter 7. See Section A.3 for an overview of such conventions.

Here, $G_{\mu\nu}$ is the Einstein tensor made out of derivatives and products of the metric $g_{\mu\nu}$, G is Newton's constant and Λ is the cosmological constant. The energy content of the universe is described by the stress-energy tensor $T_{\mu\nu}$, which, for the homogeneous and isotropic case, is

$$T^{\mu}{}_{\nu} = \mathrm{diag}(-\rho, p, p, p)\,, \tag{1.27}$$

where ρ is the energy density of the particular source being modelled, and p is its pressure, usually determined by the equation of state: $p = w\rho$. For dust the pressure is zero and $w = 0$; for radiation $w = \frac{1}{3}$; for a cosmological constant $w = -1$. The total stress-energy tensor can be a sum of contributions of the form (1.27), with each source having a different value of w.

Taking Einstein's equations (1.26), substituting the FLRW metric (1.25) for $g_{\mu\nu}$, and using for $T_{\mu\nu}$ the form (1.27), one arrives at the so-called Friedmann equations

$$H^2 = \frac{8\pi G}{3}\rho + \frac{\Lambda}{3} - \frac{k}{a^2}\,, \tag{1.28a}$$

$$\frac{\ddot{a}}{a} = -\frac{4\pi G}{3}\left(\rho + 3p\right) + \frac{\Lambda}{3}\,, \tag{1.28b}$$

and the conservation equation

$$\dot{\rho} + 3H\left(\rho + p\right) = 0\,. \tag{1.29}$$

In these equations, $H = \dot{a}/a$ is called the Hubble parameter and an over-dot denotes a derivative with respect to time. Given the curvature k and sources Λ, ρ and p, one can use the Friedmann equations to solve for the evolution of $a(t)$. Measurements suggest that the sources in our universe consists of 74% dark energy (modelled well by the cosmological constant Λ), 22% dark matter and 4% ordinary standard-model matter. Observations also indicate that the universe has been expanding since its beginnings, with a current rate $H \sim 70\ \mathrm{km}\cdot\mathrm{sec}^{-1}\cdot\mathrm{Mpc}^{-1}$ ($1\ \mathrm{Mpc} = 31\times 10^{12}\ \mathrm{km}$). The solutions to the Friedmann equations (1.28) are in excellent agreement with these observations.

The FLRW metric ansatz (1.25) and Einstein's equations (1.26) form the core of theoretical cosmology. There is a great deal more that could

be discussed — the latest results from the Wilkinson Microwave Anisotropy Probe (WMAP) [80] are particularly interesting — but we will restrict ourselves here to a brief discussion, more relevant to this thesis, of domain walls as entities that appear in the early universe.

1.4.2 Cosmological domain walls

Domain walls and kink solutions are an integral part of modern cosmology, and their appearance in cosmological models actually predates their use in extra-dimensional model building. In 1974, Yakov Zel'dovich, Igor Kobzarev and Lev Okun determined that a domain structure would be expected to appear in theories with spontaneous symmetry breaking [81]. As the universe expands its temperature decreases, and, when the temperature drops below the critical threshold associated with a given Higgs field, that Higgs field will assume a vacuum expectation value and spontaneously break a symmetry. This is known as a phase transition. Because the universe is so large, there are regions which are causally disconnected — information has not had time to travel between them — and so there is no reason for these separated regions to assume the same vacuum expectation value. As a consequence, the regions, or domains, take randomly different vacuum values following the phase transition, and domain walls form at the interface between these regions.

Note that these cosmological domain walls are two-dimensional, do not necessarily confine any fields, and are thought of as cosmological entities, or relics, which form in the early universe just like atoms form in the nucleosynthesis process. Zel'dovich et al. found that the kink solution given by equation (1.18) gives a good description of cosmological domain walls, and emphasised the fact that such relics must disappear early on or else our universe would be in a vastly different state to what we observe at the present time.

Further study was devoted to topological defects that could arise in the early universe; not only domain walls, but also strings and monopoles. The types of defects that one can expect a given theory to produce are directly related to the topology of the vacuum: the more structure there is in the symmetry of the vacuum that is spontaneously broken by a Higgs field, the more varied the allowed defects. Some details were worked out in 1976 by Tom Kibble [82], who concluded that, unless the standard cosmological

model is modified (for example, by inflation[28]), the existence of domain walls are ruled out due to the isotropy of the measured background radiation. Such analyses of the phenomenology of phase transitions in gauge theories are an important area of study, and find a wide range of application, not just to defect formation. A discussion of such phase transitions can be found in the paper by Andre Linde [85].[29]

String and domain-wall defects are inherently large objects and so one would expect gravity to play a role in their formation. In the early 1980s, Alexander Vilenkin found domain wall solutions consistent with the equations of general relativity [86, 87, 88], and it turns out that when gravity is incorporated, the only solutions are time-dependent ones. Upgrading gravity to supergravity changes the structure of spacetime and hence the formation of domain walls and their properties; see for example Cvetič, Griffies and Rey [89], and Cvetič and Soleng [90]. Investigations of the multitude of defects in supergravity gives insight to defects in superstring theories, but we will not discuss such things here.

Cosmological domain walls and domain-wall branes are generated by similar mechanisms, and similar theoretical techniques are used to analyse them. But the contexts within which they appear — early universe cosmology versus models of extra dimensions, respectively — are very different. We now return to the domain-wall branes that are the central topic of this thesis, and discuss the critically important mechanism by which gravity can be trapped to a brane.

1.5 The Randall-Sundrum warped metric

With the advent of the string-theory inspired ADD model, physicists started to take seriously the idea of using branes and large extra dimensions as tools in model building. The brane world scenario seemed to admit a realistic implementation of the standard model, as well as providing new ways to

[28] Inflation is the short period of time in the very early stages of the universe when space grows exponentially quickly, and is followed by the usual FLRW expansion. This exponential growth can eliminate domain walls and monopoles, and also solves some other interesting problems related to the big-bang scenario. See Guth [83] and Linde [84] for the original proposals of inflation.

[29] Among other things, Linde discusses the restoration of symmetry above the phase transition temperature, which has very interesting consequences. In particular, during the period when the universe was hot enough such that the electroweak symmetry was unbroken, all of the fermions, and the W and Z bosons, were massless, and the electroweak force was long ranged, like electromagnetism is today.

tackle old problems such as the hierarchy problem. But if brane worlds were to offer a compelling alternative to the traditional understanding of our universe, they would also need to make consistent predictions for cosmology.

At the end of 1998, Dvali and Henry Tye proposed a mechanism for cosmological inflation [91] (see footnote 28 regarding inflation) in the context of the ADD model. Dvali and Tye's scenario starts with multiple D-branes in the bulk, some of which are separated by relatively large distances with respect to the size of the extra dimensions. While slowly moving towards each other, the three internal spatial dimensions of these branes grow exponentially — they inflate. When they get close enough, the nature of the brane–brane interaction changes, inflation ends, and a collision occurs, where energy is dissipated into radiation on the branes. Such a mechanism provided a natural way to incorporate successful inflation in brane world models.[30] The next item to address would be FLRW expansion.

The effective Friedmann equations for a brane world with a single extra dimension were derived in early 1999 by Pierre Binétruy, Cédric Deffayet and David Langlois [93]. These equations describe the behaviour of the effective scale factor that is seen from the perspective of a brane-localised observer, and allow one to determine how the brane expands. Binétruy et al. found such behaviour to be vastly different from the usual case described by equation (1.28). In particular, the Hubble parameter in the brane-world case depended on energy density as $H^2 \sim \rho^2$, in contrast to the standard dependence $H^2 \sim \rho$. This was a serious setback for brane world models, but a setback that would be rectified, almost immediately, following the discovery of the Randall-Sundrum warped metric solution.

1.5.1 The two Randall-Sundrum scenarios

In the ADD model, the hierarchy problem is solved because the fundamental Planck scale is $M_* \sim 1$ TeV, and the observed Planck scale $M_{\mathrm{Pl}} \sim 10^{19}$ GeV is much larger due to the large volume of the extra dimensions. But this solution actually introduces a new hierarchy problem: the energy scale related to the size of the extra dimensions $1/R \sim 10^{-4}$ eV is many orders of magnitude smaller than its natural value, being the fundamental scale M_*. (Alternatively, the size of the extra dimensions $R \sim 1$ mm is many orders

[30] See Arkani-Hamed, Dimopoulos, Kaloper and March-Russell [92] for further analysis of inflation in the ADD model, including a discussion on the link to radion stabilisation.

of magnitude larger than the natural size, corresponding to M_*, which is 10^{-16} mm.) In 1999, Lisa Randall and Raman Sundrum proposed a new solution to the hierarchy problem [94], which used extra dimensions in a different way to the ADD model, and which also provided a way to confine gravity to a fundamental brane [95]. These two scenarios are known as RS1 and RS2 respectively, and we give an overview of them here, following closely the discussion in the original papers. Note that all variables in this section will be redefined, so disregard any previous meaning.

The set-up of the two RS scenarios is as follows. First, the spacetime is five-dimensional with coordinates $x^M = (x^\mu, w)$ and metric signature $+----$. The single extra dimension w is periodic with period $2L$, and the points (x^μ, w) and $(x^\mu, -w)$ are identified (so the space is $S^1/\mathbb{Z}_2$). We take the extent of w to be $-L$ to $+L$, but the reflection identity means that the independent points are only those between 0 and L. The bulk five-dimensional metric is G_{MN}, with determinant G. Second, the sources in the model consist of a bulk cosmological constant Λ, and two fundamental branes located at the boundaries of the extra dimension; the left one is at $w = 0$ and the right one at $w = L$. The metrics on these branes are the bulk metric evaluated at the appropriate points:

$$g_{\mu\nu}^{\text{left}}(x^\mu) = G_{\mu\nu}(x^\mu, 0)\,, \tag{1.30a}$$

$$g_{\mu\nu}^{\text{right}}(x^\mu) = G_{\mu\nu}(x^\mu, L)\,. \tag{1.30b}$$

Note that the branes are four-dimensional entities, so their metrics are only indexed by μ and ν. The determinants of these brane metrics are g_{left} and g_{right} respectively.

This set-up, with two branes in a five-dimensional bulk, is modelled by the action

$$\mathcal{S} = \mathcal{S}_{\text{bulk}} + \mathcal{S}_{\text{left}} + \mathcal{S}_{\text{right}}\,, \tag{1.31}$$

where the separate pieces are

$$\mathcal{S}_{\text{bulk}} = \int d^4x \int_{-L}^{L} dw \sqrt{G} M_*^3 \left(-R - 2\Lambda\right)\,, \tag{1.32a}$$

$$\mathcal{S}_{\text{left}} = \int d^4x \sqrt{-g_{\text{left}}}\left[\mathcal{L}_{\text{left}} - V_{\text{left}}\right]\,, \tag{1.32b}$$

$$\mathcal{S}_{\text{right}} = \int d^4x \sqrt{-g_{\text{right}}}\left[\mathcal{L}_{\text{right}} - V_{\text{right}}\right]\,. \tag{1.32c}$$

The branes are composed of some (unspecified for now) Lagrangian densities $\mathcal{L}_{\text{left}}$ and $\mathcal{L}_{\text{right}}$, and brane tensions V_{left} and V_{right}.

Given this action, one can now find the solutions to Einstein's equations. Randall and Sundrum assumed that the bulk metric respected four-dimensional Poincaré invariance, in anticipation that spacetime would be flat on the branes. The ansatz is therefore

$$ds^2 = e^{-2\sigma(w)}\eta_{\mu\nu}dx^\mu dx^\nu - dw^2 \,, \tag{1.33}$$

where $\eta_{\mu\nu} = \text{diag}(+1, -1, -1, -1)$ is the four-dimensional Minkowski metric. The factor $e^{-2\sigma(w)}$ is known as the warp factor, and the warp factor exponent $\sigma(w)$ is solved for using some of Einstein's equations, yielding

$$\sigma(w) = |w|\sqrt{\frac{-\Lambda}{6}} \,. \tag{1.34}$$

This solution requires $\Lambda < 0$ and hence the bulk spacetime is a slice of five-dimensional Anti-de Sitter space, or AdS_5. It is convenient to use a single energy scale, denoted k, to parameterise the set of solutions that we will get. This scale is related to the amount of curvature in the bulk, and it is assumed that such curvature is smaller than the fundamental Planck scale: $k < M_*$. The bulk cosmological constant is then

$$\Lambda = -6k^2 \,, \tag{1.35}$$

and the rest of Einstein's equations give the relations

$$V_{\text{left}} = -V_{\text{right}} = 12M_*^3 k \,, \tag{1.36}$$

which fully constrain the model. The necessity of having these specific values for the bulk cosmological constant and brane tensions in terms of k is known as the problem of fine tuning in the RS model. Such a tuning was not addressed in the original proposal, and is equivalent to imposing the condition that the effective four-dimensional spacetime has a vanishing cosmological constant.

The next thing to do is determine the effective strength of gravity from the four-dimensional perspective, by integrating out the extra dimension. This can be achieved by assuming a more general form of the five-dimensional

metric which includes the dynamics of the four-dimensional subspace; such a metric is

$$ds^2 = e^{-2\sigma(w)}\overline{g}_{\mu\nu}(x^\mu)dx^\mu dx^\nu - dw^2 \,. \tag{1.37}$$

Here, $\overline{g}_{\mu\nu}(x^\mu)$ describes the metric of four-dimensional slices at fixed w, with corresponding determinant $\overline{g}$. This is not the most general metric; for example, it ignores the dynamics associated with the radion. Nevertheless, using equation (1.37), one is now able to factorise out the w dependent part of the relevant term contained in the Ricci scalar:

$$R(x^M) \supset e^{2\sigma(w)}\overline{R}(x^\mu) \,, \tag{1.38}$$

where $\overline{R}(x^\mu)$ is the four-dimensional Ricci scalar made of $\overline{g}_{\mu\nu}(x^\mu)$. Then, using the solution for the warp factor, the bulk action (1.32a) can be expanded

$$\mathcal{S}_{\text{bulk}} \supset -\int d^4x \int_{-L}^{L} dw\; M_*^3 e^{-2k|w|}\sqrt{-\overline{g}}\,\overline{R} \,. \tag{1.39}$$

The factor multiplying $-\int d^4x\sqrt{-\overline{g}}\;\overline{R}$ is identified as the effective Planck scale:

$$M_{\text{Pl}}^2 = M_*^3 \int_{-L}^{L} dw\; e^{-2k|w|} = \frac{M_*^3}{k}\left(1 - e^{-2kL}\right) \,. \tag{1.40}$$

In summary, the RS set-up is specified by three parameters: the fundamental Planck scale M_*, the size of the extra dimension L, and the magnitude of the bulk curvature k. The solution for the metric in the bulk is the warped metric, given by equations (1.33) and (1.34), but this solution is only consistent if the sources in the model satisfy the relations given by (1.35) and (1.36). The effective Planck scale is given by equation (1.40). We now describe the two distinct scenarios to which this warped, five-dimensional geometry can be applied.

Scenario one: a solution to the hierarchy problem

In the RS1 scenario [94], the two branes are given specific, physical roles. The left brane becomes a hidden brane, while the right brane is the visible brane, our universe, and $\mathcal{L}_{\text{right}}$ contains the standard model. Now let us determine how four-dimensional gravity, whose dynamics come from $\overline{g}_{\mu\nu}$, couples to fields localised on these two branes. For the hidden brane at $w = 0$, the metric is given by equation (1.30a), which, after evaluating the warp

factor at $w = 0$, yields exactly $\overline{g}_{\mu\nu}$. Thus, the natural scale for dimensionful parameters in $\mathcal{L}_{\text{left}}$ is the effective Planck scale given by equation (1.40); there is nothing special going on here.

For the visible brane at $w = L$, things are drastically different, because the metric on this brane is

$$g^{\text{visible}}_{\mu\nu} = e^{-2kL}\overline{g}_{\mu\nu} \,, \tag{1.41}$$

which includes an exponential suppressing factor. To see how this factor modifies fields on the visible brane, consider a localised electroweak Higgs field (see equation (1.6), but ignore the coupling of Φ to other fields), which is described by the Lagrangian density

$$\mathcal{L}_{\text{visible}} \supset g^{\mu\nu}_{\text{visible}}\partial_\mu\Phi^\dagger\partial_\mu\Phi - \lambda\left(|\Phi|^2 - v^2\right)^2 \,. \tag{1.42}$$

Substituting this in the action for the visible brane (1.32c), and using equation (1.41) to expand the metric, we find

$$\mathcal{S}_{\text{visible}} \supset \int d^4x\; e^{-4kL}\sqrt{-\overline{g}}\left[e^{2kL}\overline{g}^{\mu\nu}\partial_\mu\Phi^\dagger\partial_\mu\Phi - \lambda\left(|\Phi|^2 - v^2\right)^2\right] \,. \tag{1.43}$$

Next comes the crucial step: the usual rules of QFT, in particular the interpretation of quantised fields as particles, require kinetic terms to be canonically normalised. We perform such normalisations quite extensively throughout this thesis. For the case at hand, the Higgs field must be rescaled: $\Phi = e^{kL}\Phi'$. This transforms the action (1.43) to

$$\mathcal{S}_{\text{visible}} \supset \int d^4x\; \sqrt{-\overline{g}}\left[\overline{g}^{\mu\nu}\partial_\mu\Phi'^\dagger\partial_\mu\Phi' - \lambda\left(|\Phi'|^2 - \left(ve^{-kL}\right)^2\right)^2\right] \,. \tag{1.44}$$

We see that the new, normalised, physical Higgs field Φ' has the same form as the original field Φ, except that the dimensionful parameter v is replaced by $v' = ve^{-kL}$. As Randall and Sundrum noted, this is a remarkable thing because we can take v to have its natural value, of order $M_* \sim M_{\text{Pl}}$, and yet obtain a *measured* value v' of order 1 TeV with just a mildly large $kL \sim 37$. This is a solution to the hierarchy problem.

Scenario two: an infinitely large extra dimension

The roles of the two branes are reversed in the RS2 scenario [95], where the left brane is the visible brane, and the right brane is hidden. In fact, the main result of RS2 is that the right brane can be completely removed from the set-up by making the size of the extra dimension infinite! The solution for the warp factor, and the values of Λ and the brane tensions, remain valid because they do not depend on the size L. Only $M_{\rm Pl}$ depends on L, but such dependence is insignificant for large kL, and equation (1.40) reduces to $M_{\rm Pl}^2 = M_*^3/k$ in the limit $L \to \infty$.

So the warped metric solution can be used with only a single brane in an infinite extra dimension, but does such a scenario reproduce a viable four-dimensional theory of gravity? To check that it does, one must examine the perturbations of the five-dimensional metric in the presence of the warped background solution, and ensure that, from the perspective of an observer localised to the brane, these perturbations look like the usual four-dimensional perturbations of GR. An extension of the metric (1.37) which includes such five-dimensional perturbations $H_{\mu\nu}(x^\mu, w)$ is

$$ds^2 = e^{-2\sigma(w)} \left[\eta_{\mu\nu} + H_{\mu\nu}(x^\mu, w)\right] dx^\mu dx^\nu - dw^2 \,, \tag{1.45}$$

and Einstein's equations are used to determine the equation of motion for $H_{\mu\nu}$, being

$$e^{2\sigma} \partial^\lambda \partial_\lambda H_{\mu\nu} - H''_{\mu\nu} + 4\sigma' H'_{\mu\nu} = 0 \,. \tag{1.46}$$

Note that we use $\eta^{\mu\nu}$ here to raise indices, prime denotes a derivative with respect to w, and we are working in the transverse, traceless gauge where $\partial^\mu H_{\mu\nu} = 0$ and $\eta^{\mu\nu} H_{\mu\nu} = 0$.

As we did for the domain-wall-trapped fermion, equation (1.21), the extra-dimensional behaviour of $H_{\mu\nu}$ can be determined by performing separation of variables:

$$H_{\mu\nu}(x^\mu, w) = \sum_n E_n(w) h^n_{\mu\nu}(x^\mu) \,. \tag{1.47}$$

Here we are doing a full generalised Fourier decomposition of $H_{\mu\nu}$, and the sum over n is a sum over modes, also known as Kaluza-Klein modes. The extra-dimensional profile of the $n^{\rm th}$ mode is $E_n(w)$, and $h^n_{\mu\nu}(x^\mu)$ is its

corresponding four-dimensional gravity perturbation, which is assumed to satisfy the wave equation: $\partial^\lambda \partial_\lambda h^n_{\mu\nu} = -m_n^2 h^n_{\mu\nu}$, where m_n is the mass of the mode. This separation of variables prescription is used to manipulate equation (1.46) and obtain an equation which can be solved to find the mode profiles E_n. The resulting equation is actually easier to understand (it becomes a Schrödinger-like equation) after changing variables from w to z using $dw = e^{-\sigma} dz$, and rescaling the mode profile by $E_n(w) = e^{3\sigma/2}\tilde{E}_n(z)$. The equation that determines the extra-dimensional behaviour of gravity perturbations is then

$$\left(-\frac{d^2}{dz^2} + V(z)\right)\tilde{E}_n(z) = m_n^2 \tilde{E}_n(z)\,, \tag{1.48}$$

where the potential is

$$V(z) = \frac{15}{4}\frac{k^2}{(1+k|z|)^2} - 3k\delta(z)\,. \tag{1.49}$$

This potential dictates the allowed mode solutions, and hence determines how effective four-dimensional gravity behaves for observers on the brane. $V(z)$ is often called a volcano potential, after its pictorial representation, and has a deep and narrow well centred at $w = z = 0$, which has the exact form required to trap gravity to the brane! Such trapping is due to two important qualitative features of $V(z)$: the ground state mode has $m_0 = 0$, and, while there is a continuum of positive mass modes directly on top of this ground state (there is no mass gap), the profiles corresponding to these massive modes are suppressed near $w = 0$ due to the sides of the so-called volcano. In Section 4.1 we shall discuss these features in more detail and provide a plot of the volcano potential as well as the solution for the profile $\tilde{E}_0$ of the ground state mode, the zero mode, of gravity perturbations. This zero mode is associated with the usual four-dimensional massless graviton, and is responsible for reproducing four-dimensional GR on the brane. Modifications to GR come from the massive modes, and Randall and Sundrum computed the effect these modes have on Newton's law of gravity:

$$U_{\rm grav}(r) = G_N \frac{m_A m_B}{r}\left(1 + \frac{1}{k^2 r^2}\right)\,, \tag{1.50}$$

where $G_N = k/16\pi M_*^3$ is Newton's constant, and m_A and m_B are four-

dimensional test masses separated by a distance r. In this equation, the leading term is due to the gravity zero mode, and the massive modes collectively contribute the $1/k^2r^2$ term. It is evident that, on the brane, gravity looks very much like Newtonian gravity, so long as k is large enough. Experiments have been performed to search for such deviations to gravity, and the current experimental bound for the RS2 model is $k > 1.6 \times 10^{-2}$ eV [96]. Theoretically, it is expected that k is close to the fundamental Planck scale, so it is unlikely that gravity experiments will be able to probe models with a warped metric.

A couple of the finer details of the RS2 scenario were addressed by Randall and Sundrum. It was found that the continuum gravity modes are very weakly coupled to matter on the brane, so it is rare for energy to be lost to the bulk. It was also argued that the zero mode, which extends into the extra dimension, is well isolated from the continuum modes, and so matter on the brane has very little indirect coupling to these other modes. These results, along with equation (1.50), demonstrated that the RS2 set-up — a fundamental brane in an infinite extra dimension — provided a way of realising four-dimensional gravity trapped to a subspace, a result that we will use extensively throughout this thesis. We shall now discuss some of the investigations that have followed from this discovery.

1.5.2 Beyond Randall-Sundrum

Since its inception, the Randall-Sundrum warped metric solution has found itself at the centre of a large body of research; research focusing not only on fundamental branes and string theory, but also field theoretic domain-wall brane constructions. Such studies have been numerous and cover a broad range of theoretical and phenomenological topics, ranging from the early universe, cosmology and inflation, to details of particle physics and associated model building. For general introductions to these areas, see Rubakov [97], Csáki [98] and Pérez-Lorenzana [99]. A comprehensive review of the use of D-branes in particle physics model building and cosmology can be found in Kiritsis [100].

The following sections touch briefly on a selection of this work; in particular we discuss models which use the RS metric in the context of thick branes generated by a scalar field — an idea central to this thesis. Note that references to papers will now generally be given by category, not chronology, and we will often omit names in the interest of brevity.

Fixing brane cosmology

First, let us return to the problem of cosmological expansion in brane world models, as outlined at the beginning of Section 1.5. To summarise the issue, the effective Friedmann equations have $H^2 \sim \rho^2$, in contrast to the usual case where $H^2 \sim \rho$. Guided by the RS mechanism, it was found that correct behaviour could be obtained, at least to first order, by endowing the brane with a tension which is fine tuned against a bulk cosmological constant [101, 102, 103, 104, 105, 106]. This means that one expands the brane localised energy density as $\rho = \rho_{\rm b} + \rho_{\rm s}$, where $\rho_{\rm b}$ is the brane tension (see equation (1.36)) and $\rho_{\rm s}$ is a brane-localised source (like dust or radiation). Then, assuming that the tension is much greater than the source, $\rho_{\rm b} \gg \rho_{\rm s}$, the Friedmann equation looks like $H^2 \sim (\rho_{\rm b} + \rho_{\rm s})^2 \simeq \rho_{\rm b}^2 + 2\rho_{\rm b}\rho_{\rm s}$. Putting a cosmological constant of the correct magnitude in the bulk, equation (1.35), will induce a term in the Friedmann equation that cancels $\rho_{\rm b}^2$, and one is left with the correct form $H^2 \sim \rho_{\rm s}$. See Chapter 7 for the details of this calculation, in particular Section 7.1.

Thus, by incorporating the RS idea whereby the brane has a tension and the bulk has a cosmological constant, the original analysis of brane cosmology was saved. In fact, such a cosmological analysis can be viewed as an *extension* of the RS model to include arbitrary sources on the brane, and to account for the effects of a non-Minkowski metric on the brane. Actually, the RS1 set-up has some problems in the cosmological context with a wrong-signed Friedmann equation [101], as well as stabilisation of the size of the extra dimension (the radion problem as in the ADD model), see for example Cline [107].

General RS studies

The RS warped metric was seen to have great potential as a solution to the hierarchy problem, and also provided an exciting and rich new framework for constructing models beyond the standard model. Many of the details of the RS background, as well as branes, were uncovered, and ways of improving the original RS set-up were proposed. The properties of bent (spatially curved) branes were analysed [108], and a connection between the dilaton and branes, and bulk vacuum stability was discussed [109]. Studies also focused on the general form of the effective Einstein's equations on the brane [110], the consequences of different vacuum states on either side of the brane [111],

and the reasons for having a scalar field in the five-dimensional bulk [112]. A connection between the RS scenario and the AdS/CFT correspondence[31] was also discovered, see for example the papers [114, 115, 116].

The localisation of gravity to a brane is actually a much more general phenomenon than the mechanism of the original scenario. For example, consider a brane with a large positive tension in an infinite extra dimension (RS2). In this background can be placed a second brane, with a smaller but still positive tension, to which gravity is localised *and* on which the hierarchy problem is solved [117]. It was also found that localisation of gravity to a brane is a local phenomenon which does not depend on physics far out in the bulk, and, as a consequence, the brane tension does not need to be tuned exactly against the bulk cosmological constant [118]. Furthermore, it was discovered that the fields of the standard model may not actually need to be confined to a particular brane [119, 120].

Inflation and other cosmological phenomena

A large proportion of the research into brane worlds has been in the context of cosmology, ensuring that consistent predictions are made for cosmological phenomena. As we have already seen, the usual four-dimensional Friedmann equations can be recovered in the basic RS set-up, but it is important to check the extent of such validity, for example when the finite width of the brane is taken into account [104, 121]. Other cosmological aspects of brane world models must also be checked, like inflation and gravity wave production; we will now briefly discuss such topics. For an introduction to brane world cosmology see Langlois [122], for recent reviews see [123, 124], and see Maartens [125] for a more in-depth analysis of cosmological phenomenon. A comprehensive discussion of brane inflation can be found in Tye [126].

Initial formulation of the RS set-up placed the brane(s) at fixed locations in the extra dimension, and determined the resulting warped background metric. When looking at the cosmological evolution of such a model, the background metric is generally time-dependent and can be made to expand at the location of the brane, leading to the effective Friedmann equations. It was realised quite early on that an alternative mechanism existed which yielded an expanding brane: if the background is *static* five-dimensional

[31] The AdS/CFT (Anti-de Sitter/conformal field theory) correspondence is a conjecture, made in 1997 by Juan Maldacena [113], which relates degrees of freedom between a space and its boundary.

Schwarzchild-Anti-de Sitter, then a *moving* brane samples different slices of this background metric over time, and this looks like FLRW expansion (or contraction) to brane localised observers [127, 128, 129]. These two scenarios — having a stationary brane and time-dependent bulk, or moving brane and static bulk — were shown to be equivalent and related by a coordinate transformation [130].

Implementing inflation in RS-like models has received a lot of attention, due mostly to the fact that brane worlds provide novel ways to solve some of the problems in this area. General inflating brane solutions have been found [131, 132], the issue of chaotic inflation has been discussed [133], and the use of a bulk scalar field to drive inflation has been analysed [134]. Different ways to begin and end inflation have been proposed, with brane collision and annihilation playing a significant role [135, 136, 137], and some of the usual problems related to inflation are solved in these models.

One of the main experimental signatures of events that occurred in the early stages of the universe are gravitational waves. Any theory, such as an RS based theory, that has something to say about cosmology will make certain predictions regarding the spectrum of gravitational waves that we can expect to measure. The production and evolution of such waves for brane worlds have been studied [138, 139, 140, 141, 142], and it may be possible to constrain certain RS models after measuring gravitational waves.

A very interesting result, regarding the dimensionality of spacetime, has been obtained by looking at the behaviour of many branes (a gas of branes) in multiple extra dimensions. Early studies in superstring cosmology tried to understand why, out of the nine (or ten) spatial dimensions required by the theory, we only have three seemingly infinite ones [143]. With the advent of D-branes, such a question seemed to find a plausible answer: a gas of branes of various dimensionality eventually annihilate (and possibly drive inflation), and it is natural to expect only D3-branes to survive [144, 145, 146]. There are very few theories that can give such a reason for our spacetime being four-dimensional.

Higher bulk dimensionality and intersecting branes

An obvious extension of the RS model is to have more than one extra spatial dimension. But the RS warped metric solution is particular to branes with codimension one — the bulk must have exactly one more spatial dimension

than the brane — so it is not possible to just increase the dimensionality of the bulk alone. Instead, the idea is to increase the dimensionalities of the bulk *and* brane by the same amount, place multiple branes together in the bulk, and identify our universe as the intersection of these branes [147]. For example, in a six-dimensional bulk spacetime, the intersection of two D4-branes is a three-dimensional space (along with time). Since each brane independently traps gravity, multiple branes will conspire to confine gravity to precisely their intersection.

Constructing an intersecting brane model, or a model where multiple branes meet at a vertex, is not as straightforward as placing the various branes in a bulk. The angles between the branes, their tensions, and the values of the bulk cosmological constants must obey certain relations among themselves, in order that the configuration yield a static solution for the warped metric [148, 149]. This is actually a generalisation of the fine tuning problem from the original set-up.[32]

In addition to intersecting, codimension one branes, codimension two branes have been analysed [150], interesting crystal-like configurations have been discussed [151], as have vortex-shaped defects [152, 153] and higher-dimensional extensions [154], and supergravity domain walls have been explored in multiple extra dimensions [155] and with brane junctions [156]. Nowadays, intersecting D-branes find application to string phenomenology [157, 158], where the standard model is constructed from open strings connected between branes in a specific configuration. Considering alternative topological structures for the bulk, it is possible to obtain constructions where the extra dimensions form a compact hyperbolic manifold [159, 160, 161, 162].

Stabilisation of the size of compact extra dimensions

As we discussed in the context of the ADD model, the size of the extra compact dimension in RS1, or the distance between the two branes, is actually a dynamical variable, and a mechanism is needed to ensure that this size takes an acceptable value. Goldberger and Wise proposed a solution [163] (see [164] for an alternative) which makes use of a bulk scalar field that

[32] In [148], an interesting point is raised: it seems that there is always a fine tuning relation which is independent of the angles of the brane configuration, and so such a configuration can only form dynamically (say from branes moving around, or from a set of scalar fields) if certain parameters in the theory conspire to allow it.

has different quartic potentials on the two opposite branes. After finding the background solution for this scalar field, and integrating out the extra dimension, an effective potential for the size of this dimension is obtained. The minimum of this potential is obtained only for a specific size of the extra dimension, and hence provides a stabilisation mechanism. The critical result of this mechanism is that the parameters in the potential of the bulk scalar field do not need to be fine tuned, and the hierarchy problem can be solved as per the original RS1 proposal.

A more comprehensive analysis of the Goldberger-Wise mechanism was later performed [165], along with a study of the effects of the bulk scalar on cosmology [166], and general phenomenological consequences have been determined [167]. The mechanism has found a use in many models with extra dimensions, see for example [168], and the general phenomenon of stabilisation and self-tuning has since been widely studied, for example [169, 170, 171].

Smooth and thick RS

The final topic that we will discuss, that also has its roots in the RS warped metric solution, is the use of a dynamical field to generate a domain-wall brane, in place of the fundamental branes used in the RS set-up. Quite simply, a domain-wall solution like that given by equation (1.18) has an energy density which is localised at the centre of the domain wall, and mimics the tension of a fundamental brane. From the gravity point of view, the only real difference between these two types of branes is that the domain wall is a smoothed out, or thick, version of the fundamental one. As a consequence, one is able to obtain a smoothed out version of the RS warped metric [172, 165, 173], as opposed to the sharp, or cusp-like, solution given by equation (1.34).

When constructing smooth versions of the RS scenario, it is common to use a scalar field to generate the domain-wall brane. In such a situation, it is important to not only obtain an analogue of the warped metric, but to also make sure that a four-dimensional massless gravity mode is localised to the domain wall, and that corrections to gravity, due to massive modes, are small. This was found to be the case [174], and we will rely heavily on these results in this thesis. For an explicit form of a smoothed warped metric solution, the scalar field domain-wall solution and the associated po-

tential, see Section 4.4. It is interesting that, when using a five-dimensional scalar field to generate the domain wall, a wider class of metric solutions exist. This is due to the existence of a matter field in the bulk, leading to new metric solutions which can differ from the usual scenario where the bulk contains only a cosmological constant; for example, there can be bulk singularities [175].

The thick domain-wall brane produced by a scalar field, and the associated smooth warped metric, in general form a family of solutions, parameterised by the thickness, or width, of the domain wall; for the domain wall described by equation (1.18), this width is $l = (v\sqrt{\lambda/2})^{-1}$. One would therefore expect to be able to take a controlled limit, which includes $l \to 0$, and which recovers the sharp RS warped metric. This is indeed the case; see for example [165], and also [176, 177] for related analyses. See [178] for a detailed discussion of the validity of distributional sources in general relativity. We will discuss such limiting behaviour in Chapter 3, where we perform a rigorous analysis of the thin kink limit, and the effect of this limit on coupled scalars and fermions. In this chapter we also discuss the zero mode of the domain wall — the massless Nambu-Goldstone boson associated with zero-energy-cost translations of the kink. It is important to understand the dynamics of this Nambu-Goldstone boson, because it is the lightest, and hence most accessible, mode associated with the domain wall, and it may couple to gravity in a non-trivial way [179].

A fundamental brane, a D-brane, can localise matter and gauge fields by the stringy mechanism whereby open strings end on the brane. For domain-wall branes, this problem must be solved in a different way, and we have already discussed the basic mechanisms for fermion and gauge field localisation, although not in the presence of gravity. Gravity alone does actually have the ability to trap scalar fields (see Section 4.3), but not fermions, and fermion localisation, inspired by the original mechanism due to Rubakov and Shaposhnikov, has received much attention [180, 181, 182, 183, 184, 185]. To first order, massless chiral fermions are localised to the brane, but, since we measure massive particles in our universe, the localised fermions must obtain a small mass, possibly via a localised Higgs field. Whatever the mechanism used to endow mass, in the presence of a warped metric, such localised massive particles have a non-zero probability of escaping into the bulk [186, 187]. We discuss effects related to this phenomena in Chapter 4.

Many other analyses related to thick domain-wall brane worlds have been performed. These include general localisation mechanisms [188], gravity trapping [189, 190], issues related to quantisation of localised fields [191], colliding domain-walls [192, 193, 194, 195, 196], model building [197], and generating the domain-wall using a field with a non-standard kinetic term [198]. Scalar fields are also used to generate domain walls in models with supergravity and extra dimensions, see for example [155, 156]. And there is certainly much that we have yet to discover in this rich and diverse niche of particle physics.

1.5.3 Summary of Randall-Sundrum

The Randall-Sundrum scenario is a very simple and elegant model which has two profound consequences: it provides a solution to the hierarchy problem, and opens up the possibility of having extra dimensions which are infinite in size. The set-up consists of fundamental branes, with non-zero tensions, placed in a bulk with a cosmological constant. The solution for the bulk gravitational metric is a slice of AdS_5, a warped metric, which traps gravity to the branes, and which can provide an exponential suppressing factor in effective four-dimensional terms without the use of any unnaturally large numbers. An immense amount of work has been inspired by the warped metric solution since its discovery, ranging from inflation in cosmology, through string-inspired model building with intersecting branes, to use in field theoretic model building with thick domain walls. In this thesis, we use the RS warped metric solution exclusively to trap gravity, and build upon such a gravitational background to produce a brane-localised standard model.

1.6 Overview of the thesis

Beginning with Nordström's attempt at unifying electromagnetism with scalar, relativistic gravity, we have traced the history of theoretical high-energy physics, focusing on those aspects that are most relevant to this thesis. Indeed, we will exploit many of the ideas and mechanisms which have been discussed: extra dimensions, Abelian and non-Abelian gauge theories, dynamical symmetry breaking, Nambu-Goldstone bosons, the Higgs mechanism, asymptotic freedom, the standard model of particle physics including the strong and electroweak forces, grand unification in the form of

SU(5) and E_6, domain walls, chiral fermion localisation, the Dvali-Shifman mechanism for gauge field localisation, the FLRW metric ansatz and the expansion of the universe, and the Randall-Sundrum warped metric.

From this rich and diverse history has emerged the standard model itself — a magnificent achievement with contributions from many, and which makes predictions of unsurpassed accuracy. But, as we have pointed out, there are still many unresolved issues in the field of high-energy physics, and research will continue with the aim of improving even further our understanding of nature at its most fundamental level. The latter part of our historical overview focused on one such particular direction that has seen a great amount of recent activity: brane world models of extra dimensions. It is in the spirit of such activity that this thesis finds its roots.

We are particularly motivated by the ability of extra dimensions to provide a different perspective on current problems, and hope that new insight can be gained by studying brane world models. In the area of brane worlds, we see as one of the more outstanding challenges the need to construct a complete field-theoretic version of the standard model confined to a domain-wall brane. This is to be contrasted to the string theory inspired models where the brane is a D-brane, and the true dynamics of the theory can only be resolved by an appeal to string theory. We would like to be able to describe not only the dynamics of the brane, and the formation of the domain-wall on which our universe resides, but also the mechanisms by which the matter and gauge fields are confined. Of course, we still expect our hypothetical domain-wall brane model to be embedded in some higher theory, but, by describing all elements of our model using standard field theory, we will have made a relatively conservative extension of current, well tested models. Besides this, it is interesting to see if it can be done at all — if one can write down a consistent, extra-dimensional extension of the standard model that makes testable predictions for collider experiments of the near future, then one is doing honest theoretical physics.

So that is the aim of this thesis: to consider, in the context of field theory, all the aspects related to extending the standard model to include an additional, infinite, spatial dimension. We will use a domain-wall brane, generated by a scalar field which dynamically breaks a symmetry, to ensure that gravity, gauge and matter degrees of freedom are reduced, at low energies, to four spacetime dimensions. We will construct such a model and

analyse some of its important phenomenology, including basic cosmological predictions. It is hoped that our work here can provide the foundations for a full phenomenological treatment of the model that we present, and further hope that our pointers to possible improvements can be followed. We will now outline the structure of the rest of the thesis, and the particular content of each chapter.

In Chapter 2 we examine a toy model where a pair of scalar fields, charged under a $\mathrm{U}(1) \otimes \mathrm{U}(1)$ gauge symmetry, form a background domain-wall configuration. The gauge fields themselves have a non-zero background configuration in the presence of this domain wall, and their form corresponds to semi-confinement of gauge fields. We introduce the perturbative stability analysis technique, find that the normal modes of the configuration have non-negative eigenvalues, and hence conclude that the domain wall is stable. Gravity is incorporated into the model and a smooth version of the Randall-Sundrum warped metric solution is obtained, coupled to the domain wall. In this later scenario, it seems that the background solution for the gauge fields must be identically zero.

Returning to the simplest case of generating a domain-wall brane using a single real scalar field, we show in detail in Chapter 3 how the wall is obtained, and determine its relationship to the fundamental brane in the infinitely thin wall limit. Explicit expressions for the full spectrum of modes of such a domain wall are found, corresponding to the zero mode of translation and to the massive modes which deform the background kink solution. The symmetric modified Pöschl-Teller potential arises in this context, and the behaviour of the zero mode in the thin kink limit is explored. We couple both fermions and scalars to the domain wall, determine their mode spectrum and discuss how this spectrum looks in the thin kink limit. These analyses demonstrate explicitly how a five-dimensional field can be dimensionally reduced to a tower of effective four-dimensional modes.

We add gravity to our domain-wall brane model in Chapter 4, obtain the Randall-Sundrum warped metric solution, and analyse how this affects the spectrum of localised fermions and scalars. It turns out that gravity induces a continuum in the four-dimensional spectrum, where originally there would have been a mass gap between discrete modes. Physically, this means that trapped low-energy modes, corresponding perhaps to standard model fields, have a non-zero coupling to continuum bulk modes. Using a simple toy

model, we determine the strength of such a coupling, and find that it can be made small enough to avoid experimental constraints.

Building on the techniques which trap gravity, fermions and scalars to a domain-wall brane, and using the Dvali-Shifman mechanism for gauge field localisation, we construct an SU(5) grand unified, single-generation version of the standard model in Chapter 5. In addition to the usual standard model field content, two auxiliary scalar fields are required to generate the domain wall and implement the Dvali-Shifman mechanism. The couplings between these scalars and the fermions induces a split-fermion effect, which allows the model to escape some of the usual problems with SU(5) theories. In particular, the unrealistic fermion mass relation no longer holds, and Higgs induced proton decay can be suppressed by ensuring a small overlap between relevant fields. An extension of this model to larger gauge groups is considered in Chapter 6. We find that the Dvali-Shifman mechanism is not well suited to SO(10), and instead use E_6 in combination with the clash-of-symmetries mechanism. In such a set-up, the field content for the scalar sector can be simplified, and only one fermion multiplet is needed, as opposed to two in the SU(5) model.

Having dealt with the particle physics and core model building aspects, we move on to investigate cosmological implications of domain-wall brane models in Chapter 7. The analysis for the fundamental brane scenario is extended to the thick brane case, and we attempt to reproduce an effective four-dimensional FLRW metric for the fields localised to the domain wall. For a wall of finite thickness, we find that it is not possible to define a common spacetime for all localised species of matter, and, as a consequence, different species experience a different effective four-dimensional scale factor. This is certainly an unusual effect, and it is potentially at odds with observation, but we leave a full phenomenological analysis to future work. Instead, we show that by making the domain wall thin enough, this unusual effect can be suppressed, and we are able to recover the cosmology of a fundamental brane in the limit that the domain wall is infinitely thin.

We draw our conclusions in Chapter 8 and summarise the results that are obtain throughout the course of this thesis. The issues that remain outstanding are discussed, and we point to studies that would be of interest to perform in the future. We conclude that domain-wall brane models of an infinite extra dimension are viable extensions of the standard models of particle physics and cosmology.

Chapter 2

The U(1) ⊗ U(1) toy model

Let us first put aside the ambitious idea of building a domain-wall confined standard model, and play with a toy model which shall allow us to develop some general techniques for extra-dimensional model building. The toy model that we will be using is a slight generalisation of a model put forward by Rozowsky, Volkas and Wali [199]. These authors were interested in two ideas: the clash-of-symmetries mechanism and localising gauge fields to kink solutions. Briefly, the clash-of-symmetries mechanism (see [39, 200, 201, 202], and also [203, 204, 205]) takes a symmetry group G (with independent continuous and discrete symmetries) which contains two or more isomorphic, but differently embedded, subgroups H_i. If G is broken to each H_i in different regions of space, then at the intersection of these regions, G is generally broken to the intersection of the H_i. Kink solutions find a natural place in this mechanism, as they interpolate between the differently broken vacua.

The toy model that we are going to study in this chapter is inspired by the clash-of-symmetries mechanism, with the symmetry group being

$$G = \mathrm{U}(1) \otimes \mathrm{U}(1) \otimes \mathbb{Z}_2 \,, \tag{2.1}$$

where the two U(1)'s are local gauge symmetries. We will refer to this model as the U(1) ⊗ U(1) model. Its field content consists of the gauge fields, A_1^M and A_2^M, and a pair of scalar fields, ϕ_1 and ϕ_2, charged under the gauge symmetries. The discrete groups acts as an interchange symmetry: $\phi_1 \leftrightarrow \phi_2$ and $A_1^M \leftrightarrow A_2^M$. Although the original toy model studied by Rozowsky et al. lived in a four-dimensional spacetime, the extension we make here to

five-dimensions (which has also been made in [202]) requires very little in the way of modifications. Our main aim in this chapter is to study the stability of kink solutions that one can obtain in this toy model, and the clash-of-symmetries mechanism serves only to inspire such kink solutions. A more sophisticated use of the mechanism is explored in Chapter 6, where we consider an E_6 model breaking to differently embedded SO(10)'s, and we shall discuss more details regarding the clash-of-symmetries there.

Of critical importance for any domain-wall brane model is the stability of the underlying wall itself. In general, the domain-wall configurations that we consider are time-independent solutions to the classical equations of motion. For example, this is true of the kink solution $\phi_{\rm DW}$ given by equation (1.18). Consider a set of fields $\chi_i(t,\vec{x})$ and a time-independent background configuration formed by these fields: $\chi_i^{\rm BG}(\vec{x})$. Now, take small perturbations $\delta_i(\vec{x})$ and set the initial conditions for the fields $\chi_i = \chi_i^{\rm BG} + \delta_i$. The fields χ_i will then evolve over time, but, if the solutions $\chi_i^{\rm BG}$ are stable, then χ_i will remain within a bounded "distance" of the time-independent solutions. Equivalently, the energy density of the stable configuration $\chi_i^{\rm BG}$ is at a local (or possibly global) minimum of all possible configurations. It is important to consider stability because we shall be interested in coupling other fields to the domain-wall background configuration, and excitations of these coupled fields will act to perturb the wall. Furthermore, in a quantum theory, the fields forming the domain-wall will naturally fluctuate, and the configuration must be resistant to such fluctuations.

In certain cases, it is possible to argue for or against stability using topological arguments. In the case of the canonical kink solution $\phi_{\rm DW}$, the associated potential (1.16) has degenerate minima at $\pm v$ which are topologically *disconnected*, meaning that there are no continuous transformations which can be applied to go from one minimum to the other. Thus, by using these two values as opposing boundary conditions, the resulting kink solution $\phi_{\rm DW}$ cannot be transformed into any other topologically distinct solution, such as $\phi = v$, by any finite-energy perturbation. The energy of this configuration is a global minimum for the topological class that it belongs to, and it cannot, in a sense, be "undone". For more complicated models, such as the toy model we study in this chapter where the domain-wall is formed by two scalar fields, it can be difficult to find a topological argument for stability. Instead, one can use the very general method of

linear perturbative stability analysis. Here, the normal modes of perturbations of the time-independent solutions are determined, and, if all such modes are bounded in their time-evolution, the corresponding background solutions are perturbatively, or locally, stable.

We have already discussed at length the confinement of gauge fields to domain walls using the Dvali-Shifman mechanism; see Section 1.3.3. This mechanism relies on non-perturbative aspects of non-Abelian gauge theories, and it is difficult to make quantitative statements about the modes of the gauge fields in models that rely on this mechanism. It would be advantageous to have a gauge-field localisation mechanism which was more tractable, and which could be analysed in a similar way to the localisation of fermions to a kink, as discussed in Section 1.3.1. These considerations were, as we briefly mentioned, part of the reason Rozowsky et al. wanted to study kink solutions in the $\mathrm{U}(1) \otimes \mathrm{U}(1)$ toy model, where gauge fields are naturally coupled to the scalar fields responsible for setting up the kink. Unfortunately, this simple idea does not allow for gauge field localisation: the solutions for the gauge fields have linearly rising gauge potential on one side of the domain wall, and Meissner suppression on the other, leading to semi-confinement of the associated fields. Nevertheless, this toy model is still a useful theoretical tool for understanding perturbative stability, as well as confinement of gravity using a smooth version of the Randall-Sundrum warped metric, and these are the topic we shall work through in this chapter.

In Section 2.1 we present the details of the $\mathrm{U}(1) \otimes \mathrm{U}(1)$ model, slightly generalised from that originally studied by Rozowsky et al., and display the time-independent solutions for light- and space-like gauge fields. The stability analysis method that we are going to use is outlined in Section 2.2, followed by a full investigation demonstrating the perturbative stability of the background scalar-gauge kink configuration. In Section 2.3 we extend the model to include gravity, inspired by the Randall-Sundrum set-up, and find coupled gravity-domain-wall solutions which, unfortunately, seem to require the background gauge fields to vanish. We give a summary of the chapter in Section 2.4.

2.1 The model and its kink solutions

The toy model studied here has symmetry group G given by equation (2.1), a pair of five-dimensional gauge fields A_i^M ($i = 1, 2$ and $M = t, x, y, z, w$) and

a pair of charged five-dimensional scalar fields ϕ_i. The discrete symmetry acts by interchanging the fields: $\phi_1 \leftrightarrow \phi_2$ and $A_1^M \leftrightarrow A_2^M$. The extension to five-dimensions, first made in [202], is a minor modification of the original model studied by Rozowsky et al. The model features a quartic scalar potential, coupling the scalar fields to each other, and permits domain-wall solutions which asymptote to different degenerate minima of the potential. The action is

$$\mathcal{S} = \int d^5x \, \mathcal{L} \,, \tag{2.2}$$

with Lagrangian density given by

$$\begin{aligned} \mathcal{L} = &-\frac{1}{4} F_1^{MN} F_{1MN} - \frac{1}{4} F_2^{MN} F_{2MN} \\ &+ (D^M \phi_1)^* D_M \phi_1 + (D^M \phi_2)^* D_M \phi_2 - V(\phi_1, \phi_2) \,. \end{aligned} \tag{2.3}$$

The metric is Minkowski spacetime, $\eta_{MN} = \mathrm{diag}(+1, -1, -1, -1, -1)$, the field strength tensor is defined as usual, $F_{iMN} = \partial_M A_{iN} - \partial_N A_{iM}$, and the covariant derivative is

$$D_M = \partial_M - iQ_1 A_{1M} - iQ_2 A_{2M} \,. \tag{2.4}$$

Here, Q_1 and Q_2 are the charge operators associated with the two U(1) gauge groups. Respecting the discrete $\mathbb{Z}_2$ interchange symmetry, the charges of the scalar fields under U(1) ⊗ U(1) are

$$\phi_1 \sim (e, \tilde{e}) \qquad \text{and} \qquad \phi_2 \sim (\tilde{e}, e) \,, \tag{2.5}$$

with e and $\tilde{e}$ constants. The Rozowsky et al. model took $\tilde{e} = 0$, so this is a slight generalisation, which was first introduced in [202]. The quartic potential, which must also respect the discrete symmetry, is

$$V(\phi_1, \phi_2) = \lambda_1 (\phi_1^* \phi_1 + \phi_2^* \phi_2 - v^2)^2 + \lambda_2 \phi_1^* \phi_1 \phi_2^* \phi_2 \,. \tag{2.6}$$

We work in the $\lambda_{1,2} > 0$ parameter regime, where the degenerate global minima are manifestly given by

$$|\phi_1| = v \,, \quad \phi_2 = 0 \qquad \text{and} \qquad \phi_1 = 0 \,, \quad |\phi_2| = v \,. \tag{2.7}$$

The Euler-Lagrange equations of motion for the scalar and gauge fields

are

$$D^M D_M \phi_i = -2\lambda_1 \phi_i \left(\phi_i^* \phi_i + \phi_j^* \phi_j - v^2\right) - \lambda_2 \phi_i \phi_j^* \phi_j \,, \tag{2.8a}$$

$$\partial_N F_i^{NM} = 2\,\mathrm{Im}\left(e\phi_i^* D^M \phi_i + \tilde{e}\phi_j^* D^M \phi_j\right) \,, \tag{2.8b}$$

where $i = 1$ and $j = 2$, or $i = 2$ and $j = 1$ (this notation is to be understood in subsequent equations, and, in particular, the summation convention for repeated i, j indices does not hold). With the intention of finding time-independent, domain-wall-like solutions to these equations of motion, we assume that all fields depend only on the extra-dimension w. Following Rozowsky et al., we also utilise a polar decomposition for the scalar fields: $\phi_i(w) = R_i(w)e^{i\Theta_i(w)}$. The boundary conditions that are imposed on the scalar fields should be compatible with the minima of the potential, given by the set of equations (2.7). Since we are taking the ϕ_i to depend only on w, we must choose some combination of these minima for the boundary conditions as $w \to \pm\infty$. The choice that allows for domain-wall solutions is

$$\begin{aligned} |\phi_1| = R_1 \to 0 \,, \quad |\phi_2| = R_2 \to v \quad \text{as} \quad w \to -\infty \,, \\ |\phi_1| = R_1 \to v \,, \quad |\phi_2| = R_2 \to 0 \quad \text{as} \quad w \to \infty \,, \end{aligned} \tag{2.9}$$

or vice-versa.

Since we are working with two gauge fields we have the freedom to choose two gauges, one for each A_i^M; the Lorentz gauge $\partial_M A_i^M = 0$ turns out to be the most suitable choice for both. The algebra also simplifies further if, instead of A_i^M, one considers the linear combination $\mathcal{A}_i^M = eA_i^M + \tilde{e}A_j^M$. Working with these choices, the field equations of motion given by (2.8) reduce to

$$R_i'' = -R_i \eta_{\mu\nu} \mathcal{A}_i^\mu \mathcal{A}_i^\nu + 2\lambda_1 R_i (R_i^2 + R_j^2 - v^2) + \lambda_2 R_i R_j^2 \,, \tag{2.10a}$$

$$\mathcal{A}_i^{\mu\prime\prime} = 2(e^2 + \tilde{e}^2) R_i^2 \mathcal{A}_i^\mu + 4e\tilde{e} R_j^2 \mathcal{A}_j^\mu \,, \tag{2.10b}$$

$$\mathcal{A}_i^{w\prime} = 0 \,, \tag{2.10c}$$

$$\Theta_i' = -\mathcal{A}_i^w \,, \tag{2.10d}$$

where prime denotes differentiation with respect to w, and μ, ν index t, x, y, z. We immediately see from equation (2.10c) that the $\mathcal{A}_i^w$, and hence the A_i^w, are pure gauge and do not contribute to the physics; neither do the Θ_i.

To further simplify the problem, we note that each gauge component

$\mathcal{A}_i^\mu$ exhibits the same dynamics in equation (2.10b) and appears otherwise only as part of the four-Lorentz scalar $s = \eta_{\mu\nu}\mathcal{A}_i^\mu\mathcal{A}_i^\nu$ in equation (2.10a). Thus, the qualitative physical behaviour depends on whether the gauge field configuration is space-like, light-like or time-like, corresponding respectively to $s < 0$, $s = 0$ or $s > 0$. Expressing this behaviour as the single field $\mathcal{A}_i$ we have

$$R_i'' = kR_i\mathcal{A}_i^2 + 2\lambda_1 R_i(R_i^2 + R_j^2 - v^2) + \lambda_2 R_i R_j^2 \,, \tag{2.11a}$$

$$\mathcal{A}_i'' = 2(e^2 + \tilde{e}^2)R_i^2\mathcal{A}_i + 4e\tilde{e}R_j^2\mathcal{A}_j \,, \tag{2.11b}$$

where $k = +1,\ 0,\ -1$ for space, light- and time-like gauge fields respectively. One can see that equation (2.11a) is consistent with the boundary conditions (2.9) so long as $k \geq 0$. For $k = -1$ the asymptotic behaviour of R_i is oscillatory and so we discard this time-like scenario.

Now that we have equations (2.11a) and (2.11b) in hand, we proceed to solve them, given the boundary conditions (2.9) for the R_i. In general, these equations cannot be solved analytically and we shall resort to numerics, but before we do that, let us make some remarks regarding the asymptotic behaviour of the gauge fields. If we consider equation (2.11b) with $i = 1$ and $j = 2$ and on the right side of the wall, where $w \to \infty$, $R_1 \to v$ and $R_2 \to 0$, we see that $\mathcal{A}_1'' \to 2(e^2 + \tilde{e}^2)v^2\mathcal{A}_1$, which has two solutions: an exponentially growing and exponentially decaying one. Although all measurable quantities associated with the A_i^M, such as the electric and magnetic field, arise through derivatives, the exponentially growing solution still has a derivative which grows exponentially, so we conclude that $\mathcal{A}_1$ is exponentially suppressed on the right side of the wall. Then, taking $i = 2$ and $j = 1$ in equation (2.11b), we see that $\mathcal{A}_2'' \to 0$ on this same side of the domain wall; we have used the previous result $\mathcal{A}_1 \to 0$ to obtain this condition. As we mentioned, physical quantities are computed through derivatives of A_i^M, so we are able to have $\mathcal{A}_2$ asymptoting to a general linear form — an unbounded, but physical, solution. For the other side of the wall, the conditions are interchanged: $R_1 \to 0$, $R_2 \to v$, $\mathcal{A}_2 \to 0$ and $\mathcal{A}_1$ takes a linear form.

Moving on to calculate the actual solutions, we make use of the numerical relaxation-on-a-mesh technique. Here, a function $f(w)$ is approximated by a piece-wise linear function, which is equivalent to sampling discrete values of f at fixed mesh points, and computing derivatives us-

ing difference equations. For the case at hand, the differential equations look like $f''(w) = D(w)$, where $D(w)$ contains functions evaluated at w, but no derivatives. We can turn this differential equation into the difference equation $\frac{1}{h^2}[f(w+h) - 2f(w) + f(w-h)] = D(w)$, where h is the spacing between mesh points. This equation is rearranged to obtain $f(w) = \frac{1}{2}[f(w+h) + f(w-h) - h^2 D(w)]$, which is the central equation of the numerical technique. For small h, one computes $f(w)$ as the average of its neighbouring mesh points, corrected by some small amount proportional to $D(w)$. Such a computation is done for each mesh point (using old values of the mesh) which constitutes a single iteration, and these new values are used to seed the next iteration, which continues until certain convergence criteria are reached. For solving multiple, coupled functions, it is enough to interleave the individual iterations for each function. Usually, one must dampen the iterations by taking a weighted average of the old mesh points and the new ones, but, in general, this simple relaxation technique works well, and performs efficiently enough. See Appendix B and "Numerical Recipes in C" [206] for further details.

Using this numerical technique, we consider the light-like case first, where $k = 0$. Here, the equations (2.11a) and (2.11b) semi-decouple, and the R_i can be solved for independently of the $\mathcal{A}_i$. Typical solutions are shown in the top two plots in Figure 2.1. The scalar fields assume a typical domain-wall configuration asymptoting to distinct minima of the potential. As the boundary conditions for the R_i are symmetric under w reflection, the solutions for these scalar fields are just reflections of each other. In the left plot, the boundary conditions for the two gauge fields are also reflection symmetric. In the right plot, a different boundary condition is used for $\mathcal{A}_2$. As the scalar fields do not feel the presence of the gauge fields, due to the light-like nature of the latter, the domain wall has exactly the same solution in both of these plots.

For the space-like case, $k = 1$, and the scalar and gauge fields are fully coupled. Solutions are shown in the bottom two plots in Figure 2.1 with all parameters, except k, mimicking the top two plots. Although they look similar, the light- and space-like plots on the left are slightly different. A more significant difference between these two scenarios is evident in the right plots where the boundary conditions for the two gauge fields are different. In the space-like case the scalar fields are influenced by the gauge fields and

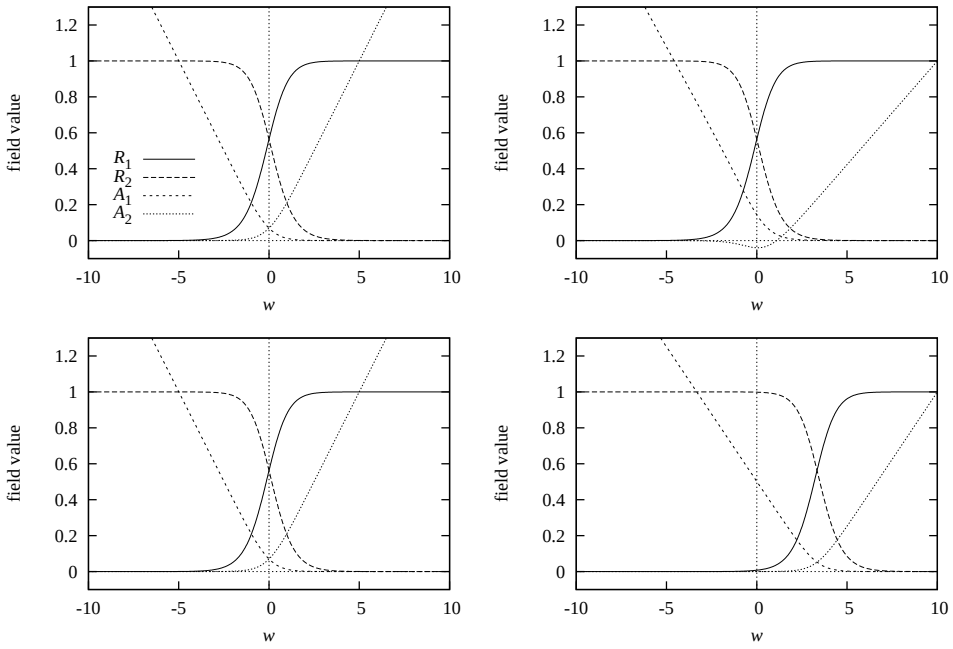

Figure 2.1: Time-independent domain-wall solutions for the two scalar and two gauge fields in the U(1) ⊗ U(1) model, plotted against the extra-dimension w. The top two plots are for the light-like case, the bottom two for the space-like case. All plots have $e = 1$, $\tilde{e} = \frac{1}{2}$, $\lambda_1 = 1$, $\lambda_2 = 2$ and $v = 1$. The plots on the left have symmetric boundary conditions for the gauge fields, those on the right asymmetric. In the light-like case, the scalar fields do not feel the gauge fields and thus do not depend on the choice of gauge field boundary conditions. This is unlike the space-like case where the scalar fields centre on the gauge fields to restore the reflection symmetry.

the favourable configuration is that with exact reflection symmetry. The boundary conditions serve to simply shift the centre of the domain wall, and the right plot on the bottom is an exact translation of the left plot. Our result is contrary to the claim by Rozowsky et al. that asymmetric boundary conditions in the space-like case are not equivalent to spatial translations of the domain-wall centre.

Disregarding the technical details, there are two important qualitative features of the solutions presented here for the U(1) ⊗ U(1) model: the reflection symmetric scalar fields which form a domain-wall configuration, and the partially suppressed gauge fields. This suppression of $\mathcal{A}_1$ under R_1, and $\mathcal{A}_2$ under R_2, is physically similar to the Meissner effect and serves to semi-localise the gauge fields. We make the physical interpretation of an infinite sheet of supercurrent confined to the wall, producing a constant

magnetic field in the region opposite the suppression.

While we have shown the existence of time-independent solutions that depend only on the extra-dimensional coordinate, we have not established their stability. In the next section we demonstrate that under small perturbations, the solutions to equations (2.11a) and (2.11b) are in fact stable.

2.2 Stability of the background configuration

The essence of the background solutions that we have found is their time independence, but, as part of a world that evolves over time, the fields that produce such a background will also evolve. We must thus ensure that the domain-wall configurations found in the previous section are not destroyed by time-dependent perturbations. As discussed earlier, a background χ_i^{BG} is stable if, given the initial conditions where small perturbations δ_i are added to the background, the evolution of such a state remains within a bounded distance of the original time-independent background. To determine such behaviour, the time-dependent fields $\chi_i(t, \vec{x})$ are expanded as the background $\chi_i(\vec{x})$ plus the normal mode $c(\vec{x})e^{i\omega t}$, and the Euler-Lagrange equations of motion are used to obtain a equation to solve for the mode eigenvalue ω (and the eigenfunction $c(\vec{x})$ if necessary). Because we are interested in small perturbations, only the terms linear in $c(\vec{x})$ are kept, hence this method determines perturbative, or local, stability. The background configuration χ_i^{BG} is then perturbatively stable if all allowed eigenvalues ω are real, because in such a case, all perturbations oscillate around the background solution.

In this section we shall apply such a technique to show that the domain-wall configuration presented in the previous section is perturbatively stable. We begin by taking the time-independent background solution for each field, including the five gauge components as part of the more convenient $\mathcal{A}_i^M$, and adding a perturbation factored as a normal mode described above. The expansion is thus

$$R_i(t, \vec{x}, w) = R_i^{\mathrm{BG}}(w) + r_i(w)e^{i\omega_r t}\,, \tag{2.12a}$$

$$\mathcal{A}_i^M(t, \vec{x}, w) = \mathcal{A}_i^{\mathrm{BG},M}(w) + a_i^M(w)e^{i\omega_a t}\,, \tag{2.12b}$$

$$\Theta_i(t, \vec{x}, w) = \Theta_i^{\mathrm{BG}}(w) + \theta_i(w)e^{i\omega_\theta t}\,, \tag{2.12c}$$

where $\vec{x} = (x, y, z)$. To eliminate clutter in the following equations, we shall omit the superscript BG for the background solutions. By the choice of an explicitly complex exponential, if the mode eigenvalue ω has solutions which are purely real, then the perturbation will be oscillatory and hence remain bounded in time. On the other hand, if any of the solutions for ω have an imaginary component, the exponential will blow up, signifying instability of the original time-independent solution.

We take the original field equations (2.8), make the substitutions given by (2.12) and simplify using the fact that the background fields satisfy equations (2.10). We work to first order in r_i, a_i^M and θ_i, and consider only independent perturbations,[1] which decouples the resulting set of equations to give

$$\left[-\partial_w^2 - \eta_{\mu\nu}\mathcal{A}_i^\mu\mathcal{A}_i^\nu + 2\lambda_1(3R_i^2 + R_j^2 - v^2) + \lambda_2 R_j^2\right] r_i = \omega_r^2 r_i \,, \tag{2.13a}$$

$$\left[-\partial_w^2 + 2(e^2 + \tilde{e}^2)R_i^2\right] a_i^M = \omega_a^2 a_i^M \,, \tag{2.13b}$$

$$\left[-\partial_w^2 - 2\frac{R_i'}{R_i}\partial_w\right] \theta_i = \omega_\theta^2 \theta_i \,. \tag{2.13c}$$

Here, the $\mathcal{A}_i^\mu$ and the R_i are the background domain-wall solutions, and we are going to need to substitute their numerical form, as found in the previous section. Note that, as before, equation (2.13b) has the same form for all of the gauge field perturbations a_i^M, and the gauge field background only appears as the four-Lorentz scalar in equation (2.13a). Thus, we shall analyse the light- and space-like scenarios separately.

Before we continue with these equations, we shall first establish a general result which will help determine the spectrum of eigenvalues for our normal modes. Given the equation

$$f''(w) + V(w)f'(w) + W(w)f(w) = 0 \,, \tag{2.14}$$

one can show that if $W(w) < 0$ for all w, then there exist no non-trivial solutions for $f(w)$ on the domain $w \in \mathbb{R}$ with $f(w) \to 0$ as $|w| \to \infty$. To

[1] By independent we mean that only one of r_i, a_i^M or θ_i are non-zero at any one time. It is possible to generalise the method to include coupled perturbations, where the eigenfunction becomes the vector $\mathbf{b}_i = (r_i, a_i^M, \theta_i)$, and the differential equation becomes the matrix-differential equation $\mathbf{M} \cdot \mathbf{b}_i = \Omega^2 \mathbf{b}_i$. The solutions for the eigenvalue Ω now correspond to both coupled and non-coupled modes. We do not perform such a generalised analysis here.

see this, consider large $-w$ with f taking a vanishingly small positive value. For non-trivial solutions, f must increase as w increases[2] and so $f' > 0$. For solutions where f becomes vanishingly small for large w, we require $f' < 0$ for some subsequent region of the w-axis. This change in the sign of the first derivative requires $f'' < 0$ for some region, in particular we must have $f'' < 0$ when $f' = 0$, i.e. at the turning point. But at this point we have $f'' = -W(w)f$ and since $f > 0$ and $W(w) < 0$ for all w, we have $f'' > 0$. Thus the function is positive with a positive gradient and can never turn back towards the w-axis. A similar argument holds when f is below the axis; it can never turn back up. Hence there are no non-trivial bounded solutions if $W(w) < 0$ for all w.

There is an alternative way of seeing this result, which relies on our experience solving Schrödinger-like equations. First, assume we have $V(w) = 0$ (which is actually the case for our equations (2.13a) and (2.13b)). Then equation (2.14) looks like a Schrödinger equation with potential $-W(w)$ and energy equal to zero. If the potential is positive for all w, that is $W(w) < 0$, then there will be no bounded solution; the potential must drop below zero for there to be a chance of a zero-energy solution. This is the result established in the previous paragraph. We can relax the assumption that $V(w) = 0$ by noting that, via a change of variables $d\tilde{w} = \Lambda(w)\, dw$ with suitable $\Lambda(w)$, one can eliminate the $V(w)f'(w)$ term in equation (2.14) and obtain a Schrödinger-like equation.

Now that we have established such a result, we return to the issue of stability. Consider equation (2.13c) with $f(w) = \theta_i(w)$ and $W(w) = \omega_\theta^2$. If $\omega_\theta^2 < 0$ then one would have $W(w) < 0$ for all w and, by the previous result, the only solution for θ_i would be the trivial one. Thus there are no negative eigenvalues for equation (2.13c) with bounded eigenfunctions θ_i. Note that the condition that the eigenfunctions θ_i be bounded does not imply that we are only accepting perturbations which are bounded. The perturbation to the background field is given in full by $\theta_i(w)e^{i\omega_\theta t}$ where, by definition of a perturbation, the $\theta_i(w)$ factor must be small and bounded. It is the nature of the temporal part $e^{i\omega_\theta t}$, and hence the eigenvalue ω_θ, that determines stability, since if solutions exist with ω_θ imaginary, then the perturbations grow exponentially over time, even though the eigenfunction $\theta_i(w)$ is bounded.

[2]Since $f(-\infty) = 0$ there must be a region where f increases if it is to attain a finite positive value.

We have shown that $\omega_\theta^2 \geq 0$ and so ω_θ is real, thus the perturbations are oscillatory, and $\Theta_i(w)$ is a stable background configuration.

For the gauge fields, inspection of equation (2.13b) yields

$$W(w) = \omega_a^2 - 2(e^2 + \tilde{e}^2)R_i^2 \,. \tag{2.15}$$

For bounded $a_i^M(w)$ we require $W(w) \geq 0$ for some non-zero domain of w. This means that we need

$$\omega_a^2 \geq 2(e^2 + \tilde{e}^2)R_i^2 \tag{2.16}$$

for some w. Since ω_a^2 is a constant it must be greater than or equal to the minimum of $2(e^2 + \tilde{e}^2)R_i^2$, hence it is non-negative. Thus we have shown that the time-independent gauge field configuration is stable under small time-dependent perturbations.

Following a similar argument, we look at the scalar fields R_i, and equation (2.13a) gives a bound on the eigenvalues:

$$\omega_r^2 \geq \min(U(w)) \,, \tag{2.17}$$

where

$$U(w) = -\eta_{\mu\nu}\mathcal{A}_i^\mu \mathcal{A}_i^\nu + 2\lambda_1(3R_i^2 + R_j^2 - v^2) + \lambda_2 R_j^2 \,. \tag{2.18}$$

It is not so clear as to the sign of this function. We analyse the light-like case first where the $\mathcal{A}_i^\mu$ terms are absent. In this case, as can be seen from equation (2.11a) with $k = 0$, the scalar field configuration, and hence $U(w)$, depend only on the parameters λ_1, λ_2 and v. Since v can be absorbed into a rescaling of the R_i, we only have two parameters to consider. A typical plot of the function $U(w)$ for the two permutations of i and j is shown on the left in Figure 2.2.

We see that $U(w) > 0$ for this particular choice of parameters, and so the eigenvalues are all positive in this case. Figure 2.3 shows the minimum of $U(w)$ for a large range of values of λ_1 and λ_2. Since all minima are positive, it must be that $\omega_r^2 > 0$ and hence the background scalar field solutions in the light-like case are stable, at least for this range of parameters.

For the space-like scenario the results are similar. The plot on the right in Figure 2.2 shows equation (2.18) with a space-like four-Lorentz scalar: $\eta_{\mu\nu}\mathcal{A}_i^\mu \mathcal{A}_i^\nu < 0$. Figure 2.4 shows the minimum of $U(w)$ for various values of

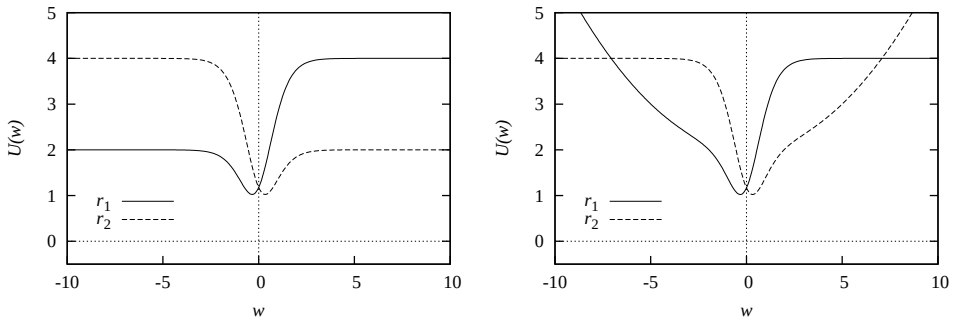

Figure 2.2: The function $U(w)$ used to determine the eigenvalues of the r_i perturbation in the light- (left plot) and space-like (right plot) cases, plotted as a function of w. The parameters and corresponding field configurations are as in the reflection symmetric cases in Figure 2.1. There are two plots in each graph corresponding to $U(w)$ with $i = 1$, $j = 2$ and $i = 2$, $j = 1$.

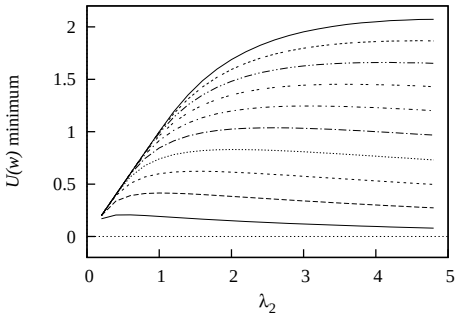

Figure 2.3: The minimum of the function $U(w)$ in the light-like case plotted against λ_2. The upper curves correspond to successively larger values of λ_1, which runs from 0.2 to 2 in steps of 0.2.

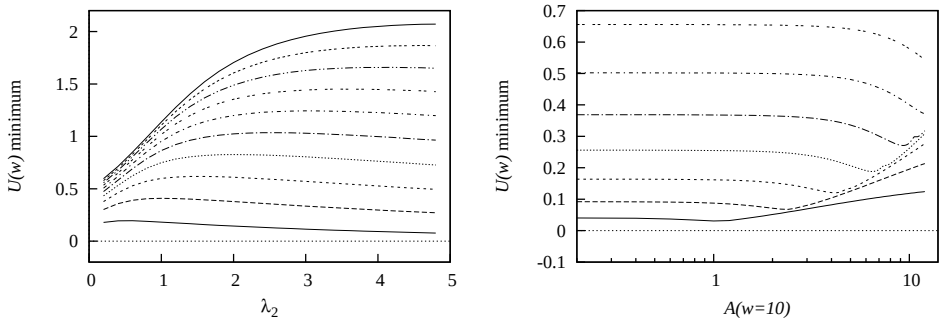

Figure 2.4: The minimum of the function $U(w)$ in the space-like case. The plot on the left is against λ_2 with upper curves corresponding to larger values of λ_1, which runs from 0.2 to 2 in steps of 0.2. The plot on the right is against the boundary condition for the gauge field with upper curves corresponding to larger values of v, which runs from 0.2 to 0.8 in steps of 0.1.

the parameters and boundary conditions for the gauge fields. It is clear that the minima are all positive and so the time-independent background scalar field configuration is also stable in the space-like case.

Since each field in the model permits time-independent solutions which are independently stable, we conclude that the domain-wall configuration as a whole is a stable one. We have also verified this analysis with explicit numerical calculation of the possible values for the mode eigenvalue ω. They were found to be all real in the large parameter space that we scanned.

2.3 Including gravity

Having analysed the U(1) ⊗ U(1) toy model in a five-dimensional Minkowski spacetime without gravity, we now proceed to include the gravitational effects of the domain wall, and obtain a smooth version of the Randall-Sundrum warped metric. To make such an extension of the model, we must include the Ricci scalar R and a bulk cosmological constant Λ in the action, and use the curved space metric g_{MN} to contract indices. Using the time-like conventions of Section A.3, the action is

$$S = \int d^5x\sqrt{g}\left[\kappa(-R - 2\Lambda) - \frac{1}{4}g^{MP}g^{NQ}f_{MNPQ} + g^{MN}t_{MN} - V(\phi_a)\right] , \tag{2.19}$$

with $\kappa = 1/16\pi G$, G is Newton's constant, and

$$f_{MNPQ} = \sum_a F_{aMN}F_{aPQ} , \tag{2.20a}$$

$$t_{MN} = \sum_a (D_M\phi_a)^* D_N\phi_a , \tag{2.20b}$$

where the field content is as before, as is the definition of the covariant derivative D_M. Although we previously gave a concrete form for the scalar field potential $V(\phi_1, \phi_2)$, we are going to leave it unspecified for now.

By varying the action with respect to the metric components g_{MN}, we obtain Einstein's equations:

$$G_{MN} = \frac{1}{2\kappa}T_{MN} + g_{MN}\Lambda , \tag{2.21}$$

where the stress-energy tensor is (see Section A.3)

$$T_{MN} = -g^{PQ} f_{MPNQ} + 2t_{MN} - g_{MN}\mathcal{L}_{\text{matter}} \,, \tag{2.22a}$$

$$\mathcal{L}_{\text{matter}} = -\frac{1}{4} g^{MP} g^{NQ} f_{MNPQ} + g^{MN} t_{MN} - V \,. \tag{2.22b}$$

We also obtain the Euler-Lagrange equations of motion by varying the individual scalar and gauge fields, respectively:

$$D_M \left(\sqrt{g}\, g^{MN} D_N \phi_i\right) = -\sqrt{g} \frac{\partial V}{\partial \phi_i^*} \,, \tag{2.23a}$$

$$\partial_M \left(\sqrt{g}\, g^{MP} g^{NQ} F_{iPQ}\right) = \sqrt{g}\, g^{NP} 2 \left[e \,\mathrm{Im}\left(\phi_i^* D_P \phi_i\right) + \tilde{e}\,\mathrm{Im}\left(\phi_j^* D_P \phi_j\right)\right] \,. \tag{2.23b}$$

To proceed, we must make an ansatz for the five-dimensional metric. We have seen in the non-gravity case that the gauge fields can be light-like or space-like, so the metric should be general enough to allow the different coordinates to behave independently. Since we are looking for domain-wall solutions that only depend on w, this is the only such dependence we shall allow for in the metric, giving the ansatz

$$ds^2 = e^{f(w)} dt^2 - e^{h(w)} dx^2 - e^{j(w)} \left(dy^2 + dz^2\right) - dw^2 \,. \tag{2.24}$$

As before, we make a polar decomposition for the ϕ_i, and also assume that the y and z components of the gauge fields are zero:

$$\phi_i = R_i(w)\, e^{i\Theta_i(w)} \,, \tag{2.25a}$$

$$A_{iM} = \left(A_i(w), B_i(w), 0, 0, Z_i(w)\right) \,. \tag{2.25b}$$

Such a choice for the gauge fields should not be overly restrictive, as it still allows for light- and space-like configurations.

We now need to determine the equations that the thirteen degrees of freedom satisfy. To simplify the algebra we define

$$\mathcal{F} = \tfrac{1}{2}\left(f + h + 2j\right) \,, \tag{2.26a}$$

$$\overline{\mathcal{F}} = \tfrac{1}{2}\left(-f + h + 2j\right) \,, \tag{2.26b}$$

$$\overline{\overline{\mathcal{F}}} = \tfrac{1}{2}\left(f - h + 2j\right) \,, \tag{2.26c}$$

and express the gauge fields, and scalar phase, in terms of the linear combinations

$$\mathcal{A}_i = eA_i + \tilde{e}A_i \,, \tag{2.27a}$$
$$\mathcal{B}_i = eB_i + \tilde{e}B_i \,, \tag{2.27b}$$
$$\mathcal{Z}_i = eZ_i + \tilde{e}Z_i - \Theta_i' \,. \tag{2.27c}$$

As before, prime denotes differentiation with respect to w. Expanding equation (2.23b) in terms of the individual fields gives

$$\mathcal{A}_i'' + \overline{\mathcal{F}}'\mathcal{A}_i' - 2(e^2+\tilde{e}^2)R_i^2\mathcal{A}_i - 4e\tilde{e}R_j^2\mathcal{A}_j = 0 \,, \tag{2.28a}$$
$$\mathcal{B}_i'' + \overline{\overline{\mathcal{F}}}'\mathcal{B}_i' - 2(e^2+\tilde{e}^2)R_i^2\mathcal{B}_i - 4e\tilde{e}R_j^2\mathcal{B}_j = 0 \,, \tag{2.28b}$$
$$\left(eR_i^2 + \tilde{e}R_j^2\right)\mathcal{Z}_i = 0 \tag{2.28c}$$

The third equation here implies $\mathcal{Z}_i = 0$ which we use to simplify the rest of the equations of motion. For the scalar field we use equation (2.23a) to obtain

$$R_i'' + \mathcal{F}'R_i' + e^{-f}\mathcal{A}_i^2 R_i - e^{-h}\mathcal{B}_i^2 R_i - e^{-i\Theta_i}\frac{\partial V}{\partial \phi_i^*} = 0 \,. \tag{2.29}$$

After some manipulation, Einstein's equations yield

$$f'' + \tfrac{1}{2}f'^2 + \tfrac{1}{3}f'h' + \tfrac{2}{3}f'j' - \tfrac{1}{3}h'j' - \tfrac{1}{6}j'^2 - \tfrac{5}{3\kappa}e^{-f}\Phi - \tfrac{1}{3\kappa}e^{-h}\Psi + \tfrac{1}{3\kappa}\Omega = 0 \,, \tag{2.30a}$$
$$h'' + \tfrac{1}{3}f'h' - \tfrac{1}{3}f'j' + \tfrac{1}{2}h'^2 + \tfrac{2}{3}h'j' - \tfrac{1}{6}j'^2 + \tfrac{1}{3\kappa}e^{-f}\Phi + \tfrac{5}{3\kappa}e^{-h}\Psi + \tfrac{1}{3\kappa}\Omega = 0 \,, \tag{2.30b}$$
$$j'' - \tfrac{1}{6}f'h' + \tfrac{1}{6}f'j' + \tfrac{1}{6}h'j' + \tfrac{5}{6}j'^2 + \tfrac{1}{3\kappa}e^{-f}\Phi - \tfrac{1}{3\kappa}e^{-h}\Psi + \tfrac{1}{3\kappa}\Omega = 0 \,, \tag{2.30c}$$

where

$$\Phi = \mathcal{A}_1^2R_1^2 + \mathcal{A}_2^2R_2^2 + \tfrac{1}{2}A_1'^2 + \tfrac{1}{2}A_2'^2 \,, \tag{2.31a}$$
$$\Psi = \mathcal{B}_1^2R_1^2 + \mathcal{B}_2^2R_2^2 + \tfrac{1}{2}B_1'^2 + \tfrac{1}{2}B_2'^2 \,, \tag{2.31b}$$
$$\Omega = R_1'^2 + R_2'^2 + V + 2\kappa\Lambda \,. \tag{2.31c}$$

First of all, let us discuss the coupled gravity-domain-wall solutions *without* the gauge fields present, so we can just set them to zero. In this case,

we can assume all three metric components are equal, $f = h = j$, and equations (2.29) and (2.30) simplify to

$$R_i'' + 2f'R_i' - e^{-i\Theta_i}\frac{\partial V}{\partial \phi_i^*} = 0\,, \tag{2.32a}$$

$$f'' + f'^2 + \tfrac{1}{3\kappa}\left[R_1'^2 + R_2'^2 + V\right] + \tfrac{2}{3}\Lambda = 0\,. \tag{2.32b}$$

Instead of the quartic potential used in the non-gravity case, we shall use a rather complicated form for V, which was engineered to obtain analytic domain-wall solutions; see Dando et al. [202] for details regarding such engineering. The potential reads

$$\begin{aligned} V(\phi_1,\phi_2) = {} & \frac{\beta^2}{v^2}\left(1+\frac{v^2}{3\kappa}\right)|\phi_1|^2|\phi_2|^2 \\ & - \frac{2\beta^2}{v^4}\left(\frac{3}{2}+\frac{v^2}{3\kappa}\right)|\phi_1|^2|\phi_2|^2\left(|\phi_1|^2+|\phi_2|^2-v^2\right) \\ & + \frac{\zeta\beta^2}{2v^2}\left(\frac{3}{2}+\frac{v^2}{3\kappa}\right)\left(|\phi_1|^2+|\phi_2|^2-v^2\right)^2\left(\eta+\frac{|\phi_1|^2+|\phi_2|^2-v^2}{v^2}\right), \end{aligned} \tag{2.33}$$

where β, v, ζ and η are parameters which must satisfy certain relations in order that V is able to support a domain-wall solution; again, see [202] for details. Using this potential, the analytic solutions to equations (2.32a) and (2.32b) are then

$$R_{1,2}(w) = \frac{v}{\sqrt{2}}\sqrt{1 \pm \tanh(\beta w)}\,, \tag{2.34a}$$

$$f(w) = -\frac{v^2}{6\kappa}\log\left(\cosh(\beta w)\right)\,. \tag{2.34b}$$

The form of R_i is that of a domain-wall, and looks qualitatively the same as the scalar fields in the non-gravity case, Figure 2.1. The solution for the metric component f is a smoothed out version of the Randall-Sundrum warped metric, and we can assume the general result for such metrics: that gravity is localised to the domain wall. For these solutions to hold, the Randall-Sundrum fine tuning condition must be satisfied, which ensures that the effective four-dimensional spacetime has a vanishing cosmological constant; it is

$$\Lambda = -\frac{\beta^2 v^4}{24\kappa^2}\,. \tag{2.35}$$

Unfortunately, we are not able to find solutions, even numeric ones, with any of the gauge field components non-zero. We shall make a few remarks about why we believe such solutions do not actually exist, or are at least difficult to find. Compare the equations for the gauge fields in the gravity-free case, equation (2.10b), and the case with gravity, equations (2.28a) and (2.28b). The only difference is the appearance, in the gravity case, of the term with a single derivative of the gauge field. So we can appeal to our argument from Section 2.1 regarding the asymptotic behaviour of the fields, and determine that, for example, as $w \to \infty$ we have $\mathcal{A}_2'' + \overline{\mathcal{F}}'\mathcal{A}_2' \to 0$. We know that for the warped metric, derivatives of the metric components approach a constant far from the domain wall, so it should be safe to assume that $\overline{\mathcal{F}}'$ approaches constant. Then we can solve for the asymptotic behaviour of the gauge field:

$$\mathcal{A}_2'(w \to \infty) \sim e^{-\overline{\mathcal{F}}}\,. \tag{2.36}$$

It does not seem as though we can recover the asymptotic behaviour that we had in the gravity-free case, as $\mathcal{A}_2'$ either exponentially grows or decays, instead of approaching a constant. The exponentially decaying solution may be physically acceptable (the other case is certainly not), but this requires something like $h = j = 0$ so that $\overline{\mathcal{F}} > 0$ (note that we expect $f, h, j < 0$ from experience with the gauge-free case, equation (2.34b)). Such a solution may be possible, but our numerical studies have not given any indication of this.

Finally, one must be careful when searching for numerical solutions to the gravity equations, as the Randall-Sundrum fine tuning condition must be satisfied, which can be a non-trivial exercise. The scalar fields that make up the domain wall contribute energy density which must be balanced against the bulk cosmological constant Λ. One very general way of determining this balance is to take the five-dimensional action (2.19), substitute in the background configuration (which may be analytical or numerical), integrate out the extra dimension, and choose a value for Λ such that the resulting four-dimensional action is identically zero. This amounts to ensuring that the four-dimensional cosmological constant is zero. If the gauge fields are non-zero, they may contribute some value to the energy density, and hence modify the required value of Λ. This possibility can be taken into account

when looking for numerical solutions by solving for Λ each iteration, but the feedback loop induced by such a calculation seems to make it difficult to find solutions.

2.4 Conclusion

In this chapter we considered a toy model based on a $\mathrm{U}(1)\otimes\mathrm{U}(1)$ gauge symmetry, and a discrete $\mathbb{Z}_2$ interchange symmetry acting on a pair of charged scalar fields. We presented the time-independent background configurations which took the form of a domain wall with semi-confined gauge fields. This configuration was found to be perturbatively stable: we looked at the normal modes of perturbations and found them to be oscillatory for a large range of parameters. Gravity was then incorporated into the model, and we presented analytic solutions, with the gauge fields set to zero, that had the form of a domain wall coupled to a smooth version of the Randall-Sundrum warped metric. A numerical investigation failed to obtain non-zero solutions for any components of the gauge fields in the case with gravity, and we made some remarks as to why we believe no solutions actually exist.

Now that we have experience solving Euler-Lagrange equations to determine background configurations, and can also analyse the perturbative stability of such configurations, we are going to move on, in the next chapter, to study the full dynamical behaviour of the classical kink solution. This will be an extension of the analysis of the normal modes: we perform a generalised Fourier expansion about the kink background and find a description of the dynamics associated with each Fourier mode in terms of an effective four-dimensional action.

Chapter 3

Kink modes and confined matter fields

Extra spatial dimensions, if they exist, must be hidden at low energies. In the language of field theory, this means that a five-dimensional field, say $\Phi(t, \vec{x}, w)$, must be somehow restricted from having any dynamics in the extra-dimension w. It is not possible to actually eliminate the w degree of freedom, but it is possible to transform it into a physically different form. Mathematically, we can perform a generalised Fourier transform on w and write the five-dimensional field as $\Phi(t, \vec{x}, w) = \sum_i \phi_i(t, \vec{x})\eta_i(w)$, where the sum is over the general Fourier modes, the $\phi_i(t, \vec{x})$ are four-dimensional fields and the $\eta_i(w)$ form the basis of the transform. After substituting such a transformation into the action of the theory, the extra-dimension can be integrated out, along with the $\eta_i(w)$, and the w degree of freedom originally present in $\Phi(t, \vec{x}, w)$ is now manifest as the infinite tower of the four-dimensional modes — the Kaluza-Klein modes. These modes form a tower because the extra-dimensional part of the kinetic term of $\Phi(t, \vec{x}, w)$ becomes a mass term after integrating over the extra dimension, and different modes have different mass.

Such a transformation of the w degree of freedom to a tower of modes is only going to be useful in extra-dimensional model building if the low-energy modes of the tower are isolated. Discrete modes, whose mass is separated by a finite amount from neighbouring modes, are modes that are completely isolated. There also exist partially isolated, or resonant, modes, which look almost discrete, but lie in the midst of a spectrum of a continuum of modes.

The trapping of gravity is an example of this: the tower of gravity modes for the situation of the Randall-Sundrum warped metric has no mass gap between the lowest mode of the tower and the continuum, yet it still produces an acceptable effective four-dimensional theory of gravity. This is because the continuum modes are highly suppressed in the vicinity of the brane, and the lowest mode looks almost discrete. This phenomenon is also manifest in the models in Chapter 4, and shall be discussed in detail there; in the current chapter we focus on the case of discrete modes. Low-mass modes that are well isolated within a spectrum (be they discrete or resonant modes) can be identified as the four-dimensional fields observed in our universe. The central problem is then coming up with a mechanism which yields such a discrete spectrum. This is precisely the role of a domain-wall brane, which has the effect of trapping particles because it is able to induce a discrete Kaluza-Klein mass spectrum, at least at low energies.

A useful and related picture to keep in mind is the behaviour of a particle trapped in a square well. Here, the Schrödinger equation is used to solve for the allowed eigen-wave-functions and associated eigen-energies of the trapped particle, and the low-energy solutions are discrete modes with a fixed wave-function. For energies larger than the depth of the well, the solutions form a continuum, corresponding to a particle that is free of the well. In the case of the domain-wall background, or kink as it shall frequently be referred to in this chapter, a similar scenario holds true: the coupling of the kink to another field, like $\Phi(t, \vec{x}, w)$, induces a well-like potential, in the extent of the extra-dimension. Utilising the general Fourier transform, the functions $\eta_i(w)$ are then the objects that feel the kink induced well, and their solutions are found by solving a Schrödinger-like equation, yielding a discrete (and continuous) mass spectrum for the four-dimensional fields $\phi_i(t, \vec{x})$.

In this chapter, we provide the details of such a trapping mechanism, and present explicit, analytic solutions for the tower of modes for both fermion and scalar fields coupled to a kink. For fermions, we extend the mechanism due to Rubakov and Shaposhnikov [45], which we discussed in Section 1.3.1, to find the full set of modes that are localised, and de-localised, in the presence of the kink. For the case of a scalar field, we demonstrate that it is possible to confine an effective four-dimensional scalar field with a quartic potential of arbitrary shape, a technique which can be used to place the

standard model electroweak Higgs field on the brane. We determine the Kaluza-Klein structure of the modes of these trapped fields, which is important for two reasons. First, for a given field, the lowest mode will be used in model building as one of the four-dimensional fields of the standard model. Second, the next few higher modes will be the first to be discovered in experiments (if our model is a faithful description of nature), will provide a signature of extra-dimensions, and allow us to probe parameters of extra-dimensional models.

We are also going to study the modes associated with the kink itself. The simple treatment in Section 1.3.1 of the canonical kink solution provided an understanding of the background solution $\phi_{DW}(w)$, but neglected all of the dynamics associated with the field that forms the kink. In this chapter, our study of the kink background retains all of the degrees of freedom, which manifest through a general Fourier transform as four-dimensional fields, in just the same way as coupled, trapped fermion and scalar fields do. During the course of such a detailed analysis of the kink, we discuss in detail the kink zero mode: the massless, Nambu-Goldstone-boson degree of freedom associated with translations of the kink background. As for the modes of coupled fermions and scalars, the behaviour of the modes of the kink will be important for a phenomenological analysis, as these modes allow us to probe the structure of the domain wall.

One important aspect of a domain-wall brane is its behaviour in the limit where it becomes infinitely thin. We expect the brane to be physically quite thin (equivalently, be constructed out of a field with a large mass), since we have not, so far, measured any effects related to our universe being localised on a brane. As part of the analyses in this chapter, of kink, fermion and scalar modes, we will determine the behaviour of the spectra of such modes in the various limits of the width of the kink. A general result is that the masses of the modes in the Kaluza-Klein towers are proportional to the inverse width of the kink, and so a thin kink ensures that the gaps in the discrete spectrum are large enough to be consistent with experiments performed so far.

We begin in Section 3.1 by presenting the toy model which supports a scalar kink and determine the full spectrum of its associated modes. We discuss the different limits of this model which give the scenarios with no kink, a thick kink and a thin kink. Issues related to the dynamics of the translation

symmetry of the kink, the kink zero mode, are discussed in detail. In Section 3.2 we add a scalar field to the kink model, and show that the kink sets up a symmetric modified Pöschl-Teller potential for the extra-dimensional component of the scalar field. We determine the modes of this potential and use them to obtain an effective four-dimensional action, discussing in detail the thin kink limit. In Section 3.3 we analyse a fermion coupled to the kink, present the full mode decomposition, and show that in the thin kink limit, the massless left-handed mode is the only surviving dynamical field. We also present an action that contains this massless four-dimensional mode coupled to a five-dimensional field. The chapter is summarised in Section 3.4. Appendix C contains analytic solutions of the potential well set up by the kink, solutions which are used extensively throughout this chapter.

Note that gravity will be ignored in the analyses presented in this chapter, and we work in a five-dimensional Minkowski spacetime. Chapter 4 deals with the situation where gravity is included.

3.1 The kink and its limits

The conventions that we follow in this chapter are as follows. The background spacetime is $4+1$-dimensional Minkowski space with metric $\eta_{MN} = \text{diag}(+1,-1,-1,-1,-1)$. Capital Latin letters index the full space, Greek letters index the $3+1$-dimensional subspace, the extra-dimensional coordinate is w and the coordinates are embedded as $x^M = (x^\mu, w)$.

We begin our analysis of the domain-wall, the kink, without any coupling to other matter (or gauge) fields, since we would like to study the formation and dynamics of this background entity in isolation. The kink is modelled by a real, five-dimensional scalar field $\Phi(x^M)$, and the action is given by

$$\mathcal{S}_\Phi = \int d^5x \left[\frac{1}{2}\partial^M\Phi\partial_M\Phi - V(\Phi)\right] , \tag{3.1}$$

with

$$V(\Phi) = \frac{a}{4m}\left(\Phi^2 - \frac{m^3}{a}\right)^2 , \tag{3.2}$$

where a is a dimensionless constant and m is the mass of Φ. The potential $V(\Phi)$ is just the usual quartic potential, but we have expressed it using rather unconventional parameters, due to the fact that we are in five-dimensions,

where the dimensionality of Φ is (energy)$^{3/2}$, and we want the explicit appearance of the mass of Φ in the potential. In four-dimensions, the same potential would look like $V_{(4d)}(\phi) = \frac{\lambda}{4}(\phi^2 - \frac{m^2}{\lambda})^2$. Note the discrete $\mathbb{Z}_2$ symmetry $\Phi \to -\Phi$ which is inherent in our model, and which ensures the topological stability of domain-wall solutions. From this action we find the Euler-Lagrange equation for Φ to be

$$\partial^M \partial_M \Phi - m^2 \Phi + \frac{a}{m}\Phi^3 = 0\,. \tag{3.3}$$

With the aim of producing an effective four-dimensional theory, Φ will initially be taken to depend only on the extra-dimensional coordinate w; this behaviour is denoted as $\phi_c(w)$, where the subscript c reminds us that ϕ_c is a solution of the classical equation of motion. This ansatz for Φ allows for a topologically stable solution to equation (3.3), which is

$$\phi_c(w) = \sqrt{\frac{m^3}{a}}\tanh\left(\frac{mw}{\sqrt{2}}\right)\,. \tag{3.4}$$

This classical kink solution interpolates between the $\mathbb{Z}_2$ degenerate minima of the potential $V(\Phi)$. The kink has constant energy per unit volume at every spatial point in the $3+1$-dimensional subspace, given by

$$\varepsilon_{\phi_c} = \int_{-\infty}^{\infty} dw \left[\frac{1}{2}(\partial_w \phi_c)^2 + V(\phi_c)\right] = \frac{2\sqrt{2}m^4}{3a}\,. \tag{3.5}$$

As discussed previously, the physically interesting parameter regime of our model is when the background configuration is that of a relatively thin kink, corresponding to large m. To make such a statement more precise, we write the two parameters of our model as

$$a = \tilde{a}\Lambda^{\alpha}\,, \tag{3.6a}$$

$$m = \tilde{m}\Lambda^{\mu}\,, \tag{3.6b}$$

with $\tilde{a}$ and $\tilde{m}$ finite and real, and consider the limit $\Lambda \to \infty$. The parameters α and μ can be adjusted so, in the limit of infinite Λ, a and m can independently vanish, diverge or stay finite. Of course, only the ratio α/μ and the individual signs of α and μ are meaningful, and we can further constrain the ratio by considering the energy density of the kink. In the

limit $\Lambda \to \infty$, the kink energy density behaves as $\varepsilon_{\phi_c} \sim \Lambda^{4\mu-\alpha}$ and must remain finite for the kink solution to be a physical one, yielding the constraint $\alpha = 4\mu$. This in turn means the amplitude of the kink has limiting behaviour $|\phi_c(w)| \sim \Lambda^{-\frac{1}{2}\mu}$. The sign of the single parameter μ now describes all possible limiting scenarios of the theory, with $\mu = 0$ corresponding to no limit being taken. If $\mu < 0$ the potential $V(\Phi)$ disappears, as does the classical kink solution[1] $\phi_c(w) \to 0$, and the action describes a massless, freely propagating, five-dimensional scalar field. The case $\mu > 0$ is the more interesting thin kink limit. Here, the width of ϕ_c tends to zero and, to keep the energy density finite, the height also vanishes. We will refer extensively to these limits in the following sections.

By assuming that $\Phi(x^M)$ depends only on w we have of course lost a lot of the dynamics of the full theory. First, since $\phi_c(w)$ breaks translational invariance along w, we expect a zero mode which can act to translate the kink. Second, if we have a thick kink, we expect there to be massive modes associated with arbitrary deformations of the kink. We now proceed to incorporate these dynamics by performing a generalised Fourier transformation of the coordinate w.

3.1.1 Kink modes and the effective model

The classical kink background $\phi_c(w)$ breaks the five-dimensional Poincaré symmetry, leaving a four-dimensional Poincaré subgroup. This makes it natural to decompose a field into a sum of products of an extra-dimensional component and a $3+1$-dimensional component. For $\Phi(x^M)$, we want this expansion to be made about the kink solution, and so we take

$$\Phi(x^\mu, w) = \phi_c(w) + \sum_i \phi_i(x^\mu)\eta_i(w)\,, \tag{3.7}$$

where $\eta_i(w)$ are a fixed orthonormal basis of the extra dimension, $\phi_i(x^\mu)$ are four-dimensional dynamical fields, and the sum over i can in general be a combination of discrete and continuous modes. We would like to determine a basis η_i such that the equations of motion for the ϕ_i describe massive scalar fields. This can be done in the standard way by taking the action for Φ given by (3.1), substituting the expansion (3.7), using the fact that ϕ_c

[1] The relevant limit is $\lim_{m\to 0} \tanh(mw/\sqrt{2})/\sqrt{m} = 0$.

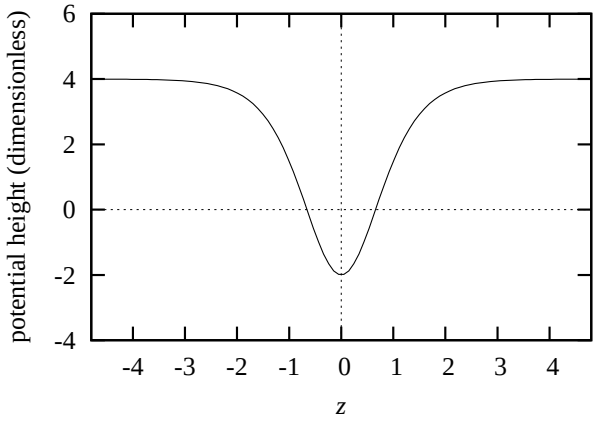

Figure 3.1: Plot of the potential well, $U(z) = 6\tanh^2 z - 2$, corresponding to the modes of the kink. Solutions of a Schrödinger-like equation with this potential give the extra-dimensional profiles of the kink modes, equations (3.11) and (3.12).

satisfies (3.3), discarding terms $\mathcal{O}(\phi_i\eta_i)^3$ and higher and using integration by parts. The effective second order action is then

$$\mathcal{S}_\Phi^{\mathcal{O}(2)} = \int d^5x \left[\frac{a}{4m}\phi_c^4 - \frac{m^5}{4a} - \frac{1}{2}\phi_i\eta_i\left(\partial^\mu\partial_\mu - \partial_w^2 + \frac{3a}{m}\phi_c^2 - m^2\right)\phi_j\eta_j\right], \tag{3.8}$$

with implicit sums over i and j which label the modes. For the ϕ_i to satisfy the massive Klein-Gordon equation with mass λ_i we require

$$\left(-\frac{d^2}{dw^2} + \frac{3a}{m}\phi_c^2 - m^2\right)\eta_i = \lambda_i^2\eta_i\,. \tag{3.9}$$

There is no sum over i on the right-hand-side of this equation.

By using the known form of ϕ_c, we can manipulate equation (3.9) to get

$$\left(-\frac{d^2}{dz^2} + 6\tanh^2 z - 2\right)\eta_i = \left(\frac{2\lambda_i^2}{m^2}\right)\eta_i\,, \tag{3.10}$$

where we have switched to the dimensionless coordinate $z = mw/\sqrt{2}$. This differential equation is a Schrödinger-like equation with a symmetric modified Pöschl-Teller potential, a plot of which is given in Figure 3.1. Analytic solutions of this potential are known in terms of hypergeometric functions, and, in general, there are both bound and continuum solutions. In Appendix C we present these solutions expressed in terms of regular functions, along with their normalisation coefficients, for a more general form of the

potential. For the kink modes at hand, equation (3.10) is equation (C.1) with $l = 2$. There are two discrete, bound modes, which have eigenvalues and eigenfunctions

$$\lambda_0^2 = 0 \qquad \eta_0(w) = E_0 \cosh^{-2} z \,, \tag{3.11a}$$

$$\lambda_1^2 = \frac{3}{2}m^2 \qquad \eta_1(w) = E_1 \sinh z \cosh^{-2} z \,, \tag{3.11b}$$

and above these bound modes lie a continuum, parameterised by the real variable q:

$$\lambda_q^2 = \frac{1}{2}(q^2+4)m^2 \,, \tag{3.12a}$$

$$\eta_q(w) = E_q e^{iqz}\left(3\tanh^2 z - (q^2+1) - 3iq\tanh z\right) \,. \tag{3.12b}$$

The bound modes $\eta_{0,1}(w)$ are square integrable normalised by equation (C.3) and the continuum modes $\eta_q(w)$ are delta function normalised by equation (C.6), the normalisation constants being

$$E_0 = \sqrt{\frac{3m}{4\sqrt{2}}}, \quad E_1 = \sqrt{\frac{3m}{2\sqrt{2}}}, \quad E_q = \sqrt{\frac{m}{2\pi\sqrt{2}(q^2+1)(q^2+4)}}. \tag{3.13}$$

Armed with the basis η_i, we return to the analysis of the full dynamics of the kink. Expanding the original action (3.1) with Φ decomposed in the η_i basis and integrating over the extra dimension gives

$$\mathcal{S}_\Phi = \int d^4x \left[-\varepsilon_{\phi_c} + \mathcal{L}_\phi\right], \tag{3.14}$$

where the ϕ kinetic, mass and self-coupling terms are

$$\begin{aligned}\mathcal{L}_\phi = {} & \frac{1}{2}\partial^\mu\phi_0\partial_\mu\phi_0 + \frac{1}{2}\partial^\mu\phi_1\partial_\mu\phi_1 - \frac{3}{4}m^2\phi_1^2 \\ & + \int_{-\infty}^{\infty} dq \left[\frac{1}{2}\partial^\mu\phi_q^*\partial_\mu\phi_q - \frac{1}{4}(q^2+4)m^2\phi_q^*\phi_q\right] \\ & - \kappa^{(3)}_{ijk}\phi_i\phi_j\phi_k - \kappa^{(4)}_{ijkl}\phi_i\phi_j\phi_k\phi_l \,. \end{aligned} \tag{3.15}$$

The fields $\phi_{0,1}(x^\mu)$ are the real valued scalars associated with the two bound modes $\eta_{0,1}(w)$. The integration over q is over the complex valued continuum modes $\phi_q(x^\mu)$ associated with $\eta_q(w)$. Note that $\phi_{-q} = \phi_q^*$ and $\eta_{-q} = \eta_q^*$ and so this integral is real. The effective cubic and quartic self-interaction

couplings are

$$\kappa^{(3)}_{ijk} = \frac{a}{m}\int_{-\infty}^{\infty} \phi_c \eta_i \eta_j \eta_k \, dw \,, \tag{3.16a}$$

$$\kappa^{(4)}_{ijkl} = \frac{a}{4m}\int_{-\infty}^{\infty} \eta_i \eta_j \eta_k \eta_l \, dw \,. \tag{3.16b}$$

For brevity, the indices i, j, k, l label bound modes, continuum modes or a mixture of both, and the sum over these labels is implied in equation (3.15). The couplings κ can be computed as their integrands are known; some are zero due to parity, some are non-zero.

Equations (3.14) and (3.15) are exact manipulations of the original five-dimensional model (3.1), and provide a description in a basis useful for investigating the effective four-dimensional behaviour. The bound modes are reminiscent of the Kaluza-Klein modes one obtains in compact extra dimensions, but, in the case at hand, the gaps in the mass spectrum are not uniform. Furthermore, the continuum modes do not have analogues in the Kaluza-Klein model and are not strictly four-dimensional, but instead form a pseudo-five-dimensional field with reduced degrees of freedom.

Consider briefly the renormalisability of the original five-dimensional action given by equation (3.1). The quartic term coming from the potential, $\frac{a}{4m}\Phi^4$, has a coefficient with negative mass-dimensionality, rendering the theory non-renormalisable. By choosing to allow such a term, we are no longer restricted (like we are in the usual, four-dimensional, renormalisable case) to writing down terms below a certain order, and we could quite happily extend the potential beyond quartic order. But the manipulations which bring us to the four-dimensional level, given by equation (3.15), do in fact leave us with a renormalisable theory if we truncate the action to just the bound states. This renormalisability of the bound states may be a useful criterion for restricting the types of terms that one begins with in the five-dimensional (or higher-dimensional) action.

3.1.2 Limiting behaviour of the kink

Now that we have such a reformulation of the kink model, we are in a position to analyse the full dynamics of the system for the three different limits of the mass m. Following our previous parameterisation, for $\mu < 0$ there is no kink and the basis $\eta_i(w)$ is replaced by a standard complex Fourier expansion. All

the dynamical components are packaged together by the Fourier transform and it is no longer sensible to perform the w integral. Instead one should consider $\Phi(x^M)$ as a free, massless, five-dimensional field.

For the thick kink case when $\mu = 0$, the spectrum consists of the energy density of the integrated kink, a zero mode, a massive bound mode and a continuum of massive complex scalars. These effective four-dimensional fields are self-coupled and coupled amongst each other via cubic and quartic interactions. In particular, the zero mode $\phi_0(x^\mu)$ and massive bound mode $\phi_1(x^\mu)$ each have a potential:

$$V_0(\phi_0) = \frac{9\sqrt{2}\,a}{140}\phi_0^4\,, \tag{3.17a}$$

$$V_1(\phi_1) = \frac{3}{2}m^2\phi_1^2 + \frac{3\pi}{32}\sqrt{\frac{3a}{2\sqrt{2}}}\,m\,\phi_1^3 + \frac{9\sqrt{2}\,a}{280}\phi_1^4\,, \tag{3.17b}$$

which are due to the non-zero values of $\kappa^{(4)}_{0000}$, $\kappa^{(3)}_{111}$ and $\kappa^{(4)}_{1111}$. Similarly, we can compute the coupling potential amongst these two bound modes to get

$$V_{0,1}(\phi_0,\phi_1) = \frac{9\pi}{64}\sqrt{\frac{3a}{2\sqrt{2}}}\,m\,\phi_0^2\phi_1 + \frac{9\sqrt{2}\,a}{70}\,\phi_0^2\phi_1^2\,. \tag{3.18}$$

Note that while ϕ_0 has no mass term it does have a non-zero potential, making it energetically unfavourable to excite the field, even though it costs zero energy to translate the kink. We can account for this unexpected result by recalling that η_0 corresponds to *infinitesimal* translations of ϕ_c. Adding any small but finite multiple of η_0 to ϕ_c will, to first order, perform a translation, but to higher order it will *deform* the kink. The energy cost of these higher order deformations are described by the potential V_0.[2] For completeness, we point out that while V_1 has a cubic term, the potential has only one extremum, which is a minimum at $\phi_1 = 0$. Any other location for the minimum would indicate that the kink solution is unstable.

We now move on to discuss the thin kink limit, where $\mu > 0$ and both m

[2]In constructing the basis η_i we linearised the action about the kink background, equation (3.8), and so it may seem that we are in error keeping the cubic and quartic terms in equation (3.17). But we are in fact allowed to keep such higher order terms, and they have no further corrections at the classical level. This is because, regardless of how we came to determine it, η_i forms a complete basis in the sense that any function of w can be faithfully represented by a particular linear combination of the η_i's. Using this basis, exact manipulations of the original five-dimensional action lead us to equation (3.17).

and a tend to infinity. In such a scenario, the kink energy density remains finite, but the masses of the bound mode ϕ_1 and the continuum modes ϕ_q go like m. Recall that these massive modes correspond to deformations in the kink, and as the kink gets thinner it also gets more rigid, requiring a larger amount of energy for a given deformation. The dynamics of the massive modes are thus frozen out, as they are no longer able to deform the kink without possessing infinite energy.

This argument can also be applied, perhaps naïvely, to the translation zero mode ϕ_0, which gets frozen out in the thin kink limit, despite remaining massless, because its corresponding potential V_0 becomes infinitely steep. This can be understood from the arguments given above: for an infinitely rigid kink, the higher order deformations due to the zero mode are forbidden and the only physical resolution is to remove the dynamics of this mode. So, in the thin kink limit, we are left with only the kink energy density ε_{ϕ_c} in the effective four-dimensional action.

At this point it seems we may have come to a counter-intuitive, and perhaps incorrect, conclusion regarding the zero mode ϕ_0. After all, even an infinitely thin kink can still be translated, and the translated configuration has the same energy density as the original configuration. Thus, it seems there should still exist a dynamical zero mode in the thin kink limit. We have not come to a definite conclusion regarding this matter, and the following subsection is devoted to a lengthy and detailed discussion of the issues involved. Recall that we are ignoring gravity in our analysis; in the gravity case, there are additional complications which arise from the interaction of the kink zero mode with a scalar degree of freedom of the metric [179].

3.1.3 Is the kink zero mode really frozen out?

The thin kink limit, as characterised by the width going to zero, or $m \to \infty$, while keeping the energy density ε_{ϕ_c} finite, still retains the property that it can be continuously translated to a shifted configuration that possesses an equivalent energy density. From Goldstone's theorem, there should exist a massless scalar field corresponding to the spontaneously broken, continuous symmetry of translation invariance.[3] It is unexpected then, that in this

[3] Although, Rajaraman makes the remark, on page 151 of his book [46], that the kink zero mode η_0 has nothing to do with massless fields, and does not correspond to a Nambu-Goldstone boson! He points out that Nambu-Goldstone bosons are the lowest state of a continuum of modes, but, in the case of the kink, η_0 corresponds to a bound state.

limit, the four-dimensional remnant of the translation symmetry, the zero mode ϕ_0, is frozen out, and the symmetry has no observable consequence at the effective four-dimensional level.

Before we launch into a discussion of this supposed contradiction, let us summarise what we believe the result to be: yes, the four-dimensional mode ϕ_0 is frozen out in the thin kink limit because, in this limit, the kink becomes infinitely rigid, and hence does not support perturbations of any kind. With no dynamical degrees of freedom left, the translation symmetry is manifest, at the four-dimensional level, by the zero energy cost associated with a specific *constant field configuration* (constant in x^μ) which has no physical consequence. This constant configuration is equivalent to shifting the mode expansion basis $\eta_i(w)$ to align it with the translated kink profile. We discuss this in detail in the following sections, and include an identification of the composite mode which is responsible for finite translations.

To give contrast to our result that the zero mode is frozen out, we also present the collective coordinate expansion, which treats the zero mode differently from the massive modes. In the effective four-dimensional action that results, the zero mode is coupled to the massive modes by derivative couplings only, and, in the limit where the massive modes decouple from the model, the zero mode still remains. We mention a reason why this particular analysis may be inequivalent to our mode expansion, and summarise the issue with a discussion of the difference between energy density and rigidity.

No dynamical degrees of freedom with a canonical kinetic term

Perhaps there exists a dynamical degree of freedom, call it $\rho_0(x^\mu)$, which is a certain linear combination of the states we have already identified, namely the set of fields $\phi_{0,1,q}$, and which survives in the infinitely thin kink limit. To follow this argument through, we assume that such a mode has a definite extra-dimensional profile, which may be unwarranted, but seems to be a reasonable assumption. If such a mode ρ_0 exists, then its extra-dimensional profile can be written as a linear combination of the basis that we have already found, $\eta_{0,1,q}$ (by virtue that the $\eta_{0,1,q}$ form a complete set for the extra-dimension w), and the same coefficients of this linear combination are then used to write ρ_0 in terms of $\phi_{0,1,q}$. We do not actually need to worry about the extra-dimensional profile of ρ_0, we just assume that it has one, and so ρ_0 manifests as a linear combination of the fields $\phi_{0,1,q}$, which we

write as

$$\rho_0 = \alpha_0\phi_0 + \beta_0\phi_1 + \int \gamma_0^*(q)\phi_q \, dq \,, \tag{3.19}$$

where α_0, β_0 and $\gamma_0(q)$ are the coefficients of the combination. We proceed to show that there are no choices for these coefficients which yield a field ρ_0 whose dynamics survive in the thin kink limit. We do this by looking at the action for ρ_0, and show that, if ρ_0 is forced to have a canonical kinetic term, its potential has coefficients which tend to infinity in the thin kink limit.

To determine the effective action for ρ_0 we will need to invert equation (3.19) to express $\phi_{0,1,q}$ in terms of ρ_0. To do this properly, we need a complete basis which includes ρ_0; call it $\rho_{0,n,q}$, where n labels the extra bound modes and q labels the extra continuum modes needed to complete the basis. Then the inverse of (3.19) is

$$\phi_0 = \alpha_0\rho_0 + \sum_n \alpha_n\rho_n + \int \alpha_r\rho_r \, dr \,, \tag{3.20a}$$

$$\phi_1 = \beta_0\rho_0 + \sum_n \beta_n\rho_n + \int \beta_r\rho_r \, dr \,, \tag{3.20b}$$

$$\phi_q = \gamma_0(q)\rho_0 + \sum_n \gamma_n(q)\rho_n + \int \gamma_r(q)\rho_r \, dr \,. \tag{3.20c}$$

Substituting this expansion in the action (3.14) gives the full action for the new fields $\rho_{0,n,q}$. We are only interested in the terms that describe ρ_0 as a self-interacting field that does not couple to any of the other fields. Keeping just these terms, the effective action is

$$\mathcal{S}_{\rho_0} = \int d^4x \left[\frac{1}{2}A^{(\mathrm{kin})}\partial^\mu\rho_0\partial_\mu\rho_0 - \frac{m^2}{2}A^{(2)}\rho_0^2 - m\sqrt{a}\,A^{(3)}\rho_0^3 - aA^{(4)}\rho_0^4\right] \,, \tag{3.21}$$

where

$$A^{(\mathrm{kin})} = \alpha_0^2 + \beta_0^2 + \int \gamma_0^*(q)\gamma_0(q) \, dq \,, \tag{3.22a}$$

$$A^{(2)} = \frac{3}{2}\beta_0^2 + \int \left(\frac{1}{2}(q^2+4)\gamma_0^*(q)\gamma_0(q)\right) \, dq \,, \tag{3.22b}$$

$$A^{(3)} = (\text{terms with at least one factor of } \beta_0 \text{ or } \gamma_0(q)) \,, \tag{3.22c}$$

$$A^{(4)} = \frac{9\sqrt{2}}{140}\alpha_0^4 + (\text{terms with at least one factor of } \beta_0 \text{ or } \gamma_0(q)) \,. \tag{3.22d}$$

In the thin kink limit, where $m \to \infty$ and $a \to \infty$ but m^4/a is kept finite, the mass of ρ_0 will tend to infinity unless $A^{(2)}$ vanishes. For $A^{(2)}$ to be identically zero, we require $\beta_0 = 0$ and $\gamma_0(q) = 0$. The requirement that the kinetic term for ρ_0 be of the canonical form implies $A^{(\mathrm{kin})} = 1$, and thus $\alpha_0 = 1$ (hence $\rho_0 = \phi_0$), and then the coefficient of the quartic term ρ_0^4 is $9\sqrt{2}\,a/140$ which freezes out ρ_0 in the thin kink limit.

Alternatively, we can choose β_0 and $\gamma_0(q)$ such that $A^{(2)}$ is not identically zero, but in the thin kink limit tends to zero in order to keep $m^2 A^{(2)}$ finite. Then, in this limit, $\beta_0 \to 0$ and $\gamma_0(q) \to 0$ and so $\alpha_0 \to 1$. The quartic coefficient $A^{(4)}$ is then dominated by the α_0^4 term which, as before, tends to infinity in the thin kink limit and freezes out ρ_0. Thus, there is no linear combination of the fields $\phi_{0,1,q}$, and hence no scalar degree of freedom, which has a canonical kinetic term, and whose dynamics survive in the infinitely thin kink limit.

This result is perhaps not so surprising: we have tried to take linear combinations of ϕ_0 as well as the massive fields $\phi_{1,q}$ to make a new massless one, and found that the only such field is actually ϕ_0. One could extend this analysis to include non-canonical kinetic terms for ρ_0, and possibly allow non-linear combinations of the fields $\phi_{0,1,q}$. But note that, if ρ_0 has an extra-dimensional profile, it can always be written as a *linear* combination of the basis, so the analysis presented here is actually quite general.

Manifestation of translation symmetry as a non-dynamical shift

The energy density ε_{ϕ_c} of the kink configuration $\phi_c(w)$ is independent of the location of the kink along the w-dimension. Thus, for a linear combination of the basis $\eta_{0,1,q}$ which just translates the kink profile, the corresponding linear combination of $\phi_{0,1,q}$ should have zero energy density. This statement needs to be made more precise, as we have just shown in the previous subsection that there is no linear combination of $\phi_{0,1,q}$ that has a vanishing potential. Instead, there exists a linear combination with a potential that vanishes only at a specific, constant (in x^μ) value of the field, corresponding to a shift of the kink. We proceed to determine this linear combination.

Consider the expansion

$$\Phi(x^M) = \phi_c(w) + \rho_0(x^\mu) s_0(w)\,, \tag{3.23}$$

where $s_0(w)$ is the profile of a finite shift of the kink, and $\rho_0(x^\mu)$ is the

corresponding four-dimensional field (unrelated to the previous ρ_0). For a given fixed shift of the kink Δw, we want to have the relation

$$\rho_0(x^\mu)s_0(w) = \phi_c(w + \Delta w) - \phi_c(w) \,. \tag{3.24}$$

For this to be true, ρ_0 must be an arbitrary constant, which we fix by normalising the profile $\int s_0^2(w)\, dw = 1$. This gives

$$s_0(w) = \sqrt{m}\, S\sigma_0(w) \,, \tag{3.25}$$

with

$$S = \frac{1}{2^{5/4}}\sqrt{\frac{\tanh\Delta z}{\Delta z - \tanh\Delta z}} \,, \tag{3.26a}$$

$$\sigma_0(w) = \frac{\tanh\Delta z\, \cosh^{-2} z}{1 + \tanh\Delta z\, \tanh z} \,. \tag{3.26b}$$

We have $z = mw/\sqrt{2}$ and $\Delta z = m\Delta w/\sqrt{2}$. For the combination $\rho_0 s_0$ to actually shift ϕ_c by an amount Δw, as given by (3.24), it is required that the field ρ_0 be a particular constant:

$$\rho_0(x^\mu) = \frac{m}{\sqrt{a}\, S} \,. \tag{3.27}$$

We now want to treat the field ρ_0 as a dynamical four-dimensional scalar degree of freedom. It will correspond to finite translations of the kink profile and we are interested in its behaviour in the thin kink limit. One can write ρ_0 as a linear combination of $\phi_{0,1,q}$, which can be determined from the linear combination needed to write s_0 in terms of $\eta_{0,1,q}$. It is then possible to determine the effective action for ρ_0 by substituting this combination in the Lagrangian (3.15). A simpler way to obtain the same result is to substitute (3.23) into the original five-dimensional action (3.1) and integrate out the extra dimension. The result is

$$\mathcal{S}_{\rho_0} = \int d^4x \left[-\varepsilon_{\phi_c} + \frac{1}{2}\partial^\mu\rho_0\partial_\mu\rho_0 - V_{\rho_0}(\rho_0) \right] \,, \tag{3.28}$$

with the effective potential

$$V_{\rho_0}(\rho_0) = \left(\frac{5}{2\tanh^2\Delta z} - \frac{5\tanh\Delta z}{6(\Delta z - \tanh\Delta z)} - \frac{3}{2} \right) \rho_0^2 \left(\sqrt{a} S\rho_0 - m \right)^2 \,. \tag{3.29}$$

Note that the potential for ρ_0 has two minima: one at $\rho_0 = 0$ and the other at precisely the value corresponding to the finite translation, given by (3.27). The energy density associated with ρ_0 is

$$\varepsilon_{\rho_0} = \frac{1}{2}(\partial_t \rho_0)^2 + \frac{1}{2}(\nabla \rho_0)^2 + V_{\rho_0}(\rho_0) \, . \tag{3.30}$$

Any dynamical behaviour of ρ_0 has non-zero, positive energy density. This energy density will vanish only when $\rho_0 = 0$ or ρ_0 is the constant (3.27) at all locations in the four-dimensional spacetime. This is the manifestation of the translation symmetry of the kink. The field ρ_0, or, equivalently, a specific linear combination of $\phi_{0,1,q}$, can assume this constant value at each point x^μ with zero energy cost. It is possible to show that the situation where the fields assume this value is equivalent to the situation where the original basis $\eta_{0,1,q}$ is shifted by the amount Δw.

So what happens to ρ_0 in the thin kink limit? The finite kink-translations that it represents should still be valid, and this is indeed the case. But these translations can only be made if the entire kink is shifted at once, corresponding to ρ_0 being a constant. This is because, in the thin kink limit, the potential V_{ρ_0} becomes infinitely steep and the dynamics of ρ_0 are frozen out, just as the ϕ_0 mode is. The only remnant of the translation symmetry at the effective, four-dimensional level is the fact that ρ_0 is allowed to be a certain constant value everywhere with no energy cost. But such a constant value has no physical consequence, and so the translation symmetry is hidden at the four-dimensional level. From this result, we make the interpretation that an infinitely thin kink is synonymous with an infinitely rigid one. Or, at the very least, this is true of the particular kink solution that we are studying in this chapter.

Collective coordinate expansion

There is an alternative way of expanding the five-dimensional field Φ, as opposed to equation (3.7), which explicitly accounts for translation invariance; it is known as the collective coordinate expansion; see Chapter 8 of Rajaraman [46]. (Such an expansion may not actually be completely general when the theory is considered to all orders, a point which shall be discussed later.) To illustrate the idea of a collective coordinate, consider a model with a complex scalar field $\chi(t, \vec{x})$ that respects a global U(1) symmetry

$\chi \to e^{i\alpha}\chi$. For any configuration of χ, the configuration $e^{i\alpha}\chi$ describes the same physics, has the same energy, and there will be a zero mode associated with such a symmetry. If we think of χ as the sum of a real field and an imaginary field, then multiplication by a phase mixes these two fields together, and the resulting real and imaginary parts are non-trivial combinations of their original counterparts. The idea of a collective coordinate is to change variables, or, in the case of field theory, to rewrite the fields, such that the action of the symmetry affects only a single field.

For the example of the U(1) symmetry, and the complex field χ, one first changes to polar fields via

$$\chi(t,\vec{x}) = \chi_r(t,\vec{x})e^{i\chi_\theta(t,\vec{x})} \,. \tag{3.31}$$

Now the U(1) symmetry acts by $\chi_\theta \to \chi_\theta + \alpha$, which is simpler than the original transformation because χ_r is left untouched. But the entity $\chi_\theta(t,\vec{x})$ is a field, and is hence an infinite set of time-dependent variables, one at each point $\vec{x}$ in space. The action of the U(1) symmetry adds the constant α to *all* of these variables, so we have not completely separated out the degree of freedom which corresponds precisely to the symmetry. We can actually arrange for the U(1) symmetry to affect only a single variable. The idea is to collect, or package, the constant component of the field χ_θ into a single variable:

$$\chi_0(t) = \frac{1}{(\text{volume})}\int \chi_\theta(t,\vec{x})d\vec{x} \,. \tag{3.32}$$

Here, $\chi_0(t)$ is the collective coordinate: a single variable which is the collection of the infinitely many variables $\chi_\theta(t,\vec{x})$ at different points in space (see equation (8.31) of Rajaraman [46]). We define the left-over field (or variables) as $\chi_{\tilde{\theta}}(t,\vec{x}) = \chi_\theta(t,\vec{x}) - \chi_0(t)$. The action of the U(1) symmetry is then $\chi_0 \to \chi_0 + \alpha$, and $\chi_{\tilde{\theta}}$ and χ_r are invariant.

We have just presented an example of an *explicit* collective coordinate, so called because $\chi_0(t)$ has an explicit formulation given by equation (3.32). Such a change of fields, from the complex valued χ to the real valued triple $(\chi_0, \chi_r, \chi_{\tilde{\theta}})$, is useful because the dynamics of the U(1) symmetry will not manifest in the analysis of χ_r and $\chi_{\tilde{\theta}}$.

Applying this idea to the translation symmetry of the kink, one aims to change fields such that the action of the translation affects only a single field. It turns out that one cannot explicitly define such a field, as was done

with χ_0, and so the definition is an implicit one, hence we work with implicit collective coordinates. In our analysis here, we follow closely Burnier and Zuleta [207]; see also Section 8.3 of Rajaraman [46].

Instead of our original basis expansion (3.7), consider the implicit collective coordinate expansion

$$\Phi(x^M) = \phi_c\left(w - Z(x^\mu)\right) + \sum_{i\neq 0} \tilde{\phi}_i(x^\mu)\eta_i\left(w - Z(x^\mu)\right) \,, \tag{3.33}$$

where $Z(x^\mu)$ is the implicitly defined collective coordinate, and replaces the zero mode $\phi_0(x^\mu)$, hence the sum over i does *not* include the mode η_0. Note that the $\eta_{1,q}$ are the same as before, but their corresponding four-dimensional partner fields $\tilde{\phi}_{1,q}$ are in general different from the original $\phi_{1,q}$. This definition is now used to expand the action (3.1) to get

$$\begin{aligned}
\mathcal{S}_\Phi = \int d^4x \Big\{ & -\varepsilon_{\phi_c} + \frac{1}{2}\varepsilon_{\phi_c}\partial^\mu Z\partial_\mu Z + \frac{1}{2}\partial^\mu\tilde{\phi}_1\partial_\mu\tilde{\phi}_1 - \frac{3}{4}m^2\tilde{\phi}_1^2 \\
& + \int_{-\infty}^{\infty} dq \left[\frac{1}{2}\partial^\mu\tilde{\phi}_q^*\partial_\mu\tilde{\phi}_q - \frac{1}{4}(q^2+4)m^2\tilde{\phi}_q^*\tilde{\phi}_q\right] \\
& - \sum_{i,j,k\neq 0}\kappa^{(3)}_{ijk}\tilde{\phi}_i\tilde{\phi}_j\tilde{\phi}_k - \sum_{i,j,k,l\neq 0}\kappa^{(4)}_{ijkl}\tilde{\phi}_i\tilde{\phi}_j\tilde{\phi}_k\tilde{\phi}_l \\
& + \sum_{i\neq 0}\pi_i^{(a)}\tilde{\phi}_i\partial^\mu Z\partial_\mu Z + \sum_{i,j\neq 0}\pi_{ij}^{(b)}\tilde{\phi}_i\tilde{\phi}_j\partial^\mu Z\partial_\mu Z \\
& + \sum_{i,j\neq 0}\pi_{ij}^{(c)}\tilde{\phi}_i\partial^\mu\tilde{\phi}_j\partial_\mu Z\Big\} \,,
\end{aligned} \tag{3.34}$$

where $\kappa^{(3)}_{ijk}$ and $\kappa^{(4)}_{ijkl}$ are defined as per (3.16), and

$$\pi_i^{(a)} = \int_{-\infty}^{\infty}\phi_c'\eta_i'\,dw \,, \tag{3.35a}$$

$$\pi_{ij}^{(b)} = \frac{1}{2}\int_{-\infty}^{\infty}\eta_i'\eta_j'\,dw \,, \tag{3.35b}$$

$$\pi_{ij}^{(c)} = \int_{-\infty}^{\infty}\eta_i\eta_j'\,dw \,. \tag{3.35c}$$

The effective four-dimensional action (3.34) is to be compared with the action obtained using our original expansion, equations (3.14) and (3.15). The terms describing the massive modes $\tilde{\phi}_{1,q}$ and their self-interactions (with

coefficients $\kappa^{(3,4)}$) are equivalent to the description of the fields $\phi_{1,q}$. The differences between the two formalisms are in the description of the zero mode. In the case at hand, the field Z does not have any potential terms, and couples to the massive modes $\tilde{\phi}_{1,q}$ only via derivatives $\partial_\mu Z$. When the thin kink limit is taken, all of the massive modes are frozen out, along with their coupling to derivatives of Z, and we are left with the action

$$\mathcal{S}_\Phi = \int d^4x \left[-\varepsilon_{\phi_c} + \frac{1}{2}\varepsilon_{\phi_c} \partial^\mu Z \partial_\mu Z \right] . \tag{3.36}$$

Recall that the energy density ε_{ϕ_c} remains finite in the thin kink limit, so, after the field redefinition $\tilde{Z} = \sqrt{\varepsilon_{\phi_c}}\, Z$, we see that this action describes a single, four-dimensional, massless scalar field.

The question now is: are the two formalisms for expanding Φ — the mode expansion (3.7) and the implicit collective coordinate expansion (3.33) — equivalent or inequivalent? If they are equivalent, which is the correct picture? Which expansion allows us to correctly interpret the zero mode as a physical field, with associated interactions? Is it $\phi_0(x^\mu)$ or $\tilde{Z}(x^\mu)$ that manifests in the effective four-dimensional theory? If they are equivalent, and if we believe that Z must be defined *implicitly*, through equation (3.33), then we should not be able to find any *explicit* combination, linear or otherwise, of $\phi_{0,1,q}$ which behaves as Z does. If this is the case, then what is wrong with our mode expansion (3.7), which should provide a completely general way of expanding an arbitrary five-dimensional field Φ?

We suspect that maybe these two formalisms are actually inequivalent. Our main motivation for this suspicion is that the collective coordinate expansion (3.33) is not general enough to express an arbitrary field $\Phi(x^M)$. For example, there are no choices of $Z(x^\mu)$ and $\tilde{\phi}_{1,q}$ which yield $\Phi(x^M) = \omega(x^\mu)\eta_0(w)$ for any $\omega(x^\mu)$. If there were, then we could write

$$\omega(x^\mu)\eta_0(w) = \phi_c(w - Z) + \sum_{i\neq 0} \tilde{\phi}_i(x^\mu)\eta_i(w - Z) . \tag{3.37}$$

Keep in mind that Z may depend on x^μ, we have just neglected to write this explicitly to keep the equation clear. Now, multiply through by $\eta_0(w - Z)$

and integrate over w:

$$\omega(x^\mu)\int \eta_0(w)\eta_0(w-Z)\,dw = \int \phi_c(w-Z)\eta_0(w-Z)\,dw + \sum_{i\neq 0}\tilde{\phi}_i(x^\mu)\int \eta_i(w-Z)\eta_0(w-Z)\,dw\,. \tag{3.38}$$

There is the freedom to shift the integrals on the right-hand-side by Z, and then, because η_0 is orthogonal to ϕ_c and $\eta_{1,q}$, we have

$$\omega(x^\mu)\int \eta_0(w)\eta_0(w-Z(x^\mu))\,dw = 0\,, \tag{3.39}$$

Since the integral in this equation will always be positive, regardless of the form of $Z(x^\mu)$, it must be that $\omega(x^\mu)=0$. Hence we have shown that the implicit collective coordinate expansion (3.33) cannot faithfully represent all possible forms of Φ, and so is less general than the mode expansion (3.7). In fact, our argument here demonstrates that by using collective coordinates, one has forbidden excitations corresponding to the zero mode η_0 from the outset!

The implicit collective coordinate expansion (3.33) may be useful in certain contexts, for example, where one is only interested in expanding a model up to a given order in perturbation theory. This is actually the case for the discussions in Rajaraman [46], where models are quantised around a classical ground state (like the kink), and perturbation theory is used to analyse the quantum excitations. In the scenario presented in this chapter, we consider the full, non-linear theory *exactly*, and in a classical context only, so perhaps it is not suitable to use the collective coordinate approach here.

Summary of unresolved issues regarding the kink zero mode

We strongly suspect that our exact treatment of the expansion of the modes of the kink, given by equation (3.7), is the correct way of analysing the dynamics of the kink. Furthermore, we believe that the zero mode ϕ_0 freezes out in the thin kink limit, as do all the massive fields. The only remnant of the translation symmetry at the four-dimensional level is a certain combination of fields taking on a certain constant value with no energy cost, corresponding to a finite shift of the infinitely thin kink. Such a constant con-

figuration has no physical consequence, and so the effective four-dimensional action contains only the energy density ε_{ϕ_c}. For the rest of this chapter, we are going to assume that this is in fact what happens.

Finally, we would like to point out that it is not clear that energy density and rigidity have a definite relationship, at least in the context of a kink. The energy density is defined by equation (3.5), and is an effective four-dimensional quantity accounting for the energy in the background kink configuration per unit four-volume. This is sometimes referred to as the tension of the brane, particularly when talking about fundamental branes. Calling the energy density the tension makes it quite easy to confuse energy density and rigidity. We would be inclined to suggest that rigidity is *not* the same as energy density (or tension), but is instead related to the malleability of the brane. For the kink considered in this chapter, the rigidity is perhaps related to the mass of the scalar field which forms the domain-wall, Φ, and when this mass is taken to infinity, it becomes impossible to deform the kink solution, even though the energy density is finite. One avenue to pursue, which may resolve this issue more clearly, is to consider a kink model with more parameters (more than just a and m) and see if one can arrange to have a finite energy density, zero width, and also a finite rigidity. In such a scenario, we would expect the zero mode associated with translations to survive in the thin kink limit.

3.2 Adding a scalar field

We have so far performed an analysis of the kink and its modes in isolation. As stated previously, we aim to use the properties of the domain wall to dynamically trap five-dimensional fields to a brane and create an effective four-dimensional model. We can achieve this if the kink is coupled to a different five-dimensional field and projects out a set of modes with the lowest mode separated from the rest by a significant mass gap. Then, if we are at energies where only the lowest bound state can be excited, the degree of freedom of propagation along the extra dimension has been lost and the bound mode is confined.

3.2.1 Scalar modes

The simplest place to start is to take another five-dimensional scalar field $\Xi(x^M)$ and couple it to the kink field. The action describing this model is the

sum of the action for Φ and an action for the new field Ξ, $\mathcal{S}_{\Phi+\Xi} = \mathcal{S}_\Phi + \mathcal{S}_\Xi$, where

$$\mathcal{S}_\Xi = \int d^5x \left[\frac{1}{2}\partial^M \Xi \partial_M \Xi - \frac{ab(b+1)}{4m}\Phi^2\Xi^2 - W(\Xi) \right] , \tag{3.40}$$

with potential

$$W(\Xi) = \frac{n^2}{2}\Xi^2 + \frac{c}{4n}\Xi^4 . \tag{3.41}$$

The parameters b and c are dimensionless, while the dimensionful parameter n is the mass of Ξ. We have chosen a strange looking Yukawa coupling constant for the $\Phi^2\Xi^2$ term because b has a physical meaning, which we elaborate on later. Note that the discrete $\mathbb{Z}_2$ symmetry $\Phi \to -\Phi$ is respected by this new action, as is the additional, independent $\mathbb{Z}_2$ symmetry $\Xi \to -\Xi$.

Following the analysis for the kink modes, we perform the general Fourier expansion

$$\Xi(x^M) = \sum_i \xi_i(x^\mu) k_i(w) , \tag{3.42}$$

where the sum over i can again be a combination of discrete and continuous parts. To obtain a suitable basis $k_i(w)$, we look at the linearised equation of motion for $\Xi(x^M)$ with $\Phi(x^M) = \phi_c(w)$:

$$\left(\partial^\mu \partial_\mu - \partial_w^2 + \frac{ab(b+1)}{2m}\phi_c^2 + n^2 \right) \xi_i k_i = 0 . \tag{3.43}$$

We want $\xi_i(x^\mu)$ to satisfy the four-dimensional Klein-Gordon equation with mass δ_i. This leads to

$$\left(-\frac{d^2}{dz^2} + b(b+1)\tanh^2 z \right) k_i = \left(\frac{2(\delta_i^2 - n^2)}{m^2} \right) k_i , \tag{3.44}$$

where $z = mw/\sqrt{2}$ as before. This Schrödinger-like equation has the same form as the one obtained for the kink modes, equation (3.10). We see that the kink sets up a symmetric modified Pöschl-Teller potential well which traps not only its own modes, but also those of a coupled scalar field. Looking to Appendix C we see that the basis k_i contains $\lceil b \rceil$ bound modes[4] (which justifies our choice for the strange Yukawa coupling constant) and a

[4] We use the standard notation $\lceil . \rceil$ for the ceiling function.

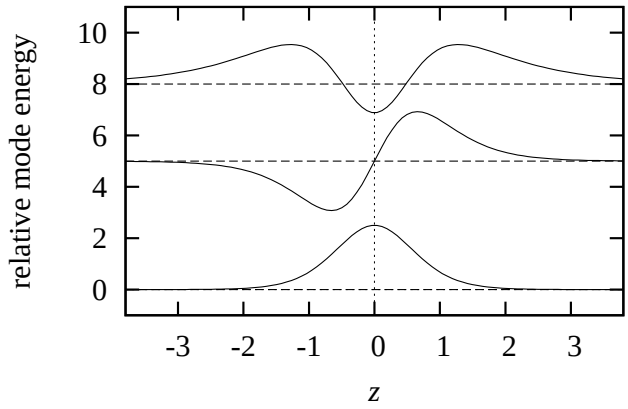

Figure 3.2: Typical extra-dimensional profiles for the lowest, discrete, bound states arising from a scalar field coupled to a kink. We have chosen $b = 3$ and $n^2 = -3m^2/2$. The modes are $k_0(w)$ at the bottom, followed by $k_1(w)$ then $k_2(w)$, plotted against the dimensionless extra-dimensional coordinate $z = mw/\sqrt{2}$.

continuum. The masses of the bound states are

$$\delta_0^2 = n^2 + \frac{1}{2}bm^2 \,, \tag{3.45a}$$

$$\delta_1^2 = n^2 + \frac{1}{2}(3b-1)m^2 \,, \tag{3.45b}$$

$$\delta_2^2 = n^2 + \frac{1}{2}(5b-4)m^2 \,, \tag{3.45c}$$

$$\vdots$$

$$\delta_i^2 = n^2 + \frac{1}{2}((2i+1)b - i^2)m^2 \,, \tag{3.45d}$$

and for the continuum we have

$$\delta_q^2 = n^2 + \frac{1}{2}\left(q^2 + b(b+1)\right)m^2 \,, \tag{3.46}$$

where $q \in \mathbb{R}$ labels the continuum modes. Unlike the modes of the kink, this spectrum of masses does not in general include a zero mode and the bottom of the spectrum is dependent on the parameters n, b and m. We also have the freedom to change the sign of n^2 in the original action and dial up any positive, zero, or negative value for the mass δ_0^2 of the ground state. We will not give explicit forms of the functions k_i; they are easily determined from Appendix C. Instead, we provide a plot of the discrete profiles k_0, k_1 and k_2 for the case where $b = 3$ and n^2 is chosen such that $\delta_0^2 = 0$; see Figure 3.2.

As before, we use the basis k_i to expand Ξ in the original action (3.40) and integrate over the extra dimension. Including the kink sector, the effective four-dimensional action is then

$$\mathcal{S}_{\Phi+\Xi} = \int d^4x \left[-\varepsilon_{\phi_c} + \mathcal{L}_\phi + \mathcal{L}_\xi\right], \tag{3.47}$$

where the kink-only part $\mathcal{L}_\phi$ is given by equation (3.15), and the Lagrangian for the additional coupled scalar is

$$\begin{aligned}\mathcal{L}_\xi = &\sum_{i=0}^{\lceil b-1\rceil}\left[\frac{1}{2}\partial^\mu\xi_i\partial_\mu\xi_i - \frac{1}{2}\delta_i^2\xi_i^2\right] + \int_{-\infty}^{\infty} dq\left[\frac{1}{2}\partial^\mu\xi_q\partial_\mu\xi_q - \frac{1}{2}\delta_q^2\xi_q^2\right] \\ &- g^{(3)}_{ijk}\phi_i\xi_j\xi_k - g^{(4)}_{ijkl}\phi_i\phi_j\xi_k\xi_l - \tau_{ijkl}\xi_i\xi_j\xi_k\xi_l\,.\end{aligned} \tag{3.48}$$

The Yukawa and self-coupling factors are

$$g^{(3)}_{ijk} = \frac{ab(b+1)}{2m}\int_{-\infty}^{\infty}\phi_c\eta_i k_j k_k\, dw\,, \tag{3.49a}$$

$$g^{(4)}_{ijkl} = \frac{ab(b+1)}{4m}\int_{-\infty}^{\infty}\eta_i\eta_j k_k k_l\, dw\,, \tag{3.49b}$$

$$\tau_{ijkl} = \frac{c}{4n}\int_{-\infty}^{\infty} k_i k_j k_k k_l\, dw\,. \tag{3.49c}$$

With this expanded four-dimensional action, we are ready to analyse the various limits of the model with the scalar field.

3.2.2 The thin kink with a scalar field

In this subsection we consider the combined five-dimensional action $\mathcal{S}_{\Phi+\Xi} = \mathcal{S}_\Phi + \mathcal{S}_\Xi$ and the various limits that arise through m, the mass of the kink. As discussed previously, we have three scenarios which are characterised by the sign of μ. In the case $\mu < 0$ there is no kink and we are left with two interacting five-dimensional fields Φ and Ξ. The thick kink scenario, $\mu = 0$, has many interacting four-dimensional scalar fields, the details given by the mass spectra of ϕ_i and ξ_i and the couplings κ, g and τ. We will not dwell on these two cases, but instead concentrate our attention on the thin kink limit and explore the parameter space of b, c and n.

It was shown in Section 3.1.2 that the thin kink limit leaves only the energy density of the domain wall in the effective four-dimensional action

(assuming the zero mode of translation is truly frozen out). The dynamics of all the scalar modes ϕ_i are removed and so the $g^{(3)}$ and $g^{(4)}$ Yukawa terms in (3.48) are eliminated.[5] With $m \to \infty$ and b finite, the masses of all the ξ_i modes will also tend to infinity and the scalar Ξ becomes completely frozen out. To leave some remnant of Ξ in the model we have two choices: either take b to zero to counter m^2, or choose n^2 such that it cancels $\frac{1}{2}bm^2$.

For the first choice, let n be finite and $b = \tilde{b}\Lambda^\beta$. Then $\delta_0^2 \sim \Lambda^{\beta+2\mu}$ and the mode ξ_0 has finite mass if $\beta + 2\mu \leq 0$. Since $b \to 0$ in the limit $\Lambda \to \infty$, there are in fact no bound modes, the basis k_i is not valid and we must consider Ξ as a five-dimensional field. The effective action for such a limit of the parameters is[6]

$$\mathcal{S}^{5\mathrm{D}}_{\Phi+\Xi} = \int d^4x \left[-\varepsilon_{\phi_c}\right] + \int d^5x \left[\frac{1}{2}\partial^M \Xi \partial_M \Xi - \frac{1}{4}bm^2\Xi^2 - W(\Xi)\right] . \quad (3.50)$$

We see that the five-dimensional field Ξ has nothing dynamical to couple to, and just picks up an addition to its Ξ^2 term. If we have the strict inequality $\beta + 2\mu < 0$, this addition to the mass will be zero.

The second choice which keeps some part of Ξ alive is to change the sign of n^2 and fine tune it to exactly cancel the infinite term in δ_0^2. An exact cancellation would render the mode ξ_0 massless; we can be more general and allow a finite mass to remain by choosing

$$n^2 = -\frac{1}{2}bm^2 + n_0^2 \,, \quad (3.51)$$

where n_0 is finite. Let us briefly comment on the situation where $b \to 0$, but not quickly enough to counter m (thus $-2\mu < \beta < 0$) and so we must choose n^2 as in equation (3.51). In this case there are again no bound modes and Ξ is a five-dimensional field with equivalent physics as described by (3.50), except the quadratic term of the generated potential is replaced by $\frac{1}{2}n_0^2\Xi^2$.

We can now restrict our analysis to the case where $\beta \geq 0$ and n^2 is of the form given by (3.51). As we have a non-zero b, there is at least one bound mode, and, in fact, only the lowest bound mode will have finite mass. The

[5] Section 3.1.3 established that the translation symmetry manifests as a linear combination of $\phi_{0,1,q}$ which can assume a non-zero constant value with zero energy cost, even in the thin kink limit. One can show that this contribution to the Yukawa terms is counteracted by shifting the k_i basis to align with the shifted kink, and then redefining ξ_i.

[6] This result uses $\tanh^2(mw/\sqrt{2}) \to 1$ as $m \to \infty$, which ignores the fact that the distribution vanishes on a set of measure zero at the origin.

dynamics of the higher bound modes and the continuum will not be part of the model as their corresponding masses are infinite. With only ξ_0 alive, the quartic coupling terms reduce to just the one with the factor τ_{0000}. Putting all these pieces together we arrive at the four-dimensional action

$$\mathcal{S}^{4\mathrm{D}}_{\Phi+\Xi} = \int d^4x \left[-\varepsilon_{\phi_c} + \frac{1}{2}\partial^\mu \xi_0 \partial_\mu \xi_0 - W_0(\xi_0) \right] , \tag{3.52}$$

with

$$W_0(\xi_0) = \frac{1}{2} n_0^2 \xi_0^2 + \frac{c}{4\sqrt{2\pi}} \frac{\sqrt{2}\,\Gamma^2(b+\frac{1}{2})\Gamma(2b)}{\sqrt{b}\,\Gamma^2(b)\Gamma(2b+\frac{1}{2})} \xi_0^4 \,. \tag{3.53}$$

For large values of b, this potential simplifies to

$$W_0(\xi_0) \xrightarrow{b\to\infty} \frac{1}{2} n_0^2 \xi_0^2 + \frac{c}{4\sqrt{2\pi}} \xi_0^4 \,. \tag{3.54}$$

This analysis shows that in the thin kink limit, a five-dimensional coupled scalar field is projected down to a single, localised, four-dimensional scalar field ξ_0. As the parameters n_0 and c are arbitrary, one can generate a phenomenologically suitable potential for ξ_0, in particular the sign of n_0^2 can be changed to yield a potential which encourages a non-zero vacuum expectation value. We mention two uses of this. Most obviously this mechanism can be used to localise the standard model electroweak Higgs field to a brane, and it should be no trouble to arrange Yukawa couplings to fermion fields for mass generation. We utilise such a method in Chapter 5 when we construct our domain-wall localised standard model.

Our second application of a localised scalar is the following. Notice that the effective potential $W_0(\xi_0)$ has the same form as the kink potential $V(\Phi)$ and can thus support a domain-wall solution. This leads to the idea of nested domain walls, which have been explored previously by Morris [208] in the context of cosmological defects. For the case of a nested brane world, generated by domain walls, consider a six-dimensional model with the two scalar fields Φ and Ξ and a suitable potential. One can use Φ to generate a domain wall and an effective five-dimensional action, and then use the lowest projected mode of Ξ in the same way to generate an effective four-dimensional action. The method used does not depend on the dimensionality and one is free to generate an arbitrary number of nestings. When actually calculating the background configuration generated by multiple scalar fields, one must

solve all the Euler-Lagrange equations of motion self-consistently, or ensure that the energy scales associated with each kink form a large hierarchy, to prevent the formation of the interior kink from de-stabilising its parent. Of course, this mechanism just deals with the formation of the domain wall. The non-trivial exercise is to check that gravity can be broken down in similar stages, and made to reproduce four-dimensional general relativity; this will not be attempted here, but see [147, 148, 149] for derivations of the Randall-Sundrum warped metric in the presence of nested and intersecting fundamental branes.

3.3 Adding a fermion field

In the previous section we performed a full analysis of the modes of a five-dimensional scalar field coupled to a kink. We showed that in the thin kink limit, an effective four-dimensional scalar field remains and could be potentially useful for model building. In direct analogy with this analysis we now consider a five-dimensional massless fermion with Yukawa coupling to Φ, find a suitable basis for decomposition, and investigate the limiting behaviour. This is a generalisation of the result first obtained by Rubakov and Shaposhnikov [45], which we discussed at length in Section 1.3.1. In fact, the four-dimensional, massless, chiral fermion that emerges in the Rubakov and Shaposhnikov set-up is exactly the lowest mode of the Kaluza-Klein tower that arises in the more general situation that we consider here. For a partially analytic analysis of massive fermion modes confined to a thick brane in the presence of gravity, see [187].

3.3.1 Fermion modes

Fermions in five-dimensions are four-component spinors and their Dirac structure is described by Γ^M $(M = 0, 1, 2, 3, 5)$ with $\{\Gamma^M, \Gamma^N\} = 2\eta^{MN}$. Specifically, we take $\Gamma^\mu = \gamma^\mu$ and $\Gamma^5 = -i\gamma^5$ where $\gamma^{\mu,5}$ are the usual gamma matrices in the Dirac representation. Our action for a massless, five-dimensional fermion $\Psi(x^M)$ coupled to the kink is $\mathcal{S}_{\Phi+\Psi} = \mathcal{S}_\Phi + \mathcal{S}_\Psi$ where the fermion action is

$$\mathcal{S}_\Psi = \int d^5x \left[\overline{\Psi} i \Gamma^M \partial_M \Psi - \sqrt{\frac{ad^2}{2m}}\, \Phi \overline{\Psi} \Psi \right] . \tag{3.55}$$

The kink parameters a and m are the same as before and d is a dimensionless coupling parameter. The Yukawa coupling constant is chosen to take an unusual form so that d represents the number of bound fermion modes, in analogy with b in the coupled scalar field case; this will be demonstrated shortly. The discrete $\mathbb{Z}_2$ symmetry takes $\Phi \to -\Phi$, so, under this symmetry, the fermion field must transform in such a way as to obtain $\overline{\Psi}\Psi \to -\overline{\Psi}\Psi$ but at the same time keep the kinetic term invariant. This can be accomplished by extending the action of the kink $\mathbb{Z}_2$ symmetry to include $w \to -w$ and $\Psi \to i\Gamma^5\Psi$. (Note that $w \to -w$ does not destroy the invariance of the scalar field kinetic terms.) This symmetry then forbids a mass term for the five-dimensional Ψ.

As with the scalar field Ξ, we expect the extra-dimensional behaviour of Ψ to be quite different to the four-dimensional part. Also, because of the Dirac structure of the fifth gamma matrix, $\Gamma^5 = -i\gamma^5$, we expect left- and right-handed projections of the four-dimensional part to behave differently. Thus we choose the general Fourier expansion

$$\Psi(x^\mu, w) = \sum_i \psi_{Li}(x^\mu) f_{Li}(w) + \sum_i \psi_{Ri}(x^\mu) f_{Ri}(w)\,, \tag{3.56}$$

where the $f_{Li}(w)$ and $f_{Ri}(w)$ are a fixed basis, the $\psi_i(x^\mu)$ are dynamical four-dimensional fields, $\gamma^5\psi_{Li} = -\psi_{Li}$, $\gamma^5\psi_{Ri} = \psi_{Ri}$ and the sum over i includes both discrete and continuous modes. To obtain the defining equations for the basis functions f_i, we impose that the ψ_i satisfy the massive Dirac equation by $i\partial\!\!\!/\psi_{Li} = \sigma_i\psi_{Ri}$ and $i\partial\!\!\!/\psi_{Ri} = \sigma_i\psi_{Li}$, where σ_i is the mass of the four-dimensional mode corresponding to the pair of spinors ψ_{Li} and ψ_{Ri}. Then, substituting the expansion (3.56) into the Dirac equation for Ψ (not given; its form is obvious from the action (3.55)), we arrive at

$$\begin{aligned}&\psi_{Li}\left(-\partial_w f_{Li} + f_{Ri}\sigma_i - \sqrt{\frac{ad^2}{2m}}\phi_c f_{Li}\right)\\ &+ \psi_{Ri}\left(\partial_w f_{Ri} + f_{Li}\sigma_i - \sqrt{\frac{ad^2}{2m}}\phi_c f_{Ri}\right) = 0\,.\end{aligned} \tag{3.57}$$

Since left and right Dirac components are independent and the ψ_i are arbitrary fields, both of the two parenthesised factors in equation (3.3.1)

must be zero. Hence the f_{Li} and f_{Ri} must satisfy a set of two first order coupled ordinary differential equations. We turn these equations into two uncoupled, second-order equations:

$$\left(-\frac{d^2}{dz^2} + d(d+1)\tanh^2 z - d\right) f_{Li} = \frac{2\sigma_i^2}{m^2} f_{Li}\,, \tag{3.58a}$$

$$\left(-\frac{d^2}{dz^2} + d(d-1)\tanh^2 z + d\right) f_{Ri} = \frac{2\sigma_i^2}{m^2} f_{Ri}\,. \tag{3.58b}$$

Again, as with the scalar field, we see that the kink sets up a symmetric modified Pöschl-Teller potential well which traps the extra-dimensional component of the fermion field. This has been noted in a similar context of fat branes in [209], and in the context of a two-dimensional Dirac equation in [210]. We use Appendix C of this thesis to obtain the solutions. The bound modes come in pairs; their masses and extra-dimensional profiles are given by

$$(\sigma_0^d)^2 = 0 \qquad \begin{cases} f_{L0}^d(w) = F_{L0}^d \cosh^{-d} z \\ f_{R0}^d(w) = 0\,, \end{cases} \tag{3.59a}$$

$$(\sigma_1^d)^2 = \frac{1}{2}(2d-1)m^2 \qquad \begin{cases} f_{L1}^d(w) = F_{L1}^d \sinh z \cosh^{-d} z \\ f_{R1}^d(w) = F_{R1}^d \cosh^{-d+1} z\,, \end{cases} \tag{3.59b}$$

$$\vdots$$

$$(\sigma_n^d)^2 = \frac{1}{2}(2nd - n^2)m^2 \qquad \begin{cases} f_{Ln}^d(w) = \dfrac{1}{\sigma_n^d}\left(\dfrac{dm}{\sqrt{2}}\tanh z - \dfrac{d}{dw}\right) f_{L,n-1}^{d-1} \\ f_{Rn}^d(w) = f_{L,n-1}^{d-1}(w)\,. \end{cases} \tag{3.59c}$$

These bound state modes are valid for all positive values of d and there are $\lceil d \rceil$ sets of modes.

For the continuum, the solutions can be found in terms of standard functions when d is a positive integer. We present here the solutions when $d = 1$ and $d = 2$ (corresponding to one and two bound states, respectively, lying below the given continuum), and a recurrence relation for larger integer

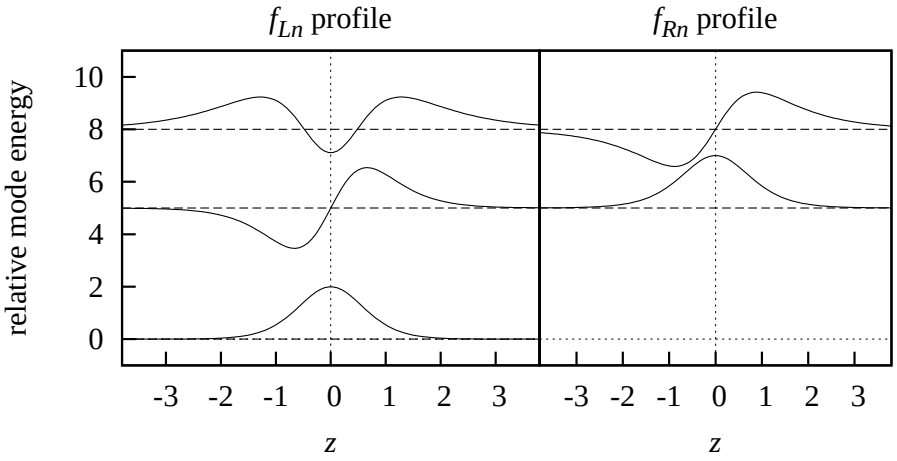

Figure 3.3: Extra-dimensional profiles for the massless, left-handed four-dimensional fermion, and two massive fermions, which arise when a five-dimensional fermion is coupled to a kink. For these plots we have taken $d = 3$. In the left panel are the left-handed modes $f_{L0}(w)$, $f_{L1}(w)$ and $f_{L2}(w)$, and in the right panel are the right-handed modes $f_{R1}(w)$ and $f_{R2}(w)$, plotted against the dimensionless extra-dimensional coordinate $z = mw/\sqrt{2}$.

values of d:

$$(\sigma_q^1)^2 = \frac{1}{2}(q^2+1)m^2 \qquad \begin{cases} f_{Lq}^1(w) = F_{Lq}^1 e^{iqz}\,(\tanh z - iq) \\ f_{Rq}^1(w) = F_{Rq}^1 e^{iqz}\,, \end{cases} \tag{3.60a}$$

$$(\sigma_q^2)^2 = \frac{1}{2}(q^2+4)m^2 \qquad \begin{cases} f_{Lq}^2(w) = F_{Lq}^2 e^{iqz}\left(3\tanh^2 z - (q^2+1) - 3iq\tanh z\right) \\ f_{Rq}^2(w) = F_{Rq}^2 e^{iqz}\,(\tanh z - iq)\,, \end{cases} \tag{3.60b}$$

$$\vdots$$

$$(\sigma_q^d)^2 = \frac{1}{2}(q^2+d^2)m^2 \qquad \begin{cases} f_{Lq}^d(w) = \dfrac{1}{\sigma_n^d}\left(\dfrac{dm}{\sqrt{2}}\tanh z - \dfrac{d}{dw}\right) f_{Lq}^{d-1} \\ f_{Rq}^d(w) = f_{Lq}^{d-1}(w)\,. \end{cases} \tag{3.60c}$$

As in previous equations, the real parameter q selects a particular continuum mode. The normalisation coefficients F_L^d and F_R^d can be computed with the help of Appendix C, specifically equation (C.7). Figure 3.3 is a plot of the discrete left- and right-handed extra-dimensional profiles, given by the equations (3.59), for the case where $d = 3$.

Using these basis functions, we expand the original action (3.55) and integrate over the extra dimension. The effective four-dimensional action, including the kink dynamics, is

$$\mathcal{S}_{\Phi+\Psi} = \int d^4x \left[-\varepsilon_{\phi_c} + \mathcal{L}_\phi + \mathcal{L}_\psi\right] , \tag{3.61}$$

where the Lagrangian for the expanded Ψ is

$$\begin{aligned}\mathcal{L}_\psi = \overline{\psi_{L0}} i\partial\!\!\!/ \psi_{L0} + \sum_{i=1}^{\lceil d-1\rceil} \overline{\psi_i}(i\partial\!\!\!/ - \sigma_i)\psi_i + \int_{-\infty}^{\infty} dq \left[\overline{\psi_q}(i\partial\!\!\!/ - \sigma_q)\psi_q\right] \\ - h_{jkl}\,\phi_j\,\overline{\psi_{Lk}}\,\psi_{Rl} - h^*_{jlk}\,\phi^*_j\,\overline{\psi_{Rk}}\,\psi_{Ll} \,.\end{aligned} \tag{3.62}$$

We have condensed the notation using $\psi_i = \psi_{Li} + \psi_{Ri}$ and similarly for ψ_q. For brevity in the Yukawa terms, the implicit sum over $j = 0, 1$ denotes a sum over the bound scalar modes ϕ_j and an integral over the continuum modes ϕ_q; similarly the sums over k and l denote sums over bound and continuum fermion modes. The effective dimensionless Yukawa coupling is

$$h_{jkl} = \sqrt{\frac{ad^2}{2m}} \int_{-\infty}^{\infty} \eta_j f^*_{Lk} f_{Rl}\, dw \,. \tag{3.63}$$

We can compute these h_{jkl}. Those of importance are the couplings between the bound kink modes and the bound fermion modes, the first few being

$$h_{0i0} = 0 \qquad (\text{for all } i)\,, \tag{3.64a}$$

$$h_{001} = \sqrt{\frac{3a}{8\sqrt{2}}} \left(\frac{d-\frac{1}{2}}{d-1}\right)^{\frac{3}{2}} \frac{\Gamma^2(d-\frac{1}{2})}{\Gamma^2(d-1)}\,, \tag{3.64b}$$

$$h_{011} = h_{101} = 0, \tag{3.64c}$$

$$h_{111} = \sqrt{\frac{3a}{8\sqrt{2}}} \frac{(d-\frac{1}{2})^{\frac{1}{2}}}{d-1} \frac{\Gamma^2(d-\frac{1}{2})}{\Gamma^2(d-1)}\,. \tag{3.64d}$$

This analysis includes the well known chiral zero mode localisation when all fermion modes except ψ_{L0} are removed from (3.62). In this reduced model, there are no Yukawa couplings between ψ_{L0} and any of the kink modes ϕ_i due to the chirality of the fermion mode.

3.3.2 Kink limits with a coupled fermion field

With the effective, four-dimensional description of the bulk fermion Ψ, equations (3.61) and (3.62), we can now consider the limits of the kink and the fate of the fermion modes. With no kink ($\mu < 0$) the basis f_i is not valid and we instead obtain a model containing the coupled five-dimensional fields Φ and Ψ. The thick kink scenario ($\mu = 0$) contains the bound-state, four-dimensional scalars ϕ_i and fermions ψ_i, the continuum modes ϕ_q and ψ_q, and couplings between these fields. The third limit, the thin kink limit ($\mu > 0$), is what we are most interested in, where the remnant of the kink sector is just the energy density (assuming the kink zero mode is frozen out). Then the Yukawa term in (3.55), which couples Ψ to Φ, reduces to simply a coupling of Ψ to the classical kink background:

$$\sqrt{\frac{ad^2}{2m}}\,\Phi\overline{\Psi}\Psi = \frac{|dm|}{\sqrt{2}}\tanh^2(z)\,\overline{\Psi}\Psi\,, \tag{3.65}$$

and we have only the parameter d left to play with. There are four scenarios, corresponding to different limiting behaviours of d, and we classify these using the previous technique for parameterising limits by writing $d = \tilde{d}\Lambda^\delta$, where $\tilde{d}$ is finite and $\Lambda \to \infty$.

In the first scenario, with $\delta = -\mu$ and so $d \to 0$, there are no bound fermion modes, and the fermion is left as a five-dimensional field with the action

$$\mathcal{S}^{\text{5D}}_{\Phi+\Psi} = \int d^4x\,[-\varepsilon_{\phi_c}] + \int d^5x\left[\overline{\Psi}i\Gamma^M\partial_M\Psi - \frac{|dm|}{\sqrt{2}}\theta(w)\overline{\Psi}\Psi\right]\,, \tag{3.66}$$

where $\theta(w)$ is the step function. The fermion in this case has an unusual mass term that changes sign across the kink. For the second scenario, with $\delta < -\mu$, we have the same situation as in the first scenario, except the mass term disappears. Third, if $-\mu < \delta < 0$, d is not going to zero fast enough to counter m, and the unusual mass term becomes infinite. In this case, the five-dimensional field Ψ is thus frozen out and we are left with just the kink energy density in our effective theory.

The fourth scenario is the most interesting to us. It has $\delta \geq 0$, and so $d > 0$ and there is at least one bound fermion mode. Because the masses of these modes go like m, all modes are frozen out *except* for the zero mode ψ_{L0}. None of the Yukawa couplings h are relevant because they couple ψ_{L0}

to higher fermion modes which are not dynamical. The effective action is then simply

$$\mathcal{S}^{\mathrm{4D}}_{\Phi+\Psi} = \int d^4x \left[-\varepsilon_{\phi_c} + \overline{\psi_{L0}} i \partial\!\!\!/ \psi_{L0} \right] , \tag{3.67}$$

which contains the dynamics of a single, four-dimensional, chiral, massless fermion, along with the energy density of the kink ε_{ϕ_c}. Thus we obtain the result of Rubakov and Shaposhnikov [45] in the thin kink limit with $d > 0$. This is of obvious importance in model building, where chiral zero modes are the basic ingredients for constructing theories with fermions, which may ultimately obtain a mass from, for example, the Higgs mechanism.

3.3.3 Four- and five-dimensional interacting fields

In all the limits of the models we have considered thus far, the dynamical fields are either exclusively four-dimensional or exclusively five-dimensional. It is possible to construct an action which, in the thin kink limit, contains interacting four- and five-dimensional fields, and we shall provide an explicit example of such a model here. Because the dynamics of the kink are frozen out in the thin kink limit, we require two extra fields from the outset: one which couples appropriately to the kink and provides a four-dimensional zero mode, and another which remains five-dimensional. To implement this idea, we take the original action for the kink, equation (3.1), and the fermion, equation (3.55), and add the scalar field Ξ with a coupling to the fermion only. The action is then

$$\mathcal{S}_{\mathrm{all}} = \mathcal{S}_\Phi + \mathcal{S}_\Psi + \int d^5x \left[\frac{1}{2} \partial^M \Xi \partial_M \Xi - s\, \Xi (\overline{\Psi} \Psi^c + \overline{\Psi^c} \Psi) \right] , \tag{3.68}$$

where s is a dimensionful coupling constant and the charge conjugate field is defined as $\Psi^c = \Gamma^2 \Gamma^5 \Psi^*$. In the coupling term, the $\overline{\Psi}\Psi^c$ form is chosen, as opposed to $\overline{\Psi}\Psi$, because we want the massless, four-dimensional, left-handed fermion (the lowest of the fermion modes) to couple to Ξ. To respect the discrete $\mathbb{Z}_2$ symmetry, we must have $\Xi \to \Xi$.

We choose the kink-fermion coupling $d \neq 0$ such that there is at least one fermion bound mode (the massless chiral mode) and follow the thin kink analysis performed previously. All the massive fermion modes are frozen out

and the Ξ coupling term becomes

$$s\,\Xi(\overline{\Psi}\Psi^c + \overline{\Psi^c}\Psi) \xrightarrow{m\to\infty} s\,(f_{L0})^2\,\Xi(\overline{\psi_{L0}}\psi^c_{L0} + \overline{\psi^c_{L0}}\psi_{L0})\,. \tag{3.69}$$

The extra-dimensional factor from the fermion zero mode becomes a delta distribution in the thin kink limit

$$(f_{L0}(w))^2 = \frac{m\,\Gamma(d+\frac{1}{2})}{\sqrt{2\pi}\,\Gamma(d)}\cosh^{-2d}\left(\frac{mw}{\sqrt{2}}\right) \xrightarrow{m\to\infty} \delta(w)\,. \tag{3.70}$$

The w integral can then be performed over the Yukawa term given by (3.69), which reduces the action (3.68) to

$$\begin{aligned}\mathcal{S}^{\mathrm{4D/5D}}_{\mathrm{all}} = &\int d^4x\,\left[-\varepsilon_{\phi_c} + \overline{\psi_{L0}}i\partial\!\!\!/\psi_{L0} - s\,\Xi|_{w=0}(\overline{\psi_{L0}}\psi^c_{L0} + \overline{\psi^c_{L0}}\psi_{L0})\right] \\ &+ \int d^5x\,\left[\frac{1}{2}\partial^M\Xi\partial_M\Xi\right]\,.\end{aligned} \tag{3.71}$$

This is a dynamically generated model describing a four-dimensional zero mode ψ_{L0} coupled at the extra-dimensional point $w = 0$ to a five-dimensional field Ξ. The situation can easily be reversed to have Ψ five-dimensional and coupling at $w = 0$ to the four-dimensional ground state mode of Ξ. Extensions to multiple four and five-dimensional fields are also easily obtained.

3.4 Conclusion

The main aim of this thesis is to construct a domain-wall brane version of the standard model, which, first and foremost, requires a comprehensive understanding of the dynamics of the underlying domain wall. The kink solution, equation (3.4), is an attractive candidate for the domain wall, as it can localise not only massless, chiral fermions but also scalars with arbitrary quartic potentials, as demonstrated in this chapter. We have also provided a detailed analysis of the modes of the kink and localised matter fields, and provided analytic solutions for the extra-dimensional profiles of these modes.

In particular, in Section 3.1 we discussed the classical kink solution, determined its modes, and investigated the behaviour of these mode degrees-of-freedom in the limits of no kink, a thick kink and a thin kink. Due to the quartic potential which sets up the kink profile, the Kaluza-Klein spectrum

consists of a massless bound mode, a massive bound mode and a massive continuum. In the thin kink limit all the massive modes freeze out as their mass becomes infinite. The dynamics of the zero mode of translation also freeze out in this limit, due to a divergent quartic self coupling, and we are lead to the physical interpretation that an infinitely thin kink is infinitely rigid. We discussed in detail why we believe our approach is more general than the collective coordinate approach. The conclusion that we reach is that, in the thin kink limit, only the finite energy density of the kink remains in the effective four-dimensional action.

A full analysis of a second scalar field coupled to the kink was performed in Section 3.2. We showed that such a scalar field is trapped by the kink in a symmetric modified Pöschl-Teller potential well, and we gave the mass spectrum that results from such a trapping. In the thin kink limit, this extra scalar field could either freeze out completely, be a free five-dimensional field, or have just its ground state mode in an effective four-dimensional action. We showed that in this latter case, an arbitrary quartic potential could be generated for this mode and it could thus be used as a standard model electroweak Higgs field. We incorporate such a mechanism in the model constructed in Chapter 5.

Our final analysis, performed in Section 3.3, was that of a fermion coupled to the kink, and its resulting mode decomposition. This generalised the result, due to Rubakov and Shaposhnikov [45], that a left-handed, massless, four-dimensional fermion can be localised to the kink solution. The full spectrum of four-dimensional fields consist of a left-handed zero mode, a certain number of pairs of left- and right-handed modes and a continuum of pairs. In the thin kink limit, we showed that the fermion can either freeze out completely, be five-dimensional with or without a mass term, or reproduce the result of a localised four-dimensional, massless, left-handed mode. We also provided an explicit example of a model where the kink localised a left-handed, zero mode fermion, and this fermion was coupled, at a single point in the extra-dimension, to a full five-dimensional scalar field.

The analyses presented in this chapter demonstrate explicitly how a five-dimensional field can be dimensionally reduced to a tower of effective four-dimensional modes. Furthermore, the mechanisms discussed here form the basic tools necessary to write down the standard model, without gauge fields, on a dynamically generated brane in five-dimensions. The details of

the spectrum of the decomposed five-dimensional fields will be necessary to compute phenomenology associated with interactions between the massless and massive modes, and knowledge of the mass spectra can also be used, in conjunction with experimental data, to put an upper bound on the width of the brane. There remains the outstanding problem of the zero mode of translation of the kink, whose dynamics may be frozen out in the thin kink limit.

Chapter 4

Warped gravity and matter spectra

Prior to the discovery by Randall and Sundrum of the warped metric solution, little thought had been put into the possibility of there existing an infinite extra-dimension. Since gravity is described by the curvature of spacetime, an infinite extra-dimension would necessarily allow gravity to propagate in more than the usual four-dimensions, leading to, for example, an unacceptable law of gravitational attraction. As we have seen in Chapter 3, it is possible to transform the extra degree of freedom associated with an infinite extra-dimension into a Kaluza-Klein tower of modes, and arrange for only the lowest-energy mode to be excited. Randall and Sundrum showed [95] that such a technique can be applied to gravity: at low-energies, it is possible to reproduce four-dimensional gravity on a brane living in a non-compact five-dimensional Anti-de Sitter bulk. We detailed such a set-up in Section 1.5.1. In particular, the key ingredients of the Randall-Sundrum (RS) model are a negative bulk cosmological constant and a positive brane tension, and these two quantities must be tuned against each other. The time-independent solution to Einstein's equations is then a warped metric respecting four-dimensional Poincaré invariance, and such a metric essentially traps gravity to the brane, due to the existence of a localised zero mode graviton in the Kaluza-Klein tower.

As discussed in Section 1.5.2, the trapping of gravity to a brane can be extended to the situation where the brane manifests as a domain wall, or a kink, and the RS warped metric becomes smoothed out, or regu-

larised [165, 173, 174, 211, 188, 202, 182]. A kink also provides a natural mechanism for confining both fermion and scalar fields to a thick four-dimensional slice of a five-dimensional bulk, a mechanism which we explored in detail in Chapter 3. These two ideas for trapping gravity and matter fields find a natural union: they both use a kink background to dynamically generate the brane, and they both transform the extra-dimensional degree of freedom to a tower of modes. Furthermore, if our ultimate aim is to construct a realistic, infinite extra-dimensional version of our current model of the universe, we shall certainly need to describe both gravity and matter together, and also eventually incorporate gauge fields.[1] It is thus important to ensure that gravity, which becomes an integral part of the domain-wall background configuration, does not destroy the desirable features of the matter localisation. This chapter is therefore dedicated to an analysis of the general features of localised fermions and scalars in smoothed, field-theoretical versions of the RS scenario. We demonstrate that, despite some interesting modifications to the associated Kaluza-Klein spectra, the mechanisms of Chapter 3 can still be used to trap matter fields.

Recall that the Kaluza-Klein spectra of matter fields, of fermions and scalars, in general begins with a discrete set of modes (see equations (3.11), (3.45) and (3.59)), followed by a continuum which begins at the *non-zero* height of the trapping potential (see equations (3.12), (3.46) and (3.60)). For the case of scalar field localisation, it was first noted by Bajc and Gabadadze [212] that with gravity included, the scalar continuum modes can begin at *zero* energy. Dubovsky, Rubakov and Tinyakov [186] found that this could be the case for fermions also, and that introducing a five-dimensional mass term can produce massive, localised, meta-stable states. Due to their coupling to the low lying continuum modes, these meta-stable states can tunnel into the bulk and have a finite lifetime. Ringeval, Peter and Uzan [187] considered a specific model and determined the full mass spectrum of the meta-stable, or quasi-localised, modes and demonstrated that their lifetime could be made longer than the age of the universe.

In this chapter we present a general analytic argument which demon-

[1] We emphasise that, in this thesis, we are mostly concerned with classical field theory, so combining gravity and particle physics is as straightforward as combining their individual actions. On the occasions where we appeal to quantum field theory, we consider it in a curved spacetime. We do not enter the regime of quantum gravity.

strates these facts explicitly: in the presence of RS2-like gravity, both scalar and fermion fields exhibit a continuum of properly normalisable modes starting at zero mass. Briefly, we show that the potential well set up by the kink, the well that traps the matter fields, is warped down to zero height at large distances from the centre of the domain wall. The warping is due to gravity, and the resulting potential well is qualitatively similar to the volcano potential which traps the graviton in the RS model. If the matter fields have discrete modes present in their spectra in the gravity-free case, these become resonances in the gravity-induced continuum, and represent quasi-localised states. Off-resonant matter modes are highly suppressed on the brane, in direct analogy with the continuum gravity modes. We argue that, in the presence of interactions, the low-energy, non-resonant continuum modes will couple only very weakly to the resonant modes localised on the brane, and we present numerical calculations for a toy model which supports this argument. Thus, despite the introduction of continuum modes, four-dimensional physics can still be reproduced at low energies, and we can confidently use such a trapping mechanism in model building, as we shall proceed to do in Chapters 5 and 6.

This chapter is structured as follows. In Section 4.1 we discuss the RS warped metric solution, with emphasis on the structure of the volcano potential in both the original set-up and in a scenario where the domain wall is generated by a kink. Section 4.2 gives an analysis of localised fermions in the presence of a warped metric, demonstrating that the fermion mass spectrum has a continuum beginning at zero, and that the modes can still be properly normalised in the presence of gravity. We repeat such a gravitational analysis for a trapped scalar field in Section 4.3, and a similar conclusion is reached: the scalar continuum modes begin at zero mass. As we outlined in Section 3.2.2, it is possible to obtain discrete scalar modes with tachyonic mass in order to realise, for example, the Higgs mechanism; we show that this can still be done when gravity is included in the model. In Section 4.4 we consider a specific toy model to demonstrate more clearly the effect of gravity, and provide numerical support to the claim that the gravity induced continuum modes are only weakly coupled to a brane-localised zero mode. Section 4.5 concludes the chapter.

4.1 Randall-Sundrum and the volcano potential

The spectrum corresponding to the effective four-dimensional graviton in the RS model was shown to consist of a single massless mode, followed by a continuum of massive modes starting arbitrarily close to the zero mode [95]. The zero mode graviton is responsible for reproducing the Newtonian force law, and the integrated effect of the continuum modes at the position of the brane is negligible at low energies, due to the suppression of their wave-functions near the brane; see equation (1.50). Csáki et al. have shown [174] that the same result holds for the situation of regularised RS-like spacetimes, where the brane is dynamically generated by a field.

In both the original set-up and the regularised version, the spectrum of gravity modes is obtained by looking at a Schrödinger-like differential equation for the extra-dimensional profiles of the modes. We performed this type of calculation in Chapter 3, where the potential in the differential equation took the form of a symmetric modified Pöschl-Teller potential, which looks qualitatively like a smooth version of the canonical square well studied in basic quantum mechanics. For the graviton, the corresponding potential is modified further, and takes the shape of a volcano: it has a deep well centred on the brane, tall barriers either side of the centre, and tapers off to zero height at large distances into the bulk (along the extra-dimension). We now proceed to give explicit expressions for the volcano potential, as a warm-up to the more complicated, but qualitatively similar, behaviour of trapped matter fields in the presence of gravity.

In this chapter we consider a five-dimensional spacetime, $x^M = (x^\mu, w)$, and utilise the RS metric ansatz:

$$ds^2 = e^{-2\sigma(w)}\eta_{\mu\nu}dx^\mu dx^\nu - dw^2 \,. \tag{4.1}$$

To analyse the behaviour of gravity modes for this ansatz, one adds perturbations $H_{\mu\nu}(x^\mu, w)$ to the metric,

$$ds^2 = e^{-2\sigma(w)}\left[\eta_{\mu\nu} + H_{\mu\nu}(x^\mu, w)\right] dx^\mu dx^\nu - dw^2 \,, \tag{4.2}$$

and Einstein's equations are then used to obtain the equation of motion for $H_{\mu\nu}$, with a background specified by the (arbitrary for now) function $\sigma(w)$; see equation (1.46) for the resulting Einstein's equation, and also the

surrounding discussion. The extra-dimensional dependence of $H_{\mu\nu}$ is separated from the four-dimensional behaviour by the expansion $H_{\mu\nu}(x^\mu, w) = \sum_n h^n_{\mu\nu}(x^\mu)E_n(w)$, where the mode $h^n_{\mu\nu}$ is assumed to satisfy $\partial^\lambda\partial_\lambda h^n_{\mu\nu} = -m_n^2 h^n_{\mu\nu}$ with m_n the mass of the mode. A Schrödinger-like equation is obtained by going to conformal coordinates z, where $dw = e^{-\sigma}dz$, and rescaling the mode profile by $E_n(w) = e^{3\sigma/2}\tilde{E}_n(z)$. As a result, the extra-dimensional behaviour of gravity perturbations is described by the equation

$$-\frac{d^2\tilde{E}_n(z)}{dz^2} + U_{\rm grav}(z)\tilde{E}_n(z) = m_n^2\tilde{E}_n(z)\,, \tag{4.3}$$

where the effective trapping potential is given by

$$U_{\rm grav}(z) = \frac{9}{4}\left(\frac{d\sigma}{dz}\right)^2 - \frac{3}{2}\frac{d^2\sigma}{dz^2}\,. \tag{4.4}$$

In the case of the fundamental brane, the solution for the warp factor exponent is $\sigma_{\rm RS}(w) = k|w|$, (see equation (1.34)) where $k > 0$ is a parameter of the model, and the bulk five-dimensional cosmological constant is fine tuned to $\Lambda_{\rm RS} = -6k^2$. The corresponding potential for the graviton is then found to be

$$U_{\rm grav}(z) = \frac{15}{4}\frac{k^2}{(1+k|z|)^2} - 3k^2\delta(kz)\,. \tag{4.5}$$

This is the volcano potential. Because we have an infinitely thin brane, the well of the volcano, the $-3k^2\delta(kz)$ term, is also infinitely thin. Nevertheless, this well supports a bound state, corresponding to the zero mode graviton, and its profile is

$$\tilde{E}_0(z) = \sqrt{k}\,(1+k|z|)^{-\frac{3}{2}}\,. \tag{4.6}$$

The normalisation of this profile is determined by $\int_{-\infty}^{\infty}\tilde{E}_0^2(z)\,dz = 1$. Plots of $U_{\rm grav}$ and $\tilde{E}_0$ are given in Figure 4.1. It can be seen that the sides of the volcano decay to zero height for large $k|z|$, and hence this potential allows solutions with an arbitrarily small eigenvalue m_n. These solutions are the continuum gravity modes, and they are suppressed in the region $kz \sim 0$ due to the relatively large barrier set up by the sides of the volcano. This is in contrast to the zero mode $\tilde{E}_0$, which attains its largest value at $kz = 0$, and decays to zero away from the brane.

Moving on from the fundamental brane scenario, we want to consider a set-up where the brane is generated by the classical background configura-

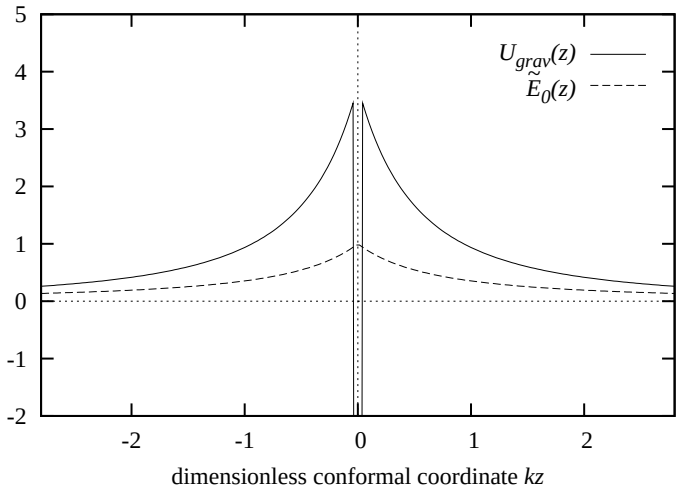

Figure 4.1: Plot of the volcano-shaped graviton trapping potential $U_{\rm grav}(z)$ and the zero mode profile $\tilde{E}_0(z)$ for the Randall-Sundrum warped metric with an infinitely thin brane. $U_{\rm grav}(z)$ is plotted in units of k^2, and $\tilde{E}_0(z)$ in units of $\sqrt{k}$. The narrow well in the centre of the plot schematically represents a negative delta distribution.

tion of a scalar field, or, in general, a set of scalar fields $\Phi_j(x^M)$. To this end, we take the Einstein-Hilbert action, using the time-like sign conventions of Section A.3, and minimally couple the Φ_j to gravity as usual, to obtain the background action

$$\mathcal{S}_{bg} = \int d^5x\sqrt{G}\Big[M_*^3(-R-2\Lambda) + \frac{1}{2}G^{MN}\partial_M\Phi_j\partial_N\Phi_j - V(\Phi)\Big]\,, \qquad (4.7)$$

where G_{MN} is the five-dimensional metric, G its determinant, M_* is the five-dimensional Planck mass, R the five-dimensional Ricci scalar, and Λ the bulk cosmological constant. There is an implicit sum over j, and the scalar potential $V(\Phi)$ can take any form, so long as it respects the $\mathbb{Z}_2$ symmetry $\Phi_j \to -\Phi_j\ \forall\ j$. Such a symmetry ensures that the global minimum of $V(\Phi)$ is at least doubly degenerate, and attained for (say) $\Phi_j = \pm\Phi_j^{\rm min}$. We also require this $\mathbb{Z}_2$ to be independent of any continuous symmetries of the theory.

To determine the background configuration, we must solve the coupled Einstein and Klein-Gordon equations associated with (4.7); the solutions will of course depend on the specific choice of the potential $V(\Phi)$. The ansatz for the metric is as per the fundamental brane set-up, equation (4.1). We also suppose there exists a solution $\phi_j(w)$ depending only on the coordinate

w, satisfying the boundary conditions $\phi_j \to \pm\Phi_j^{\min}$ as $w \to \pm\infty$. Such a solution for the scalar fields is topologically stable. Various authors [165, 173, 211, 188, 213, 202, 182] have found configurations compatible with the assumptions made here, and, in general, the warp factor exponent σ takes the form of a smooth even function of w with asymptotic behaviour $\sigma \to \mu|w|$ as $|w| \to \infty$, where μ is some mass scale. This is a generalisation of the RS2 model, where $\sigma = k|w|$ everywhere.

Allowing ourselves to make some more quantitative remarks, we shall make use of a particular background solution found by Kobayashi, Koyama and Soda [213], where a single, real scalar field $\phi(w)$ forms the domain wall. The stability of the solution is demonstrated in Reference [213]. The warp factor and scalar field take the form,[2]

$$\sigma(w) = a \log[\cosh(lw)] \,, \tag{4.8a}$$

$$\phi(w) = D \arctan[\sinh(lw)] \,, \tag{4.8b}$$

where a and l are free parameters of the model (along with M_*) and $D^2 = 6aM_*^3$. Physically, l controls the width of the domain wall, and a can be used to adjust the strength of gravity at the effective four-dimensional level via the relationship

$$M_{\rm Pl}^2 = \frac{M_*^3}{l} \frac{\sqrt{\pi}\,\Gamma(a)}{\Gamma(a+\frac{1}{2})} \,. \tag{4.9}$$

The limiting behaviour of this equation is $M_{\rm Pl}^2 \to M_*^3/la$ for $a \to 0$ and $M_{\rm Pl}^2 \to M_*^3\sqrt{\pi}/l\sqrt{a}$ for $a \to \infty$; see equation (A.9). Thus, smaller a corresponds to weaker four-dimensional gravity (larger $M_{\rm Pl}$).

The solutions (4.8) correspond to a five-dimensional cosmological constant $\Lambda = -6a^2l^2$, and a scalar field potential

$$V(\Phi) = 3al^2M_*^3(1+4a)\cos^2\left(\frac{\phi}{D}\right) \,. \tag{4.10}$$

The RS thin-brane limit corresponds to taking $a \to 0$ and $l \to \infty$ while keeping the product al finite. One can then make the identification $k = al$, where k is the single parameter of the RS2 model.

For this smooth, analytic case, the volcano potential is, as one would ex-

[2]The functional form of this solution appears different to that given in Reference [213], but it is in fact equivalent.

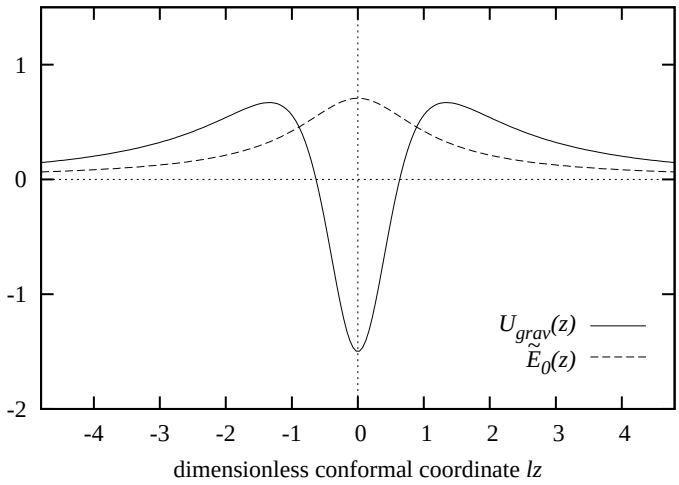

Figure 4.2: Plot of the volcano-shaped graviton trapping potential $U_{\rm grav}(z)$ and the zero mode profile $\tilde{E}_0(z)$ for domain-wall brane model with a smooth warped metric. We have taken $a = 1$ in the model described by equation (4.8) to get analytic solutions for the plot. $U_{\rm grav}(z)$ is plotted in units of l^2, and $\tilde{E}_0(z)$ in units of $\sqrt{l}$.

pect, a smooth version of equation (4.5). In order that we can actually solve the conformal coordinate transformation, we choose $a = 1$. This restriction in relaxed in Section 4.4 where we use numerical techniques to solve the equations. For now, with $a = 1$, we just want to get a feel for the smooth form of the solutions. In terms of the conformal coordinate, the volcano potential is

$$U_{\rm grav}(z) = \frac{l^2}{(1+(lz)^2)^2}\left(\frac{15}{4}(lz)^2 - \frac{3}{2}\right) , \tag{4.11}$$

and it supports the zero mode profile

$$\tilde{E}_0(z) = \sqrt{\frac{l}{2}}\left(1+(lz)^2\right)^{-\frac{3}{4}} , \tag{4.12}$$

which is normalised, as before, by demanding $\int_{-\infty}^{\infty} \tilde{E}_0^2(z)\, dz = 1$. The potential and zero mode are plotted in Figure 4.2. Again, notice how the height of $U_{\rm grav}$ tapers to zero as $z \to \pm\infty$, implying the existence of a continuum of modes arbitrarily close to the zero mode.

We found in Chapter 3 that fermions and scalars are trapped to a kink-generated domain wall by a potential well, which looks qualitatively like that shown in Figure 3.1. In the following two sections, we demonstrate

that this well is modified by the presence of a warped gravitational metric, and takes the form of a smooth volcano potential, very similar in nature to U_{grav} plotted in Figure 4.2. Thus, the Kaluza-Klein spectra associated with four-dimension matter fields is also modified to include a continuum beginning at zero mass. Despite the presence of continuum modes, we show, in Section 4.4, that effective four-dimensional behaviour is retained at low enough energies.

4.2 Fermions in the presence of gravity

We begin this section with a brief review of the situation without gravity, following closely the discussion in Section 3.3.1; this gives us a chance to introduce our notation. Gravity is then added to the model and we demonstrate how a continuum of modes are induced, and how the original discrete modes in the Kaluza-Klein tower become resonances. It is also shown that the fermion modes can be properly normalised in the presence of gravity.

Consider the five-dimensional background action (4.7) *without* gravity. In particular, this action generalises the model of Section 3.3.1 by including any number of scalar fields Φ_j. Now introduce a fermion field Ψ, and Yukawa-couple it to the domain wall. Its action will be

$$\mathcal{S}_\Psi = \int d^5x \left[i\overline{\Psi}\Gamma^A \partial_A \Psi - g_j \Phi_j \overline{\Psi}\Psi \right] , \tag{4.13}$$

where the g_j are Yukawa coupling constants and $\Gamma^A = (\Gamma^\mu, \Gamma^5) = (\gamma^\mu, -i\gamma^5)$, with $\gamma^{\mu,5}$ the usual four-dimensional Dirac matrices and chirality operator, respectively. The action of the $\mathbb{Z}_2$ symmetry (which acts on the Φ_j as $\Phi_j \to -\Phi_j$) is extended to include $w \to -w$ and $\Psi \to i\Gamma^5\Psi$. For simplicity we have also imposed a global U(1) symmetry $\Psi \to e^{i\theta}\Psi$, to forbid a term $g'_j \Phi \overline{\Psi}\Psi^c$ + h.c. We now look to solve the Dirac equation in the classical background of the domain wall. As per equation (3.56), we separate variables by expanding Ψ in a generalised Fourier series:

$$\Psi(x^\mu, w) = \sum_n \psi_L^n(x^\mu) f_L^n(w) + \sum_n \psi_R^n(x^\mu) f_R^n(w) , \tag{4.14}$$

where the fields $\psi_{L,R}^n$ are left- and right-handed four-dimensional spinors: $\gamma^5 \psi_{L,R} = \mp \psi_{L,R}$, $i\gamma^\mu \partial_\mu \psi_L^n = m_n \psi_R^n$ and $i\gamma^\mu \partial_\mu \psi_R^n = m_n \psi_L^n$, where m_n is

the mass of the n^{th} mode. The sum over n generally includes an integral over continuum parts. The basis functions $f^n_{L,R}$ are found by solving the five-dimensional Dirac equation with the above assumptions for $\psi_{L,R}$, which yields

$$-{f^n_{L,R}}'' + W_{L,R} f^n_{L,R} = m_n^2 f^n_{L,R} \,, \tag{4.15}$$

where primes denote differentiation with respect to w, and

$$W_{L,R}(w) = (g_j \phi_j)^2 \mp g_j \phi_j' \,. \tag{4.16}$$

Here, and in subsequent equations, it is understood that f^n_L is solved for using the potential $W_L(w)$ with the *minus* sign, while f^n_R has the plus sign.

Equation (4.15) is just a Schrödinger-like equation with eigenvalue m_n^2. The potential $W_{L,R}$ is a finite well, and $W_{L,R} \to (g_j \Phi_j^{\min})^2 > 0$ as $w \to \pm\infty$. This asymptotic value corresponds to the eigenvalue of the beginning of the continuum modes. The four-dimensional fermion spectrum therefore contains a massless left-handed particle, a finite number of massive Dirac particles with discrete masses, and a continuum of massive Dirac particles beginning at $m_{\text{cont}} = g_j \Phi_j^{\min}$. Explicit solutions for a specific model are presented in Section 3.3.

To include gravity in this model, we need to add the Einstein-Hilbert term to the action, and minimally couple the fields Φ and Ψ to gravity as usual. Formulating fermions in curved spacetime requires the introduction of the vielbein ${e_A}^N$ (here A is an "internal" Lorentz index) and the spin connection ω_N, in order that $\overline{\Psi}\Gamma^A \partial_A \Psi$ be upgraded to a general coordinate, and locally Lorentz, invariant object; see Section A.4 for material pertaining to the vielbein formalism. A suitable choice for the vielbeins, which reproduces the metric described by equation (4.1), and the associated spin connection, are

$$ {e_A}^\mu = \delta^\mu_A e^\sigma \,, \qquad {e_A}^5 = \delta^5_A \,, \tag{4.17a}$$

$$ \omega_\mu = \frac{i}{2} \sigma' e^{-\sigma} \gamma_\mu \gamma^5 \,, \qquad \omega_5 = 0 \,. \tag{4.17b}$$

The total action is then the sum of the background action (4.7) and the fermion action

$$\mathcal{S}_\Psi = \int d^5x \sqrt{G} \left[i \overline{\Psi} \Gamma^A {e_A}^N (\partial_N + \omega_N) \Psi - g_j \Phi_j \overline{\Psi} \Psi \right] \,. \tag{4.18}$$

The resulting Dirac equation is

$$\left[\gamma^5\partial_w + ie^{\sigma}\gamma^{\mu}\partial_{\mu} - 2\sigma'\gamma^5 - g_j\phi_j(w)\right]\Psi(x^{\mu},w) = 0\,. \tag{4.19}$$

We again decompose Ψ into four-dimensional chiral components, and obtain equations for the extra-dimensional profiles $f_{L,R}$. As long as the value $g_j\Phi_j^{\min}$ is large enough, there still exists a left-handed, massless mode; see, for example, [212, 182]. For $m_n > 0$ we get the following two (one each for f_L^n and f_R^n) equations:

$$-{f_{L,R}^n}'' + 5\sigma' {f_{L,R}^n}' + \left[2\sigma'' - 6\sigma'^2 + \tilde{W}_{L,R}\right] f_{L,R}^n = m_n^2 e^{2\sigma} f_{L,R}^n\,, \tag{4.20}$$

where

$$\tilde{W}_{L,R} = (g_j\phi_j)^2 \mp g_j\phi_j' \pm g_j\phi_j\sigma'\,. \tag{4.21}$$

The inclusion of gravity has meant that equation (4.20) is no longer simply a Schrödinger equation, so we cannot directly apply our knowledge of one-dimensional quantum mechanics. It is however possible to transform equation (4.20) into a Schrödinger-like equation, as we did in Section 4.1 when obtaining the volcano potential. Specifically, we let $f_{L,R}^n = e^{2\sigma}\tilde{f}_{L,R}^n$, and change coordinates to $z(w)$ such that $dz = e^{\sigma}dw$. This change of coordinates takes us to conformal coordinates, where the metric is conformally flat: $ds^2 = e^{-2\sigma(w(z))}(\eta_{\mu\nu}dx^{\mu}dx^{\nu} - dz^2)$. Equation (4.20) then becomes

$$-\frac{d^2\tilde{f}_{L,R}^n}{dz^2} + \left(e^{-2\sigma}\tilde{W}_{L,R}\right)\tilde{f}_{L,R}^n = m_n^2\tilde{f}_{L,R}^n\,, \tag{4.22}$$

and we thus identify the effective potential

$$\tilde{W}_{L,R}^{\text{eff}} = e^{-2\sigma}\tilde{W}_{L,R}\,. \tag{4.23}$$

As $|w| \to \infty$, $\sigma \sim \mu|w|$, where μ is, as before, some mass scale. In terms of z, this asymptotic behaviour becomes $e^{-2\sigma} \sim 1/(\mu z)^2$ as $|z| \to \infty$. For this limiting value of $|z|$, we have $\tilde{W}_{L,R} \to$ constant, and therefore the effective potential decays towards zero at large distances from the brane (see Figure 4.3 for some specific cases). Indeed, it is qualitatively the same as the volcano potentials, studied in Section 4.1, that arise in the analysis of the graviton sector. Particles subjected to $\tilde{W}_{L,R}^{\text{eff}}$ are essentially free asymptotically (at large $|z|$), so there is a continuum of delta-function normalisable

solutions for all $m_n^2 > 0$. We will now show that normalisability of $\tilde{f}_{L,R}^n$ implies appropriate normalisability of $f_{L,R}^n$, and conclude that our dimensionally reduced theory contains a continuum of fermions starting at zero mass.

The $\tilde{f}_L^n$ satisfy an ordinary Schrödinger-like equation with a continuum of eigenvalues, and therefore are delta-function orthonormalisable:

$$\int_{-\infty}^{\infty} \tilde{f}_L^{n*} \tilde{f}_L^{n'} \, dz = \delta(n - n') \, . \tag{4.24}$$

On the other hand, the normalisation condition for the f_L^n can be derived by demanding that integrating the action (4.18) over w leads to a properly normalised, four-dimensional kinetic term for the field ψ_L^n, namely

$$\int d^4x \int dw \, \sqrt{G} \left[i\overline{\Psi} \Gamma^A e_A{}^\mu \partial_\mu \Psi \right] \supset \int d^4x \int dn \, i\overline{\psi}_L^n \gamma^\alpha \partial_\alpha \psi_L^n \, . \tag{4.25}$$

Here, the integral over n is an integral over the continuum modes. Note that there will be no mixing of f_L^n and $f_R^{n'}$ in the kinetic terms due to the properties of chiral fermions. Substituting in the expressions for the vielbein and metric, this condition becomes

$$\int_{-\infty}^{\infty} e^{-3\sigma} f_L^{n*} f_L^{n'} \, dw = \delta(n - n') \, , \tag{4.26}$$

However, if we write f_L^n in terms of $\tilde{f}_L^n$ and use $dw = e^{-\sigma} dz$, we find that

$$\int_{-\infty}^{\infty} e^{-3\sigma} f_L^{n*} f_L^{n'} \, dw = \int_{-\infty}^{\infty} \tilde{f}_L^{n*} \tilde{f}_L^{n'} \, dz \, . \tag{4.27}$$

So the normalisation integral for the f_L^n is equivalent to the normalisation integral for the $\tilde{f}_L^n$. The same conclusion is reached for the right-handed profiles f_R^n. Therefore, there is a continuum of normalisable fermion modes in the theory, starting at zero four-dimensional mass. Despite this, the zero modes still form an effective four-dimensional theory at low energies, and we can understand this as follows.

Flat space corresponds to $\sigma \equiv 0$, and we have seen that, in this case, the low-energy spectrum consists of a finite number of particles with discrete masses. The reason for this is that the effective potential of the analogue Schrödinger system, given by equation (4.16), asymptotes to a non-zero

value. The discrete spectrum corresponds to modes bound in the potential well, near $w = 0$, with eigenvalue less that the asymptotic height of the potential.

Suppose now that σ is non-zero, but grows only very slowly with increasing $|w|$. In this case, the effective potential of equation (4.23) approximates that of equation (4.16) near the brane, then decays towards zero as $|w| \to \infty$. We thus have a localised, non-zero potential in the form of a narrow well flanked by wide barriers. The low-energy continuum eigenfunctions of such a system will generically have very small amplitudes at the position of the well, due to the potential barrier which they must tunnel through when coming in from the bulk.

So, although arbitrarily light fermions will exist in the theory, their wavefunctions will be strongly suppressed at the position of the brane, where the zero mode resides. These light modes are effectively "localised at infinity". This leads to a very small probability of these low-energy continuum modes interacting with any zero modes that are present in the model (and there will, in general, be multiple fermion zero modes; for example, one for each of the fermions in the standard model).

There is one more generic feature which we expect to occur. Certain discrete energies will resonate with the potential, and the corresponding states will thus have a much larger probability of being found on the brane. These are the remnants of the discrete bound states in the flat space case, and become coincident with them in the zero-gravity limit. What happens if one of these resonant modes is produced in a high-energy process on the brane? Any particle produced on the brane will have a wavefunction truly localised to the brane, and thus cannot correspond exactly to a single mode ψ^n, which has a wavefunction oscillatory as $|z| \to \infty$. Instead such a particle will be a wavepacket made from the continuum modes, with a Fourier spectrum peaked around one of the resonances (see Figure 4.4 for an example). It is therefore not a true energy or mass eigenstate, and, as the various components evolve to an out-of-phase configuration, the wavefunction will leak off the brane. The particle then has some probability of escaping the brane, which justifies the moniker "quasi-stable" or "quasi-localised" for the resonant modes. It is these resonant, quasi-localised states that are investigated by Ringeval et al. [187].

Quantitative calculations confirming the above conclusions will be given

for a particular toy model in Section 4.4. But first, we will show that the introduction of a continuum of modes, starting from zero energy, is true also for the spectrum of a localised scalar field.

4.3 Localised scalar fields with gravity

As well as fermions, it is desirable for model building purposes to be able to localise scalar fields to the wall. We analysed the modes of a scalar in the gravity-free case in Section 3.2, and found a similar spectrum to that of a localised fermion, except that the mass-squared of the lightest scalar mode depends on parameters in the five-dimensional theory. The lowest scalar state can even be arranged to have a tachyonic mass, so as to realise the Higgs mechanism in the low-energy theory. We will now examine the effects of gravity on these results.

Consider a five-dimensional scalar field $\Xi(x^M)$ described by the combined action of equation (4.7) and the additional piece

$$\mathcal{S}_\Xi = \int d^5x\,\sqrt{G}\left[G^{MN}(\partial_M\Xi)^\dagger\partial_N\Xi - H(\Phi,\Xi)\right]\,, \tag{4.28}$$

where H specifies the coupling of Ξ to itself and to the domain wall, the latter of which is a particular classical configuration $\phi_j(w)$ of the five-dimensional fields $\Phi_j(x^M)$. The linearised equation of motion for Ξ is given by

$$\partial_M\left(\sqrt{G}\,G^{MN}\partial_N\Xi\right) + \sqrt{G}\,U(\phi_j)\Xi = 0\,, \tag{4.29}$$

where U is independent of Ξ, and defined by $\frac{\partial H}{\partial\Xi^\dagger} = U\Xi + \mathcal{O}(\Xi^2)$. We solve this exactly the same way as in the fermion case: by separating variables

$$\Xi(x^\mu, w) = \sum_n \xi^n(x^\mu)h^n(w)\,, \tag{4.30}$$

where each $\xi^n(x^\mu)$ satisfies the four-dimensional Klein-Gordon equation

$$\partial^\mu\partial_\mu\xi^n + m_n^2\xi^n = 0\,. \tag{4.31}$$

The analogue of equation (4.20) is then

$$-h^{n\prime\prime} + 4\sigma' h^{n\prime} + Uh^n = e^{2\sigma}m_n^2 h^n\,. \tag{4.32}$$

We can convert this to a Schrödinger-like equation by again going to the conformal coordinate z, as well as making the substitution $h^n = e^{\frac{3}{2}\sigma}\tilde{h}^n$. This yields

$$-\frac{d^2\tilde{h}^n}{dz^2} + \left[\frac{9}{4}\left(\frac{d\sigma}{dz}\right)^2 - \frac{3}{2}\frac{d^2\sigma}{dz^2} + e^{-2\sigma}U\right]\tilde{h}^n = m_n^2\tilde{h}^n\,, \tag{4.33}$$

which is to be compared with the fermion version, equation (4.22). Analysing the asymptotic behaviour of equation (4.33), we find that, as $|z| \to \infty$, $\sigma \sim \log|z|$ and $U \to$ *constant*. Thus we see immediately that, as in the fermion case, the effective potential for the scalar modes decays towards zero far from the brane. Therefore the low-energy scalar spectrum also contains a continuum of modes of arbitrarily small mass, which are properly normalisable, as can be shown by a calculation analogous to that described previously for the fermions.

If $U \equiv 0$, the equation (4.33) is in fact identical to that satisfied by four-dimensional gravitons, the latter being equation (4.3). In this case then, we know that there is a single zero mode, followed by a continuum of modes starting arbitrarily close to $m_n^2 = 0$. The low-lying continuum modes are strongly suppressed on the brane; for example, their contribution to a static potential generated by Ξ exchange between two sources on the brane separated by r, is suppressed by $1/(\mu r)^2$ relative to the contribution of the zero mode (recall that μ is a large mass scale). This is analogous to the RS2 corrections to Newton's law of gravity, equation (1.50).

For non-zero U, the spectrum is modified from the graviton case, the significant difference being the possible introduction of resonant modes (in the absence of fine-tuning of parameters, there will no longer be a zero mode). As in the fermion case, these resonant modes correspond to the discrete bound modes in the corresponding gravity-free theory and we expect the first of these modes to occur for $m_n \sim \mu$. Unlike the fermion case, if appropriate coupling to the domain-wall is included, such that U makes some negative contribution to the effective potential, then there may be bound state solutions with $m_n^2 < 0$, as in the gravity-free case where the spectrum is given by equation (3.45). This signals an instability in the system, and implies that Ξ is non-zero in the stable background configuration. In this case we would have to instead solve the coupled Einstein and Klein-Gordon equations including the Φ_j fields *and* Ξ.

This set-up can be used for interesting model building, in which a symmetry is broken on the brane but restored in the bulk. This idea has been used in the flat space case in the Dvali-Shifman mechanism [57]. We sketch the reasoning following Witten [214]. Take the scalar potential

$$H(\Phi, \Xi) = (g'\Phi^2 - u^2)\Xi^\dagger\Xi + \tau(\Xi^\dagger\Xi)^2 \,, \tag{4.34}$$

where we have specialised to a single background field Φ, and we assume $g'\Phi^{\min} - u^2 > 0$ such that $(\Phi, \Xi) = (\pm\Phi^{\min}, 0)$ are still the global minima of the potential, and we must have $\Xi \to 0$ as $|w| \to \infty$. If Φ forms a domain wall, then $\Phi \sim 0$ inside the wall, so that the leading term of $H(\Phi, \Xi)$ is $\sim -u^2\Xi^\dagger\Xi$, suggesting that the $\Xi = 0$ solution is unstable there. This will show up as a negative eigenvalue $m_n^2 < 0$ in equation (4.33), and solving for a consistent set of background solutions will yield a background Ξ that is peaked on the brane and tending to zero in the bulk. Putting Ξ in a non-trivial representation of some gauge group will induce spontaneous breaking of that group on the brane, a mechanism which can be used, for example, to realise the standard model Higgs mechanism on the brane; this is what we shall do in Chapter 5.

In the stable case, U will asymptotically approach some constant positive value U_0. As $|z| \to \infty$, we can approximate the effective potential in equation (4.33) as

$$V_{\text{eff}} \sim \frac{1}{z^2}\left(\frac{15}{4} + \frac{U_0}{\mu^2}\right) \,. \tag{4.35}$$

Again, we can appeal to the results of Csáki et al. [174], where it is shown that for a potential that behaves asymptotically as $\alpha(\alpha+1)/z^2$, the amplitudes of modes with small m_n are suppressed by $(m_n/\mu)^{\alpha-1}$. Therefore the coupling to the domain wall actually reduces the effect of the continuum modes on low-energy physics.

4.4 Toy model calculation

We would like to study a fermion field $\Psi(x^M)$ in a kink background to illustrate the existence and suppression of the low-lying continuum modes. For the background, we shall use the smooth, analytic model from Section 4.1, where a single, real scalar field $\Phi(x^M)$ formed the kink. The action for this background is (4.7), the scalar potential is (4.10) and the classical solutions

for $\sigma(w)$ and $\phi(w)$ are given by equation (4.8). We again impose a global $U(1)$ symmetry $\Psi \to e^{i\theta}\Psi$ so that Ψ only couples to the background via a term $g\Phi\overline{\Psi}\Psi$. For the sake of examining interactions later, we also include an additional scalar field $\Xi(x^M)$, which $U(1)$ acts on via $\Xi \to e^{2i\theta}\Xi$, to mediate interactions between Ψ quanta.[3] In addition to the background action describing gravity and Φ, we have the action for the two matter fields:

$$\mathcal{S}_{\Psi\Xi} = \int d^5x\sqrt{G}\Big[i\overline{\Psi}\Gamma^A e_A{}^M(\partial_M + \omega_M)\Psi - g\Phi\overline{\Psi}\Psi \\ + \partial^M\Xi^\dagger\partial_M\Xi - g'\Phi^2\Xi^\dagger\Xi - u^2\,\Xi^\dagger\Xi - \tau(\Xi^\dagger\Xi)^2 - \lambda(\Xi\overline{\Psi}\Psi^c + \text{h.c.})\Big]\,. \tag{4.36}$$

Here, the charge conjugate is $\Psi^c = \Gamma^2\Gamma^5\Psi^*$. For our background solution to remain stable, $\Xi = 0$ must be the stable solution, that is equation (4.33) must not have any negative eigenvalues. Choosing $u^2 > 0$ suffices to guarantee this.

The effective Schrödinger-like equation which determines the modes of the fermion field is found as described in Section 4.2. For various values of a (which controls the strength of four-dimensional gravity as per equation (4.9)), the resulting effective potential felt by the left-chiral component of the fermion is plotted in Figure 4.3. It does indeed asymptote to zero when gravity is included ($a > 0$), implying the existence of a continuum of arbitrarily light modes. There is of course a zero mode which is localised to the brane — all other modes are, however, oscillatory at infinity.

Using this toy model, we want to quantify our argument that the light continuum modes do not overly influence physics on the brane. In our model, the dominant process by which the continuum could be detected is two zero mode particles annihilating to produce two continuum particles via exchange of a Ξ quantum, so this is the process we shall consider. As explained at the end of Section 4.2, a Ξ quantum produced on the brane will not correspond to a single mass mode, but will be a wavepacket initially localised on the brane. The creation of such a wavepacket on the brane, and the ensuing shape of the wavepacket as it evolves over time, will be a complicated issue,

[3] It is necessary to introduce a field other than Φ, because the fermion zero mode is chiral, and thus does not interact with Φ via the term $g\Phi\overline{\Psi}\Psi$. Additionally, while the modes of Φ mix with scalar gravitational degrees of freedom, the global $U(1)$ symmetry prevents such a mixing of Ξ modes.

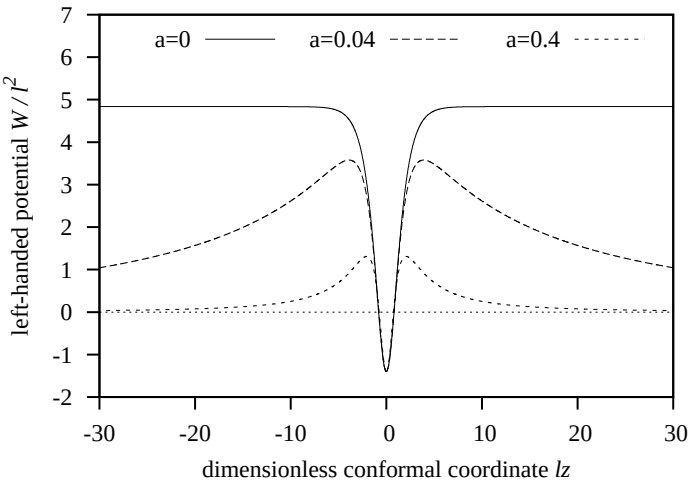

Figure 4.3: An example of the effective Schrödinger potential, $\tilde{W}_L^{\text{eff}}$, defined by equation (4.23), which traps a left-handed fermion field. The kink background configuration is as per equation (4.8). The three plots correspond to no gravity ($a = 0$), "weak" gravity ($a = 0.04$), and "strong" gravity ($a = 0.4$). The horizontal line is $W = 0$. All three plots have $gD = 1.4\,l$ for the fermion-kink coupling.

and is not considered here. Instead, we will simply take $\cosh^{-1}(lz)$ as a typical localised profile[4] and assume that a Ξ quantum is produced with the normalised, extra-dimensional wavefunction $\tilde{h}_{\text{typ}}(z) = \sqrt{l/2}\,\cosh^{-1}(lz)$. We have computed the Fourier decomposition of $\tilde{h}_{\text{typ}}(z)$ in terms of the mass eigenmodes $\tilde{h}^n(z)$ (the eigenfunctions of equation (4.33)); these Fourier amplitudes are

$$F^n = \left(\int_{-\infty}^{\infty} \tilde{h}_{\text{typ}} \tilde{h}^n \, dz \right)^2 . \tag{4.37}$$

The spectrum is sharply peaked at a mass corresponding to the first resonant mode, as expected, and as shown in Figure 4.4. See Section B.2 for details of the numerical method used to obtain the extra-dimensional profiles.

We now proceed to calculate the effective coupling of the fermion modes to this particle in the dimensionally reduced theory. This will give us a quantitative estimate of the likelihood of continuum fermion modes being produced by on-brane dynamics through s-channel annihilation. It will also be a valid estimate for t-channel scattering of localised zero modes with bulk continuum modes.

[4]Results should be almost identical for any profile which decays exponentially beyond $|z| \sim 1/l$.

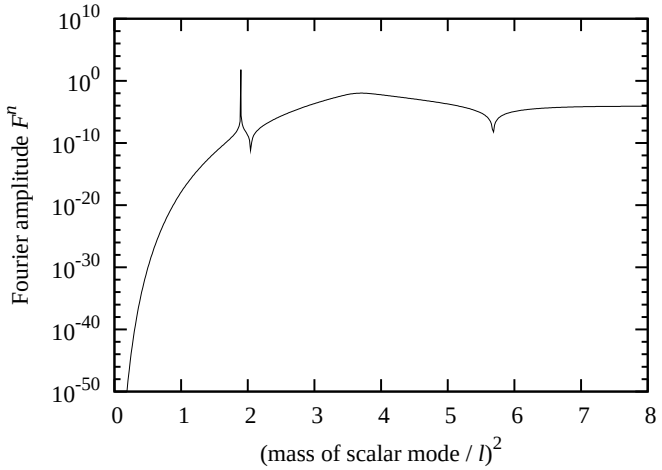

Figure 4.4: Fourier decomposition of the extra-dimensional profile $\tilde{h}_{\rm typ}(z) = \sqrt{l/2}\,\cosh^{-1}(lz)$ in terms of the scalar modes $\tilde{h}^n(z)$. The latter, being the eigenfunctions of equation (4.33), are indexed by their eigenvalue on the horizontal axis (rather than the abstract label n). The kink background is given by equation (4.8) and potential $U = g'\phi^2 + u^2$. The amplitude is defined by equation (4.37), and the parameters are $a = 0.04$, $g'D^2 = 1.2\,l^2$ and $u^2 = l^2$. The typical brane-localised mode $\tilde{h}_{\rm typ}(z)$ is comprised almost entirely of the first resonant mode with eigenvalue $m^2_{\rm res} \simeq 1.9\,l^2$.

The effective coupling constant between the fermion modes of Ψ and the localised Ξ particle is given by the five-dimensional Yukawa coupling constant λ multiplied by the overlap integral of their extra-dimensional wavefunctions. For the fermion mode with extra-dimensional dependence $f^n(w)$, the coupling will be

$$\begin{aligned}\lambda^{(4)}_n &= \lambda \int_{-\infty}^{\infty} e^{-4\sigma}\, h_{\rm typ}(w) \left(f^n(w)\right)^2 dw \\ &= \lambda \int_{-\infty}^{\infty} e^{\frac{1}{2}\sigma}\, \tilde{h}_{\rm typ}(z) \left(\tilde{f}^n(z)\right)^2 dz \\ &= \lambda \sqrt{\frac{l}{2}} \int_{-\infty}^{\infty} e^{\frac{1}{2}\sigma} \frac{\left(\tilde{f}^n(z)\right)^2}{\cosh lz}\, dz\,. \end{aligned} \tag{4.38}$$

The results for the case $a = 0.04$ are plotted in Figure 4.5, contrasted with the results in the gravity-free case.[5] It is clear that the four-dimensional coupling constants go quickly to zero for modes with masses much less than

[5]Note that what is plotted is really "interaction strength per continuum mode" with mode energy used on the horizontal axis to label a particular mode number. An integral over some finite range of modes is required to yield a finite on-brane effect.

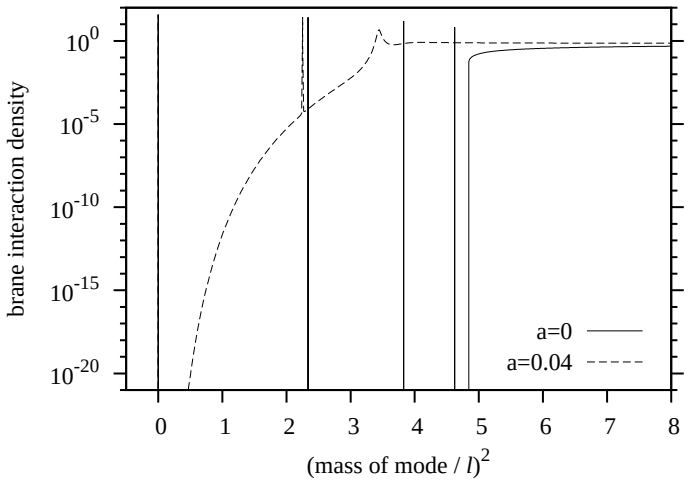

Figure 4.5: The "interaction per continuum mode", $\lambda_n^{(4)}/\lambda\sqrt{l}$, for continuum fermion modes interacting with a typical bound mode on the brane. Both the gravity-free ($a = 0$) and "weak" gravity ($a = 0.04$) cases are shown. The fermion zero mode remains bound in the presence of gravity (hidden by the gravity-free plot), while a continuum is introduced for all positive energies. It is clear that at energies well below l, the continuum modes are essentially decoupled from those on the brane. The coupling becomes relatively strong for energies greater than the maximum of the effective potential. The fermion coupling strength is $gD = 1.4\,l$.

the inverse width l of the domain wall. Plots displaying similar resonant behaviour for fermions localised to a domain wall have been obtained by Almeida et al. [215].

Such behaviour is of course easy to understand, based on the discussion of Section 4.2. Modes with energy much less than l see a wide potential barrier preventing them from penetrating to the brane, where the Ξ particle resides. At an energy approximately equal to l, we see the first resonant mode, which does not suffer the generic suppression near the brane. Continuum modes with energy above the barrier height ($\sim 5l^2$ for the gravity-free case and $\sim 3.5l^2$ for weak gravity) are free to roam in the vicinity of the brane, hence their coupling is of order unity. We have explicitly plotted the profiles of a resonant mode and a (slightly) off-resonant mode in Figure 4.6 to illustrate the amplification of one, and suppression of the other, on the brane.

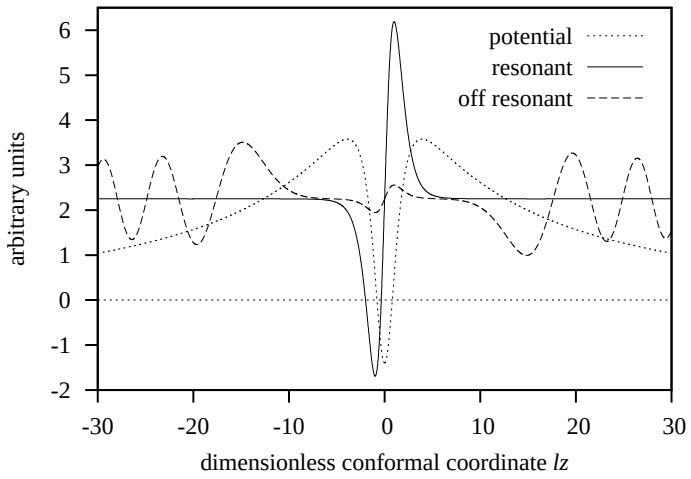

Figure 4.6: The extra-dimensional profiles of the fermion resonant mode at $(E/l)^2 \simeq 2.3$, and a fermion mode off-resonance by 2.0×10^{-4} in units of $(E/l)^2$. We are in the "weak" gravity case with $a = 0.04$. The profiles are not plotted on the same scale; in reality, each is normalised to the same amplitude *at infinity* (since the normalisation condition is dominated by the behaviour of the wavefunction at infinity). Thus the contrast is much more dramatic even than it appears here.

4.5 Conclusion

In this chapter we looked at the effect the Randall-Sundrum warped metric has on the trapping capability of a kink background, and the resulting modifications to the spectra of localised matter fields. As a warm-up, we discussed in Section 4.1 the volcano potential which determines the extra-dimensional profiles of graviton modes. For such a potential, the graviton zero mode lies directly beneath a tower of continuum modes. We then proceeded to show that a similar spectrum of continuum modes is introduced into the Kaluza-Klein tower of fermion and scalar modes discussed previously in Chapter 3. We also demonstrated, by studying a toy-model, that the effect of the gravity-induced continuum can be neglected at low-energies, and so the phenomenology of our domain-wall set-up is not necessarily counter to experiment.

In particular, Section 4.2 analysed the behaviour of a fermion field coupled to a generic, gravitating, scalar domain wall in five-dimensions. The spectrum of the low-energy effective four-dimensional theory was found to consist of a massless fermion of fixed chirality, and a continuum of states with all possible masses $m > 0$. The massless mode is bound to the brane,

while the continuum modes are oscillatory far from the brane. In Section 4.3, we showed that a scalar field coupled to the same background also yields a continuum of arbitrarily light states.

Coupling constants in the low energy theory will be determined by overlap integrals between the extra-dimensional profiles of the fields involved. Generically, continuum modes are strongly suppressed on the brane, and thus should interact only very weakly with the zero modes and other localised fields. We have demonstrated this effect (see Section 4.4) by explicitly computing the overlap integrals for a typical toy model. It should be possible within specific models to arrange for the integrated effects of these modes to be small enough, so as not to contradict known low-energy phenomenology. Nevertheless, at higher energies it may be important to consider the effects of such modes.

There will be a finite number of resonant modes which *will* manifest on the brane; these are the remnants of the bound states of the analogue Schrödinger system in the non-gravitating case. The lowest of these modes will have a mass approximately equal to the inverse width of the domain wall, which would need to be sufficiently large in a realistic model.

Note that we have assumed throughout that the four-dimensional metric on the brane is Minkowskian. Cosmologically, it may be desirable to allow it to be de Sitter; in this case, by dimensional analysis, the continuum matter modes will begin at a mass $m \sim \sqrt{\Lambda_4}$, where Λ_4 is the effective cosmological constant on the brane. This effect is demonstrated explicitly for gravitons by Karch and Randall [118]. For our universe, such a shifting of the beginning of the continuum modes is very small, and would be negligible for collider phenomenology. A more drastic consequence of a de Sitter, or any non-Minkowskian, spacetime is detailed in Chapter 7.

The analysis presented in this paper would form the basis of an investigation of the low-energy phenomenology of a realistic model; for example, of the model we present in Chapter 5.

Chapter 5

The SU(5) model

Having developed and discussed the machinery for constructing a domain-wall brane, for confining scalars and chiral fermions, and for assimilating the Randall-Sundrum warped metric so that gravity is also localised, we proceed, in this chapter, to write down the standard model localised to a brane. Actually, the model presented here will not be exactly the standard model: our action is invariant under a local SU(5) symmetry, and we consider only a single generation of fermions (although the extension to three generations is straightforward). We are also going to ignore the issue of neutrino mass. Nevertheless, we believe that our SU(5) domain-wall brane model, extended to three generations, is the *simplest* way to have the standard model emerge from an effective, field-theory model of an infinite extra dimension. Indeed, our construction introduces only the bare minimum of scalar fields necessary to generate the requisite domain wall, and these fields end up playing an additional role in the splitting of the fermions and Higgs fields in the extra dimension, nullifying the usual $m_e = m_d$ relation of minimal, four-dimensional SU(5) models.

Our focus in this chapter is on model-building rather than detailed phenomenology. We are going to give a general overview of our domain-wall brane model and explain the dynamics behind the formation of the kink background. We shall then provide an explicit example of such a background, and discuss how the elements of the usual, four-dimensional standard model emerge. This will hopefully provide convincing evidence that our model has good phenomenology, and serves to inspire a more comprehensive phenomenological study.

As has been the theme throughout this thesis so far, our model is motivated by a desire to treat extra-dimensions on the same footing as existing dimensions. Our single, extra, spatial dimension is therefore infinite in extent, and the action of our model respects five-dimensional Poincaré invariance. The four dimensions that constitute our observable universe are then *a low-energy approximation*, valid only because of the dynamical formation of a domain-wall brane. This wall is created jointly by a real singlet-Higgs field $\eta(x^M)$ configured as a kink, and an SU(5) adjoint-Higgs field $\chi(x^M)$ that is non-zero inside the wall, but vanishes asymptotically far from the brane. Five-dimensional fermions Yukawa coupled to the background scalar fields provide localised, four-dimensional, chiral zero modes, as per the set-ups detailed in Chapters 3 and 4. The standard model Higgs doublet is similarly localised using the techniques developed in these earlier chapters. Localised gravity is generated via the Randall-Sundrum warped metric, generalised to the case where the brane is smooth and extended in the extra dimension.

One thing that has remained outstanding in the developments made so far in this thesis is the mechanism by which gauge fields are to be localised to the domain wall. In Chapter 2 we played with a toy model which allowed for semi-localisation of U(1) gauge fields using a standard field-theoretic analysis. As far as we are aware, it does not seem possible to get such a field-theoretic model to work and to properly localise massless gauge fields. We are therefore going to resort to using the Dvali-Shifman (DS) mechanism [57], outlined in Section 1.3.3, which relies on the confinement property of non-Abelian gauge theories — a non-perturbative feature which allows only qualitative statements to be made (unless one moves into the arena of numerical lattice-gauge-theory). Actually, phrasing it as 'resorting' to the DS mechanism is really underplaying the situation: DS requires a *larger* gauge symmetry in the bulk, larger than the symmetry localised to the brane, leading immediately to the decision that our full action be SU(5) invariant. The standard model gauge group, being a maximal subgroup of SU(5), is then exactly the symmetry group which is localised to the brane! As we have already mentioned, we believe our model to be the minimal, infinite extra-dimensional, field-theory model which subsumes the standard model, and this belief is supported by the seeming necessity of DS and the subsequent simplification of the gauge and fermion sectors inherent in using a grand unified theory.

Aside from its calculational complexities, the DS mechanism is yet to be proven to work in the five-dimensional context. Pure Yang-Mills theory is not renormalisable in more than four-dimensions, and, as a consequence, the physics of five-dimensional confinement — the underlying feature of our implementation of DS — is not properly understood. We shall show in this chapter that *if* one takes the DS mechanism to work in five-dimensions, *then* our domain-wall-localised standard model follows readily. The gauge symmetry is then required to be SU(5) in the bulk, spontaneously broken, via the adjoint χ, to

$$G_{\rm SM} = {\rm SU}(3)_C \otimes {\rm SU}(2)_L \otimes {\rm U}(1)_Y \tag{5.1}$$

inside the domain wall. Provided that the SU(5) theory in the bulk exhibits confinement, the standard model gauge bosons are thus localised to the interior of the domain wall. We hope that our model spurs rigorous studies of the DS mechanism in five-dimensions, to either confirm it or disprove it. Were it to be confirmed, then our general model-building set-up, exemplified in this chapter, would provide a clear pathway to the construction of phenomenologically-realistic effective theories of domain-wall-localised fields.

Inherent in our model is the split fermion mechanism [67]. The five-dimensional bulk fermions Ψ_5 and Ψ_{10}, in non-trivial representations of SU(5), are coupled to both background scalar fields η and χ. When χ breaks the SU(5) gauge symmetry to the standard model gauge group, components of Ψ_5 and Ψ_{10} with different ${\rm U}(1)_Y$ hypercharges are localised to *different* positions along the bulk direction. The Higgs doublet of the standard model emerges from the bulk Higgs Φ, along with its colour triplet SU(5) partner, and they are localised and split in analogy with the fermion sector. There is some control over the structure and extent of the splitting of the fermion and Higgs fields, and we can use this to our advantage to, for example, suppress coloured-Higgs-induced proton decay. Furthermore, because four-dimensional fermion masses are computed from overlap integrals of profile functions, and because these profiles are different for fermions with different hypercharges, our model automatically avoids the usual SU(5) mass relation $m_e = m_d$.

There is an important loose end that we are not going to address in this

thesis: gauge coupling constant unification. For such an analysis to proceed, we must look at the three-generation version of our model, since it is the full spectrum of particles, and their associated Kaluza-Klein excitations, that will determine the running of the coupling constants. We shall expand on this point in Section 5.3.1.

In Section 5.1 we review the DS mechanism, and include a discussion of the open questions related to confinement in five-dimensional, non-Abelian gauge theories. Our SU(5) model is described in Section 5.2, and we explain how the domain-wall background forms and how the standard model can be recovered. In Section 5.3, we provide an explicit, analytic example of a background configuration, and show how the split fermion and split Higgs mechanism works. We also look at the effective electroweak sector, present formulae for the fermion masses, and outline the effect of gravity in the form of the warped metric. Section 5.4 discusses the relationships among the various scales in our model, and Section 5.5 concludes the chapter.

5.1 The Dvali-Shifman mechanism

We have given an overview of the DS mechanism in Section 1.3.3. It seems that this is the most plausible way of localising gauge bosons to a domain wall. The mechanism requires a confining non-Abelian gauge theory in the bulk, where the symmetry G is broken to a subgroup group H inside the domain wall. Massless gauge bosons corresponding to H are then localised to the region where the symmetry is broken; they are localised to the wall. Since we are attempting to place the standard model on a domain wall, the minimal choice is to take $G = \mathrm{SU}(5)$ and $H = \mathrm{SU}(3)_C \otimes \mathrm{SU}(2)_L \otimes \mathrm{U}(1)_Y$, which is exactly what we shall do in this chapter. Having been led to such an appropriate choice of gauge symmetry, and drawing on the mechanisms for fermion, scalar and gravity confinement, the precise construction of our extra-dimensional SU(5) model follows quite naturally.

Before we present the model, let us make some specific remarks about DS and gauge field confinement. We have seen examples of how effective four-dimensional couplings arise from integrals over products of extra-dimensional profiles; for example, equation (3.16). In general, modes that have different profiles will have different four-dimensional couplings. Imagine that the gauge coupling constant of (say) $\mathrm{U}(1)_Y$ was an effective quantity,

computed by evaluating such an overlap integral of the profiles of fermions and the gauge field. Each particle in the effective four-dimensional theory will potentially have a different coupling to the four-dimensional gauge field, which is disastrous, since we know that ratios of the hypercharge Y have definite values. If the five-dimensional fermions already begin with the correct hypercharge (in our SU(5) model they do because the bulk fermions are non-trivial SU(5) multiplets), then the overlap integrals for all the modes (or at least the zero modes) must be equal to each other in order that the hypercharge ratios be preserved. This could be accomplished by severely restricting the layout of the profiles. For example, in models with compact extra-dimensions, one can give the zero modes of the gauge fields a constant profile [67]. For the case of an infinite extra-dimension, we have seen that the ground state mode of a localised field has a Gaussian-shaped profile, and so it would seem nearly impossible to organise gauge overlap integrals that were equal for all fermions. It seems necessary therefore that a successful mechanism of gauge field localisation involve a non-standard way of computing effective gauge coupling constants. For DS, this is hidden in the non-perturbative physics of confinement.

Confinement seems to be the key to the DS mechanism. In a *four*-dimensional spacetime, the truth of DS is well established [58, 60, 59], and we shall review, briefly, the arguments. Following Dvali and Shifman [57], let us consider the simple toy example of $G = \mathrm{SU}(2)$ broken, on the wall, to $H = \mathrm{U}(1)$. Place a U(1) source charge inside the wall. The bulk respects the non-Abelian SU(2) symmetry and is in the confinement phase, and so the electric field lines of the source charge cannot penetrate this region. Instead, the field lines are repelled from the domain-wall-bulk interface and the effective dimensionality of the Coulomb field is thus reduced by one. If we adopt the 't Hooft-Mandelstam proposal that confinement arises from the magnetic dual of superconductivity [216, 217], then this repulsion of field lines from the interface is understood from the dual Meissner effect [58, 60].

Now place the U(1) source charge in the bulk. Electric field lines emanating from the source are, by confinement, expelled from the bulk. The most energetically favourable configuration is that of an electric flux tube that starts at the source and ends on the domain wall [58, 60, 59]. Once inside the wall the field lines are able to spread out in the plane of the wall because G has broken to H, which is no longer a confining group. The flux

tube acts to funnel the bulk-originating field lines back to the domain wall, giving the illusion that the charge is actually located entirely within the wall. The electric field configuration looks the same at large distances inside the wall irrespective of the position of the source in the bulk. Upgrading this picture to the situation where the source is extended in the bulk direction — it has an arbitrary bulk profile — it follows that the long range Coulomb field is independent of how the profile depends on the coordinate perpendicular to the wall (which is, in our case, the extra dimension). This is the physics responsible for ensuring that different particles, with different profiles, couple to the gauge fields with equal strength; we have gauge coupling universality. We shall assume that this result holds in our five-dimensional implementation of DS: that the different extra-dimensional profiles of the trapped matter fields do not preclude the gauge universality of H.

The extension to a non-Abelian H, which is what we shall need for the standard model gauge group, is straightforward: the arguments above generalise to the case of chromoelectric field line expulsion from the bulk.

Another perspective on the localisation physics is provided by the mass gap of non-Abelian theories [57]. In the bulk, because of confinement, the gauge bosons of H cannot propagate alone, but instead form constituents of propagating, *massive* G glueballs. In the $G = \mathrm{SU}(2)$ and $H = \mathrm{U}(1)$ example, the U(1) gauge boson, which is both massless and free inside the wall, must somehow incorporate itself into a massive SU(2) glueball if it is to propagate into the bulk. But such an event must be paid for in terms of the energy required to bridge the mass gap. Thus any U(1) gauge boson inside the wall is dynamically constrained to remain there. If H has non-Abelian factors that are themselves in confinement phase inside the wall, then the mass gap suppression corresponds to the H glueballs inside the wall being less massive than the G glueballs in the bulk.

These arguments are rather convincing because they rest on the well-established confinement property for asymptotically-free non-Abelian gauge theories in 3+1-dimensions. In the 4+1-dimensional case, the DS mechanism is a conjecture because 4+1-dimensional confinement (or lack thereof) is not properly understood. The main issue is that pure Yang-Mills theory is not renormalisable in $4+1$-dimensions (or larger). At the level of lattice gauge calculations, this corresponds to the lack of a physical limit when taking the lattice spacing to zero. To expand on this point, it is known that $4+1$-

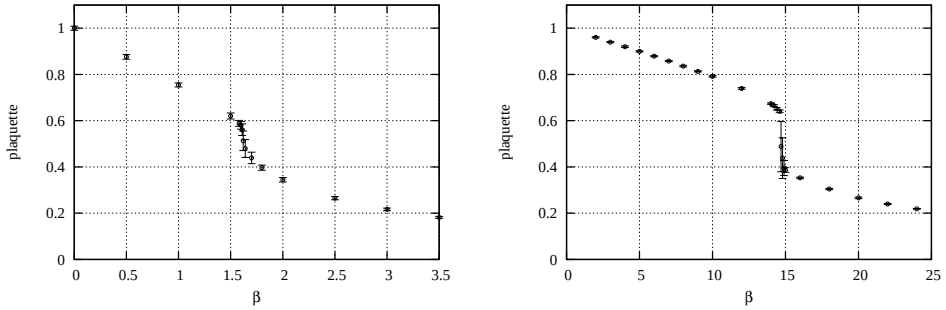

(a) (b)

Figure 5.1: Plot of the average plaquette (defined in Creutz [218]) as a function of the inverse lattice temperature β, which is proportional to the inverse of the square of the gauge coupling constant. The plot in (a) is for SU(2) Yang-Mills (computed to check against Figure 1 of [218]), and (b) is for SU(5) Yang-Mills. The calculations were performed in $4+1$-dimensions with 3^5 lattice points. Each point represents 300 sweeps of the lattice, and the total length of the error bars indicate two standard deviations. A phase transition is discernible in both of these plots, giving good evidence that the corresponding gauge theories exhibit confinement in five-dimensions.

dimensional SU(2) has a first order phase transition for finite lattice spacing; see Creutz [218]. We have verified this conclusion for $4+1$-dimensional SU(5) (see Figure 5.1) and so presumably SU(5) has a confining phase for sufficiently large values of the gauge coupling constant. This analysis cannot be extended to the continuum limit, and so we must be content with $4+1$-dimensional SU(5) exhibiting confinement *below* a relevant cutoff of the theory. Thus we consider $4+1$-dimensional DS to be an effective mechanism, valid below this cutoff, which does the job of confining gauge fields to the domain wall. As we remark below, any field theoretic brane-world model is non-renormalisable and hence must be defined with an ultraviolet cutoff, so in our context we do not need to take the continuum limit.

To the best of our knowledge, the DS mechanism has not been directly checked in $4+1$-dimensions, which would require more than just an analysis of the phase structure of pure Yang-Mills theory. But we are encouraged by lattice gauge calculations in $2+1$-dimensions (see Laine et al. [219]) which do verify the mechanism. We shall assume that it works also in $4+1$-dimensions, and show that realistic model building is then quite possible.

5.2 The model

As stated at the start of Section 5.1, the DS mechanism immediately motivates that the bulk should respect at least an SU(5) gauge symmetry. Since we would like to construct a "minimal" domain-wall-localised standard model, it would be pertinent to have the bulk, and the action, respect exactly an SU(5) symmetry. There are in fact no model-building obstacles to making this minimal choice, and DS implies that the field used to break SU(5) to $G_{\rm SM}$ is also the field that confines the standard model gauge bosons to the wall. In Chapter 6 we are going to relax this minimality condition and consider an E_6 invariant action breaking to SO(10) in the bulk, and SU(5) on the brane.

For now, we are concerned with our SU(5) domain-wall model. The spacetime coordinate is $x^M = (x^\mu, w)$ with $M = (0,1,2,3,5)$, $\mu = (0,1,2,3)$. The gauge field is $X^M(x^N) = X^M_a(x^N)t_a$, where t_a $(a = 1,\ldots,24)$ are the generators of SU(5), normalised to $\mathrm{Tr}(t_a t_b) = \frac{1}{2}\delta_{ab}$. The field strength tensor is $\mathcal{F}^{MN}_a$ and g_5 will be the gauge coupling constant. The five-dimensional matter content is:

$$\text{scalars:} \quad \eta \sim \mathbf{1}\,,\ \chi \sim \mathbf{24}\,,\ \Phi \sim \mathbf{5}^*\,, \tag{5.2a}$$

$$\text{fermions:} \quad \Psi_5 \sim \mathbf{5}^*\,,\ \Psi_{10} \sim \mathbf{10}\,. \tag{5.2b}$$

The scalar field $\eta(x^M)$ is real, $\chi(x^M)$ is conveniently represented as a 5×5 Hermitian traceless matrix, while $\Phi(x^M)$ is a fivefold column vector of complex fields. In four-dimensions chiral spinors are eigen-spinors of the Dirac matrix γ^5, but in five-dimensions γ^5 is used as one of the generators of the Clifford algebra, and is associated with Lorentz transformations in the extra dimension. Chirality does therefore not exist in five-dimensions, and both $\Psi_5(x^M)$ and $\Psi_{10}(x^M)$ are Dirac fields, represented here by a fivefold vector and 5×5 antisymmetric matrix respectively. As mentioned previously, we are only considering one quark-lepton family here. This is for the sake of simplicity, and so we are able to better explore the model-building machinery related to the dimensional reduction. Once we have this under control, it is straightforward to generalise our model to three generations. The neutrino mass question is also deferred to future work.

Under a local $U \in \mathrm{SU}(5)$ transformation, the matter fields behave as

$$\eta \to \eta\,, \qquad \chi \to U\chi U^\dagger\,, \qquad \Phi \to U^*\Phi\,, \tag{5.3a}$$

$$\Psi_5 \to U^*\Psi_5\,, \qquad \Psi_{10} \to U\Psi_{10}U^T\,. \tag{5.3b}$$

We also impose a discrete, reflection symmetry which serves to facilitate the formation of a stable domain wall. This symmetry acts as

$$w \to -w\,, \tag{5.4a}$$

$$\eta \to -\eta\,, \qquad \chi \to -\chi\,, \tag{5.4b}$$

$$\Psi_5 \to i\Gamma^5\Psi_5\,, \qquad \Psi_{10} \to i\Gamma^5\Psi_{10}\,, \tag{5.4c}$$

with X^M and Φ left untouched. Here, the five-dimensional (flat-space) Dirac matrices are $\Gamma^A = (\gamma^\alpha, -i\gamma^5)$ and satisfy $\{\Gamma^A, \Gamma^B\} = 2\eta^{AB}$, where $\eta_{AB} = \mathrm{diag}(+1, -1, -1, -1, -1)$.

We have given the field content and the symmetries. Our model also includes gravity and the full action is

$$\mathcal{S} = \int d^5x\sqrt{G}\left[M_*^3(-R - 2\Lambda) + T - Y_{\mathrm{DW}} - Y_5 - V\right]\,, \tag{5.5}$$

where G is the determinant of the metric, M_* the five-dimensional gravitational mass scale, R the scalar curvature and Λ the bulk cosmological constant. Note that we are using the time-like sign conventions of Section A.3. The rest of the action consists of all the gauge invariant and discrete-reflection-symmetry invariant kinetic and potential terms that can be constructed using the gauge and matter fields. These terms include minimal coupling to gravity. For the kinetic terms we have

$$\begin{aligned} T = &-\frac{1}{4}G^{MN}G^{PQ}\,\mathrm{Tr}\,(\mathcal{F}_{a\,MP}\mathcal{F}_{a\,NQ}) \\ &+ \frac{1}{2}G^{MN}\partial_M\eta\partial_N\eta + G^{MN}\,\mathrm{Tr}\left[(D_M\chi)^\dagger D_N\chi\right] \\ &+ G^{MN}\,(D_M\Phi)^\dagger\,D_N\Phi \\ &+ i\overline{\Psi}_5\Gamma^A e_A{}^M D_M\Psi_5 + \mathrm{Tr}\left(i\overline{\Psi}_{10}\Gamma^A e_A{}^M D_M\Psi_{10}\right)\,. \end{aligned} \tag{5.6}$$

The symbol D_M stands for the appropriate general-coordinate covariant and gauge-covariant derivative. For the fermions, this derivative includes the spin-connection, and for this we require the vielbein $e_A{}^M$; see the dis-

cussions in Section 4.2 and Section A.4. $Y_{\rm DW}$ has the Yukawa couplings of the fermions to the kink background fields η and χ,

$$\begin{aligned} Y_{\rm DW} = {} & h_{5\eta}\overline{\Psi}_5\Psi_5\eta + h_{5\chi}\overline{\Psi}_5\chi^T\Psi_5 \\ & + h_{10\eta}\,\mathrm{Tr}\left(\overline{\Psi}_{10}\Psi_{10}\right)\eta - 2h_{10\chi}\,\mathrm{Tr}\left(\overline{\Psi}_{10}\chi\Psi_{10}\right)\,, \end{aligned} \tag{5.7}$$

and Y_5 is the SU(5) Yukawa Lagrangian used to generate quark and lepton masses:

$$Y_5 = h_-\overline{(\Psi_5)^c}\Psi_{10}\Phi + h_+\epsilon^{ijklm}\overline{(\Psi_{10})^c}_{ij}(\Psi_{10})_{kl}(\Phi^*)_m + \text{h.c.} \tag{5.8}$$

The last term is written in SU(5) index notation with ϵ^{ijklm} the totally anti-symmetric tensor. Charge conjugation of five-dimensional fermions is defined by $\Psi^c = \Gamma^2\Gamma^5\Psi^*$. Finally, we have the Higgs potential $V = V_{\eta\chi} + V_{\rm rest}$, where

$$\begin{aligned} V_{\eta\chi} = {} & (c\eta^2 - \mu_\chi^2)\,\mathrm{Tr}(\chi^2) + \lambda_1\eta\,\mathrm{Tr}(\chi^3) + \lambda_2\left[\mathrm{Tr}(\chi^2)\right]^2 \\ & + \lambda_3\,\mathrm{Tr}(\chi^4) + l(\eta^2 - v^2)^2\,, \end{aligned} \tag{5.9a}$$

$$\begin{aligned} V_{\rm rest} = {} & \mu_\Phi^2\Phi^\dagger\Phi + \lambda_4(\Phi^\dagger\Phi)^2 + \lambda_5\Phi^\dagger\Phi\eta^2 + 2\lambda_6\Phi^\dagger\Phi\,\mathrm{Tr}(\chi^2) \\ & + \lambda_7\Phi^\dagger(\chi^T)^2\Phi + \lambda_8\Phi^\dagger\chi^T\Phi\eta\,. \end{aligned} \tag{5.9b}$$

To summarise, the model contains the gravitational parameters M_* and Λ, the gauge coupling g_5, the fermion Yukawa constants $h_{5\eta}$, $h_{5\chi}$, $h_{10\eta}$, $h_{10\chi}$, h_- and h_+, and the scalar parameters c, l, v, μ_χ, μ_Φ and $\lambda_{1\text{–}8}$.

Disregard gravity for the moment and consider the ultraviolet behaviour of our model. Since we are in five-dimensions, we cannot renormalise the theory, and so, as is usual in these kinds of models, we assume an implicit ultraviolet cut-off $\Lambda_{\rm UV}$. We do not commit to the nature of physics beyond this scale, and have nothing to say about how our model emerges as the low-energy limit of the putative ultraviolet completion; we simple assume that it does. In line with the discussion at the end of Section 3.1.1 regarding renormalisable terms at the effective level, our action is perhaps best considered as the set of lowest-dimensional operators, consistent with the given symmetries, of a non-renormalisable, effective five-dimensional theory. The relationship of $\Lambda_{\rm UV}$ to the other scales in the model is discussed in Section 5.4.

Now that we have the theory described in full, we turn to a discussion of how the domain-wall background forms, the ground state matter modes that are localised to the wall, and how these modes result in an effective, four-dimensional standard model. A specific background configuration, along with explicit solutions for the extra-dimensional profiles, will be presented in Section 5.3. For now, we outline these features in general terms.

The first thing to do is find a background configuration for η, χ and the metric which solves Einstein's equations and the Euler-Lagrange equations. Of course, we need to specify boundary conditions in order to pick out solutions with the requisite Randall-Sundrum, domain-wall structure. The ansatz for the metric is, as usual, the warped form

$$ds^2 = e^{-2\sigma(w)}\eta_{\mu\nu}dx^\mu dx^\nu - dw^2 \,, \tag{5.10}$$

with asymptotic behaviour $\sigma(w) \to \sim |w|$ as $|w| \to \infty$. The proportionality constant for the asymptotic behaviour of $\sigma(w)$ will depend on the bulk cosmological constant Λ, and the usual Randall-Sundrum fine-tuning condition must be imposed to ensure a Minkowski brane. This will, in turn, relate Λ to the width and height of the kink solution.

Having the Randall-Sundrum warped metric guarantees localised gravity. To localise the fermions and Higgs, we need η to form a kink, and we need χ to form a Gaussian-like profile, centred on the domain wall, to implement the DS mechanism and localise the gauge bosons.[1] Because we aim to localise the standard model, we also need to make sure that χ breaks SU(5) in the direction of $G_{\rm SM}$. Recall that χ is a 5×5 matrix that transforms as the **24** of SU(5), so we can write it as $\chi = \chi_a t_a$. Let us define the first generator t_1 to be the component associated with the weak-hypercharge generator:

$$t_1 = \frac{1}{2\sqrt{15}}\,\mathrm{diag}(2, 2, 2, -3, -3) \,. \tag{5.11}$$

Our desired symmetry breaking pattern can then be achieved by choosing to have, at the background solution level, $\chi_1 \neq 0$ and the rest of the components

[1] As pointed out by Dvali and Shifman [57], as well as localising gauge bosons the confining bulk can localise gauge non-singlet fermions and scalar fields. However, for our application, we have to retain the seemingly redundant localisation-to-a-kink mechanism. The DS mechanism on its own will not suffice because it will localise vector-like fermions, not massless chiral fermions. The kink configuration is necessary for the spontaneous generation of chirality in the four-dimensional effective theory.

$\chi_{2\text{–}24}$ vanishing.

Since w is the extra dimension, we look for background solutions where η and χ_1 depend only this coordinate, as is the case for the metric function $\sigma(w)$. The boundary conditions for the scalar fields are

$$\eta(w = -\infty) = -v\,, \qquad \eta(w = +\infty) = +v\,, \tag{5.12a}$$

$$\chi_1(w = -\infty) = 0\,, \qquad \chi_1(w = +\infty) = 0\,. \tag{5.12b}$$

These values correspond to degenerate global minima of $V_{\eta\chi}$. The spontaneously broken reflection symmetry ensures topological stability for the domain wall configuration.

For a significant region of parameter space, the coupled Einstein's and Klein-Gordon equations (not given) admit numerical solutions compatible with our ansatz for the metric and our choice of scalar-field boundary conditions. The solutions have σ a smooth, even function of w with Randall-Sundrum asymptotic behaviour, η forms the usual kink profile, and χ_1 is Gaussian shaped. The matter fields Ψ_5, Ψ_{10} and Φ propagate in this background, and appropriate Kaluza-Klein towers of modes are induced. Our classical analysis of the associated mode profiles is encumbered in this particular model by the non-perturbative physics of the DS mechanism. We are going to assume that such difficulties can be avoided, at least in the first instance, because the SU(5) confinement dynamics are suppressed within the wall. Outside the wall, the non-perturbative SU(5) physics makes calculating impossible, at least in the absence of dedicated lattice-gauge-theory machinery. Since the localisation profiles of the Kaluza-Klein modes are peaked near the centre of the wall, where the bulk symmetry is broken, ignoring the non-perturbative corrections is approximately valid. We continue this discussion in Section 5.3.1.

Assuming that it is safe to do so, analysis of our model proceeds by performing a general Fourier expansion of the fermion and Higgs fields. For now, we are just going to be interested in the lowest modes of the towers: the fermion zero modes, the Higgs-doublet tachyonic mode, and the lowest coloured-scalar mode. The two fermion multiplets contain precisely the fermion content of the standard model, as per equation (1.12). Each individual Dirac spinor will be localised via the kink profile η in the usual way, but, due to the different $\mathrm{U}(1)_Y$ hypercharges, each component couples

differently to the additional SU(5)-charged scalar χ_1. This additional coupling is large enough to significantly influence the effective trapping potential that appears in the Schrödinger-like equation for the extra-dimensional profiles. Therefore, the different components of Ψ_5 and Ψ_{10} feel different background configurations, and their Kaluza-Klein towers are subsequently localised at different positions in the extra dimension — the split fermion mechanism [67], as introduced in Section 1.3.4. The terms responsible for the fermion localisation come from Y_{DW}, and the associated parameters are $h_{5\eta}$, $h_{5\chi}$, $h_{10\eta}$ and $h_{10\chi}$.

The splitting phenomenon also applies to the Higgs multiplet Φ. This field contains the five-dimensional Higgs-doublet $\Phi_w(x^M)$ along with the five-dimensional coloured-scalar $\Phi_c(x^M)$. These two components have different $\mathrm{U}(1)_Y$ hypercharges, and, by the previous argument, are localised to different positions inside the domain-wall region. Here, the $\lambda_{5\text{–}8}$ terms in V_{rest} control this trapping, and the parameters can be adjusted to shift the location of the modes. The additional parameter μ_Φ^2 in equation (5.9b) is used to manipulate the overall height of the effective trapping potential and obtain a tachyonic ground state mode for Φ_w; see equation (3.45) and the discussion towards the end of Section 3.2.2. Let the lowest modes of Φ_w and Φ_c have mass-squared m_w^2 and m_c^2 respectively. It turns out that there is sufficient parameter freedom to allow both $m_w^2 < 0$ and $m_c^2 > 0$, thus setting the stage for an effective Mexican-hat potential for the associated lowest mode $\phi_w(x^\mu)$, while keeping the lowest coloured-scalar mode $\phi_c(x^\mu)$ massive. This ensures that electroweak symmetry breaking can be implemented on the brane, giving masses to the chiral, fermion zero modes, while $\mathrm{SU}(3)_C$ remains an exact symmetry.

We can now see how natural resolutions arise to some of the usual problems with an SU(5) grand unified theory. The mass relation $m_e = m_d$ is *not* obtained because the four-dimensional Yukawa couplings, and hence the masses of the four-dimensional modes, depend on overlap integrals in the extra dimension. These will be different for fermions with different $\mathrm{U}(1)_Y$ hypercharge (like e and d) because of the layout of the fermion localisation profiles. The splitting of the profiles can also alleviate the issue of proton decay. The coloured-scalar ϕ_c can induce such a decay through the reaction $p \to \pi^0 e^+$ via the Yukawa terms $\overline{u}_R (e_R)^c \phi_c^*$ and $\overline{d}_R (u_R)^c \phi_c$. This effect can be suppressed by making the relevant profile overlaps very small. For exam-

ple, splitting u_R and d_R so that that they overlap exponentially little would suffice; see, for example, Coulthurst, McDonald and McKellar [220].

In Chapter 4 we discussed how the spectrum of localised matter fields is modified in the presence of Randall-Sundrum-like warped gravity. These effects will be present in our SU(5) model. In particular, a continuum of fermion and Higgs fields will be present, starting at zero four-dimensional mass, although they will only couple very weakly to the modes that are bound to the brane. The question of the influence that a warped metric has on the gauge boson spectrum is left as work for the future, but we suspect the effect to be negligible since, in the region close to the domain wall, the scale of gravity is far weaker than the physics related to the gauge boson localisation.

The next section gives an explicit, analytic form for the background configuration which allows us to give concrete expressions, and plots, for the profiles of the ground state fermion and Higgs fields. We shall also discuss the effective electroweak sector and derive the fermion masses.

5.3 Aspects of the model

The exposition of our theory, which is defined by equation (5.5), begins with gravity turned off, and we follow the general mode analysis of Chapter 3. This will allow us to focus on the purely particle-physics aspects of the model. Modifications due to gravity are then discussed towards the end, in Section 5.3.3. The gravity-free background consists of the configuration of the coupled scalar fields η and χ_1, which generally take the form of a kink and Gaussian, respectively. Purely for the sake of giving a concrete, analytic example, we can impose the parameter conditions

$$\lambda_1 = 0 \,, \tag{5.13a}$$

$$2\mu_\chi^2(c - \tilde{\lambda}) + (2c\tilde{\lambda} - 4l\tilde{\lambda} - c^2)v^2 = 0 \,, \tag{5.13b}$$

with $\tilde{\lambda} \equiv \lambda_2 + \frac{7}{30}\lambda_3$. This permits the solution

$$\eta(w) = v \tanh(kw) \,, \tag{5.14a}$$

$$\chi_1(w) = A \cosh^{-1}(kw) \,, \tag{5.14b}$$

where $k^2 = cv^2 - \mu_\chi^2$ and $A^2 = (2\mu_\chi^2 - cv^2)/\tilde{\lambda}$. As before, the adjoint field $\chi = \chi_a t_a$ has, at the classical solution level, all components except χ_1 vanish. Since χ_1 is associated with t_1, defined by equation (5.11), it induces $\mathrm{SU}(5) \to G_{\mathrm{SM}}$ within the domain wall, a region with width of order $1/k$. By the DS mechanism, the gauge bosons associated with G_{SM} are localised to this small region. For the field η, its form is the canonical kink solution, and serves to trap the fermions Ψ_5 and Ψ_{10}, and the Higgs Φ, to the brane. We have checked numerically that configurations such as equation (5.14) are perturbatively stable against the formation of additional, non-zero χ components.

With these background solutions, we now proceed to provide explicit forms of the matter trapping potentials, and give examples of how the split fermions, and split Higgs, can be arranged in the extra dimension.

5.3.1 The fermion and Higgs fields

The five-dimensional fermions couple to the background w-dependent scalar fields as per Y_{DW}, and a Kaluza-Klein tower of four-dimensional modes is induced. A full mode decomposition analysis involves writing a bulk fermion field as a sum over the product of four-dimensional fields and their associated profiles. The Dirac equation is then used to solve for the forms of the profiles. So far in this thesis we have come across singlet fermions, which are just usual Dirac spinors, and the extra-dimensional profile of each component of the spinor satisfies an identical differential equation. Thus we were justified in performing the expansions of equations (3.56) and (4.14), where a single profile multiplies each component of the spinor. For the case at hand, as we have discussed already, the extra-dimensional profiles of fermion components with different hypercharges are going to solve different equations. Thus we must expand each hypercharge component of the multiplets Ψ_5 and Ψ_{10} with different profile functions. In what follows, the notation for one of these five-dimensional components is $\Psi_{nY}(x^M)$, where $n = 5$, 10 and Y is the hypercharge. The same story is true for the scalar Φ, and here the two components are Φ_w and Φ_c.

One may wonder about the validity of a full mode decomposition in the presence of the non-perturbative physics of the DS mechanism, a discussion which we began in Section 5.2. Consider the case of the expansion of a generic scalar: $\Xi(x^M) = \sum_n \xi_n(x^\mu)k_n(w)$. From a mathematical point of

view, the set of mode functions k_n is just some complete set of functions that permits the decomposition of Ξ without loss of generality, and so one has the usual freedom to change basis by changing the mode-function set. This is a pertinent observation for theories that employ the non-perturbative quantum-field-theoretic DS mechanism. Say Ξ is a gauge singlet, and is hence immune to DS. Then our mode decomposition, whereby the ξ_n satisfy the massive Klein-Gordon equation, constitutes a "sensible" choice of basis functions, where "sensible" means that each (bound) profile k_n corresponds to a physical, propagating state in the effective four-dimensional theory. Now take Ξ to transform non-trivially under the gauge symmetry and to feel the non-perturbative nature of the bulk. Although it may not be a "sensible" way of doing things, there is no problem in using the same mode decomposition that we used for the singlet field, because that is simply a mathematically-valid recasting of Ξ as an infinite set of ξ_n components. If the bulk is indeed in confinement phase, then the gauge non-singlet ξ_n fields will not propagate as free particles, so their physical interpretation will be as constituent particles. This is conceptually no different from expressing the QCD Lagrangian in terms of quarks and gluons even though the propagating states are hadrons.

We are not actually going to perform a full mode decomposition for the five-dimensional fields in our model. Instead, we are just interested in the physics that emerges from the fermion zero modes and the ground state Higgs modes. These low-energy modes have profiles which are sharply peaked inside the domain wall, and so to a first approximation we need not be concerned with interpretive complications that arise because of the non-perturbative bulk. As we have just emphasised, we are free to choose any set of basis functions (profiles) that we like, and we are going to choose those that have a physically sensible interpretation in the non-DS scenario, and, furthermore, we are only going to consider the ground state mode of this basis. Our assumption is that in doing so we capture the essential physics of the low-energy, four-dimensional effective theory, and that taking into account the higher modes and a proper treatment of DS does not significantly alter our results.

Let us first consider the fermions. To analyse the localisation of the chiral, zero mode, the full mode expansion is unnecessary. Instead, it suffices to solve the Dirac equations with a simple separation of variables for each

hypercharge component:

$$\Psi_{nY}(x^\mu, w) = f_{nY}(w)\ \psi_{nY,L}(x^\mu)\,, \tag{5.15}$$

where the $\psi_{nY,L}(x^\mu)$ are four-dimensional, massless, left-chiral fields: they satisfy $i\gamma^\alpha\partial_\alpha\,\psi_{nY,L} = 0$ and $\gamma^5\psi_{nY,L} = -\psi_{nY,L}$. These fields have weak-hypercharge Y and their corresponding extra-dimensional profiles are $f_{nY}(w)$. With this separation, the Dirac equations for the five-dimensional fermion components are

$$\left[i\Gamma^A\partial_A - h_{n\eta}\eta(w) - \sqrt{\frac{3}{5}}\frac{Y}{2}\,h_{n\chi}\chi_1(w)\right]\Psi_{nY}(x^\mu, w) = 0\,. \tag{5.16}$$

As pointed out earlier, $n = 5$, 10 and Y is the $\mathrm{U}(1)_Y$ hypercharge associated with the component Ψ_{nY}. Equation (5.16) is manifestly different for the various components, vindicating our earlier claim that the SU(5) structure of our model automatically gives different localisation points and profiles to the different standard model components. The zeroes of

$$b_{nY}(w) \equiv h_{n\eta}\eta(w) + \sqrt{\frac{3}{5}}\frac{Y}{2}\,h_{n\chi}\chi_1(w) \tag{5.17}$$

are the localisation centres of the associated profiles, these profiles being

$$f_{nY}(w) \propto e^{-\int_0^w b_{nY}(w')\,dw'}\,. \tag{5.18}$$

Here, the proportionality constant is determined by normalising f_{nY}^2 to unity. To localise four-dimensional, left-chiral fields, all the b_{nY} must pass through zero with positive slope; this constrains the signs and magnitudes of the parameters $h_{n\eta}$ and $h_{n\chi}$. Sample solutions of the split profiles f_{nY} are given in Figure 5.2.

Moving on to the localisation of the Higgs field Φ, we are again only interested in the lowest mode of the full Kaluza-Klein tower, and so perform a simple separation of variables for the doublet and triplet components:

$$\Phi_{w,c}(x^\mu, w) = p_{w,c}(w)\ \phi_{w,c}(x^\mu)\,, \tag{5.19}$$

where $\phi_{w,c}(x^\mu)$ are required to satisfy a massive four-dimensional Klein-Gordon equation with mass-squared parameters $m_{w,c}^2$. The two profiles,

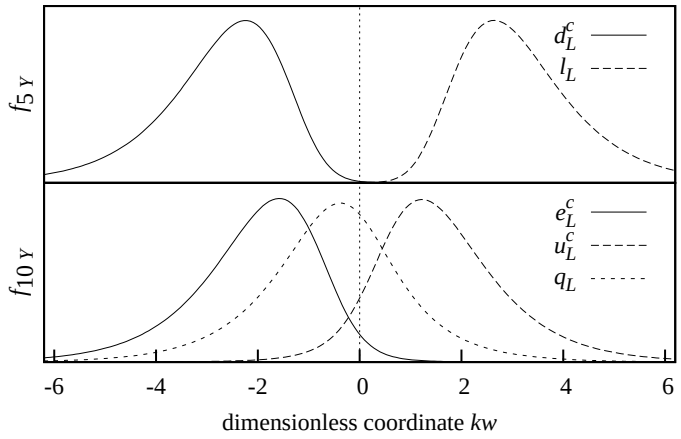

Figure 5.2: Typical extra-dimensional profiles $f_{nY}(w)$ for the fermion components contained in the $\mathbf{5}^*$ (top) and the **10** (bottom). The fields η and χ_1 are as per equation (5.14) and we are plotting equation (5.18) with parameter choices $v = A = 1$, $h_{n\eta} = 1$, $h_{5\chi} = 6$ and $h_{10\chi} = 1$. The profiles are normalised such that $\int dw f_{nY}^2(w) = 1$.

$p_w(w)$ and $p_c(w)$, obey the Schrödinger-like equation

$$-\frac{d^2 p_{w,c}(w)}{dw^2} + W_Y(w) p_{w,c}(w) = m_{w,c}^2 p_{w,c}(w) \,, \tag{5.20}$$

with a weak-hypercharge-dependent effective potential

$$W_Y(w) = \mu_\Phi^2 + \lambda_5 \eta^2 + \lambda_6 \chi_1^2 + \frac{3Y^2}{20}\lambda_7 \chi_1^2 + \sqrt{\frac{3}{5}}\frac{Y}{2}\lambda_8 \eta \chi_1 \,. \tag{5.21}$$

The hypercharges are: $Y(\phi_w, \phi_c) = (-1, \frac{2}{3})$.

We can actually determine the full spectrum of localised and delocalised Φ modes by finding all the eigenfunctions, and associated eigenvalues, of equation (5.20). Of this spectrum, we are only interested here in the lowest mass eigenstates. As mentioned previously, there is sufficient parameter freedom to allow $m_w^2 < 0$ while keeping $m_c^2 > 0$, which enables the four-dimensional mode ϕ_w to act as the usual standard model Higgs, and prevents ϕ_c from breaking the colour gauge group $\mathrm{SU}(3)_C$. An example of the effective potentials $W_Y(w)$, which support such eigenvalues, are given in Figure 5.3. Note that if $m_w^2 < 0$, one really needs to solve for the background configuration of η, χ and Φ *simultaneously*, to ensure that the back-reaction of the tachyonic ϕ_w does not destroy the domain wall. Since the energy

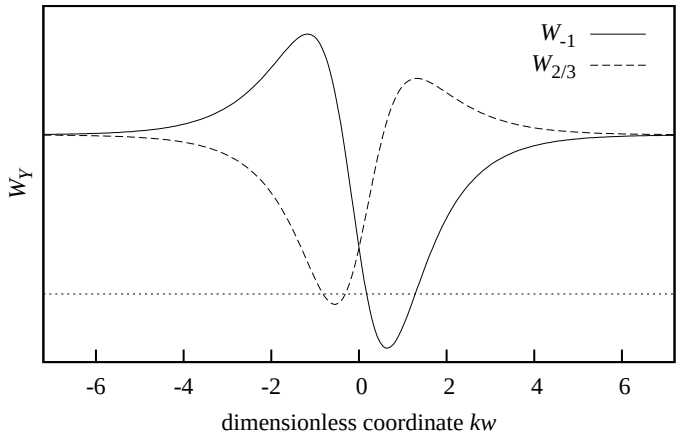

Figure 5.3: Example potential profiles $W_Y(w)$, given by equation (5.21), which trap the Higgs doublet Φ_w and coloured scalar Φ_c. The straight horizontal line is $W_Y = 0$. Parameters are chosen such that the lowest eigenstate of W_{-1} ($W_{2/3}$) has a negative (positive) eigenvalue. This gives the four-dimensional Higgs doublet ϕ_w a tachyonic mass on the brane while keeping the coloured scalar ϕ_c heavy.

scale of ϕ_w condensation is much lower than that of the other background scalars, we assume the back-reaction to be negligible, and the domain wall stable. Actually, due to the shape of the profile p_w, the background configuration associated with ϕ_w is like a mini version of DS all over again: the Φ_w component of Φ is breaking $G_{\rm SM} \to {\rm SU}(3)_C \otimes {\rm U}(1)_{\rm EM}$, but only inside the domain wall.

Recall that the scalar spectrum also contains the kink translation zero mode, which is potentially frozen out in the thin kink limit, as discussed at length in Section 3.1.3. If this mode does not freeze out, or if the kink is not thin enough, then the translation mode must be dealt with in some other way, possibly using gravity, following Shaposhnikov et al. [179].

As mentioned at the beginning of this chapter, gauge coupling constant evolution cannot be examined until a proper phenomenological parameter fitting is done, preferably with three generations. This is because the higher mass modes both depend on these parameters and affect the coupling constant evolution. Since the higher mass modes are split SU(5) multiplets, the running will be different from standard four-dimensional, non-supersymmetric SU(5), and successful unification may, in fact, be possible. Note that coupling constants run logarithmically, not through a power-law, in the effective four-dimensional theory of localised fields.

5.3.2 Effective Higgs sector and fermion masses

Having solved the Schrödinger-like equation (5.20) for the profile p_w and mass-squared eigenvalue m_w^2, we are able to determine the effective four-dimensional action for the ground-state Higgs mode ϕ_w. We consider only those terms that contain ϕ_w alone; for example, we ignore the terms coupling this Higgs to the gauge fields. From T we obtain the usual kinetic term, diagonal and canonically normalised due to the orthonormality of the eigenfunctions. The effective potential for ϕ_w comes entirely from V_{rest}; the μ_Φ^2 and $\lambda_{5\text{–}8}$ terms induce the trapping potential and conspire to produce a value for m_w^2, while the λ_4 term yields a quartic interaction. The resulting effective action is quite simply

$$\mathcal{S}_{\phi_w} = \int d^4x \left[\partial^\alpha \phi_w^\dagger \partial_\alpha \phi_w - m_w^2 \phi_w^\dagger \phi_w - \kappa_w (\phi_w^\dagger \phi_w)^2\right] , \tag{5.22}$$

where the (dimensionless) quartic coupling constant is

$$\kappa_w = \lambda_4 \int (p_w)^4 \, dw \, . \tag{5.23}$$

Note that p_w is a real-valued profile. Since we have arranged for m_w^2 to be negative, ϕ_w will pick up a VEV. More precisely, it is the lower component of this Higgs doublet (the uncharged component) that picks up the VEV. It is

$$\langle \phi_w \rangle = \sqrt{\frac{-m_w^2}{\kappa_w}} \, . \tag{5.24}$$

Now we would like to consider the fermions; their kinetic terms and their mass terms. What follows is a bit of a notational nightmare because we begin with five-dimensional, Dirac, SU(5) multiplets, Ψ_5 and Ψ_{10}, and end up with four-dimensional, chiral spinors. For the following deconstruction, it may be helpful to refer to equation (1.12) and Figure 1.1.

The five-dimensional multiplet Ψ_5 contains the five-dimensional, Dirac, anti-down quark Ψ_{d^c} and the five-dimensional, Dirac lepton-doublet Ψ_l. The latter is made up of the electron Ψ_e and the electron-neutrino Ψ_ν, both of which are still five-dimensional Dirac fields. These components are separated into an extra-dimensional profile and a four-dimensional spinor. As per previous discussions, the kink background localises a four-dimensional, left-chiral projection of these spinors, and in this chapter we are only con-

sidering this ground state. So, we define, $\Psi_{d^c} = f_{d^c}\psi_{d^c}$, where $f_{d^c}(w)$ is the profile associated with the four-dimensional, left-handed field $\psi_{d^c}(x^\mu)$, which is to be identified with the degrees of freedom of the anti-down quark of the standard model. In the notation used in equation (5.15), we identify $f_{d^c} \equiv f_{(n=5,Y=2/3)}$. For the lepton-doublet field, both components of the doublet have the same profile, so we can write $\Psi_l = f_l\psi_l$, as well as $\Psi_e = f_l\psi_e$ and $\Psi_\nu = f_l\psi_\nu$. Here, $f_l \equiv f_{(n=5,Y=-1)}$ is the profile, and $\psi_l(x^\mu)$ is the four-dimensional, left-chiral lepton-doublet of the standard model, with components $\psi_e(x^\mu)$ and $\psi_\nu(x^\mu)$. Just to be clear, we have $\psi_l = (\psi_e, \psi_\nu)$.

The multiplet Ψ_{10} contains $\Psi_{u^c} = f_{u^c}\psi_{u^c}$, $\Psi_{e^c} = f_{e^c}\psi_{e^c}$ and $\Psi_q = f_q\psi_q$, with a factor of $1/\sqrt{2}$, as per equation (1.12). The latter field is the quark-doublet and contains $\Psi_u = f_q\psi_u$ and $\Psi_d = f_q\psi_d$. The fields ψ_{u^c}, ψ_{e^c}, ψ_u and ψ_d are four-dimensional, left-chiral fields that are identified with the anti-up quark, anti-electron, up quark and down quark respectively. These, together with the left-chiral fields from Ψ_5, make up precisely the fermion content of the standard model.

Our next task is to extract the relevant terms from Y_5 which give mass to the four-dimensional fermions. We are interested in those terms which couple individual components of Ψ_5 and Ψ_{10} to Φ_w, where the latter is defined by $\Phi = (\Phi_c, \Phi_w)$. There are two such terms in the Ψ_5-Ψ_{10}-Φ coupling:

$$\overline{(\Psi_5)^c}\Psi_{10}\Phi \supset \frac{1}{\sqrt{2}}\left[\overline{(\Psi_{d^c})^c}\Psi_q\Phi_w + \epsilon^{ij}\overline{(\Psi_l)^c}_i\Psi_{e^c}(\Phi_w)_j\right] , \tag{5.25}$$

where $\epsilon^{12} = -\epsilon^{21} = 1$, and the i, j indices on the fields work, for example, as $(\Psi_l)_1 = \Psi_e$. Be careful with the superscript-c notation here: Ψ^c is the five-dimensional charge conjugate of Ψ (defined earlier), but Ψ_{d^c} is just notation to remind us that this field is to be identified with an anti-down quark (we could have called it $\Psi_{\text{anti-}d}$ instead). The Ψ_{10}-Ψ_{10}-Φ coupling contains one other relevant term:

$$\epsilon^{ijklm}\overline{(\Psi_{10})^c}_{ij}(\Psi_{10})_{kl}(\Phi^*)_m \supset 4\epsilon^{ij}\overline{(\Psi_{u^c})^c}(\Psi_q)_i(\Phi_w^*)_j \, . \tag{5.26}$$

By using expansions of the form $\Psi_X = f_X\psi_X$ (X labels some fermion) and $\Phi_w = p_w\phi_w$, and by making the replacement $(\phi_w)_2 \to \langle\phi_w\rangle$, we obtain, from equations (5.25) and (5.26), bi-linear terms which couple each fermion with their anti-fermion partner. For example, ψ_e is paired with ψ_{e^c}. These

terms are exactly the requisite fermion mass terms. Each four-dimensional, left-chiral spinor field will also have a kinetic term, which is canonically normalised because the f_X^2 are normalised to unity.

Considering just those terms which serve to describe the massive, propagating electron at the effective four-dimensional level, we obtain the action

$$\mathcal{S}_e = \int d^4x \left[\overline{\psi_e}\, i\gamma^\alpha \partial_\alpha \psi_e + \overline{\psi_{e^c}}\, i\gamma^\alpha \partial_\alpha \psi_{e^c} + \kappa_e \langle \phi_w \rangle \overline{(\psi_e)^c} \psi_{e^c} + \text{h.c.} \right] . \quad (5.27)$$

Recall that both ψ_e and ψ_{e^c} are left-chiral fields. The charge conjugate in equation (5.27) is now the usual *four-dimensional* charge conjugate: $\psi^c = \gamma^2 \psi^*$. The coupling constant is computed as the overlap integral

$$\kappa_e = \frac{i h_-}{\sqrt{2}} \int f_l \, f_{e^c} \, p_w \, dw \, , \quad (5.28)$$

and the mass of the electron is identified as

$$m_e = |\kappa_e| \langle \phi_w \rangle \, . \quad (5.29)$$

For the sake of completeness, let us define the Dirac field $e = \psi_e + (\psi_{e^c})^c$ which has $\mathrm{U}(1)_{\mathrm{EM}}$ electric charge -1. The action (5.27) can then be written in the more familiar form

$$\mathcal{S}_e = \int d^4x \, [\overline{e}\, i\gamma^\alpha \partial_\alpha e - m_e \overline{e} e] \, . \quad (5.30)$$

The story is the same for the down and up quarks. The fields ψ_d and ψ_{d^c} form a Dirac pair, as do ψ_u and ψ_{u^c}. Their effective actions are analogous to equation (5.27), but with coupling constants

$$\kappa_d = \frac{i h_-}{\sqrt{2}} \int f_{d^c} \, f_q \, p_w \, dw \, , \quad (5.31a)$$

$$\kappa_u = 4 i h_+ \int f_{u^c} \, f_q \, p_w \, dw \, , \quad (5.31b)$$

and corresponding masses

$$m_d = |\kappa_d| \langle \phi_w \rangle \, , \quad (5.32a)$$

$$m_u = |\kappa_u| \langle \phi_w \rangle \, . \quad (5.32b)$$

For the single-generation standard model that we have reproduced here,

it is obvious that there are enough parameters to fit the quark and lepton masses. The profiles f_l, f_{e^c}, f_{d^c}, f_q and p_w can be adjusted to obtain the correct ratio m_e/m_d, then h_- can be chosen to fix the absolute value.[2] The parameter h_+ independently controls m_u. For the three-generation case, it is plausible that sufficient parameter freedom exists, though this has not been rigorously proven as yet. It is a complicated problem, because the physical observables depend on profile functions which depend in complicated ways on the Lagrangian parameters. There may also be diagonalisation issues in the profile sector, as the Schrödinger-like equations will contain terms which mix the three generations ($h_{n\eta}$ and $h_{n\chi}$ will be 3×3 matrices). Corrections to the classical calculations due to the effect of the non-perturbative bulk will also exist at some level.

5.3.3 Including gravity

The previous analysis has been performed in the absence of gravity. To include gravity, using the ansatz for the metric given by equation (5.10), we must find a background configuration for σ, η and χ_1 that satisfies Einstein's equations and the Klein-Gordon equations. As in the gravity-free case, analytic solutions exist for a restricted set of parameters. For notational convenience, define $a = v^2/6M_*^3$. Then, for the special parameter choices

$$\lambda_1 = 0\,, \tag{5.33a}$$

$$c = 2l + \frac{\tilde{\lambda}}{2}\,, \tag{5.33b}$$

$$\mu_\chi^2 = \frac{lv^2}{1+2a} + \frac{\tilde{\lambda}v^2}{4}\left(\frac{3+8a}{1+2a}\right)\,, \tag{5.33c}$$

we are able to obtain the convenient analytical solutions

$$\eta(w) = v\tanh(kw)\,, \tag{5.34a}$$

$$\chi_1(w) = v\cosh^{-1}(kw)\,, \tag{5.34b}$$

$$\sigma(w) = a\log\left[\cosh(kw)\right]\,, \tag{5.34c}$$

[2] There may be other physics, like proton decay, that dictate the layout of some of the profiles. There should be enough freedom in all of the parameters to satisfy these constraints and the mass constraint.

where

$$k^2 = \frac{cv^2 - \mu_\chi^2}{1 + 4a}\,, \tag{5.35}$$

and the fine-tuned cosmological constant is $\Lambda = -6a^2k^2$. Recall that we have defined $\tilde{\lambda} \equiv \lambda_2 + \frac{7}{30}\lambda_3$.

Our metric solution is a smoothed out version of the Randall-Sundrum warped metric, and the linearised graviton fluctuation equation has a confined zero-mode that is identified as the usual graviton, as discussed in detail in Section 4.1. Thus, our SU(5) model contains an effective description of four-dimensional gravity trapped to the dynamically generated brane.

In the presence of gravity, the four-dimensional fermion spectrum still contains a localised zero mode for each species. However, the trapping potentials of the Ψ_5 and Ψ_{10} fields are now driven towards zero far from the brane, since the physics there is dominated by the warp factor. The fermion trapping potentials are thus volcano-like, and, in analogy with the graviton modes, arbitrarily light fermions plague the original spectra. This effect is discussed in detail in Chapter 4, and it is shown there that such continuum fermion modes interact only very weakly with brane-localised processes. The Φ spectrum similarly contains a localised standard-model Higgs doublet plus a continuum starting at zero mass. Because the eigenvalue of the Higgs doublet (the mass squared) is negative, it still retains a mass gap to the beginning of the continuum modes.

The analysis of the induced continuum modes is affected by the DS phenomenon because the fermions and scalar transform non-trivially under SU(5). Since the continuum modes penetrate into the bulk, they feel the full effects of the confinement-phase physics we assume holds there. We therefore expect the low-mass continuum modes to manifest physically as the constituents of massive "hadrons" in the bulk, as opposed to a single continuum mode associated with, say, ψ_e. But these low-mass hadrons still have to tunnel through the volcano-like potential barriers to get inside the domain wall and interact with the matter localised there. Since the non-perturbative effects switch off near the wall, the situation discussed in Chapter 4 is regained and, with some plausibility, we reach the same conclusions regarding suppression of brane-bulk mode interaction.

In summary, we are confident that the analysis of our SU(5) model performed in the gravity-free case in Section 5.3.1 and Section 5.3.2 remains

valid when gravity is switched on. The ground state modes of Ψ_5, Ψ_{10} and Φ remain the same, as do the forms of their effective actions. The overlap integrals will now include factors with various powers of the warp factor $e^{-2\sigma}$, but such a modification has little qualitative effect, and we still retain enough freedom in our choice of parameters to fit, for example, the fermion masses. The four-dimensional, low-energy effective action therefore describes the single-generation standard model in a Minkowski background, with minimal coupling to four-dimensional gravity.

5.4 Relationships among the scales

Having described the construction of the model, it is now worth surveying the various scales it contains and how they should relate to each other. Of the many scales in the model, four need careful consideration:

- the ultraviolet cutoff $\Lambda_{\rm UV}$,
- the SU(5) breaking scale on the brane, $\Lambda_{\rm SU(5)} \sim [\chi_1(w=0)]^{2/3}$,
- the bulk SU(5) confinement scale $\Lambda_{\rm conf}$, and
- the domain-wall inverse width $\Lambda_{\rm DW} \equiv k$.

All of these scales must be well above the electroweak scale. Within the four, the required hierarchy is

$$\Lambda_{\rm UV} > \Lambda_{\rm SU(5)} > \Lambda_{\rm conf} > \Lambda_{\rm DW} \, . \tag{5.36}$$

For obvious reasons, the UV cut-off must be the highest scale in the theory. The SU(5) breaking scale on the brane must be higher than the SU(5) bulk confinement scale, because we need to suppress the SU(5) confinement dynamics on the brane. If the opposite were the case, then the dynamics of the field χ would be everywhere dominated by the strong SU(5) interactions, and our classical background scalar field configuration would have no physical relevance. Finally, the SU(5) bulk glueball radius scale must be smaller than the width of the domain wall in order for the DS effect to work, as discussed in the lattice gauge analysis of Laine et al. [219]. This translates into the confinement scale being higher than the inverse wall width.

The UV, domain-wall-width and SU(5) breaking scales are governed by free parameters, so the required hierarchy amongst those three can always be achieved. The SU(5) confinement scale is in principle to be calculated from the bulk SU(5) gauge theory. Because we are in five-dimensions, this gauge theory has a UV cutoff, and so $\Lambda_{\rm conf}$ will depend on $\Lambda_{\rm UV}$, as well as the dimensionful gauge coupling constant g_5. If the qualitative behaviour of the pure Yang-Mills theory discussed in Section 5.1 also holds for the complete theory, then we expect there to be a critical coupling $g_c(\Lambda_{\rm UV})$ above which the theory is confining. The hypothetical lattice gauge theory calculation would have to allow values of $g_5 > g_c$ to furnish a $\Lambda_{\rm conf}$ that obeyed equation (5.36). This calculation is left as work for the future.

5.5 Conclusion

We have proposed in this chapter a domain-wall brane model of an infinite extra-dimension, which respects SU(5) gauge symmetry and reproduces, at the low-energy, four-dimensional level, the single-generation standard model, or something very close to it, and general relativity. Our model draws on the techniques developed in earlier chapters for realising a dynamically generated domain-wall brane, and for dynamically localising gravity, fermions and scalars. The background configuration is formed by the scalars η and χ, along with the Randall-Sundrum warped metric solution. The five-dimensional fermion multiplets Ψ_5 and Ψ_{10} propagate in this background, and left-chiral zero modes are projected out and appear in the effective four-dimensional action. The five-dimensional Higgs Φ plays the similar role of providing a four-dimensional electroweak Higgs doublet. Gauge boson localisation is postulated by way of the Dvali-Shifman mechanism, and we discussed in Section 5.1 why we believe this mechanism to be necessary, and, a reasonably promising solution provided five-dimensional Yang-Mills exhibits confinement. In essence, what we have shown is that it is quite straightforward to construct a domain-wall-localised standard model if confinement exists for an SU(5) gauge theory bulk.

In Section 5.2 we presented the model: the field content, the symmetries, the action and the boundary conditions which lead to the requisite domain-wall background. Section 5.3 discussed aspects of the model, utilising a specific analytic background solution. In particular, we derived expres-

sions for the profiles of the localised, zero mode fermions (in the gravity-free case), and demonstrated how to obtain a tachyonic Higgs doublet, while keeping the coloured-Higgs massive. The effective electroweak sector was determined, as were the masses m_e, m_d and m_u. We noted that the usual tree-level SU(5) relation $m_d = m_e$ is automatically absent in our model, and that coloured-Higgs-induced proton decay can be suppressed via the splitting of the extra-dimensional profiles. We also gave analytic solutions for the background in the case where gravity took the form of a smoothed out version of the Randall-Sundrum warped metric. It was argued that the qualitative, low-energy features of our model remain intact in the presence of gravity. The relationships between the various scales of the model were outlined in Section 5.4.

There are a number of open problems to be addressed within the model-building framework exemplified in this chapter. The extension to three generations of fermions should be relatively straightforward, along with non-zero neutrino masses. More difficult would be the exercise of fitting the parameters of the model to experimental data, including CKM and PMNS mixing. One would also need to determine if, after doing such a fit, there remains enough parameter freedom to obey the experimental bounds on proton decay. Following this, a study could proceed to determine how the effective four-dimensional $G_{\rm SM}$ gauge coupling constants unify into a five-dimensional SU(5) gauge coupling constant. The phenomenological implications of the gauge bosons that are massive inside the domain wall must also be understood, especially for the physics of proton decay. The kink translation zero mode requires a more rigorous treatment in the case with gravity turned on.

Most importantly, one needs to confirm the veracity of the DS mechanism in five-dimensions. If DS works, then a whole world of domain-wall brane model building is opened up, of which the SU(5) model presented in this chapter is but an example. If DS does not work, then it is not at all clear that realistic field-theoretic domain-wall brane models exist when the extra dimension is infinite in extent. This is really the crux of the current thesis: we are confident that the mechanisms for gravity, fermion and scalar localisation are robust, but that for gauge boson localisation still remains an open question. We have put forward the DS mechanism as the most promising candidate to resolve this question, and we hope that our efforts lead to renewed interest in the issue of confinement in higher-dimensional

gauge theories.

An extension of the work presented in this chapter, more along the model-building line than the phenomenological one, is the enlarging of the gauge symmetry of the action. In Chapter 6 we consider E_6 grand unification, and demonstrate that it is possible to reduce the pair of fields η and χ to a single scalar, which plays the dual role of kink formation and Dvali-Shifman symmetry breaking, and implements the clash-of-symmetries mechanism.

Chapter 6

E_6 invariance and the clash of symmetries

Among the many possible extensions of the SU(5) domain-wall model constructed in Chapter 5, we are inspired initially to explore the potential of a larger gauge group. Given that the Dvali-Shifman (DS) mechanism works in five-dimensions and offers a whole new world of extra-dimensional model building, we find ourselves with the urge to see just how vast this new world is. We would like to test if the minimal, and seemingly very natural, choice of SU(5) is truly the best way to proceed, as we may be able to extract more model-building-power by considering larger gauge groups in the context of extra-dimensions, domain-walls and the DS mechanism. When constructing a model, the choice of symmetries — in particular the gauge invariance of the action — is perhaps the most important decision, as they dictate not only the allowed structure of terms in the action, but also determine the physical processes of the quantum field theory. It therefore seems that we are justified in spending more of our time exploring the core choices underlying our construction, as opposed to concentrating on phenomenological studies. Such explorations aim to enhance, and ultimately simplify, our domain-wall brane model of an infinite extra-dimension, which may end up being a viable description of physics beyond the standard model.

These musings provide the motivation for this chapter, in which we consider extensions of SU(5) to both the groups SO(10) and E_6. It turns out that the latter finds the more natural application in the context of a do-

main wall which incorporates DS, and we sketch the basic structure of such an E_6 model, including the configuration of the kink and the layout of the fermion profiles. In addition to drawing on the techniques and mechanisms of previous chapters, the ideas in the current chapter rely on quite a bit of non-trivial group theory, and we shall spend some time reviewing and developing the necessary background. The DS mechanism plays a significant role in the dynamics of our construction, and does so in conjunction with the clash of symmetries.

The clash-of-symmetries (CoS) mechanism [39, 199, 202, 200, 203, 204, 205] was first discussed in Chapter 2, and is crucial to the formation of the domain-wall branes studied in this chapter. In this context, the CoS phenomenon automatically arises when the simple $\mathbb{Z}_2$ kink (for example, η in Chapter 5) is extended to a theory with a continuous internal symmetry group G in addition to the discrete symmetry. Upgrading the scalar-field associated with the kink to a non-trivial representation of G, the domain-wall configuration induces a disconnected vacuum manifold topology due to the broken discrete symmetry. In addition, the kink spontaneously breaks G to a subgroup H. Two classes of domain-wall solutions exist: those which respect the same H at all values of the bulk coordinate w, and those where the unbroken subgroup varies in the bulk. We shall call the first class "non-CoS domain walls", contrasted with the "CoS domain walls" of the second class. The latter domain wall configurations arise when the subgroups respected asymptotically (at $w = \pm\infty$) are isomorphic but *differently embedded* subgroups, H and H'. The symmetry group at finite w is typically the intersection $H \cap H'$, which is of course smaller than both H and H'.

Take note of this last observation: we have a smaller symmetry in the non-asymptotic region, the region around the centre of the domain wall, than we do in the bulk. This is almost exactly the set-up required to implement the DS mechanism![1] It is not exactly the original DS idea, and the difference is subtle, but extremely important. In DS, the bulk symmetries on either side of the domain wall are *equivalent*, not just isomorphic, and the smaller symmetry group which is "sandwiched" between these bulk symmetries is induced by a scalar field in a non-trivial representation, with a profile engineered for the sole task of breaking the symmetry at the required location. Furthermore, as exemplified by the SU(5) model of Chapter 5, the

[1] See Section 1.3.3 and Section 5.1 for detailed discussions of the DS mechanism.

symmetry that is asymptotically restored in the bulk in the DS set-up is the symmetry of the action. This contrasts the clash-of-symmetries scenario, where the bulk symmetries H and H' are subgroups of G, the latter being the full symmetry of the action.

The fact that the full symmetry G is asymptotically restored is clearly not a necessary condition for gauge boson localisation. In the CoS situation, the symmetry $H \cap H'$, which is respected in the vicinity of the brane, is a subgroup of both H and H'. By the DS reasoning, provided H and H' contain confining, non-Abelian factors, at least some of the gauge bosons of $H \cap H'$ will be localised, and so the CoS mechanism will generically, and automatically, give rise to DS-like gauge-boson localisation. This alternative realisation of the DS mechanism seems conceptually neater and more advanced than the original, because it can be achieved using scalars in a single irreducible representation of G. The original requires two multiplets: a G-singlet to form a kink, which in turn forces a G-multiplet to condense in the core of the wall.

We shall show in the sections that follow that the CoS-DS confluence discussed above can naturally produce an SU(5) effective theory on the brane. The action of this theory is invariant under local $G = \mathrm{E}_6$ transformations, and, in addition to the five-dimensional gauge fields, contains a scalar field in the adjoint representation, the **78**, and a five-dimensional fermion in the **27**. The CoS mechanism is implemented by breaking G, using the scalar, to $H = \mathrm{SO}(10) \otimes \mathrm{U}(1)_E$ on one side of the domain wall, and to $H' = \mathrm{SO}(10)' \otimes \mathrm{U}(1)_{E'}$ on the other side. The intersection of these two asymptotic bulk symmetries is $\mathrm{SU}(5) \otimes \mathrm{U}(1) \otimes \mathrm{U}(1)$, where the SU(5) here is the common subgroup of SO(10) and SO(10)′. Assuming that DS works in five-dimensions, and taking the SO(10)'s as confining in the bulk, the gauge bosons associated with SU(5) are localised to the domain wall. By Yukawa coupling the fermion field to the scalar, we can localise four-dimensional, left-chiral zero modes as usual. Due to the group-theoretic structure of this coupling, out of the twenty-seven Dirac components, only seventeen are localised, and together they transform as a $\mathbf{5}^* \oplus \mathbf{10} \oplus \mathbf{1} \oplus \mathbf{1}$ of the localised SU(5). This is a remarkable feature of our model, as such a spectrum of fermions zero-modes contains just what we need to emulate the standard model, with very little "excess baggage".

Before we delve into the details of the E_6 model, we shall first review the

clash-of-symmetries idea in Section 6.1. This is followed, in Section 6.2, with a discussion of SO(10) domain walls, featuring both the CoS and DS mechanisms, and we explain here why the further extension to E_6 is necessary. In Section 6.3 we provide an in-depth analysis of the invariants of E_6 and the structure of the global minima that break this group to $SO(10) \otimes U(1)$. A preliminary version of the E_6 model is then presented in Section 6.4, and we give plots of the domain-wall background configuration and fermion localisation profiles. Conclusions are drawn in Section 6.5.

6.1 The clash of symmetries

Symmetries play a huge role in models of our universe, and understanding how such symmetries can be broken is of fundamental importance to a physicist. The standard Higgs mechanism, where a doublet scalar field breaks $SU(2)_L \otimes U(1)_Y \to U(1)_{EM}$, has the Higgs field assuming a constant background configuration. In the clash-of-symmetries scenario, the background scalar field is spatially-varying and can break a symmetry to a smaller subgroup than is accessible by the constant configuration of the same field. Since the physics we observe seems quite homogeneous and isotropic, such hypothetical, spatially-dependent symmetry breaking finds a much more natural home in the context of extra dimensions. Here, then, we might hope to construct models with large symmetries, and appeal to such mechanisms as the clash-of-symmetries to provide us with "large" symmetry breaking power. The technical details of the CoS mechanism draw on some interesting group theory, and we review such matters in this section.

At the heart of the clash-of-symmetries mechanism is the fact that, for a group G and a subgroup $H \in G$, it is generally possible to embed H in G in a number of different ways. Let us consider a concrete example: let G be the dihedral group D_3 defined by

$$D_3 = \langle x,\ y \mid x^2 = e,\ y^3 = e,\ (xy)^2 = e \rangle\ , \tag{6.1a}$$

$$= \{e,\ x,\ y,\ y^2,\ xy,\ xy^2\}\ , \tag{6.1b}$$

where e is the identity element. First consider the subgroup $H = \{e,\ x\}$, which is isomorphic to $\mathbb{Z}_2$, and compute its set of left cosets defined by $G/H \equiv \{gH : g \in G\}$. We are using the notation whereby $gH \equiv \{gh : h \in$

$H\}$ for some $g \in G$. The coset set is

$$G/H = \{H,\ yH,\ y^2H\}\,. \tag{6.2}$$

Note that H is not a normal subgroup of G and so the set of cosets G/H does not form a group with respect to the multiplication operator from G. Nevertheless, we can act on a particular element of G/H with some element $g \in G$, the result of which will be some, in general different, element of G/H. For example, $x \in G$ acting on $yH \in G/H$ (by pre-multiplication) yields $y^2H \in G/H$, while x acting on H yields H. As exemplified by the latter example, an interesting question is the following: what set of elements of G act on a given element of G/H to yield that same element of G/H back again? In other words, what are the symmetries of the elements of G/H?

For our example, the subgroup $H \subset G$ is the symmetry of the element $H \in G/H$, $yHy^2 = \{1,\ xy\}$ is the symmetry of the element yH, and $y^2Hy = \{1,\ xy^2\}$ is the symmetry of the element y^2H. These three *groups*, namely H, yHy^2 and y^2Hy, are all isomorphic to each other (they are all isomorphic to $\mathbb{Z}_2$), they are all subgroups of G, but they are differently embedded within G. We have thus found the three distinct embeddings of $\mathbb{Z}_2$ within D_3. Similarly, one can take $H' = \{1,\ y,\ y^2\}$ to find $G/H' = \{H',\ xH'\}$ whose two elements respect the symmetries H' and $xH'x = \{1,\ y^2,\ y\}$ respectively, showing that D_3 contains two copies of $\mathbb{Z}_3$. This idea of multiple embeddings is a recurrent idea of this chapter.

Moving on from the pure mathematics of groups and embeddings, we want to see how such ideas apply in the context of the internal symmetries of an action. To this end, consider a theory whose symmetry group is the direct product of a continuous symmetry G and a discrete symmetry Z. It is important for us that Z is *not* a subgroup of G. In this generic theory we need there to be a scalar, call it χ, which transforms non-trivially under G and Z, and which has a potential, referred to in what follows as the Higgs potential. Of course, this Higgs potential will remain invariant when G and/or Z acts on the associated scalar field χ. Suppose the global minima of the potential spontaneously break G to some subgroup H, and simultaneously break Z to a smaller discrete group Z'. This means that the ground state configuration — the vacuum — for χ respects only the restricted symmetries H and Z'. Acting on this vacuum with elements from

H or Z' leaves the vacuum expectation value (VEV) of χ unchanged, but acting with an element from G or Z will, in general, transform the VEV to a different, but degenerate, form. This motivates us to consider the set of degenerate vacua that are related by $G \otimes Z$ transformations:

$$\mathcal{W} = \{|0\rangle,\ g|0\rangle,\ z|0\rangle,\ gz|0\rangle,\ \ldots\}\,. \tag{6.3}$$

Here, $|0\rangle$ is the vacuum state corresponding to the VEV of χ which is invariant when χ is acted upon by elements from the subgroup $H \otimes Z'$. The other vacuum states in $\mathcal{W}$ are obtained by acting on χ — denoted notationally as acting on $|0\rangle$ — with elements from $G \otimes Z$ which are *outside* $H \otimes Z'$, that is $(g, z) \in G \otimes Z$ but $(g, z) \notin G \otimes Z$. These vacuum states are degenerate in energy with $|0\rangle$, but have χ assuming a different VEV. There is a direct correspondence between the set $\mathcal{W}$ and the coset space $(G/H) \otimes (Z/Z')$: $|0\rangle$ plays the role of the identity element $H \otimes Z'$, and the vacuum states $gz|0\rangle$ mimic the left cosets; compare $\mathcal{W}$ with equation (6.2).

At this point, it may be helpful to keep in mind two examples. First, consider the canonical kink, where χ is a real singlet, and the potential is a quartic potential. There are no continuous symmetries, only a discrete symmetry $Z = \mathbb{Z}_2$ which acts as $\chi \to -\chi$. The quartic potential breaks Z to the trivial group (which contains the single identity-element e), so the coset space is $\mathbb{Z}_2/\{e\} = \mathbb{Z}_2$, and there are two vacua. If the potential is defined by equation (1.16), then these two vacua are $\chi = v$ and $\chi = -v$, so $\mathcal{W} = \{v, -v\}$. Note that these vacua are related precisely by the action of $\mathbb{Z}_2$. Second, we can upgrade this picture to a continuous symmetry by taking χ to be complex, $G = \mathrm{U}(1)$ and Z the trivial group. The associated potential breaks G to $\{e\}$, the coset space is thus $\mathrm{U}(1)/\{e\} = \mathrm{U}(1)$, and there is now a continuum of U(1)-related vacua: $\mathcal{W} = \{ve^{i\alpha} : \alpha \in \mathbb{R}\}$.

For the sake of definiteness, we take $Z = \mathbb{Z}_2 = \{e, z : z^2 = e\}$ in the following exposition, with the $\mathbb{Z}_2$ completely broken, so the coset space of the discrete symmetry sector is $\mathbb{Z}_2$, and the total coset space is $(G/H) \otimes \mathbb{Z}_2$. Because of this broken discrete symmetry, the vacuum manifold $\mathcal{W}$ consists of two disconnected copies related by the broken element $z \in \mathbb{Z}_2$. This generalises the simple $\mathbb{Z}_2$ kink situation outlined above, where the vacuum manifold consisted of the two disconnected points v and $-v$ related by $\mathbb{Z}_2$. Each such point is now expanded into a non-trivial manifold whose "size"

is related to the "size" of G/H. We shall label these disconnected sets of vacua as $\mathcal{V}$ and $\mathcal{V}_z$ such that $\mathcal{W} = \mathcal{V} \cup \mathcal{V}_z$ and $\mathcal{V} \cap \mathcal{V}_z$ is the empty set. The $\mathbb{Z}_2$ must not be a subgroup of G for these two pieces to exist.

Let us make it clear what we mean by the vacuum manifold $\mathcal{V}$. It is a set of degenerate vacuum states corresponding to different VEVs for χ, related by elements of G:

$$\mathcal{V} = \{g|0\rangle : g \in G\} . \tag{6.4}$$

Of course, $|0\rangle$ is invariant under the subgroup H, so if $g \in H$ in equation (6.4) then we do not move to a different vacuum. Our notation for an element of $\mathcal{V}$ shall be $|0; g\rangle \equiv g|0\rangle$. As for the other piece of the vacuum manifold, $\mathcal{V}_z$, we cannot get to any of its vacua acting with elements of G because we required the discrete group $\mathbb{Z}_2$ to live outside G. This other piece is thus generated by acting with the discrete transform $z \in \mathbb{Z}_2$ to get

$$\mathcal{V}_z = \{gz|0\rangle : g \in G\} . \tag{6.5}$$

The vacuum $|0\rangle_z \equiv z|0\rangle$ is the $\mathbb{Z}_2$ image of $|0\rangle$, and the full manifold of $\mathcal{V}_z$ is generated by applying z to $|0; g\rangle$ for all g, or, equivalently, because the continuous and discrete symmetries commute, applying all g to $|0\rangle_z$. Note that the Higgs potential is G- and Z-invariant, so all elements of $\mathcal{V}$ and $\mathcal{V}_z$ are degenerate in energy. The two large circles in Figure 6.1 schematically represent the two disconnected vacuum manifolds, and the black solid dots represent particular vacua.

By construction, the symmetry of the vacuum $|0\rangle$ is H. But what about the other states $|0; g\rangle$? The answer is that for a given $g \in G$, the vacuum $|0; g\rangle$ is symmetric under the subgroup gHg^{-1}. This is easy to verify:

$$gHg^{-1}|0; g\rangle = (gHg^{-1})g|0\rangle = gH|0\rangle = g|0\rangle = |0; g\rangle . \tag{6.6}$$

The subgroup $H_g = gHg^{-1}$ is isomorphic to H, but if H is not a normal subgroup (which is the case if G is a simple Lie group) then H and H_g are comprised of different elements of the parent group G. We therefore obtain the result that the degenerate vacua $|0\rangle$ and $|0; g\rangle$ respect *differently embedded but otherwise isomorphic subgroups*, given by H and H_g respectively. As for elements of $\mathcal{V}_z$, their corresponding symmetries follow easily because the groups G and Z commute. When we apply H to $|0\rangle_z = z|0\rangle$ the elements of H go straight through z to act on $|0\rangle$, leaving it invariant. Similarly, H_g is

the symmetry of the vacuum $|0;g\rangle_z$.

These results are in direct analogy with our previous D_3 example, where the elements of the coset set $D_3/\mathbb{Z}_2$ were invariant under three differently embedded versions of $\mathbb{Z}_2$. For the case of a discrete, finite group, the number of embeddings of H is equal to the number of elements in the coset G/H. For a continuous G there is an uncountable infinity of vacua $|0;g\rangle$, corresponding to all the possible g, so there exists an uncountable infinity of differently-embedded but isomorphic subgroups H_g. However, we can impose a restriction such that the number of embeddings is actually finite. Let the Cartan subalgebra $\mathcal{G}_C$ of G be a certain particular set of generators, corresponding to a particular choice of basis for the Lie algebra. If we require that the Cartan subalgebras of two subgroups H_{g_1} and H_{g_2} are both subspaces of $\mathcal{G}_C$, then the number of distinct embeddings is finite. A familiar example of this concerns the SU(2) subgroups of SU(3). While there are an uncountable infinity of ways of embedding SU(2) in SU(3), there are only three embeddings that have the SU(2) Cartan subalgebras as subspaces of the given Cartan-subalgebra space of SU(3). These are usually called I-spin, U-spin and V-spin. When we refer to "different embeddings" later on in the chapter, this is what we shall mean.[2]

We have now established the structure of the vacuum manifold $\mathcal{V} \cup \mathcal{V}_z$, and the basic symmetry properties of the individual vacua. It is probably obvious that we are going to construct domain-wall configurations that interpolate between various vacuum states. For a kink-like profile in an infinite extra-dimension w, we need to pick two vacua, one for the scalar field to asymptotically approach as $w \to -\infty$, and the other for $w \to +\infty$. If the chosen vacua are either both from $\mathcal{V}$, or both from $\mathcal{V}_z$, then the "domain wall" configurations are not topologically stable: they are in the same topological class as any of the spatially-homogeneous vacua $|0;g\rangle$, or respectively $|0;g\rangle_z$, and will dynamically decay to one of these vacuum configurations. They may be metastable, depending on the Higgs potential topography, so while they are of some interest we shall not consider them further here.

[2]Note that taking linear combinations of Cartan generators to define different embeddings is in accord with Dynkin's general theory of embeddings [221]. In that formalism, the embedding of an algebra $\mathcal{H}$ into a simple or semi-simple algebra $\mathcal{G}$ is fully defined by a mapping F from the Cartan subalgebra of $\mathcal{H}$ into the Cartan subalgebra of $\mathcal{G}$, as per $H_\alpha \to F(H_\alpha) = \sum_{a=1}^{n} F_{\alpha a} G_a$, where H_α $(\alpha = 1, 2, \ldots, m)$ and G_a $(a = 1, 2, \ldots, n)$ are the Cartan generators of $\mathcal{H}$ and $\mathcal{G}$, respectively. The matrix $(F_{\alpha a})$ is the defining matrix of the embedding, and two embeddings are different if their defining matrices are different.

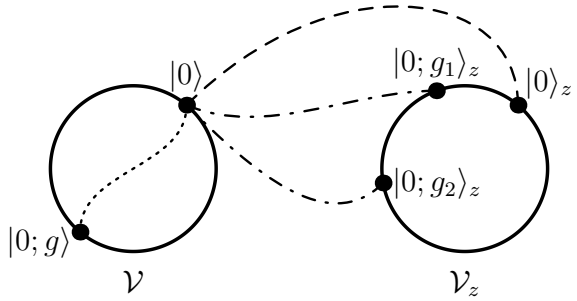

Figure 6.1: The vacuum manifold of a $G \otimes \mathbb{Z}_2 \to H$ model and some typical choices for domain-wall configurations. The two circles schematically depict the disconnected vacuum manifolds $\mathcal{V}$ and $\mathcal{V}_z$ corresponding to the coset space $(G/H)\otimes \mathbb{Z}_2$. Each point along the left $\mathcal{V}$ circle corresponds to a vacuum $|0;g\rangle$ for some $g \in G$, with the corresponding situation for $\mathcal{V}_z$ shown with the right circle. The three broken lines represent possible domain-wall configurations, with the endpoints at $w = \pm\infty$ on various choices of vacua. The dotted line represents a possible non-topological domain-wall configuration. The dashed line represents a non-CoS domain wall, while the two dash-dotted lines are CoS domain walls.

Topologically non-trivial domain-wall configurations have one boundary condition from $\mathcal{V}$ and the other from $\mathcal{V}_z$. Because of the continuous symmetry G, there is an uncountable infinity of such choices, and thus potentially an uncountable infinity of domain-wall solutions, all within the same non-trivial topological class. This potential richness has no analogue for the simple $\mathbb{Z}_2$ kink. Figure 6.1 illustrates some of the possible domain-wall configurations.

In the case of a topologically non-trivial configuration, suppose that the boundary condition at $w = -\infty$ is $|0\rangle$ and at $w = +\infty$ it is $|0\rangle_z$. As we have already established, both of these vacua respect the same symmetry H. A domain-wall configuration that interpolates between these vacua is then expected to respect the same subgroup H at all w. This is an example of a non-CoS domain wall, and it is shown in Figure 6.1. Clearly, taking the vacua as any pair $|0;g\rangle$ and $|0;g\rangle_z$ produces a similar outcome; the resulting configuration is nothing more than the g transform of the original one. A non-CoS domain wall is the simplest possible generalisation of a $\mathbb{Z}_2$ kink for a G-invariant theory.

There is, however, a more interesting way to configure a topologically non-trivial domain wall: choose the vacuum to be $|0\rangle$ at $w = -\infty$ and for $w = +\infty$ take it to be $|0;g\rangle_z$ for some $g \neq e$. In such a set-up, the Higgs potential breaks G asymptotically to the differently-embedded but isomorphic

subgroups H and H_g, respectively at $-\infty$ and $+\infty$, and this defines a CoS-style domain wall [39, 199, 200, 202].[3] At finite w, the configuration would be expected to respect the smaller group $H \cap H_g$ due to the fact that the solution has to "reconcile" boundary conditions that have different stability groups that "clash".[4]

Now let us make some remarks about the energy-densities of the domain walls that we have identified. For the non-CoS domain walls, there are an infinite family of configurations, trivially related to each other by global transformations $g \in G$. They all have the same energy density, because the Hamiltonian is invariant under G. The domain walls that implement the clash-of-symmetries have a more complicated spectrum. Consider two configurations, $\chi_1(w)$ and $\chi_2(w)$, with χ_1 interpolating between $|0\rangle$ and $|0; g_1\rangle_z$, while χ_2 interpolates between $|0\rangle$ and $|0; g_2\rangle_z$, such that $g_1 \neq g_2$. For the moment, suppose that G is a global but not a local symmetry. These two solutions *cannot* be transformed into each other by a *global* G-transformation because they share the same vacuum $|0\rangle$ at, say, $w = -\infty$, but different vacua at $w = +\infty$. Their configurations therefore trace different paths through the Higgs potential topography, and they would be expected to have different energy densities. As a corollary, the non-CoS solutions should have a different energy density from the CoS solutions (put $g_1 = e$ and re-run the previous argument).

All the solutions that interpolate between vacua from $\mathcal{V}$ to $\mathcal{V}_z$ are in the same topological class, so finite-energy dynamical evolution between them is allowed. Hence, the special configurations within that topological class that minimise the energy density will be topologically stable. The others should be unstable to decay to the minimum-energy configurations, which play the role of "vacua" for the "kink-sector". This general reasoning cannot tell you which configuration has the minimum energy-density: this must be calculated within a specific model. For example, in the toy model considered by Davidson et al. [39] the sign of a Higgs potential parameter determined whether the non-CoS or a CoS solution was energetically favoured.

[3] See also Pogosian and Vachaspati [203, 204, 205] for related works, and Dvali and Shifman [222] for soliton-induced supersymmetry breaking.

[4] The usual outcome has $H \cap H_g$ as the symmetry respected at non-asymptotic values of w, although the specifics depend on the scenario in question. Sometimes there is enhanced symmetry at $w = 0$ because some of the scalar multiplet components instantaneously vanish there; see [200, 201].

Suppose now that G is a gauge symmetry, and specify that, at the level of the solutions, the gauge fields A_M vanish. The non-CoS configurations remain connected through global transformations, and thus still have the same energy-densities. Unlike the case where G was a global symmetry, two CoS scalar field configurations, χ_1 and χ_2, can now be written as local G-transforms of each other. Suppose that

$$\chi_2(w) = U(w)\chi_1(w) \,, \tag{6.7}$$

where $U(w)$ is an element of the local symmetry group G. Then the original first solution

$$\chi = \chi_1(w) \,, \qquad A_M = 0 \tag{6.8}$$

is gauge-equivalent to

$$\chi = \chi_2(w) \,, \qquad A_M = -\frac{1}{g_*}(\partial_M U)U^\dagger \,, \tag{6.9}$$

where g_* is the gauge coupling constant, but it is *not* gauge-equivalent to

$$\chi = \chi_2(w) \,, \qquad A_M = 0 \,, \tag{6.10}$$

which is the original second solution. Thus the two solutions given by equations (6.8) and (6.10) have different energy densities, even though the scalar-field portions are related by a local symmetry transformation. Although $A_M = -\frac{1}{g_*}(\partial_M U)U^\dagger$ is a pure-gauge configuration, it contributes to the energy density through the χ-A_M interaction terms.

Setting the gauge fields to zero at the solution-level is basically a convenient choice of gauge, one we shall adopt for the rest of this chapter. Of course the solutions can be made to look very different by gauge-transforming them, but their physical consequences cannot change. This circumstance is no different from the monopole or local-string cases, where the solutions look different in different gauges. Actually, it is no more complicated than the usual homogeneous VEV case. If $\langle\chi\rangle$ is such a homogeneous VEV, then it can be gauge-transformed to a non-homogeneous configuration $U(x)\langle\chi\rangle$ but the scalar gradient energy is cancelled by the gauge-field contribution.[5]

[5]It has not been proven that the minimum-energy domain-wall configuration must have a gauge-field sector that is gauge-equivalent to zero, which appears to be a loose end. We are making the assumption that it is in fact true for the purposes of this chapter.

6.2 Attempt at an SO(10) model

With the clash-of-symmetries mechanism now a cogent part of our model-building toolkit, we want to look at extending the SU(5) model of Chapter 5 to, in the first instance, an SO(10) invariant theory. In fact, our construction is not going to work correctly, due to the non-confinement of some of the gauge bosons of the standard model. Nevertheless, it gives us a chance to introduce a working implementation of the clash-of-symmetries, combined with Dvali-Shifman gauge boson localisation, in a more straightforward context than the E_6 set-up.

Actually, most of the work has already been done constructing the requisite SO(10) model: Shin and Volkas [200] analysed O(10) kinks, and we shall borrow liberally from their construction. The main thing we need to do is reinterpret their kink configurations in the context of DS, in order to determine which gauge bosons are localised to the domain-wall region. We shall first recapitulate the model of Shin and Volkas (refer to their original work for more details), and then discuss the DS features.

Let $\chi(x^M)$ be a scalar multiplet in the adjoint representation, the **45**, of SO(10). The most general quartic Higgs potential for such a scalar field is

$$V = \frac{1}{2}\mu^2 \operatorname{Tr}(\chi^2) + \frac{1}{4}\lambda_1 \operatorname{Tr}(\chi^2)^2 + \frac{1}{4}\lambda_2 \operatorname{Tr}(\chi^4)\,, \tag{6.11}$$

where $\chi(x^M) = f_\alpha(x^M)\hat{X}^\alpha$ with the $\hat{X}$'s being matrix representations of the generators in the fundamental of SO(10) while the f_α's are the components of the adjoint multiplet. The matrix χ is antisymmetric and transforms as per $\chi \to A\chi A^T$ where A is an SO(10) fundamental-representation matrix. The parameter μ^2 is chosen to be positive since $\operatorname{Tr}(\chi^2)$ is negative definite. The cubic invariant $\operatorname{Tr}(\chi^3)$ identically vanishes so there is an accidental discrete $\mathbb{Z}_2$ symmetry, $\chi \to -\chi$, which shall play the role of Z in the clash-of-symmetries. It is not a subgroup of O(10).

The global minimisation of such a potential was performed by Li [223], and see also Kaymakcalan et al. [224]. Using an SO(10) transformation, one may always bring a VEV pattern into the standard form

$$\chi = \operatorname{diag}(f_1\,\epsilon,\, f_2\,\epsilon,\, f_3\,\epsilon,\, f_4\,\epsilon,\, f_5\,\epsilon)\,, \tag{6.12}$$

where the $f_i(x^M)$ are real fields and $\epsilon \equiv i\,\sigma_2 = \left(\begin{smallmatrix} 0 & 1 \\ -1 & 0 \end{smallmatrix}\right)$. The five independent

fields f_i correspond to the five generators in the SO(10) Cartan subalgebra. In this basis, the Higgs potential (6.11) becomes

$$V = -\mu^2 \sum_{i=1}^{5} f_i^2 + \lambda_1 \left(\sum_{i=1}^{5} f_i^2 \right)^2 + \frac{1}{2}\lambda_2 \sum_{i=1}^{5} f_i^4 \,. \tag{6.13}$$

For $\lambda_2 > 0$, the global minima of V are attained when $f_i^2 = f_{\min}^2$ for all i, where

$$f_{\min}^2 \equiv \frac{\mu^2}{10\lambda_1 + \lambda_2} \,, \tag{6.14}$$

and the corresponding unbroken subgroup of SO(10) is $H = \mathrm{U}(5)$. The values of f_i at the minima are specified up to a sign that can be chosen independently for each component: $f_i = \pm f_{\min}$. Different choices for these signs correspond to two features: different embeddings of U(5) in SO(10) and also a choice of which $\mathbb{Z}_2$ sector the minimum lies in.

To explore the effect of these sign choices further, let us have a look at the structure of the possible domain-wall configurations in the model. Suppose that at $w = -\infty$, we choose the boundary condition

$$\chi(-\infty) = -f_{\min}^{(5)} \equiv -f_{\min}\,\mathrm{diag}(\epsilon,\, \epsilon,\, \epsilon,\, \epsilon,\, \epsilon) \,. \tag{6.15}$$

This defines a certain U(5) unbroken at $w = -\infty$, and the VEV lies in one of the two disconnected pieces of the vacuum manifold. At $w = +\infty$, we have a choice of three vacua that give rise to physically distinct scenarios, and they are to be selected from the second vacuum manifold which is disconnected from the first by the spontaneously broken $\mathbb{Z}_2$:

$$\chi(+\infty) = \begin{cases} f_{\min}^{(5)} \equiv f_{\min}\,\mathrm{diag}(\epsilon,\, \epsilon,\, \epsilon,\, \epsilon,\, \epsilon) \\ f_{\min}^{(3,2)} \equiv f_{\min}\,\mathrm{diag}(\epsilon,\, \epsilon,\, \epsilon,\, -\epsilon,\, -\epsilon) \\ f_{\min}^{(4,1)} \equiv f_{\min}\,\mathrm{diag}(\epsilon,\, -\epsilon,\, -\epsilon,\, -\epsilon,\, -\epsilon) \end{cases} . \tag{6.16}$$

Permutations of the minus signs in the last two of these vacua are just a trivial rearrangement of the representation-space and need not be separately considered. Also, vacua with an odd number of minus signs on the right-hand side of equation (6.16) are continuously connected to $\chi(-\infty)$ by SO(10); they give rise to non-topological domain walls, like the dotted line in Figure 6.1, and shall not be considered here.

The three vacua in equation (6.16) are invariant under differently embedded subgroups of SO(10): $U(5)_1$, $U(5)_2$ and $U(5)_3$. The superscripts (5), $(3,2)$ and $(4,1)$ denote the numbers of plus and minus signs in the VEVs and they also serve to describe the unbroken symmetry of the domain wall at finite w — the symmetry left over after the "clash". These are, respectively,

$$\mathrm{U}(5)\,, \qquad \mathrm{U}(3)\otimes\mathrm{U}(2) \quad \text{and} \qquad \mathrm{U}(4)\otimes\mathrm{U}(1)\,, \tag{6.17}$$

and they arise for the following reasons. The ansatz for domain-wall configurations that interpolate between the stated boundary conditions is $\chi(w) = h(w)\chi(-\infty)+g(w)\chi(+\infty)$, where h asymptotes from 1 to 0, and g from 0 to 1, for w going from $-\infty$ to $+\infty$. The first configuration, which interpolates between $-f_{\min}$ and $+f_{\min}$ for all components $f_i(w)$, breaks SO(10) to $U(5)_1$ at all values of w, because the relative magnitudes of the components are always the same at a given w. It is a non-CoS domain wall, like the dashed line in Figure 6.1, and we do not consider it further.

The second configuration has an equal-magnitude 3×3 block (of 2×2 submatrices), and an equal-magnitude 2×2 block. The unbroken symmetry is then $\mathrm{U}(5)_1\cap\mathrm{U}(5)_2 = \mathrm{U}(3)\otimes\mathrm{U}(2)$. Similarly, the third configuration's block structure leads to $\mathrm{U}(5)_1\cap\mathrm{U}(5)_3 = \mathrm{U}(4)\otimes\mathrm{U}(1)$. One can solve the Euler-Lagrange equations to determine the exact form of the domain-wall profiles, and further compute their relative energy densities. It turns out that for certain parameter choices analytic solutions exist, and in this case the third configuration, the one corresponding to $f_{\min}^{(4,1)}$, has the lowest energy of the three, and so is the topologically stable one [200]. It may be that, in other parameter regions, one of the other configurations is the stable one, and we shall assume such a thing can be arranged in the following discussion, although it is of no great consequence if it cannot.

Given this exposition of an SO(10) domain-wall brane model, we would now like to examine the localisation of the gauge bosons associated with the unbroken symmetry groups, using the framework of the DS mechanism. Consider first the configuration which has an unbroken SU(4) on the brane. This symmetry group is embedded in $SU(5)_1$ on the $w<0$ side of the wall, and $SU(5)_3$ on the $w>0$ side. Drawing on the dynamics of the DS mechanism, the SU(4) gauge bosons are thus localised to the wall because, by assumption, both $SU(5)_1$ and $SU(5)_3$ are in confinement phase in their

respective bulk regions. This establishes the connection between clash-of-symmetries and Dvali-Shifman by way of an explicit, rigorously worked-out solution. Unfortunately, we cannot turn such a toy model into something phenomenologically acceptable, since the standard model gauge group cannot be realised.

Now consider the second configuration, with the symmetry

$$\mathrm{U}(3) \otimes \mathrm{U}(2) = \mathrm{SU}(3) \otimes \mathrm{SU}(2) \otimes \mathrm{U}(1) \otimes \mathrm{U}(1) \tag{6.18}$$

on the brane; this is closer to what we need for a realistic model. The gauge bosons associated with the $\mathrm{SU}(3) \otimes \mathrm{SU}(2)$ factor in equation (6.18) are localised via the DS mechanism because this factor is a subgroup of both $\mathrm{SU}(5)_1$ (the bulk symmetry for $w < 0$) and $\mathrm{SU}(5)_2$ (the bulk symmetry for $w > 0$). However, to recover the standard model, we also require a DS-localised $\mathrm{U}(1)_Y$ factor, and this turns out to be a problem.

Let us examine the generators of the two U(1)'s in equation (6.18) to see how their associated gauge fields fare in a DS context. The asymptotic gauge groups can be written as

$$\mathrm{U}(5)_1 = \mathrm{SU}(5)_1 \otimes \mathrm{U}(1)_{X_1} \qquad \text{and} \qquad \mathrm{U}(5)_2 = \mathrm{SU}(5)_2 \otimes \mathrm{U}(1)_{X_2}\,. \tag{6.19}$$

Denote by Y_1 the hypercharge generator inside $\mathrm{SU}(5)_1$, and Y_2 the one inside $\mathrm{SU}(5)_2$. The two U(1)'s in equation (6.18) can be taken to be generated either by Y_1 and X_1, or by Y_2 and X_2, and each pair can be written as linear combinations of the other pair, as per our previous discussion of the relationship between the two groups H and H_g. Now, either Y_1 or Y_2 can be the physical hypercharge Y, and which one is selected will be an accident of spontaneous symmetry breaking.[6] At some energy above the electroweak scale, the breaking

$$\mathrm{U}(1)_{Y_1} \otimes \mathrm{U}(1)_{X_1} = \mathrm{U}(1)_{Y_2} \otimes \mathrm{U}(1)_{X_2} \longrightarrow \mathrm{U}(1)_Y, \tag{6.20}$$

with either $Y = Y_1$ or $Y = Y_2$, will have to take place to produce an effective standard model at low-energies (this will require an additional Higgs field). Suppose $Y = Y_1$ is spontaneously selected, and so $\mathrm{U}(1)_Y$ originates from

[6] It cannot be that $Y_1 = Y_2$ because, by construction of the clash-of-symmetries configuration, $\mathrm{SU}(5)_1 \neq \mathrm{SU}(5)_2$.

inside $SU(5)_1$. By the DS mechanism, the hypercharge gauge boson is thus unable to propagate into the $w < 0$ bulk, where its parent group is unbroken and confining. But this is not the case for the $w > 0$ region. The generator $Y = Y_1$ is a linear combination of Y_2 and X_2, and so the hypercharge gauge field is a linear combination of the gauge fields associated with Y_2 and X_2. The Y_2 portion of the hypercharge gauge field is forbidden from entering the $w > 0$ region of the bulk, since there it must form part of an $SU(5)_2$ singlet, but the X_2 portion has no such restriction. The X_2 portion is immune from the DS effect because the associated group $U(1)_{X_2}$ is Abelian and not confining. After electroweak symmetry breaking, this will imply that both the photon and neutral Z boson will leak into the $w > 0$ bulk, which is phenomenologically ruled out. In the reverse situation, where the physical Y is actually Y_2, leakage of these bosons into $w < 0$ will occur.

So our extension to SO(10), using the clash of symmetries, does not seem to allow for localised standard-model gauge bosons. For the configuration where $U(4) \otimes U(1)$ is the symmetry on the brane we obtain a localised SU(4) factor, which is no good from the point of view of the standard model gauge group. The other clash-of-symmetries configuration had equation (6.18) as the brane symmetry, but only the gluons and the two charged W bosons were fully localised, corresponding to the embedding of the group $SU(3) \otimes SU(2)$ in confining SU(5)'s on either side of the wall. The photon and Z boson were semi-delocalised to one half of the bulk. In order to localise these latter two fields, we must arrange for the $U(1)_Y$ to be part of a confining group on *both* sides of the domain wall. One way do achieve this is to have, instead of a localised standard model, a localised grand unified model, because localisation of a GUT group guarantees localisation of its constituent subgroups, which includes $U(1)_Y$. Following this idea, we would be inclined to first try and localise an SU(5) GUT to the brane, which would seem to dictate having SO(10) as the confining parent-group in the bulk. The clash-of-symmetries mechanism requires the action to be invariant under a yet larger symmetry, leading us to consider E_6.

6.3 Structure of the E_6 invariants

The failure of the SO(10) model motivates us to consider an E_6 invariant theory. Given this, our first task is to engineer an E_6 symmetric Higgs

potential which has global minima that break

$$E_6 \to SO(10) \otimes U(1) , \tag{6.21}$$

the latter of which is a maximal subgroup. To implement the clash-of-symmetries, the Higgs potential must be able to break E_6 to differently embedded subgroups. Furthermore, we need to identify which particular embedding each minimum corresponds to, which will allow us to make correct choices for the boundary conditions of the scalar field. This section is devoted to such an analysis, and the results are used later on to construct a model that incorporates some promising features.

The scalar field that will play the simultaneous role of symmetry breaking, kink formation and DS gauge boson localisation is the adjoint multiplet $\chi(x^M)$. It shall be represented by

$$\chi(x^M) = \sum_{\alpha=1}^{78} f_\alpha(x^M)\hat{X}^\alpha , \tag{6.22}$$

where the seventy-eight $\hat{X}$'s are matrix representations of the generators for the **27** of E_6, and the seventy-eight $f(x^M)$'s are five-dimensional field components. This adjoint transforms as

$$\chi \to U\chi U^\dagger , \tag{6.23}$$

where U is an E_6 transformation in an appropriate matrix representation.

The Higgs potential for χ is constructed out of adjoint invariants, which, according to equations (6.22) and (6.23), are

$$I_n = \mathrm{Tr}(\chi^n) = \mathrm{Tr}(\hat{X}^{\alpha_1}\hat{X}^{\alpha_2}\cdots\hat{X}^{\alpha_n})f_{\alpha_1}f_{\alpha_2}\cdots f_{\alpha_n} , \tag{6.24}$$

which are simply the n^{th} order Casimir invariants. According to Racah [225] and Harvey [226], the independent invariants are

$$I_2,\ I_5,\ I_6,\ I_8,\ I_9,\ I_{12}. \tag{6.25}$$

Note the presence in this list of invariants with odd powers, namely I_5 and I_9. This means that the discrete $\mathbb{Z}_2$ symmetry $\chi \to -\chi$ is not a subgroup of E_6, since such a negation of χ (all the components f_α of χ) will also negate

the odd invariants. We shall exploit this feature later on.

Using these invariants, the most general Higgs potential is the sum of products of a free parameter and various I_n's. We are in five-dimensions and there is no reason to stop writing down terms at, say, quartic order in χ. In fact, we are going to need higher-order terms to get the requisite symmetry breaking patterns. Thus, the Higgs potential is

$$\begin{aligned} V_{\text{full}} = {} & \tau_1 I_2 + \tau_2 I_2^2 + \tau_3 I_5 + \tau_4 I_2^3 + \tau_5 I_6 + \tau_6 I_2 I_5 \\ & + \tau_7 I_2^4 + \tau_8 I_2 I_6 + \tau_9 I_8 + \tau_{10} I_2^2 I_5 + \tau_{11} I_9 \\ & + \tau_{12} I_2^5 + \tau_{13} I_2^2 I_6 + \tau_{14} I_2 I_8 + \tau_{15} I_5^2 \\ & + \tau_{16} I_2^3 I_5 + \tau_{17} I_2 I_9 + \tau_{18} I_5 I_6 + \tau_{19} I_2^6 \\ & + \tau_{20} I_2^3 I_6 + \tau_{21} I_2^2 I_8 + \tau_{22} I_2 I_5^2 + \tau_{23} I_6^2 + \tau_{24} I_{12} + \dots \,, \end{aligned} \tag{6.26}$$

where we have stopped writing at twelfth order. At this point in the game, we are faced with the rather daunting task of analysing the global minima of V_{full}, which contains seventy-eight fields and traces of products of 27×27 matrices.

To make life a bit easier, we note that one can always transform any VEV pattern to a standard form given by linear combinations of just the six generators in the Cartan subalgebra of E_6. This reduces our space to six fields and renders the problem much more tractable. The corresponding generators, the six diagonal generators T_a $(a = 1, \dots, 6)$, are given as the columns in Table 6.1. To be clear, we write out the first two:

$$T_1 = \frac{1}{12}\,\text{diag}\,(4,\ -2\cdot\mathbb{1}_{10\times 10},\ \mathbb{1}_{16\times 16})\ , \tag{6.27a}$$

$$T_2 = \frac{1}{4\sqrt{15}}\,\text{diag}\,(0,\ 2\cdot\mathbb{1}_{5\times 5},\ -2\cdot\mathbb{1}_{5\times 5},\ -5,\ 3\cdot\mathbb{1}_{5\times 5},\ -\mathbb{1}_{10\times 10})\ , \tag{6.27b}$$

where $\mathbb{1}_{n\times n}$ is the $n \times n$ identity matrix. The orthonormalisation condition for the generators is

$$\text{Tr}(T_a T_b) = \frac{1}{2}\delta_{ab}\ . \tag{6.28}$$

These generators can be found by examining the U(1) charges that emerge from the branching of the **27**. For example, under

$$\text{E}_6 \to \text{SO}(10) \otimes \text{U}(1)_{T_1} \to [\,\text{SU}(5) \otimes \text{U}(1)_{T_2}\,] \otimes \text{U}(1)_{T_1}\ , \tag{6.29}$$

the fundamental representation of E_6 branches as

$$\begin{aligned}\mathbf{27} &\to \mathbf{1}(4) + \mathbf{10}(-2) + \mathbf{16}(1) && \text{(6.30a)}\\ &\to \mathbf{1}(4,0) + [\,\mathbf{5}(-2,2) + \mathbf{5}^*(-2,-2)\,] \\ &\qquad + [\,\mathbf{1}(1,-5) + \mathbf{5}^*(1,3) + \mathbf{10}(1,-1)\,]\,. && \text{(6.30b)}\end{aligned}$$

Here, the bold-face number is the dimension of the multiplet. For the first line, the number in the parenthesis is the $U(1)_{T_1}$ hypercharge, multiplied by 12 to reduce clutter. In the second and third lines, the two parenthesised numbers are the $U(1)_{T_1}$ and $U(1)_{T_2}$ charges respectively, where the second of these is multiplied by $4\sqrt{15}$.

To understand the Higgs potential V_{full} we need to understand the group-theoretic structure of each invariant in isolation. Knowing the extrema of the I_n will allow us to determine the locations of the vacua needed to implement the clash of symmetries.

Let us begin with I_2. Because of the normalisation defined by equation (6.28), we have

$$I_2 = \mathrm{Tr}(\chi^2) = \frac{1}{2}\left(f_1^2 + f_2^2 + f_3^2 + f_4^2 + f_5^2 + f_6^2\right)\,, \tag{6.31}$$

where the six fields f_a are those associated with the six diagonal generators T_a. This invariant is isotropic (it has a global O(6) symmetry) and has a single minimum at $f_a = 0$ for all a. This trivial solution for χ does not break E_6 at all, but we shall find a use for I_2 later on.

The rest of the invariants are not isotropic, and their minima and maxima are defined by certain sextuplets of values corresponding to the six f_a. We must determine these values. Actually, we are essentially done: the sextuplets are the rows of Table 6.1, while the columns are the generators. *The diagonal generators themselves play the remarkable dual-role of telling us exactly where the extrema of the non-isotropic invariants lie.* Taking linear combinations of the generators, where the coefficients are given by the weight vectors for the fundamental of E_6 (which is what each row corresponds to), defines all twenty-seven embeddings of $SO(10) \otimes U(1)$ in E_6. They hence tell us the values for the f_a needed to achieve the requisite vacua. We have yet to find a group-theoretic argument as to why such a statement is true, and for now we are content with providing a proof by explicit computation.

pos.	$60T_1$ $20f_1$	$60T_2$ $20f_2$	$60T_3$ $20f_3$	$60T_4$ $20f_4$	$60T_5$ $20f_5$	$60T_6$ $20f_6$
1	20	0	0	0	0	0
2	-10	$2\sqrt{15}$	$3\sqrt{10}$	$-5\sqrt{6}$	0	0
3	-10	$2\sqrt{15}$	$3\sqrt{10}$	$5\sqrt{6}$	0	0
4	-10	$2\sqrt{15}$	$-2\sqrt{10}$	0	$5\sqrt{2}$	$5\sqrt{6}$
5	-10	$2\sqrt{15}$	$-2\sqrt{10}$	0	$5\sqrt{2}$	$-5\sqrt{6}$
6	-10	$2\sqrt{15}$	$-2\sqrt{10}$	0	$-10\sqrt{2}$	0
7	-10	$-2\sqrt{15}$	$-3\sqrt{10}$	$5\sqrt{6}$	0	0
8	-10	$-2\sqrt{15}$	$-3\sqrt{10}$	$-5\sqrt{6}$	0	0
9	-10	$-2\sqrt{15}$	$2\sqrt{10}$	0	$-5\sqrt{2}$	$-5\sqrt{6}$
10	-10	$-2\sqrt{15}$	$2\sqrt{10}$	0	$-5\sqrt{2}$	$5\sqrt{6}$
11	-10	$-2\sqrt{15}$	$2\sqrt{10}$	0	$10\sqrt{2}$	0
12	5	$-5\sqrt{15}$	0	0	0	0
13	5	$3\sqrt{15}$	$-3\sqrt{10}$	$5\sqrt{6}$	0	0
14	5	$3\sqrt{15}$	$-3\sqrt{10}$	$-5\sqrt{6}$	0	0
15	5	$3\sqrt{15}$	$2\sqrt{10}$	0	$-5\sqrt{2}$	$-5\sqrt{6}$
16	5	$3\sqrt{15}$	$2\sqrt{10}$	0	$-5\sqrt{2}$	$5\sqrt{6}$
17	5	$3\sqrt{15}$	$2\sqrt{10}$	0	$10\sqrt{2}$	0
18	5	$-\sqrt{15}$	$\sqrt{10}$	$-5\sqrt{6}$	$5\sqrt{2}$	$5\sqrt{6}$
19	5	$-\sqrt{15}$	$\sqrt{10}$	$-5\sqrt{6}$	$5\sqrt{2}$	$-5\sqrt{6}$
20	5	$-\sqrt{15}$	$\sqrt{10}$	$-5\sqrt{6}$	$-10\sqrt{2}$	0
21	5	$-\sqrt{15}$	$\sqrt{10}$	$5\sqrt{6}$	$5\sqrt{2}$	$5\sqrt{6}$
22	5	$-\sqrt{15}$	$\sqrt{10}$	$5\sqrt{6}$	$5\sqrt{2}$	$-5\sqrt{6}$
23	5	$-\sqrt{15}$	$\sqrt{10}$	$5\sqrt{6}$	$-10\sqrt{2}$	0
24	5	$-\sqrt{15}$	$-4\sqrt{10}$	0	$-5\sqrt{2}$	$-5\sqrt{6}$
25	5	$-\sqrt{15}$	$-4\sqrt{10}$	0	$-5\sqrt{2}$	$5\sqrt{6}$
26	5	$-\sqrt{15}$	$-4\sqrt{10}$	0	$10\sqrt{2}$	0
27	5	$-\sqrt{15}$	$6\sqrt{10}$	0	0	0

Table 6.1: The six diagonal generators $T_{1\text{–}6}$ of E_6. Also the coefficients $f_{1\text{–}6}$ of these generators that yield a linear combination that breaks $E_6 \to SO(10) \otimes U(1)$. The diagonal elements of the generator T_n are found by taking the n^{th} column and multiplying it by 1/60. The "pos." column is just the position of the entry in the diagonal matrix. There also exist twenty-seven distinct linear combinations of $T_{1\text{–}6}$ that yield a diagonal matrix which is just a rearrangement of T_1. These linear combinations are given by $\sum_{a=1}^{6} f_a T_a$, where the sextuplet $f_{1\text{–}6}$ takes values from one of the rows of the table, multiplied by 1/20, and are exactly the weight vectors for the fundamental representation of E_6. The negatives of such linear combinations are also valid rearrangements. The "pos." column specifies which position the lone 1/3 element appears in the diagonal matrix of the permuted version of T_1. Figure 6.2 gives a pictorial representation of the twenty-seven rearranged versions of the generator T_1. We can make the physical interpretation that, for an adjoint field χ, the vacuum state $\langle\chi\rangle \propto \sum_{a=1}^{6} f_a T_a$ breaks $E_6 \to SO(10) \otimes U(1)$.

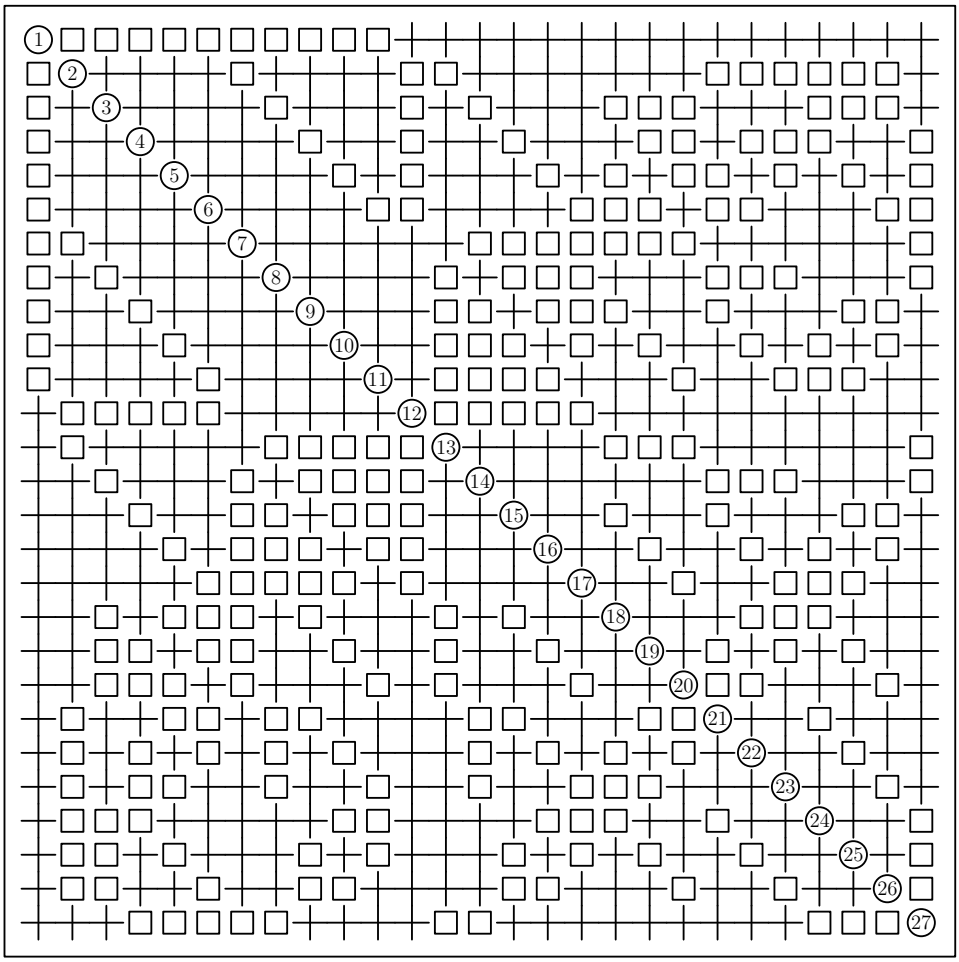

Figure 6.2: A pictorial representation of the twenty-seven rearrangements of the diagonal generator T_1 of E_6. Each rearrangement can be reconstructed from one of the twenty-seven rows (or columns) of symbols in this picture. To find the diagonal entries of the n^{th} rearrangement, read along the n^{th} row and translate the symbols according to: circles $\bigcirc$ correspond to the single $1/3$ entry, squares $\square$ to $-1/6$ and crosses $+$ to $1/12$ (note that adjacent crosses are touching). The number in the centre of each circle tells its row and column number (being the same). Row n of this picture corresponds precisely to row n of Table 6.1 in the sense that the linear combination $\sum_{a=1}^{6} f_a T_a$, where the $f_{1\text{–}6}$ are chosen from row n of Table 6.1, yields the rearranged version of the generator T_1 represented by the symbols of row n in this picture. This picture also provides a simple encoding telling the group that is the intersection of any possible combination of two of the twenty-seven differently embedded $\mathrm{SO}(10) \otimes \mathrm{U}(1)$ subgroups. If m and n are the rows corresponding to the two rearranged generators that correspond to two particular embeddings, then the symbol in row m, column n (equivalently column m, row n) tells the intersection H of these two groups: a circle $\bigcirc$ is $H = \mathrm{SO}(10) \otimes \mathrm{U}(1)$, a square $\square$ is $H = \mathrm{SO}(8) \otimes \mathrm{U}(1)^2$, and a cross $+$ is $H = \mathrm{SU}(5) \otimes \mathrm{U}(1)^2$. The picture is symmetric along the diagonal.

6.3.1 Truncated analysis of I_6

For now, we are just going to concentrate on the even invariant I_6 with only f_1, f_2 and f_3 non-zero. This allows us to make clear the method used to analyse the more general case with all f_a included. In the truncated case, the sextic invariant is

$$I_6 = \mathrm{Tr}\left[(f_1T_1 + f_2T_2 + f_3T_3)^6\right] \ . \tag{6.32}$$

To facilitate in visualising its structure, we go to spherical-polar coordinates $(r,\ \theta,\ \phi)$ via

$$f_1 = r\sin\phi\cos\theta\ , \quad f_2 = r\sin\phi\sin\theta\ , \quad f_3 = r\cos\phi\ , \tag{6.33}$$

where the domains are $r \geq 0$, $-\pi < \theta \leq \pi$ and $0 \leq \phi \leq \pi$. Equation (6.32) now takes the form

$$\begin{aligned} I_6 = \frac{r^6}{518400}\Big[&710\cos^6\phi + 144\sin\phi\ \cos^5\phi\left(\sqrt{10}\cos\theta - \sqrt{6}\sin\theta\right) \\ &+ 30\sin^2\phi\ \cos^4\phi\left(51 + 4\cos 2\theta - 4\sqrt{15}\sin 2\theta\right) \\ &+ 60\sqrt{2}\ \sin^3\phi\ \cos^3\phi\ \sin\theta\left(2\sqrt{3} + 3\sqrt{3}\cos 2\theta - \sqrt{5}\sin 2\theta\right) \\ &- 45\sin^4\phi\ \cos^2\phi\left(-34 + 2\cos 2\theta + 7\cos 4\theta - 2\sqrt{15}\sin 2\theta + \sqrt{15}\sin 4\theta\right) \\ &+ \frac{3}{2}\sin^6\phi\Big(440 + 15\cos 2\theta + 84\cos 4\theta + 11\cos 6\theta - 15\sqrt{15}\sin 2\theta \\ &\qquad + 12\sqrt{15}\sin 4\theta - 3\sqrt{15}\sin 6\theta\Big)\Big] \end{aligned} \tag{6.34}$$

Note how the radial dependence r factors out completely, leaving us with just a two-dimensional parameter space to study.

Take, for the moment, the slice of the sextic invariant where $\phi = \pi/2$ and so $f_3 = 0$. This simplifies our analysis further to just linear combinations of T_1 and T_2, parameterised by the single variable θ. A plot of the resulting invariant, $I_6(\phi = \pi/2)/r_6$, is given in Figure 6.3. While the minima of this function break E_6 to certain subgroups and have interesting properties in their own right, we are concerned here with the four[7] degenerate, global maxima which break E_6 to the maximal subgroup $SO(10) \otimes U(1)$. Since breaking to $SO(10) \otimes U(1)$ occurs at a maximum within this invariant, we shall need to negate I_6 when using it for model building purposes (by having

[7]There are five maxima in the figure, but we ignore the one on the far left as it is equivalent to that on the far right, and we have specified $\theta > -\pi$.

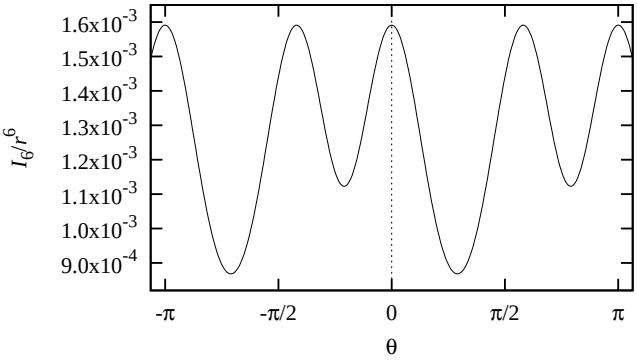

Figure 6.3: Plot of the sextic invariant I_6/r^6 as a function of θ for the slice $\phi = \pi/2$. Starting from the left, and not including the repeated extrema at $\theta = -\pi$, there are four global maxima at $\theta = -\arccos(1/4)$, 0, $\arccos(-1/4)$, π. In reference to Table 6.1, these correspond respectively to entry 12, entry 1, negative of entry 12 and negative of entry 1. Such linear combinations of the generators break E_6 to differently embedded $SO(10) \otimes U(1)$ subgroups.

$\tau_5 < 0$ in equation (6.26)). This is discussed further in Section 6.3.2; for now we are concerned with determining the precise locations of the relevant extrema in the sextic invariant.

The four global maxima in Figure 6.3 are given by $\theta = -\arccos(1/4)$, $\theta = 0$, $\theta = \arccos(-1/4)$ and $\theta = \pi$. This translates, respectively, to four different vacuum values for $\chi = f_a T_a$:

$$\frac{\langle\chi_1\rangle}{r} = \frac{1}{4}T_1 - \frac{\sqrt{15}}{4}T_2\,, \tag{6.35a}$$

$$\frac{\langle\chi_2\rangle}{r} = T_1\,, \tag{6.35b}$$

$$\frac{\langle\chi_3\rangle}{r} = -\frac{1}{4}T_1 + \frac{\sqrt{15}}{4}T_2\,, \tag{6.35c}$$

$$\frac{\langle\chi_4\rangle}{r} = -T_1\,. \tag{6.35d}$$

These vacuum values are constant, 27×27 matrices. Writing them out explicitly (not shown here), we find that all four of these vacuum values have the exact same diagonal entries as T_1, but they come with a different ordering. Therefore, we can easily evaluate the sextic invariant:

$$\frac{I_6}{r^6} = \mathrm{Tr}\left(\langle\chi_{1\text{–}4}\rangle^6\right) = \mathrm{Tr}\left(T_1^6\right) = \frac{11}{6912} \simeq 1.591 \times 10^{-3}\,. \tag{6.36}$$

This value is precisely the value of the maxima in Figure 6.3, as it should be. The particular ordering of entries in a given matrix representation of

a group correspond only to some (convenient or otherwise) choice of basis. Since T_1 is associated with the embedding of an $SO(10) \otimes U(1)$ structure in E_6, we conclude that all four vacua described by equation (6.35) break $E_6 \to SO(10) \otimes U(1)$. From the point of view of the particular basis that we have chosen to do our physical analysis in, say that defined by $T_{1\text{–}6}$, the four vacua $\langle \chi_{1\text{–}4} \rangle$ break E_6 to isomorphic but differently embedded $SO(10) \otimes U(1)$ maximal subgroups.[8] An implementation of the clash-of-symmetries mechanism is now imminent, but, before we do such a thing, we shall complete our analysis of the invariants.

Looking to Table 6.1, we see that the linear combinations of equation (6.35) that give rise to the different embeddings are exactly the first and twelfth rows of the table (up to some overall factor). But this table was originally constructed by writing the six diagonal generators as the columns! It is in fact true that the other twenty-five rows of this table correspond to all other possible linear combinations of the six generators which yield a diagonal matrix which is just a re-ordering of T_1. To be clear, the generators are given by each of the six columns multiplied by 1/60, and the possible sextuplets of values $(f_1,\ f_2,\ f_3,\ f_4,\ f_5,\ f_6)$ that define the vacuum state $\langle \chi \rangle = f_a T_a$ are given by the twenty-seven rows multiplied by 1/20. Note that only the ratio of these two normalisation factors, being 3, is meaningful; in constructing Table 6.1 we just wanted to minimise clutter, and keep all the elements normalised to the same factor. This "rearrangement property" seems truly remarkable, and we suspect that some (unknown to us) aspect of group theory can tell us what is really going on here. We conjecture that this property is true for all simple Lie groups.[9]

For reference, Figure 6.2 provides a pictorial representation of the twenty-seven possible rearrangements of the diagonal generator T_1. Row n in this figure correspond to the linear combination given by row n in Table 6.1. See the caption of Figure 6.2 for the mapping of the symbols ($\bigcirc$, $\square$, $+$) to the

[8] An explicit calculation which establishes that the embeddings are in fact different is given in Section IV of Paper 2 in the author's list of publications.

[9] This discovery came late in the course of the current thesis, and we have not had time to explore it fully. This "rearrangement conjecture" is true also for the diagonal generators of SU(2), SU(3) and SU(5), where, if $\mathrm{Tr}(T_a T_b) = \delta_{ab}/2$ is the associated normalisation, then the coefficients of the linear combinations are the diagonal entries multiplied by 2, $\sqrt{3}$ and $\sqrt{5/2}$, respectively (in the E_6 case this factor is 3). One may also inquire about the rearrangement of the entries of the other diagonal generators (not just T_1). It seems, in the case of SU(3) at least, that permutations of the coefficients (permutations of the rows) define linear combinations that yield rearranged versions of the other diagonal generators. This requires more study.

appropriate fractions. From this figure one can also determine the symmetry group that is the intersection of two differently embedded $SO(10) \otimes U(1)$ subgroups. This is done by examining the two rows of symbols corresponding to the two embeddings, and counting the number of columns that have squares in both rows, those columns that have a square in one row and a cross in the other row, and so on. We shall not provide the details of this as it is straightforward. Quite amazingly though, this figure actually tells you the answer up front: the intersection of two $SO(10) \otimes U(1)$ subgroups corresponding to rows m and n is given by the symbol in row m and column n (equivalently column m and row n)! There are three possibilities: $SO(10) \otimes U(1)$ (if the two embeddings are the same), $SO(8) \otimes U(1)^2$ and $SU(5) \otimes U(1)^2$. Again, see the caption of the figure for the mapping of the symbols to these groups. We shall draw on these results later.

One more interesting property of the degenerate vacua requires explaining. As exemplified by $\langle\chi_4\rangle$, we can trivially modify T_1 by negating all of its elements. This yields a distinct vacuum in the I_6 topography, which breaks E_6 to a different $SO(10) \otimes U(1)$ embedding than does the related $\langle\chi_2\rangle$. Note that $\langle\chi_3\rangle = -\langle\chi_1\rangle$, so these two vacua are similarly related. Therefore, the twenty-seven rows of Table 6.1 also have a $\mathbb{Z}_2$ partner, obtained by negating each element in the row. We shall return to this observation in our discussion of the full space of extrema of the invariants.

Returning to the analysis of I_6, we relax the restriction on ϕ and consider the two-dimensional structure of the sextic invariant given by equation (6.34). The easiest way to visualise this equation is via a contour plot, which is what is shown in Figure 6.4. The previous plot in Figure 6.3 is subsumed in this three-dimensional graph as the horizontal line at $\phi = \pi/2$. The maxima are marked with a black + sign, and there are two additional ones that correspond to VEVs which are degenerate with those in equation (6.35). The one at the bottom left is located at $\theta = -\arccos(\sqrt{5/8})$, $\phi = \arccos(\sqrt{9/10})$ and that at the top right at $\theta = \arccos(-\sqrt{5/8})$, $\phi = \arccos(-\sqrt{9/10})$. The corresponding vacua are, respectively,

$$\frac{\langle\chi_5\rangle}{r} = \frac{1}{4}T_1 - \frac{\sqrt{15}}{20}T_2 + \frac{3}{\sqrt{10}}T_3\,, \tag{6.37a}$$

$$\frac{\langle\chi_6\rangle}{r} = -\frac{1}{4}T_1 + \frac{\sqrt{15}}{20}T_2 - \frac{3}{\sqrt{10}}T_3\,. \tag{6.37b}$$

They correspond to the twenty-seventh row of Table 6.1.

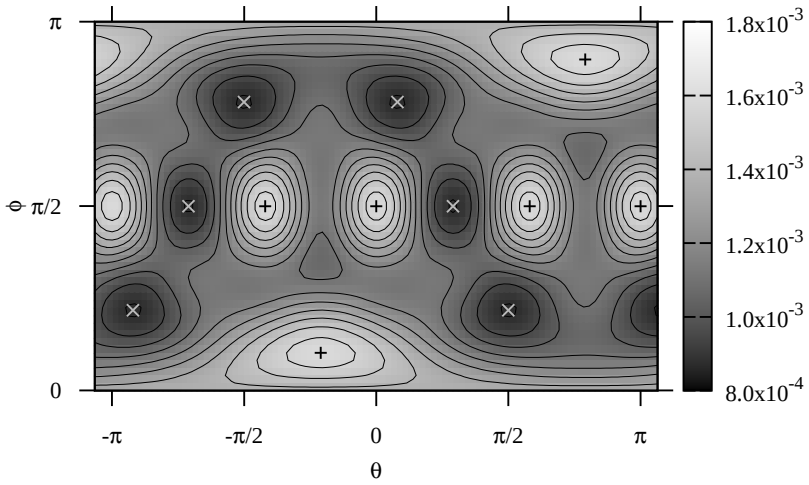

Figure 6.4: Contour plot of the sextic invariant I_6/r^6 as a function of θ and ϕ. The degenerate global maxima breaking E_6 to various $SO(10)\otimes U(1)$ subgroups are marked with black + signs, while the local minima are indicated with gray $\times$ signs. The row of four maxima along $\phi = \pi/2$ correspond to the global maxima displayed in Figure 6.3. The two additional maxima correspond to entry 27 in Table 6.1.

6.3.2 The full analysis

Our analysis of I_6 can be extended to include all six Cartan components. Going to six-dimensional hyperspherical polar coordinates involves writing the coefficients $f_{1\text{–}6}$ in terms of the modulus $r \geq 0$, the azimuthal angle $-\pi < \theta \leq \pi$ and four zenith angles $0 \leq \phi_{1,2,3,4} \leq \pi$. As before, the parameter r factors out and the group-theoretic structure of the sextic invariant is determined entirely by the angles $(\theta, \phi_{1\text{–}4})$. The domain of this space is finite, so the search for extrema finds an adequate realisation in a numerical scan. We have performed such a scan by making small, finite steps systematically through the parameter space, and computing the derivative of I_6 (with respect to each parameter[10]) at each point to determine if it is a minimum, maximum or saddle point.[11]

This numerical study found fifty-four global maxima. Analytic expressions for the locations of these maxima were subsequently reverse engineered. The corresponding values of $f_{1\text{–}6}$ are given exactly by the twenty-seven rows of Table 6.1, multiplied by $1/20$ for half of the maxima, and multiplied by $-1/20$ for the other half. As discussed previously, the linear combination

[10] A general, analytic expression for the derivative can be found easily by hand, which we then evaluated numerically at each point.

[11] We used 214 steps for θ and 107 steps for each of $\phi_{1\text{–}4}$ which gives about 2.8×10^{10} points in total, and the scan took roughly 53 hours.

$f_a T_a$ is simply a rearrangement of the entries in T_1, possibly with an overall factor of -1. A rather neat fact is the following. In Table 6.1, the "pos." (position) column specifies the location of the SO(10)-singlet $\frac{1}{3}$ element in the permuted version of T_1, where the permutation is given by the sextuplet in that particular row. For example, if we pick the f_a to be given by row eighteen, then the linear combination $f_a T_a$ has a single $\frac{1}{3}$ entry at the eighteenth position in the diagonal 27×27 matrix. This feature manifests clearly in Figure 6.2 as the circles along the diagonal. Physically, these linear combinations, the rearrangements, all yield a vacuum structure which breaks E_6 to $SO(10) \otimes U(1)$, and so we are able to use I_6 to do such breaking in fifty-four different ways, where the doubling is due to the choice of overall sign for the VEV.

Moving on to the other even invariants, I_8 and I_{12}, we have found them to have exactly the same qualitative structure as I_6. The plots of the truncated versions of these higher-power invariants, corresponding to Figures 6.3 and 6.4, are very similar, and a full numerical search of the extrema of I_8 and I_{12} revealed again the fifty-four degenerate maxima given by Table 6.1. For the odd invariants I_5 and I_9 we found twenty-seven global maxima, corresponding to the positive versions of the rows of Table 6.1, along with twenty-seven global minima, corresponding to the negative versions of the rows. This result tells us that the $\mathbb{Z}_2$ negation-relation between the two sets of twenty-seven global maxima in the even invariants actually lies outside E_6, as the odd invariants change sign (so they are not invariant) under the action of such a $\mathbb{Z}_2$.

This latter result is very useful from the point of view of the clash of symmetries. If we *impose* that our E_6 theory is also invariant under such a $\mathbb{Z}_2$, where $\chi \to -\chi$, then we eliminate any terms in the Higgs potential which have odd powers of odd invariants (like τ_3 and τ_6 in equation (6.26)), and so induce a vacuum manifold with two disconnected copies, as per Figure 6.1. If we are careful with our choices for the rest of the parameters, then the vacuum structure of each piece of the manifold will have as their global minima the $SO(10) \otimes U(1)$'s that we have identified. The two copies will each have twenty-seven degenerate global maxima that break $E_6 \to SO(10) \otimes U(1)$, and these vacua will further be degenerate among the two copies. Of course, we need our vacua to be minima to have stable kink configurations, which can be easily achieved by taking the coefficient of, say, I_6 to be negative. To ensure that the Higgs potential is then bounded from below, just add terms

proportional to positive $(I_2)^m$ as appropriate. This will not destroy the vacuum structure because I_2 is isotropic, as per equation (6.31).

Finally, we remark on a group-theoretic aspect of the number of embeddings of $SO(10) \otimes U(1)$ in E_6. They must correspond, physically speaking, to choosing different $SU(3) \otimes SU(2)$ subgroups for colour and weak-isospin. According to the $SU(3) \otimes SU(3) \otimes SU(3)$ maximal subgroup of E_6, there are three independent choices for the colour group. The weak-isospin group can then be selected as the I-, U- or V-spin subgroup of either of the two remaining SU(3)'s. This gives $3 \times 6 = 18$ choices for $SU(3) \otimes SU(2)$ embeddings. By an explicit calculation,[12] it is found that each $SU(3) \otimes SU(2)$ is contained in the intersection of three different SO(10)'s, which suggests there should be $18 \times 3 = 54$ embeddings of SO(10). However, recognising that SO(10) contains an $SU(2) \otimes SU(2)$ subgroup, we see that the correct number of independent embeddings is actually $54/2 = 27$.

6.4 An E_6 domain-wall model

Having performed a rather comprehensive analysis of the structure of the Higgs potential for an E_6 adjoint field, we proceed in this section to piece together, and analyse, the basic ingredients for an E_6 invariant domain-wall brane model of an infinite extra dimension. The clash-of-symmetries and Dvali-Shifman mechanisms play a large role in determining the structure of the kink background configuration, and, after obtaining the solution for the kink, we shall analyse the spectrum of localised fermions.

In our model there is a single background scalar field: the adjoint χ. This Higgs potential will be a restricted version of V_{full}, which is given by equation (6.26). For clash-of-symmetries sake, we require a discrete $\mathbb{Z}_2$ symmetry which lies outside E_6, and this can be arranged by imposing $\chi \to -\chi$ as a symmetry, as discussed in Section 6.3.2. This eliminates odd powers of odd invariants. We have also discussed how any one of the invariants I_n with $n \neq 2$ provide us with global extrema that break $E_6 \to SO(10) \otimes U(1)$. The lowest order Higgs potential compatible with such constraints is the order-six potential

$$V = V_0 - \lambda_1 I_2 + \lambda_2 (I_2)^2 + \frac{4}{3}\lambda_3 (I_2)^3 - 2304\kappa I_6 \,, \tag{6.38}$$

where some peculiar numbers and signs have been inserted for later conve-

[12] See Paper 2 in the author's list of publications.

nience. Recall that we need I_6 to appear with a negative coefficient to have the $\mathrm{SO}(10) \otimes \mathrm{U}(1)$ vacua the global *minima*. We also need the I_2 term negative to encourage a non-zero VEV (so that $\chi = 0$ is not a minimum), and the $(I_2)^3$ term positive to ensure that the potential is bounded from below. Additional constraints on the parameters shall be derived in Section 6.4.1.

The potential V will induce $\mathrm{E}_6 \to \mathrm{SO}(10) \otimes \mathrm{U}(1)$, and for the clash-of-symmetries we require two vacua for χ that are *not* related by the $\mathbb{Z}_2$. Acceptable choices for the minima are those defined by rows one and twelve of Table 6.1. Let us make some re-definitions to simplify the notation a bit. Take $E = T_1$ and $X = T_2$. The first minimum is obtained by breaking in the direction of E, and its $\mathbb{Z}_2$ pair, in the direction of $-E$. Recall from Section 6.1 that both of these minima respect the same symmetry, which we denote simply by

$$H = \mathrm{SO}(10) \otimes \mathrm{U}(1)_E \,. \tag{6.39}$$

Furthermore, we shall label the two respective vacua by

$$|0\rangle = (10, +) \qquad \text{and} \qquad |0\rangle_z = (10, -) \,, \tag{6.40}$$

where a '+' sign indicates that the vacuum lies in the $\mathcal{V}$ piece of the manifold, and a '$-$' sign indicates the $\mathcal{V}_z$ piece.

The second pair of minima come from considering the linear combination of row twelve of Table 6.1:

$$E' = \frac{1}{4}E - \frac{\sqrt{15}}{4}X \,. \tag{6.41}$$

The corresponding rearranged X is

$$X' = -\frac{\sqrt{15}}{4}E - \frac{1}{4}X \,, \tag{6.42}$$

and is found by demanding $\mathrm{Tr}(E'X') = 0$. Breaking in the direction of E' leaves the vacuum respecting the symmetry group[13]

$$H_g = \mathrm{SO}(10)' \otimes \mathrm{U}(1)_{E'} \,, \tag{6.43}$$

and the two vacua are

$$|0; g\rangle = (10', +) \qquad \text{and} \qquad |0; g\rangle_z = (10', -) \,. \tag{6.44}$$

[13] This embedding has been used previously in unified model building [227, 228, 229, 230].

As per the discussion in Section 6.1, and as represented in Figure 6.1, the topological CoS domain wall connects $(10,+)$ and $(10',-)$, accompanied by a CoS anti-domain-wall connecting $(10,-)$ and $(10',+)$. The symmetry on the wall is $H \cap H_g$, which can be determined by reading off the symbol at row twelve, column one of Figure 6.2. It is a cross, meaning that the intersection group is [14]

$$[\,\mathrm{SO}(10)\otimes\mathrm{U}(1)_E\,]\cap[\,\mathrm{SO}(10)'\otimes\mathrm{U}(1)_{E'}\,]=\mathrm{SU}(5)\otimes\mathrm{U}(1)_E\otimes\mathrm{U}(1)_{E'}\,. \quad (6.45)$$

Since SU(5) is fully contained in both SO(10) and SO(10)′, the Dvali-Shifman mechanism localises all the SU(5) gauge bosons to the domain wall, including the photon and the neutral Z boson. This vindicates our efforts in upgrading from an SO(10) invariant action to an E_6 invariant one. Note that the additional U(1)'s are there because adjoint configurations cannot rank-reduce.

There also exists the topological non-CoS domain wall that connects $(10,+)$ with $(10,-)$ and breaks E_6 to $\mathrm{SO}(10)\otimes\mathrm{U}(1)_E$ at all w, as well as the non-CoS configuration interpolating between $(10',+)$ and $(10',-)$, breaking E_6 to $\mathrm{SO}(10)'\otimes\mathrm{U}(1)_{E'}$ at all w. The non-topological kinks are those connecting $(10,+)$ to $(10',+)$, and $(10,-)$ to $(10',-)$, which are both CoS-like.

6.4.1 Domain-wall solutions

We are now going to solve the Euler-Lagrange equations for χ, with the potential V given by equation (6.38), to find kinks giving an explicit realisation of the symmetry breaking defined by equation (6.45). Since the requisite vacua can be obtained with linear combinations of only E and X — equivalently E' and X', or even E and E' — we need only consider two of the seventy-eight components of χ:

$$\chi = f_E E + f_X X \equiv \tilde{f}_E E + f_{E'} E'\,, \quad (6.46)$$

with the relationships

$$\tilde{f}_E \equiv f_E + \frac{1}{\sqrt{15}} f_X\,, \qquad f_{E'} \equiv -\frac{4}{\sqrt{15}} f_X\,. \quad (6.47)$$

[14] See Section IV of Paper 2 in the author's list of publications for a more in-depth analysis which examines the flipping of the roles of the SU(5) multiplets.

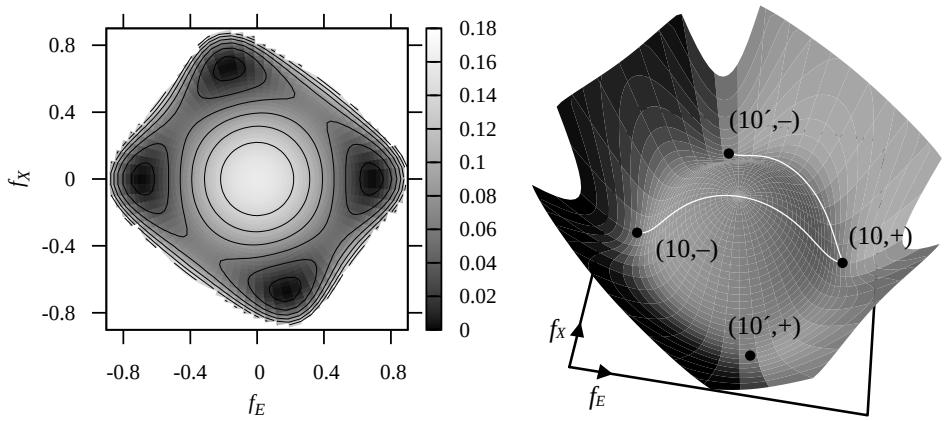

(a) (b)

Figure 6.5: (a) Contour plot of the Higgs potential as a function of the two field components f_E and f_X. The darkest regions are the global minima in the order $(10,+)$, $(10',-)$, $(10,-)$ and $(10',+)$ reading anticlockwise from the rightmost minimum. The light area near the origin is a local maximum. (b) Three-dimensional plot of the Higgs potential as a function of the two field components f_E and f_X. The white lines show the clash-of-symmetries domain wall (topmost) and the non-CoS domain wall (bottommost). The parameters used in both plots are $\kappa = 0.8$, $\lambda_1 = 1.0$, $\lambda_2 = 0$, $\lambda_3 = 22.0$ and $V_0 = -0.1589$.

Here, the specific linear combinations have been determined according to equation (6.41). The (E, X) basis is more convenient for solving the Euler-Lagrange equations, because E and X are orthogonal as per equation (6.28). The (E, E') basis, however, is the simplest one for thinking about the two embeddings.

To provide a visual aid for the following analysis, we have provided a contour plot in Figure 6.5a of the Higgs potential $V(f_E, f_X)$ for a certain choice of parameters; V is defined by equation (6.38) and has χ as per equation (6.46). It is important to realise that although the minima $(10,+)$ and $(10',+)$ [similarly $(10,-)$ and $(10',-)$] look as though they are disconnected by E_6, this is just an illusion created by only plotting the two-dimensional $(f_E,\ f_X)$ slice through the seventy-eight-dimensional adjoint representation space. Minima with opposite parities are definitely disconnected from each other.

Our aim is to find kink solutions for such a Higgs potential. The VEVs we want for the boundary conditions are

$$(\tilde{f}_E,\ f_{E'}) = v\,(1,\ 0)\,, \tag{6.48}$$

on one side of the wall, say $w \to -\infty$. This corresponds to the vacuum $(10, +)$ and breaks $E_6 \to SO(10) \otimes U(1)_E$. The other VEV, for the other side of the wall, is

$$(\tilde{f}_E,\ f_{E'}) = -v\,(0,\ 1)\,, \tag{6.49}$$

which is the vacuum $(10', -)$ giving $E_6 \to SO(10)' \otimes U(1)_{E'}$. The relative minus sign between equations (6.48) and (6.49) ensures that we connect vacua from the disconnected manifolds $\mathcal{V}$ and $\mathcal{V}_z$, while the flipping from $(1,\ 0)$ to $(0,\ 1)$ ensures a CoS configuration. The minus sign also leads to a remarkable outcome for fermion zero-mode localisation, which is explained in the next subsection. In terms of the (E, X) basis, these same VEVs are

$$(f_E,\ f_X) = \begin{cases} v\,(1,\ 0) & \text{for} \quad w \to -\infty \\ v\left(-\frac{1}{4},\ \frac{\sqrt{15}}{4}\right) & \text{for} \quad w \to +\infty \end{cases}\,. \tag{6.50}$$

The "direction" of the boundary conditions, the pairs of values in equation (6.50), are fixed because we knew *a priori* exactly the form of the E_6 breaking at the boundaries. The "magnitude", given by $v > 0$, must be determined, and will depend on the particular parameters in the Higgs potential (and may not exist in certain parameter regimes).

Our task of analysing the Higgs potential V in order to determine v is quite straightforward, so long as we draw on the results of Section 6.3. By construction, we know that the boundary conditions we have chosen are global extrema of I_6. We also know that I_2 is isotropic. Therefore, if we substitute in either of the set of boundaries given by equation (6.50) into the invariants, we obtain

$$I_2 = \frac{1}{2}v^2\,, \tag{6.51a}$$

$$I_6 = \frac{11}{6912}v^6\,. \tag{6.51b}$$

Here, we have used, respectively, equations (6.31) and (6.36). In other words, when the fields f_E and f_X are "pointing", with magnitude v, in the direction of an extrema of I_6, as they are at the boundaries, we can write equation (6.38) as

$$V = V_0 - \frac{\lambda_1}{2}v^2 + \frac{\lambda_2}{4}v^4 + \frac{\lambda_3}{6}v^6 - \frac{11\kappa}{3}v^6\,. \tag{6.52}$$

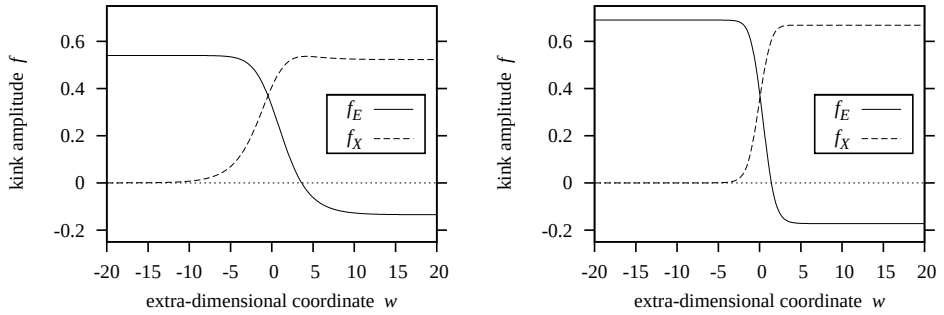

Figure 6.6: Clash-of-symmetries domain-wall solutions interpolating between $(10,+)$ at $w=-\infty$ and $(10',-)$ at $w=+\infty$. The isomorphic but differently embedded subgroups at these boundaries are $\mathrm{SO}(10)\otimes\mathrm{U}(1)_E$ and $\mathrm{SO}(10)'\otimes\mathrm{U}(1)_{E'}$ respectively, corresponding to row 1 and negative of row 12 of Table 6.1. Their intersection (clash) is the subgroup $\mathrm{SU}(5)\otimes\mathrm{U}(1)^2$. The parameters used in the left plot are $\kappa=0.2$, $\lambda_1=1.5$, $\lambda_2=0$, $\lambda_3=22.0$; those in the right plot are $\kappa=0.8$, $\lambda_1=1.0$, $\lambda_2=0$, $\lambda_3=22.0$.

In the examples presented below, we further simplify the Higgs potential by setting $\lambda_2=0$ as the associated term does not play an important role. It is then easy to show that the degenerate minima are obtained for

$$v=\left(\frac{\lambda_1}{\lambda_3-22\kappa}\right)^{1/4}, \tag{6.53}$$

so we must take $\lambda_3>22\kappa$. The value of V at this minimum is

$$V_{\min}=V_0-\frac{1}{3}\sqrt{\frac{\lambda_1^3}{\lambda_3-22\kappa}}\,, \tag{6.54}$$

and we choose V_0 such that $V_{\min}=0$ in order to produce finite energy-densities for the domain-wall configurations.

Having understood the global minima, we may now solve the Euler-Lagrange equations

$$f_X''(w)=\frac{\partial V}{\partial f_X}\,,\qquad f_E''(w)=\frac{\partial V}{\partial f_E}\,, \tag{6.55}$$

using as our boundary conditions the VEVs defined by equations (6.50) and (6.53). Numerical solutions for CoS domain-walls interpolating between $(10,+)$ at $w=-\infty$ and $(10',-)$ at $w=+\infty$ with two different parameter choices are displayed in Figure 6.6.

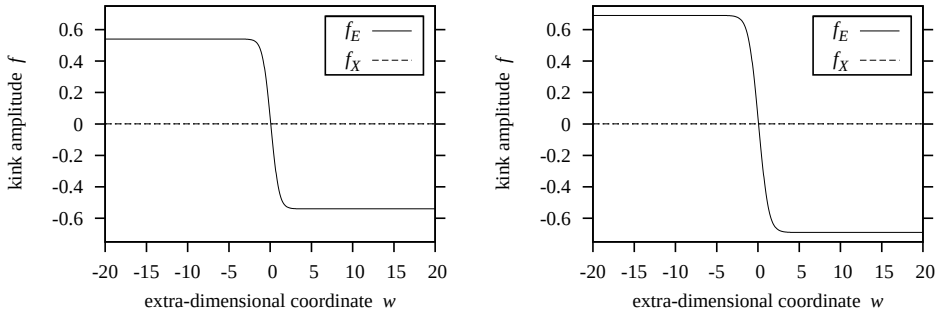

Figure 6.7: Non-clash-of-symmetries domain-wall solutions interpolating between $(10,+)$ at $w=-\infty$ and $(10,-)$ at $w=+\infty$. These boundaries respect the same $\mathrm{SO}(10)\otimes\mathrm{U}(1)$ subgroup, so there is no clash. The parameters used in the left plot are $\kappa=0.2$, $\lambda_1=1.5$, $\lambda_2=0$, $\lambda_3=22.0$; those in the right plot are $\kappa=0.8$, $\lambda_1=1.0$, $\lambda_2=0$, $\lambda_3=22.0$.

Figure 6.7 depicts non-CoS domain-wall solutions for the same parameter choices. The boundary conditions for such configurations are different to the CoS scenario: the function f_X is required to asymptote to zero as $|w|\to\infty$, while f_E interpolates from v to $-v$. The solution has f_X identically zero, and f_E takes the form of the archetypal kink. This means that the non-CoS configurations feel the large potential-energy maximum at $f_X=f_E=0$, shown at the centre in Figure 6.5a, while the CoS configuration "skirts around" that central maximum. This immediately implies that the CoS solutions have lower energy density than the non-CoS solutions. Although they are in the same topological class, the CoS domain walls are stable while the non-CoS domain walls are unstable. Figure 6.5b shows a three-dimensional plot of the potential and where the two domain-wall configurations sit with respect to the topography. There is a tall maximum at the origin, and a corrugated valley encircling it, with four low points at the VEVs. Figure 6.8 compares the energy densities of CoS and non-CoS domain walls.

Let us summarise the kink solutions we have found. We were looking for background configurations of the adjoint χ with boundary conditions that broken E_6 to differently embedded $\mathrm{SO}(10)\otimes\mathrm{U}(1)$ subgroups. As our reference vacuum, the one at $w=-\infty$, we used $(10,+)$, which corresponds to χ breaking in the direction of the diagonal generator E. For $w=+\infty$, we used both $(10',-)$ and $(10,-)$, which correspond to breaking in the direction of $-E'$ and $-E$ respectively. We needed to interpolate from a '+' vacuum

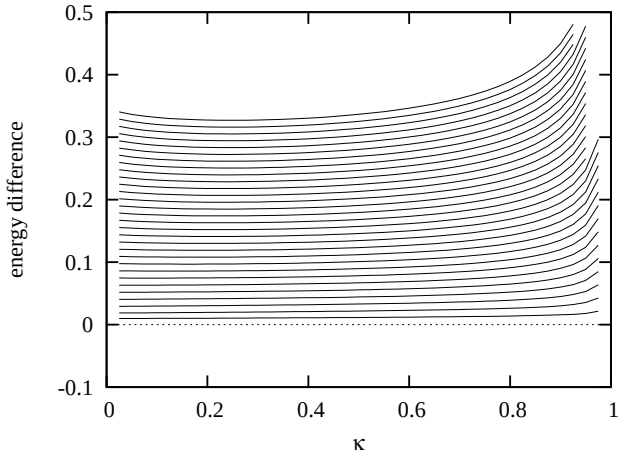

Figure 6.8: The difference in energy densities between the non-CoS and CoS domain wall solutions, $E_{\text{non-CoS}} - E_{\text{CoS}}$. We have numerically scanned through the parameter space with $0 < \kappa < 1$ along the horizontal axis, and each successive curve represents a different λ_1, beginning at $\lambda_1 = 0.05$ at the bottom and increasing in steps of 0.05 to $\lambda_1 = 1.5$ at the top. The energy difference is always positive, so the CoS domain wall has a lower energy. We set $\lambda_2 = 0$ for simplicity.

to a '$-$' vacuum to obtain topological kinks. The first set of boundary conditions gives a clash-of-symmetries set-up, with $\mathrm{SU}(5) \otimes \mathrm{U}(1)^2$ as the symmetry group respected at non-asymptotic values of w, and the second a non-clash-of-symmetries set-up, where $\mathrm{SO}(10) \otimes \mathrm{U}(1)$ is the symmetry at all w.

Think about this in terms of the twenty-seven different linear combinations of the diagonal generators $T_{1\text{–}6}$ that yield just a rearranged version of T_1, as per Table 6.1. It is helpful to refer to Figure 6.2 to visualise these twenty-seven different rearrangements, and we shall label the n^{th} rearrangement, the n^{th} row, as $T_1^{(n)}$, with $T_1^{(1)} \equiv T_1$. When χ assumes a VEV in the direction of $T_1^{(n)}$ for a given n, it breaks E_6 to one of the twenty-seven differently embedded $\mathrm{SO}(10) \otimes \mathrm{U}(1)$ subgroups. If we take $T_1^{(1)}$ as the direction of the χ vacuum at $w = -\infty$, then we have a choice of twenty-seven directions for the vacuum at $w = +\infty$, one for each of the rearranged versions of T_1 (with a negative sign to get topological kinks). The kink solutions we have been studying in this section correspond to choosing $-T_1^{(12)}$ for the CoS set-up and $-T_1^{(1)}$ for the non-CoS set-up.

It is natural to inquire about the properties of the kink configurations for the other twenty-five choices of boundary conditions at $w = +\infty$. What

is the common subgroup — the clash group — of the differently embedded SO(10)'s that is respected at non-asymptotic values of w? What are the relative energy densities of these different kink solutions? We have performed a preliminary analysis to uncover answers to these questions. The clash group can be easily determined by examining Figure 6.2. Using any of the ten rearranged generators $-T_1^{(2\text{–}11)}$ as the direction that χ breaks to at $w = -\infty$ produces kinks which have $\mathrm{SO}(8) \otimes \mathrm{U}(1)^2$ as the intersection of the two differently embedded $\mathrm{SO}(10) \otimes \mathrm{U}(1)$ groups. The other sixteen choices, being $-T_1^{(12\text{–}27)}$, yield $\mathrm{SU}(5) \otimes \mathrm{U}(1)^2$ as the intersection, or clash, group. As for the relative energy densities, for the (very tiny) parameter space that we have checked, the ten SO(8) configurations have *lower* energy density than the sixteen SU(5) ones. Note that for a given set of parameters in the Higgs potential, all ten SO(8) solutions have the same energy density, and, similarly, all sixteen SU(5) solutions have the same energy density among themselves. The single non-CoS solution, corresponding to choosing $-T_1^{(1)}$ at $w = -\infty$, has an energy density which is greater than all the other configurations.[15]

This is a rather unpleasant outcome because it means that our SU(5) kink solutions, as per Figure 6.6, are *unstable* to decay to one of the SO(8) configurations. The instability arises from the fact that there exists an E_6 transformation which is able to continuously transform the boundaries of the SU(5) configuration to that of the SO(8) one. Such an E_6 transformation comes at only a finite energy cost, so if the kink begins in the SU(5) form, it will eventually evolve to the more energetically favourable SO(8) form.

In Figure 6.9 we have plotted the kink profiles $f_{1\text{–}6}$ for a typical SO(8)-inducing background. To be clear, we have taken $\chi = \sum_{a=1}^{6} f_a T_a$, with $f_{1\text{–}6}$ in the direction of $T_1^{(1)}$ at $w = -\infty$ and in the direction of $-T_1^{(4)}$ at $w = +\infty$. Even though more of the f_a are non-zero for this configuration as compared with that in Figure 6.6, the internal structure of the invariants I_n in the Higgs potential (6.38) is such that the associated energy density is lower in the SO(8) case, at least for our particular choice of parameters and

[15] This particular analysis of the relative energy densities was performed towards the end of the current thesis, following the discovery of the rearrangement property of T_1, and we have not had time to properly understand its consequences. The preliminary results presented here do not appear in the associated publication (Paper 2 in the author's list of publications) which assumes that the SU(5) configuration, having a lower energy density than the non-CoS kink solution, has the lowest energy density of all possible configurations.

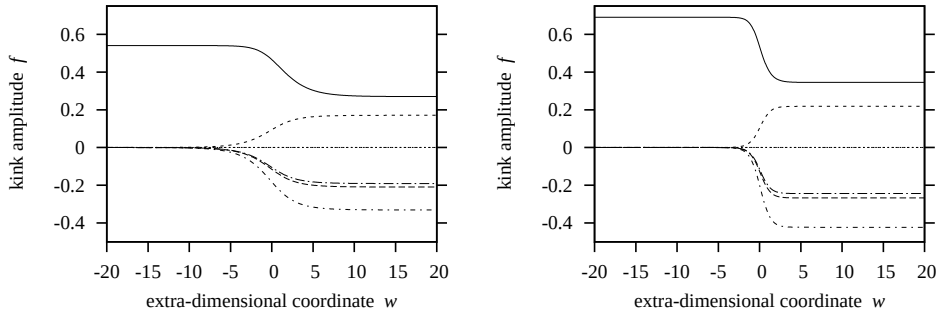

Figure 6.9: Clash-of-symmetries domain-wall solutions interpolating from the diagonal generator T_1 at $w = -\infty$ (corresponding to row 1 in Table 6.1, what we are calling $(10, +)$) to the negative of the rearranged generator corresponding to row 4 in Table 6.1, at $w = +\infty$. We must take the negative of this latter generator to yield topological kinks. These boundary conditions break E_6 to isomorphic but differently embedded $SO(10) \otimes U(1)$ subgroups, the intersection of these particular embeddings (their clash) being $SO(8) \otimes U(1)^2$, in contrast to the $SU(5) \otimes U(1)^2$ clash depicted in Figure 6.6. Reading from top to bottom on the far right side of the figure, the six components of χ are $f_1 \equiv f_E$, f_3, f_4 (which is zero everywhere), f_5, $f_2 \equiv f_X$ and f_6. The parameters used in the left plot are $\kappa = 0.2$, $\lambda_1 = 1.5$, $\lambda_2 = 0$, $\lambda_3 = 22.0$; those in the right plot are $\kappa = 0.8$, $\lambda_1 = 1.0$, $\lambda_2 = 0$, $\lambda_3 = 22.0$.

our particular choice for the form of the Higgs potential.

We may be able to save our SU(5) model by exploiting this last observation: a different form of the Higgs potential could result in solutions that have the lowest energy density for the SU(5) configurations. At our disposal are the invariants I_2, $(I_5)^2$, I_6, I_8, $(I_9)^2$, I_{12}, and their products. This gives quite a lot of room for exploration, and there is hope that one could find some region of parameter space for some form of the potential which allows for an SU(5)-clash configuration that is energetically favoured over the SO(8) and non-CoS configurations. The corresponding kink solutions will be qualitatively the same as those given in Figure 6.6 because the boundary conditions are exactly the same. For the sake of the fermion localisation analysis performed in the following subsection, we shall assume that stable SU(5) solutions can be found, and we shall use those solutions depicted in Figure 6.6 as representative of the putative, stable solutions.

6.4.2 Localisation of fermion zero modes

The clash-of-symmetries E_6 domain wall solutions described in Section 6.4.1 are a good starting point for the creation of domain-wall brane models

whereby the effective four-dimensional theory is SU(5)-invariant. To actually create such a model, fermions, additional Higgs bosons and gravitons have to be incorporated. In this subsection, we demonstrate that a phenomenologically-acceptable fermion localisation pattern is obtained using the simplest possible mechanism. This is actually quite a remarkable result, and we shall explain why. As previously pointed out, the domain-wall configurations that we have found which yield SU(5) invariance on the brane are unstable. However, we shall assume that one can find a suitable Higgs potential for χ which supports appropriate, stable solutions, and we make the following analysis under such an assumption.

There are enough degrees of freedom in the **27** of E_6 for a single generation of the standard model. So this is what we begin with:

$$\Psi \sim \mathbf{27} \,. \tag{6.56}$$

It is coupled to the adjoint scalar, as per

$$\mathcal{L}_Y = -h\overline{\Psi}\chi\Psi \,, \tag{6.57}$$

where h is the coupling constant. We now substitute in the background, clash-of-symmetries domain-wall configuration for χ and solve the resulting Dirac equations. They take the form

$$i\Gamma^M \partial_M \Psi^{(E,X)}(x^\mu, w) - h\left[f_E(w)E + f_X(w)X\right]\Psi^{(E,X)}(x^\mu, w) = 0 \,. \tag{6.58}$$

The notation $\Psi^{(E,X)}$ signifies the component of the **27** with the specified (E, X) charges, as given in equation (6.30b). The various components couple to different background field configurations,

$$b^{(E,X)}(w) = f_E(w)E + f_X(w)X \,, \tag{6.59}$$

given by the domain-wall configuration and the charges. This is in direct analogy with the splitting of the fermions in the SU(5) model considered in Chapter 5, in particular, this equation for $b^{(E,X)}$ mimics equation (5.17).

The five-dimensional Dirac matrices are, as usual, $\Gamma^M = (\gamma^\mu, -i\gamma^5)$, and we look for separated-variable solutions $\Psi(x^\mu, w) = F(w)\ \psi(x^\mu)$. As in the analyses of previous chapters, we demand that ψ have definite chiral-

ity, $\gamma^5\psi = \pm\psi$, and obeys the four-dimensional, massless Dirac equation, $i\gamma^\mu\partial_\mu\psi = 0$. Following the analysis that lead to equation (5.18), the profiles for the case at hand have solutions given by

$$F^{(E,X)}(w) = N^{(E,X)}e^{-h\int_0^w b^{(E,X)}(w')dw'}\,, \tag{6.60}$$

where N is a normalisation factor. For the profile $F^{(E,X)}$ to represent localisation, it must be square-integrable with respect to w. For this to happen, $b^{(E,X)}$ must pass through zero. If so, and it is an increasing function of w (kink-like), then a left-handed zero-mode occurs for $h > 0$, while a right-handed mode for $h < 0$. If $b^{(E,X)}$ passes through zero as a decreasing function (anti-kink-like), then a left-handed zero-mode occurs for $h < 0$, and a right-handed one for $h > 0$.

Figure 6.10 show the kink-like functions $b^{(E,X)}$ for the two parameter choices we have been using as examples. Let us take h to be negative, and we shall show that this yields an appropriate spectrum of localised fermions. Using the notation $D(12E, 4\sqrt{15}X)$ for the separate fermion multiplets inside the **27** (where D is the size of the multiplet in accord with equation (6.30)), the following lists the corresponding $b^{(E,X)}$ functions and states the localisation outcome. The latter is either "localised as left-handed (LH) zero-mode" or "localised as right-handed (RH) zero-mode" or "delocalised". We have

$$\mathbf{1}(4,0): \quad \frac{1}{3}f_E \qquad \text{localised LH}\,, \tag{6.61a}$$

$$\mathbf{5}(-2,2): \quad \frac{1}{2}\left(\frac{1}{\sqrt{15}}f_X - \frac{1}{3}f_E\right) \qquad \text{localised RH}\,, \tag{6.61b}$$

$$\mathbf{5}^*(-2,-2): \quad -\frac{1}{2}\left(\frac{1}{\sqrt{15}}f_X + \frac{1}{3}f_E\right) \qquad \text{delocalised}\,, \tag{6.61c}$$

$$\mathbf{1}(1,-5): \quad \frac{1}{4}\left(-\frac{5}{\sqrt{15}}f_X + \frac{1}{3}f_E\right) \qquad \text{localised LH}\,, \tag{6.61d}$$

$$\mathbf{5}^*(1,3): \quad \frac{1}{4}\left(\frac{3}{\sqrt{15}}f_X + \frac{1}{3}f_E\right) \qquad \text{delocalised}\,, \tag{6.61e}$$

$$\mathbf{10}(1,-1): \quad \frac{1}{4}\left(-\frac{1}{\sqrt{15}}f_X + \frac{1}{3}f_E\right) \qquad \text{localised LH}\,. \tag{6.61f}$$

The two $\mathbf{5}^*$'s are delocalised because the associated field never goes through zero. The **5** and the **10** are localised at $w = 0$ with opposite chiralities because their background fields are kink-like and anti-kink-like, respectively.

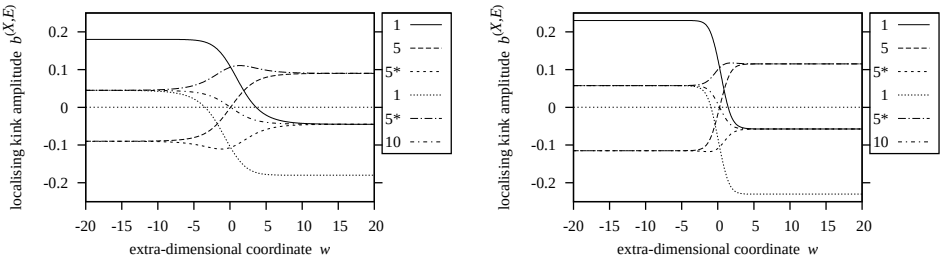

Figure 6.10: Clash-of-symmetries fermion localising profiles interpolating between $(10, +)$ at $w = -\infty$ and $(10', -)$ at $w = +\infty$. These profiles correspond to the kink backgrounds displayed in Figure 6.6. The top to bottom order of the SU(5) fermion multiplets in the key to the right of the plots matches the order in equation (6.61). The parameters used in the left plot are $\kappa = 0.2$, $\lambda_1 = 1.5$, $\lambda_2 = 0$, $\lambda_3 = 22.0$; those in the right plot are $\kappa = 0.8$, $\lambda_1 = 1.0$, $\lambda_2 = 0$, $\lambda_3 = 22.0$.

The two singlets are localised at non-zero w values, so the overall spectrum is "split". Refer to Figure 6.10.

This is a remarkable outcome for two reasons. First, because the **5** is localised with right-handed chirality, it is equivalent to a left-handed-localised $\mathbf{5}^*$. Thus the localised spectrum consists of left-handed zero-modes in the SU(5) representation

$$\mathbf{5}^* \oplus \mathbf{10} \oplus \mathbf{1} \oplus \mathbf{1} \,. \tag{6.62}$$

In other words we have one standard generation of fermions plus two singlet neutrinos. Second, apart from the extra singlet, all the exotic fermions in the **27** of E_6 are delocalised and thus do not feature in the effective four-dimensional theory on the brane. These benign outcomes depend crucially on the boundary condition choice embodied by the clash-of-symmetries domain-wall solution, including the $\mathbb{Z}_2$ minus sign.

There is an amusing aspect to this spectrum. It resembles a usual SO(10) family plus an extra singlet. However, the left-handed $\mathbf{5}^*$, which is obtained from a five-dimensional **5**, and the **10** do not come from a **16** of either SO(10) or SO(10)′.

At this point we are done with the initial analysis of our E_6 model. It is beyond the scope of this chapter, and this thesis, to search for a stable SU(5)-inducing kink background and to construct a proper realisation of the standard model, although such things would be of great interest to explore.

6.5 Conclusion

We find it extremely encouraging that our attempt to construct an E_6 invariant domain-wall brane model has lead, with only the minimal of ingredients, to the beginnings of a realistic set-up. Only a single background scalar field χ, in the adjoint of E_6, is required to form the domain wall, implement the Dvali-Shifman mechanism and localise SU(5) gauge bosons, and further localise the correct fermion spectrum. Unfortunately, these promising features of our set-up are marred by our inability to find a stable kink background configuration, but we remain optimistic that one can find a suitable Higgs potential which supports a stable solution.

The clash-of-symmetries played an integral role in out set-up, and we gave a detailed exposition of it in Section 6.1. We pointed out that there exists a general connection between the clash-of-symmetries mechanism and the Dvali-Shifman mechanism, since, in the former case, one generically has a smaller symmetry group "sandwiched" between two larger groups, which is exactly the kind of configuration needed to implement Dvali-Shifman gauge-boson localisation.

In trying to extend our SU(5) model of Chapter 5, we first looked, in Section 6.2, at having an SO(10) invariant action, breaking to U(5) in the bulk. Such a set-up did not lead to a phenomenologically-realistic symmetry group on the brane, hence the need to consider the larger group E_6. Before we could attempt to construct the E_6 model, we needed to first analyse the structure of the invariants I_n. Section 6.3 was devoted to such a study, and we discovered a truly remarkable "rearrangement property": the diagonal generators of E_6 explicitly tell you the exact coefficients needed to form linear combinations of the same generators which yield the first generator with rearranged diagonal entries. Such a fact can be used to find all twenty-seven embeddings of $SO(10) \otimes U(1)$ in E_6. A full analysis of all the independent invariants was performed, and we discussed how to engineer a Higgs potential which exploits these differently embedded subgroups.

Section 6.4 relied on these findings and used two such embeddings, along with their negative $\mathbb{Z}_2$ partners, to implement the clash-of-symmetries mechanism in an E_6 setting. The adjoint χ broke E_6 to $SO(10) \otimes U(1)_E$ on one side of the domain wall, and broke to $SO(10)' \otimes U(1)_{E'}$ on the other side; these groups are isomorphic, but embedded differently in E_6. Via the

clash-of-symmetries, the intersection of these groups, being $SU(5) \otimes U(1)^2$, is the symmetry on the brane. Because the brane-localised SU(5) is contained in both SO(10) and SO(10)′, which are confining groups, the gauge bosons associated with SU(5) are localised to the domain-wall region by the Dvali-Shifman argument. We also found kink configurations which have $SO(8) \otimes U(1)^2$ as the symmetry on the brane, this group being the intersection of two other, differently embedded $SO(10) \otimes U(1)$ subgroups. For the Higgs potential that we analysed, this set-up is the energetically favourable one, but since it has SO(8) gauge bosons confined to the domain-wall region, it is unsuitable for model building purposes. We hope that a different form of the Higgs potential for χ will allow for a stable SU(5)-brane configuration.

If such a stable kink can be found, it opens up the possibility of constructing a grand-unified-theory dynamically localised to a brane in an infinite extra-dimension. As a step towards such a model, we looked at the coupling of a five-dimensional fermion, in the **27** of E_6, to the domain-wall background. This minimal construction produced a realistic spectrum of localised fermion zero-modes, which is a non-trivial outcome.

To complete a realistic model one needs to add gravity, in the form of the Randall-Sundrum warped metric, which is expected to be a straightforward exercise. One also needs to to arrange for the additional spontaneous symmetry breaking cascade $SU(5) \otimes U(1)^2 \to SU(3) \otimes SU(2) \otimes U(1)_Y \to SU(3) \otimes U(1)_Q$. To achieve this, suitable additional Higgs multiplets need to be introduced, and their background field configurations have to be nonzero inside the domain wall to trigger the additional spontaneous symmetry breaking. This is in direct analogy with the breaking of electroweak symmetry on the brane in the SU(5) model of Chapter 5. There, the localised electroweak doublet is arranged to have an effective four-dimensional tachyonic mass, and a similar set-up seems feasible for the E_6 model.

In constructing a realistic E_6 model, it would be of great interest to find the minimal model, minimal in the field content as well as minimal in the number of parameters. While this is certainly a valid path to take next — we even have all the necessary tools at our fingertips — we are not going to attempt such E_6 model building in this thesis. Instead, we shall change tack to a direction of study that is just as important as particle physics and model building. The next chapter rounds out this thesis by studying the cosmology of domain-wall branes.

Chapter 7

Cosmology of domain-wall branes

Now that we have dealt with the core model building and particle physics aspects of domain-wall brane models, we move on to consider their cosmological properties. While it is necessary to have a given model agree with particle physics experiments, one must also take into account early universe cosmology, as there exist direct links between this early era and the behaviour of particles at the fundamental level. These links have been exploited in the past decades — most notably by the measurement of the cosmic microwave background — to provide a new window into the inner workings of nature, and to provide extra data to confirm, or rule out, models of cosmology and particle physics.

The domain-wall brane models that we have constructed in this thesis are particularly vulnerable to cosmological constraints because the early universe was hot enough to probe the physics of the extra dimension. In this chapter we show how to define a consistent domain-wall brane cosmology that provides one with the theoretical tools necessary for analysing the modifications to standard cosmology due to a brane dynamically generated by a scalar field. The usual Friedmann, Lemaître, Robertson-Walker (FLRW) metric (see Section 1.4 for a review) is recovered in the region of the brane, but, remarkably, with an effective scale factor $a_{\text{eff}}(t)$ that depends on particle energy and on particle species. As a consequence, domain-wall brane models generically predict a breakdown of the weak equivalence principle on sufficiently small scales. This unusual effect comes from the extended na-

ture of particles confined to a domain-wall brane — their extra-dimensional profiles have non-zero width — and the fact that they feel an "average" of the bulk spacetime. We demonstrate how to recover the standard results of fundamental brane cosmology in the infinitely-thin domain-wall limit, and comment on how our results have the potential to place bounds on parameters such as the thickness of domain-wall branes.

As discussed in Section 1.5, the cosmology of brane-world models where the brane is an infinitely-thin, fundamental entity has a history which is entwined with the discovery of the Randall-Sundrum warped metric. The main outcome of such studies was the deviation of brane-world cosmology from the standard cosmology at temperatures above a particular *normalcy temperature*. See the initial series of papers [93, 101, 102, 105], and also [103, 106]. More in line with the topic of the current thesis, the cosmology of thick fundamental branes has also been analysed [104, 121]. Here, the underlying nature of a fundamental brane was generically modelled as a small but finite width, and effective four-dimensional quantities were obtained by averaging their corresponding five-dimensional quantities over the width of the brane. This produced corrections to the cosmology of the infinitely-thin brane. For the case at hand, where the brane is modelled by a scalar field, this averaging procedure yields, heuristically, a weighted average. The effective four-dimensional scale factor for a given field is computed by "averaging" the five-dimensional metric components, with a weight given by the extra-dimensional profile of the associated field. As we shall see, this leads to some interesting and unexpected features.

The structure of this chapter is as follows. In Section 7.1 we review the relevant points of fundamental brane cosmology, where the FLRW metric ansatz is extended to five-dimensions and the corrections to the usual Friedmann equation are derived. We then discuss in Section 7.2 how one can define a sensible cosmological metric for a dynamically generated domain-wall brane. This is followed by the derivation of the effective, four-dimensional cosmological metrics that are experienced by confined scalar and fermion fields. The effective scale factor can be identified from such a metric. In Section 7.3 we verify that our results reproduce those of fundamental-brane cosmology in the thin wall limit, and we then conclude in Section 7.4.

7.1 Fundamental-brane cosmology

In this section we summarise previous results for the cosmological evolution of a fundamental brane with localised sources (see [93, 101, 105] for details, and [231] for an extension to higher codimension). The idea is to take a five-dimensional bulk spacetime, include brane, bulk and brane-localised stress-energy sources, and solve the five-dimensional Einstein equations. The brane is considered to be a fundamental object and is modelled by a delta distribution, with the total action being

$$\mathcal{S} = \int d^5x\sqrt{-g}\; M_*^3(R - 2\Lambda) \; + \int d^5x\sqrt{-g_{\rm brane}}\; \delta(w)\mathcal{L}_{\rm brane}\;, \qquad (7.1)$$

where M_* is the five-dimensional gravitational mass scale, Λ is the bulk cosmological constant and g and $g_{\rm brane}$ are the determinants of the metric in the bulk and on the brane respectively. The delta-function localises $\mathcal{L}_{\rm brane}$ to the brane, which includes the brane tension and standard model fields. In this chapter we are using the space-like metric of Section A.3.

Since we are interested in cosmological solutions, we consider sources that are homogeneous and isotropic in the three spatial dimensions. The most general metric consistent with these symmetries is

$$ds_5^2 = -n^2(t,w)dt^2 + a^2(t,w)\gamma_{ij}dx^i dx^j + b^2(t,w)dw^2\;, \qquad (7.2)$$

where i, j run over the three spatial dimensions, and γ_{ij} is the metric of the three-space, which may be positively curved, flat or negatively curved. Note that it is possible to make a change of coordinates of the t-w subspace so as to reduce the two metric functions n and b to a single function, say $\hat{n}$, to obtain the sub-line-element $\hat{n}(\hat{t},\hat{w})(-d\hat{t}^2 + d\hat{w}^2)$. This is not a useful set of coordinates to use for the problem at hand, so we stick with our original ansatz.

Einstein's equations are

$$G_{MN} \equiv R_{MN} - \frac{1}{2}g_{MN}R = \frac{1}{2M_*^3}T_{MN} - g_{MN}\Lambda\;, \qquad (7.3)$$

where M, N are five-dimensional indices. The brane tension and brane-localised sources are represented jointly by the four-dimensional density ρ_b

and pressure p_b and appear in the stress-energy tensor as

$$T^M{}_N = \delta(by)\,\mathrm{diag}(-\rho_b, p_b, p_b, p_b, 0)\,. \tag{7.4}$$

For the case of the metric ansatz given by equation (7.2), the non-zero components of the Einstein tensor read

$$G_{00} = 3\left[\frac{\dot{a}}{a}\left(\frac{\dot{a}}{a}+\frac{\dot{b}}{b}\right) - \frac{n^2}{b^2}\left(\frac{a''}{a}+\frac{a'}{a}\left(\frac{a'}{a}-\frac{b'}{b}\right)\right)\right]\,, \tag{7.5a}$$

$$\begin{aligned} G_{ij} = {}& \gamma_{ij}\frac{a^2}{b^2}\left[\frac{a'}{a}\left(\frac{a'}{a}+2\frac{n'}{n}\right) - \frac{b'}{b}\left(\frac{n'}{n}+2\frac{a'}{a}\right) + 2\frac{a''}{a}+\frac{n''}{n}\right] \\ & + \gamma_{ij}\frac{a^2}{n^2}\left[\frac{\dot{a}}{a}\left(-\frac{\dot{a}}{a}+2\frac{\dot{n}}{n}\right) - 2\frac{\ddot{a}}{a} + \frac{\dot{b}}{b}\left(-2\frac{\dot{a}}{a}+\frac{\dot{n}}{n}\right) - \frac{\ddot{b}}{b}\right]\,, \end{aligned} \tag{7.5b}$$

$$G_{05} = 3\left(\frac{n'}{n}\frac{\dot{a}}{a}+\frac{a'}{a}\frac{\dot{b}}{b}-\frac{\dot{a}'}{a}\right)\,, \tag{7.5c}$$

$$G_{55} = 3\left[\frac{a'}{a}\left(\frac{a'}{a}+\frac{n'}{n}\right) - \frac{b^2}{n^2}\left(\frac{\dot{a}}{a}\left(\frac{\dot{a}}{a}-\frac{\dot{n}}{n}\right)+\frac{\ddot{a}}{a}\right)\right]\,. \tag{7.5d}$$

Here, the indices 0 and 5 correspond to t and w respectively, a dot denotes a derivative with respect to t, and a prime with respect to w.

For general values of Λ, ρ_b and p_b, Einstein's equations will yield time-dependent solutions, corresponding, for example, to an expanding spacetime on the brane. Before exploring such solutions, we note that it is possible to fine tune the sources to produce a time-independent background. This corresponds exactly to the scenario of Randall and Sundrum [94, 95] who demonstrated that gravity is localised to a fundamental brane tuned in such a way.

The specific choice necessary is that the brane source be pure tension (corresponding to a four-dimensional cosmological constant) $\rho_b = -p_b = \sigma$, tuned against the bulk cosmological constant according to

$$\sigma = \sqrt{-24M_*^6\Lambda}\,. \tag{7.6}$$

Note that this implies that the bulk geometry must be five-dimensional Anti-de Sitter space AdS_5, with $\Lambda < 0$. The corresponding metric solution is then

$$ds_5^2 = e^{-2\mu|w|}(-dt^2 + \gamma_{ij}dx^i dx^j) + dw^2\,, \tag{7.7}$$

where

$$\mu \equiv \sqrt{\frac{-\Lambda}{6}} = \frac{\sigma}{12M_*^3} \,. \tag{7.8}$$

Moving back to the general time-dependent case, one solves the five-dimensional version of Einstein's equations by imposing the Israel matching conditions — calculating the discontinuities in the derivatives of the metric components across $w = 0$, and relating these to the delta-distribution sources (see [93]). It turns out that the behaviours of ρ_b, p_b and the metric components evaluated at $w = 0$ are independent of the metric solutions in the bulk, and obey

$$\dot{\rho}_b + 3H_0(\rho_b + p_b) = 0 \,, \tag{7.9a}$$

$$H_0^2 = \frac{\rho_b^2}{144M_*^6} + \frac{\Lambda}{6} - \frac{k}{a_0^2} + \frac{\mathcal{C}}{a_0^4} \,, \tag{7.9b}$$

where the parameter k takes values $+1, 0, -1$ according to whether the metric γ_{ij} describes positively-curved, flat, or negatively-curved spatial three-sections. Time has been rescaled such that $n_0(t) \equiv n(t, w = 0) = 1$. The integration constant $\mathcal{C}$ represents an effective radiation term, or so-called "dark radiation" (see [105] for bounds on this term from nucleosynthesis), and for simplicity we set $\mathcal{C} = 0$ from now on.

The effective four-dimensional scale factor a_0 is the five-dimensional metric component $a(t, w)$ evaluated on the brane $a_0(t) \equiv a(t, w = 0)$ and H_0 is the corresponding Hubble parameter. Equation (7.9a) describes the usual four-dimensional conservation of energy on the brane (the continuity equation) and equation (7.9b) is the modified Friedmann equation. Due to the proportionality $H_0 \sim \rho_b$ instead of the usual $H_0 \sim \sqrt{\rho_b}$, this Friedmann equation seems at odds with observation. The clue to fixing this problem comes from considering the time-independent Randall-Sundrum solution, where the brane tension contributed an energy that exactly cancelled the bulk cosmological constant. Guided by this, one writes the total brane source ρ_b, p_b as a sum of a background brane tension σ and some other general brane source ρ, p; namely

$$\rho_b = \sigma + \rho \,, \tag{7.10}$$

$$p_b = -\sigma + p \,, \tag{7.11}$$

where σ is defined as in (7.6). The effective Friedmann equation for a_0 now reads

$$H_0^2 = \frac{\sigma}{72M_*^6}\rho + \frac{1}{144M_*^6}\rho^2 - \frac{k}{a_0^2}\,. \tag{7.12}$$

If we assume ρ is small compared to σ, then the ρ^2 term gives small corrections to the usual behaviour and the evolution of a_0 is driven to first order by ρ, with the proportionality constant playing the role of the effective Planck mass via

$$M_{\rm Pl}^2 \equiv \frac{12M_*^6}{\sigma} = \frac{6M_*^3}{\sqrt{-6\Lambda}}\,. \tag{7.13}$$

An important feature of cosmology in codimension-one brane-worlds is that this entire analysis is independent of the behaviour of the metric components in the bulk. Nevertheless, it is possible to find bulk solutions, and since we will make use of them in a later section we provide them here. For $\mathcal{C} = 0$ they read [105, 122]

$$n(t,w) = e^{-\mu|w|} - \tilde{\epsilon}\sinh(\mu|w|)\,, \tag{7.14a}$$

$$a(t,w) = a_0(t)[e^{-\mu|w|} - \epsilon\sinh(\mu|w|)]\,, \tag{7.14b}$$

$$b(t,w) = 1\,, \tag{7.14c}$$

with μ defined as in (7.8) and

$$\epsilon \equiv \frac{\rho}{\sigma}\,, \tag{7.15a}$$

$$\tilde{\epsilon} \equiv \epsilon + \frac{\dot{\epsilon}}{H_0}\,. \tag{7.15b}$$

Note that for $\epsilon = 0$ and $k = 0$ we recover the RS warped-metric solution given by equation (7.7).

The parameter ϵ measures the energy density in matter and radiation, relative to the tension of the brane. In terms of this parameter, the Friedmann equation (7.12) is

$$H_0^2 = \frac{1}{6M_{\rm Pl}^2}\left(1 + \frac{\epsilon}{2}\right)\rho - \frac{k}{a_0^2}\,, \tag{7.16}$$

demonstrating that $\epsilon \ll 1$ is required to recover conventional cosmology. The earliest direct evidence for our standard cosmological evolution is provided by primordial (big bang) nucleosynthesis (BBN), which takes place

at temperatures of order an MeV. Therefore, we are safe from cosmological constraints if we choose $\sigma \gg (1\text{MeV})^4$.

Finally, we briefly discuss the extension of these results to fundamental branes with finite thickness [104, 121]. In these scenarios the brane and brane-localised sources are modelled as stress-energies distributed over the finite thickness of the brane. The effective four-dimensional quantities, such as the scale factor, energy density and pressure, are defined to be the spatial average, over the extent of the brane in the extra dimension, of their corresponding five-dimensional quantities. One then rewrites Einstein's equations in terms of these averaged quantities and identifies corrections to the infinitely-thin brane scenario. This averaging prescription is an important first step in understanding cosmology away from the infinitely-thin brane limit. However, a more complete treatment is essential, since, for example, in the Minkowski domain-wall set-up, one needs to expand the five-dimensional fields in KK modes and integrate over the full extent of the extra dimension. The rest of this chapter is devoted to the development of a more complete averaging framework, within which it is possible to analyse the cosmology of domain-wall brane scenarios.

7.2 The extension to a domain-wall brane

Our main goal in this chapter is to extend the analysis of the previous section to the case in which the brane is topological defect – a domain wall generated by a scalar field. The central problem is how to identify the effective four-dimensional scale factor (the analogue of a_0) and the equations that describe its time evolution. As we shall see, this question turns out to have an interesting and nontrivial resolution, which may have specific implications for the signatures of such field-theoretic brane-worlds.

As exemplified in Chapter 4, the creation of a domain-wall brane coupled to gravity is quite straightforward, and we shall follow closely the construction from said chapter. Beginning with a scalar field χ and a suitable potential, boundary conditions are chosen so that χ develops a kink-like profile, which can be thought of as a w-dependent vacuum expectation value. As $w \to \pm\infty$, the value of χ approaches vacuum and its energy density rapidly approaches zero. However, due to the topology of the vacuum (in general a discrete symmetry is required), a domain wall forms around $w = 0$.

The combination of gradient and vacuum energy in the core of this object plays an analogous role to the brane tension σ in the fundamental case of the previous section. The shape of the distribution of stress-energy due to the w-dependent profile of χ is a smooth version of the fundamental delta-function brane. In the non-cosmological case, that is when one seeks the Minkowski metric on the brane, the solution for the metric then yields a correspondingly smooth version of the $e^{-\mu|w|}$ warp factor in (7.7).

Because this domain-wall brane is extended in the extra-dimension w, any fields that were previously brane-localised by the delta function are no longer strictly located at $w = 0$. Rather, such fields (typically the standard model fields) must first be written as full five-dimensional fields, which are coupled to χ in such a way as to produce a Kaluza-Klein tower of four-dimensional fields on the domain wall. Such a procedure was detailed in Chapter 3 for the case of a Minkowski brane. We saw there that the ground state profile of the four-dimensional tower has a Gaussian like shape which, when squared,[1] reduces to a delta-distribution in the limit of an infinitely-thin domain wall.

Here we are interested in the more general cosmological case. Our objective is to understand the effective four-dimensional metric on such a domain-wall brane and how the localised fields propagate in that spacetime. In the fundamental-brane case, four-dimensional fields are located at exactly $w = 0$ and have no w degrees of freedom. The four-dimensional metric they feel is thus just the five-dimensional metric evaluated at $w = 0$, and for the RS metric (7.7) this slice is just four-dimensional Minkowski spacetime. For the cosmological metric (7.2) the slice at $w = 0$ has the form

$$ds^2 = -n^2(t, w = 0)dt^2 + a^2(t, w = 0)\gamma_{ij}dx^i dx^j \, . \tag{7.17}$$

By scaling t such that $n(t, w = 0) = 1$, it is clear that the effective four-dimensional metric is of the FLRW form, with the effective scale factor defined by $a_{\text{eff}}(t) = a_0(t) \equiv a(t, w = 0)$. The solutions to the five-dimensional Einstein equations given in the previous section then describe how a_{eff} evolves, and hence describe the spacetime in which the localised fields propagate. In this fundamental-brane scenario, each field has the same time (with the same normalisation) and feels the same scale factor, and so it is sensi-

[1] The squaring of the extra-dimensional profile comes from the normalisation of the kinetic term, which is quadratic in the field, hence quadratic in the profile.

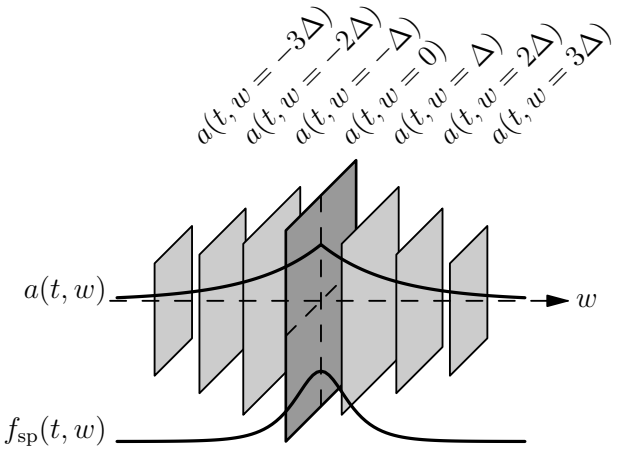

Figure 7.1: A schematic representation of "dimensional parallax" for a species of particle with extra-dimensional profile $f_{\rm sp}(t, w)$. The four-dimensional particle associated with this profile experiences a weighted average of the scale factor $a(t, w)$, the latter of which depends on the extra-dimension w. Different species will generally have different profiles, and thus feel a different effective scale factor.

ble to say that the effective four-dimensional metric is unique and defined by (7.17).

For the domain-wall brane scenario things are quite different and, as we demonstrate explicitly below, we are led to abandon the question "what is the effective scale factor on the brane?", and allow that *different fields may propagate in different spacetimes*. The essential reason for this comes from the extended nature of the profiles, as the associated fields are now sensitive to the metric around $w = 0$, not just the slice exactly at $w = 0$. Since the cosmological evolution of the slices in the vicinity of the brane are misaligned (they expand at different rates), there is a kind of "dimensional parallax" effect, whereby different species of particle are subject to a different averaging (they have a different perspective) of the slices. Figure 7.1 displays a schematic representation of this effect for a generic extra-dimensional profile $f_{\rm sp}(t, w)$. We shall explain in the following subsection why such a profile depends on time.

Note that for the Minkowski domain-wall brane with a smoothed-out version of the RS metric (7.7), things are much simpler because each four-dimensional slice is proportional to Minkowski spacetime. Therefore, the Minkowski part essentially factorises out of the averaging integral and each field feels the same spacetime.

The analysis in Section 7.1 determined the effective scale factor a_0 in the case of a general brane-localised source parameterised by ρ and p. For the domain-wall brane scenario, we need to look at the sources from the more fundamental level of classical fields. The general strategy is to identify the kinetic term in the action for the relevant field, integrate out the extra dimension w, and then to match the resulting four-dimensional effective action to the canonical four-dimensional action for such a field in an FLRW background.

7.2.1 A localised scalar field

We begin by considering a scalar field, turning to fermions in the next subsection. We take the five-dimensional metric given by equation (7.2) and a five-dimensional scalar field $\Phi(t, x^i, w)$ separated, for reasons we shall expand on below, as $\Phi(t, x^i, w) = f(t, w)\phi(t, x^i)$. The objective is to determine the effective four-dimensional spacetime on which the relevant four-dimensional field ϕ propagates.

The action for a five-dimensional scalar $\Phi(t, x^i, w)$ with metric g_{MN} is

$$\mathcal{S}_5 = \int d^5x\, \sqrt{g} \left[-\frac{1}{2} g^{MN} \partial_M \Phi \partial_N \Phi - U(\Phi) \right] , \tag{7.18}$$

where the potential U may contain couplings of Φ to the domain-wall field (to localise Φ) or couplings to other fields. Using the metric ansatz (7.2) we then obtain

$$\begin{aligned} \mathcal{S}_5 = \int d^5x\, & na^3 b\sqrt{\gamma} \times \\ & \left[-\frac{1}{2} \big(- n^{-2}\dot{\Phi}^2 + a^{-2}\gamma^{ij}\partial_i\Phi\, \partial_j\Phi + b^{-2}(\partial_w\Phi)^2 \big) - U(\Phi) \right] . \end{aligned} \tag{7.19}$$

By analogy with the flat case, our first instinct might be to separate variables by writing $\Phi(t, x^i, w) = \sum_n f_n(t, w)\pi_n(x^i)$. However, in the case of a time-dependent metric such an expansion makes it difficult to identify a four-dimensional scalar field, since the time dependence of, for example, a four-dimensional plane wave, is consumed by the profile f_n, and π becomes merely a static spatial wave. The next obvious suggestion is to instead write $\Phi(t, x^i, w) = \sum_n f_n(w)\phi_n(t, x^i)$, so that ϕ_n can be identified as a four-dimensional Kaluza-Klein mode with extra-dimensional profile f_n. Here

however, we encounter a different problem, namely that the time variation of the metric components implies that the extra-dimensional profile will in general change with time.

We overcome these obstacles by noting that there are really two time scales in the problem: the cosmological time scale of the evolution of the background metric, and the time scale associated with particle physics processes. With this in mind, we consider the following separation of variables

$$\Phi(t, x^i, w) = \sum_n f_n(t, w)\phi_n(t, x^i) \,. \tag{7.20}$$

The possible ambiguity in the time dependence (whether it appears in f_n or ϕ_n) is resolved by the requirement that ϕ_n satisfies the four-dimensional Euler-Lagrange equation, which shall be specified below. In order for ϕ_n to be identified as a propagating four-dimensional field, it must also carry the majority of the time dependence, hence we impose the condition $\dot{f}_n/f_n \ll \dot{\phi}_n/\phi_n$. These requirements formally identify the class of solutions for f_n that we are allowing.

One should consider this prescription a separation of scales, rather than a strict separation of variables. Quantitatively, $\dot{\phi}_n/\phi_n \sim E$ where E is the energy of the particle, and $\dot{f}_n/f_n \sim H$ where H is the Hubble constant. In natural units we have $H \sim 10^{-32}$eV, which is tiny compared to the typical energy of a particle. In what follows, we therefore neglect all time derivatives of f_n and of the metric components n, a and b, since they are much smaller than the other terms in the action.

From now on we focus on a single mode of the KK tower and drop the subscript n. Then, with the prescription (7.20) and the assumptions regarding small time-derivatives, the action (7.19) becomes

$$\begin{aligned}\mathcal{S}_5 = \int d^4x\sqrt{\gamma}\int dw \,\times \\ \left[-\frac{1}{2}\left(-\frac{a^3 b}{n}f^2\dot{\phi}^2 + nabf^2\gamma^{ij}\partial_i\phi\,\partial_j\phi + \frac{na^3}{b}f'^2\phi^2\right) - na^3 bU\right] \,.\end{aligned} \tag{7.21}$$

The third term, proportional to ϕ^2, will contribute to the potential U. Integrating over the extra-dimension yields the four-dimensional effective action

$$\mathcal{S}_4 = \int d^4x\sqrt{\gamma}\left[-\frac{1}{2}\left(-F(t)\dot{\phi}^2 + G(t)\gamma^{ij}\partial_i\phi\partial_j\phi\right) + \ldots\right] \,, \tag{7.22}$$

where we have written only the kinetic terms explicitly, and defined

$$F(t) \equiv \int f^2 \frac{a^3 b}{n}\, dw\,, \qquad\qquad G(t) \equiv \int f^2 nab\, dw\,. \tag{7.23}$$

The action (7.22) is almost what we are looking for, but what remains is to correctly identify the four-dimensional line element describing the space-time within which ϕ propagates. To do this, we match to the prototype line element

$$ds_4^2 = -T^2(t)dt^2 + X^2(t)\gamma_{ij}dx^i dx^j\,, \tag{7.24}$$

and the corresponding prototype action

$$\mathcal{S}_4^{(\mathrm{proto})} = \int d^4x\, T(t)X^3(t)\sqrt{\gamma}\, \left[-\frac{1}{2}\left(-T^{-2}(t)\dot{\phi}^2 + X^{-2}(t)\gamma^{ij}\partial_i\phi\partial_j\phi\right)\right]. \tag{7.25}$$

Here, we are again just focusing on the kinetic and gradient terms. Matching the effective action (7.22) with the four-dimensional prototype (7.25) we then obtain

$$F(t) = T^{-1}(t)X^3(t)\,, \qquad\qquad G(t) = T(t)X(t)\,. \tag{7.26}$$

Solving for $T(t)$ and $X(t)$ gives

$$T(t) = F^{-1/4}(t)G^{3/4}(t) = \left(\int f^2 \frac{a^3 b}{n}\, dw\right)^{-1/4} \left(\int f^2 nab\, dw\right)^{3/4}\,, \tag{7.27a}$$

$$X(t) = F^{1/4}(t)G^{1/4}(t) = \left(\int f^2 \frac{a^3 b}{n}\, dw\right)^{1/4} \left(\int f^2 nab\, dw\right)^{1/4}\,. \tag{7.27b}$$

The time-dependent functions $T(t)$ and $X(t)$ define, along with (7.24), the effective four-dimensional line element followed by the field ϕ. As we shall soon demonstrate, we are free to rescale f by an arbitrary (slowly varying) function of time, and we can use this freedom to fix $T = 1$. This corresponds to choosing a canonical time coordinate. The scale factor for ϕ is then precisely

$$a_\phi(t) = X(t)\,. \tag{7.28}$$

Notice that the temporal behaviour of $X(t)$ (and hence a_ϕ) is inherited from the time-dependence of the metric components and possibly $f(t, w)$, all of which are taken to be slowly varying.

This result for the effective scale factor immediately raises two important points. The first is that scalar modes with different profile functions will have different definitions of the scale factor a_ϕ. Thus, it is not possible to define a unique scale factor for this four-dimensional effective theory. Instead, each four-dimensional scalar field, whether it arises from a different five-dimensional field, or is merely a different KK mode of the same five-dimensional field, propagates according to a different effective four-dimensional metric.

The second interesting point is that the procedure above will yield a different result for a fermionic field (and also other spin fields) due to the difference arising from the spin connection in the kinetic term. We will follow this point up in the next section where we explicitly perform the relevant calculation for a fermion.

As a consistency check, we consider equation (7.27) in the limit of an infinitely-thin domain wall. In such a limit, the square of a typical ground state profile f becomes proportional to a delta-function distribution: $f^2 \to \delta(bw)$. This comes from the kinetic term for ϕ, which is quadratic in f, and must be normalised such that, in the thin brane limit, $\int f^2 d(bw) = 1$. The integrals for $T(t)$ and $X(t)$ can then be performed analytically yielding $T(t) = n(t, w = 0)$ and $X(t) = a(t, w = 0)$. These coincide with the fundamental brane case, in which the four-dimensional metric is the five-dimensional metric evaluated on the brane.

A further check on our derivation can be made by looking at the separable (but less general) version of the cosmological metric, given by

$$ds_5^2 = c^2(w)[-dt^2 + \hat{a}^2(t)\gamma_{ij}dx^i dx^j] + \hat{b}^2(w)dw^2 \,. \tag{7.29}$$

This ansatz allows for AdS_4 and dS_4 brane solutions, as detailed in [118, 108, 165, 175, 232, 112, 211, 182]. The effective four-dimensional metric for ϕ then has $T(t) = (\int f^2 c^2 \hat{b}\, dw)^{1/2}$ and $X(t) = \hat{a}(t)(\int f^2 c^2 \hat{b}\, dw)^{1/2}$. Note that T is constant (f will be time-independent; see later) and we can normalise f to make $T = 1$, and then find that $X(t) = \hat{a}(t)$. In this case we again recover the known result, namely that all fields on the brane feel the same metric.

To complete this formal analysis of Φ we determine the differential equation satisfied by the profile function $f(t, w)$. Our definitions above for the

separation of scales ensure that ϕ behaves as a four-dimensional scalar field in a spacetime characterised by $T(t)$ and $X(t)$. This means that ϕ will satisfy the Euler-Lagrange equation

$$-\frac{1}{T^2}\ddot{\phi}+\frac{1}{X^2}\gamma^{ij}\left(\partial_i\partial_j\phi-\Gamma^{(3)\,k}_{\;\;ij}\partial_k\phi\right)=m^2\phi\,, \tag{7.30}$$

where $\Gamma^{(3)\,k}_{\;\;ij}$ are the connection coefficients associated with the 3-space metric γ_{ij} and m is the effective four-dimensional mass of ϕ. The parenthesised term on the left hand side is simply the double covariant-derivative of ϕ with respect to γ_{ij}. Note that we are ignoring time derivatives of $T(t)$ and $X(t)$, which are much smaller that the derivatives of ϕ.

Now consider the five-dimensional Euler-Lagrange equation for Φ:

$$g^{MN}\left(\partial_M\partial_N\Phi-\Gamma^{(5)\,P}_{\;\;MN}\partial_P\Phi\right)=\frac{\partial U}{\partial\Phi}\,, \tag{7.31}$$

where $\Gamma^{(5)\,P}_{\;\;MN}$ are the five-dimensional connection coefficients. We first separate variables, neglect time derivatives of n, a, b and f, and use equation (7.30) to eliminate the spatial derivatives of ϕ (thus the four-dimensional mass will appear). We then linearise the equation, yielding

$$\left[f''+\left(\frac{n'}{n}+\frac{3a'}{a}-\frac{b'}{b}\right)f'+b^2\left(m^2\frac{X^2}{a^2}-U^{(1)}\right)f\right]\phi \\ +\frac{b^2}{a^2}\left(\frac{X^2}{T^2}-\frac{a^2}{n^2}\right)f\ddot{\phi}=0\,, \tag{7.32}$$

where $U^{(1)}$ is defined by $\partial U/\partial\Phi=U^{(1)}\Phi+\mathcal{O}(\Phi^2)$. Notice the appearance of the $\ddot{\phi}$ term, which is absent when we specialise to Minkowski spacetime on the brane. There are two reasons for this. First, there is a mismatch between the five-dimensional ratio of the time and three-space metric factors, and the corresponding effective four-dimensional ratio; $a^2/n^2\neq X^2/T^2$. For a Minkowski brane these ratios are equal because each four-dimensional slice of the five-dimensional metric is proportional to Minkowski spacetime. Second, we have employed a separation of scales rather than the usual separation of variables (which did not work in this setting). This $\ddot{\phi}$ term then quantifies the *inability of the domain-wall brane to localise proper four-dimensional effective fields*, at least in a cosmological background.

To proceed, we need to eliminate the ϕ and $\ddot{\phi}$ factors so that we have an

equation that can, at least in principle, be used to solve for f. To this end we solve the four-dimensional Euler-Lagrange equation (7.30) (in flat space; $k = 0$) and find "plane waves" of the form

$$\phi(t, x^i) \propto \exp(-iT^2Et + iX^2\gamma_{ij}p^ix^j) \,, \tag{7.33}$$

where E is the energy of the wave, p^i is its momentum, and $T^2E^2 = X^2\gamma_{ij}p^ip^j + m^2$. Then $\ddot{\phi} = -E^2T^4\phi$, and equation (7.32) becomes

$$f'' + \left(\frac{n'}{n} + \frac{3a'}{a} - \frac{b'}{b}\right) f' + b^2 \left[m^2\frac{X^2}{a^2} - U^{(1)} - \frac{E^2T^4}{a^2}\left(\frac{X^2}{T^2} - \frac{a^2}{n^2}\right)\right] f = 0 \,. \tag{7.34}$$

Usually, such an equation depends only on m, implying that although different masses in the KK tower of four-dimensional fields (ϕ_0, ϕ_1, etc.) have different profiles, these profiles are independent of the energy. Here, however, the equation also depends on E, so that quanta with the same mass but different *energies* (or momenta) have different profiles. On the surface, equation (7.34) looks linear and homogeneous in f, but it is in fact a non-linear, integro-differential equation, since both $T(t)$ and $X(t)$ are defined in terms of f. Nevertheless, this equation still has the property that f can be rescaled by a w-independent factor, so long as the eigenvalues m and E are also appropriately rescaled to compensate for the change in $T(t)$ and $X(t)$. In fact, since $\dot{f} \ll E$, as discussed previously, we may even take this factor to have a (mild) time-dependence. As we advertised earlier, the rescaling of f can be used to choose a canonical time coordinate, corresponding to fixing $T = 1$, which is achievable precisely because $T(t)$ depends on f.

As a check on our derivation, for the separable cosmological metric (7.29) the factor $X^2/T^2 - a^2/n^2$ vanishes, and equation (7.34) simplifies to the known result (compare with equation (4.32))

$$f'' + \left(\frac{4c'}{c} - \frac{\hat{b}'}{\hat{b}}\right) f' + \hat{b}^2 \left[m^2\frac{1}{c^2} - U^{(1)}\right] f = 0 \,. \tag{7.35}$$

Note the lack of time dependence, implying that f is a function of w only. The profile also no longer depends on the energy of the mode, just its mass, as usual.

Let us summarise our results for scalar fields. Given a five-dimensional background metric, described by the functions $n(t, w)$, $a(t, w)$, $b(t, w)$, and

a generic coupling potential $U(\Phi)$, we may solve equation (7.34) for $f(t,w)$. The particular solution depends on a mass eigenvalue m and an energy E. We may then use this solution $f(t,w)$ to determine $T(t)$ and $X(t)$ through equation (7.27). What results is the four-dimensional spacetime, described by $T(t)$ and $X(t)$, on which a four-dimensional quantum field ϕ with mass m and energy E propagates. We are free to rescale $f(t,w)$ to impose $T=1$, so that $X(t)$ can then be interpreted as the effective FLRW scale factor. The crucial result to note is that *the scale factor depends on the type of field, its coupling potential, and its four-dimensional mass and momentum.*

7.2.2 Localised fermions

We now turn to fermions, and perform an analogous calculation to determine the effective scale factor describing the four-dimensional spacetime on which a localised fermion field propagates.

For a five-dimensional fermion $\Psi(t,x^i,w)$ the action is

$$\mathcal{S}_{5,\Psi} = \int d^5x\ \sqrt{g}\ \left[\overline{\Psi}\Gamma^A E_A{}^M(\partial_M+\omega_M)\Psi - U_\Psi\overline{\Psi}\Psi\right]\ , \tag{7.36}$$

where Γ^A are the five-dimensional flat-space gamma matrices, $E_A{}^M$ are the vielbeins and ω_M is the spin connection.[2] The gamma-matrices obey $\{\Gamma^A,\Gamma^B\}=2\eta^{AB}$, with $\eta^{AB}=\mathrm{diag}(-1,1,1,1,1)$. The coefficient U_Ψ of the mass term will in general be a function of other fields, to allow, for example, coupling of the fermion to the domain wall.

As for a scalar field, we perform a separation of scales in time and separation of variables in space,[3]

$$\Psi(t,x^i,w) = u(t,w)\ \psi(t,x^i)\ , \tag{7.37}$$

and expand the kinetic terms, ignoring $\dot{u}$. The action becomes

$$\mathcal{S}_{5,\Psi} = \int d^4x \int dw\ na^3b\sqrt{\gamma}\ \left[u^2\,\overline{\psi}\left(-n^{-1}\gamma^0\dot{\psi}+a^{-1}\gamma^a e_a{}^j\partial_j\psi\right)+\ldots\right]\ , \tag{7.38}$$

where γ^0, γ^a are the four-dimensional, flat-space gamma matrices defined by

[2] We are using A, B to denote five-dimensional flat-space indices and M, N to denote five-dimensional curved-space indices. See Section A.4.

[3] There is a subtlety here: we are assuming that all four components of the Dirac spinor ψ have the same profile u, which may not be warranted. We expand on this later.

$\{\gamma^\alpha, \gamma^\beta\} = 2\eta^{\alpha\beta}$, and $e_a{}^j$ are vielbeins for the three-dimensional space, with γ_{ij} the metric.[4] As before, we require that the correct powers of $n(t,w)$, $a(t,w)$ and $b(t,w)$ match with the relevant terms in the prototype four-dimensional fermion action

$$\mathcal{S}^{(\text{proto})}_{4,\psi} = \int d^4x\, T_\psi(t) X^3_\psi(t) \sqrt{\gamma}\, \overline{\psi} \left(-T^{-1}_\psi(t) \gamma^0 \dot{\psi} + X^{-1}_\psi(t) \gamma^a e_a{}^j \partial_j \psi \right) , \tag{7.39}$$

where we have used the prototype line element

$$ds^2_4 = -T^2_\psi(t) dt^2 + X^2_\psi(t) \gamma_{ij} dx^i dx^j \, . \tag{7.40}$$

Matching the coefficients of the kinetic and gradient terms yields

$$F_\psi(t) = \int u^2 a^3 b \, dw = X^3_\psi(t) \, , \tag{7.41a}$$

$$G_\psi(t) = \int u^2 n a^2 b \, dw = T_\psi(t) X^2_\psi(t) \, , \tag{7.41b}$$

which may be inverted to give

$$T_\psi(t) = F^{-2/3}_\psi(t) G_\psi(t) = \left(\int u^2 a^3 b \, dw \right)^{-2/3} \left(\int u^2 n a^2 b \, dw \right) , \tag{7.42a}$$

$$X_\psi(t) = F^{1/3}_\psi(t) = \left(\int u^2 a^3 b \, dw \right)^{1/3} . \tag{7.42b}$$

These results are similar to the scalar case. As there, we can rescale $u(t,w)$ by a slowly varying function of time to enforce $T_\psi = 1$, so that ψ describes a four-dimensional fermion field in a spacetime with effective scale factor $a_\psi(t) = X(t)$. Again, the definition of the effective scale factor depends on the profile of the particular KK mode ψ that one is interested in. As before, in the infinitely-thin domain-wall limit $u^2 \to \delta(bw)$ and $T_\psi(t) \to n(t, w=0)$, $X_\psi(t) \to a(t, w=0)$, which recovers the known delta-function brane result. For the separable cosmological metric (7.29), T_ψ is a constant and, after normalising u such that $T_\psi = 1$, we have $X_\psi(t) = \hat{a}(t)$; the standard result.

To identify the equation satisfied by $u(t,w)$, we impose the requirement that ψ satisfies the four-dimensional Euler-Lagrange equation with mass

[4] $\alpha, \beta = 0, 1, 2, 3$ are the four-dimensional, flat-spacetime indices, while $a = 1, 2, 3$ is a three-dimensional flat-space index.

m_ψ and use this to eliminate the spatial derivatives of ψ from the five-dimensional Euler-Lagrange equation for Ψ. This yields

$$\left[u' + \left(\frac{n'}{2n} + \frac{3a'}{2a}\right) u\right] \gamma^5 \psi + b \left(m_\psi \frac{X}{a} - U_\Psi\right) u\psi - \frac{b}{a}\left(\frac{X_\psi}{T_\psi} - \frac{a}{n}\right) u\gamma^0 \dot{\psi} = 0\,, \tag{7.43}$$

where $\gamma^5 = i\gamma^0\gamma^1\gamma^2\gamma^3$. This has a similar structure to the scalar version (7.32); in particular, the $\dot{\psi}$ term quantifies the deviation from ψ being a four-dimensional field in the usual, infinitely-thin brane definition.

The appearance of γ^0 and γ^5 in equation (7.43) means localised states on the domain wall have an unusual Dirac structure. In the Minkowski-brane case, the $\gamma^0\dot{\phi}$ term is absent and this leads to the localisation of chiral states, which are eigenspinors of γ^5. With the presence of γ^0, one would naïvely seek Dirac states which are eigenspinors of both γ^0 and γ^5, which is impossible! It therefore seems that the time-dependent background metric leads to unconventionally localised spinor states.

To understand this problem more deeply, consider seeking solutions to equation (7.43) when $\psi = \psi_L$ (and $u = u_L$) is left-chiral; that is, $\gamma^5\psi_L = -\psi_L$ and $m_{\psi_L} = 0$. Using a plane wave solution for ψ_L and expanding its Weyl components in order to evaluate $\gamma^0\dot{\psi}_L$, we obtain two independent equations for u_L:

$$u_L' + \left(\frac{n'}{2n} + \frac{3a'}{2a}\right) u_L + bU_\Psi u_L = 0\,, \tag{7.44a}$$

$$\frac{b}{a}\left(\frac{X_{\psi_L}}{T_{\psi_L}} - \frac{a}{n}\right) u_L E_{\psi_L} T_{\psi_L}^2 = 0\,, \tag{7.44b}$$

where E_{ψ_L} is the energy of the chiral plane-wave spinor ψ_L. With a non-trivial background, the only solution to equation (7.44b) is $u_L = 0$. Thus there are no localised left-chiral spinors. It may be possible to rectify this problem and find localised states which have a certain definite spinor structure by relaxing the separation ansatz. Recall that each component of the Dirac spinor was assumed to have the same profile u, as per equation (7.37), which may be an overly strict assumption. The resolution of this problem is left for the future.

7.2.3 The effective Newton's constant

We shall now briefly discuss how to determine the effective Planck mass, and hence Newton's constant, describing the strength of gravity on the brane.[5] Usually, one expands the five-dimensional Ricci scalar in the Einstein-Hilbert action in terms of its four-dimensional counterpart, and the numerical pre-factor is identified as the Planck mass. For example, in the RS2 model one uses the metric

$$ds_5^2 = e^{-2\mu|w|} g^{(4)}_{\mu\nu}(x^\mu) dx^\mu dx^\nu + dw^2 \,, \tag{7.45}$$

for which the Einstein-Hilbert action can be written as

$$\mathcal{S}_{\rm EH} = \int d^4x \int dw \sqrt{-g}\; M_*^3 R \tag{7.46a}$$

$$\supset \int d^4x \int dw\; e^{-4\mu|w|} \sqrt{-g^{(4)}}\; M_*^3\; e^{2\mu|w|} R^{(4)} \,, \tag{7.46b}$$

where $R^{(4)}$ is the four-dimensional Ricci scalar associated with $g^{(4)}_{\mu\nu}$. One then identifies the effective four-dimensional Planck mass as

$$M_{\rm Pl}^2 \equiv M_*^3 \int_{-\infty}^{\infty} e^{-2\mu|w|} dw = \frac{M_*^3}{\mu} \,, \tag{7.47}$$

which agrees with the result obtained from the effective Friedmann equation in the fundamental brane scenario, equation (7.13).

Following this approach for domain-wall cosmology, we begin by considering how the four-dimensional Ricci scalar is embedded in the five-dimensional one. However, there is a problem with this approach, because the metric factors for t and x^i behave differently at the five-dimensional level, and so the five-dimensional Ricci scalar does not separate into a four-dimensional piece plus other terms. To make progress, one might consider restricting attention to the three-dimensional Ricci scalar (constructed from the three-dimensional spatial metric γ_{ij}), which does separate, and identifying its pre-factor in the Einstein-Hilbert action as the Planck mass. In other words, we consider just the three spatial components of the metric perturbations to determine the gravitational coupling, instead of using the temporal and spatial components together.

[5] We are concerned here with the definition of the Planck mass for use in cosmological situations, such as in equation (7.16), as opposed to its use in Cavendish-like experiments.

Explicitly, we first write the five-dimensional metric in the general form

$$ds_5^2 = -n^2(t,w)dt^2 + a^2(t,w)\xi_{ij}(t,x^i)dx^i dx^j + b^2(t,w)dw^2 \,. \tag{7.48}$$

The five-dimensional Einstein-Hilbert action can then be expanded as

$$\mathcal{S}_{\rm EH} = \int d^4x \int dw \sqrt{-g}\; M_*^3 R \tag{7.49a}$$

$$\supset \int d^4x \int dw\; na^3 b\sqrt{\xi}\; M_*^3\; a^{-2} R^{(3)} \,, \tag{7.49b}$$

where $R^{(3)}$ is the Ricci scalar constructed from ξ_{ij}. The goal is to match this to the four-dimensional prototype Einstein-Hilbert action associated with the general prototype metric

$$ds_4^2 = -T_M^2(t)dt^2 + X_M^2(t)\xi_{ij}(t,x^i)dx^i dx^j \,, \tag{7.50}$$

which yields

$$\mathcal{S}_{\rm EH}^{\rm (proto)} = \int d^4x \sqrt{-g^{(4)}}\; M_{\rm Pl}^2 R^{(4)} \tag{7.51a}$$

$$\supset \int d^4x\; T_M(t) X_M^3(t)\sqrt{\xi}\; M_{\rm Pl}^2\; X_M^{-2}(t) R^{(3)} \,. \tag{7.51b}$$

By comparing equations (7.49b) and (7.51b), we can infer that the five-dimensional theory produces three-dimensional (three spatial) metric perturbations with effective Planck mass

$$M_{\rm Pl}^2 \equiv \frac{M_*^3}{T_M(t)X_M(t)} \int nab\; dw \,. \tag{7.52}$$

This result requires us to specify the four-dimensional spacetime, by specifying $T_M(t)$ and $X_M(t)$, before we can know the Planck mass. As shown in the previous subsections, the four-dimensional spacetime is dependent on the particle species, and so we obtain a *species dependent Planck mass*. This may not be so surprising given that each species follows a different line element, but it is also possible that the assumption of matching only the three-dimensional Ricci scalar is unwarranted.

Perhaps a more sophisticated calculation would try to elucidate the effective four-dimensional Einstein equation, or at least the leading order contribution. Ultimately, we would like to identify $1/2M_{\rm Pl}^2$ as the constant

of proportionality between the dominant (first order) contributions to the four-dimensional Einstein tensor ${}^{(1)}G^{(4)}_{\mu\nu}$ and the stress-energy tensor ${}^{(1)}T^{(4)}_{\mu\nu}$ for a given field in the thin, large-tension brane limit. One possible way to perform this calculation would be to analyse the equations of motion for metric perturbations. In the case of fundamental-brane cosmology, much of the ground-work for such an analysis has been performed; see for example [138, 139, 141]. For a domain-wall brane, extra complications arise, again due to the averaging of the metric over the extra dimension. Further, it seems that in order to identify the four-dimensional metric perturbations, one is forced to perform a separation of scales for the metric perturbations themselves, as in the scalar and fermion case. Such a calculation is beyond the scope of this chapter, and for our purposes here we adopt equation (7.52) as an approximate definition of the effective Planck mass.

7.3 Effective scale factor for a thin domain wall

Having developed the general framework for a domain wall with localised matter fields and the associated four-dimensional metric, we would like to better understand the behaviour of the effective scale factors a_ϕ and a_ψ. These will, of course, depend on the details of the domain wall construction. Furthermore, we need to solve explicitly for the metric components $n(t,w)$, $a(t,w)$ and $b(t,w)$ in the presence of this domain wall. We are unable to find analytic solutions for a coupled domain-wall gravity system, and numerical solutions are beyond the scope of this initial work.[6] To make progress, we will assume that the domain wall is extremely thin and that therefore the solutions for the metric components are well approximated by the set of equations (7.14).

The profiles of the domain-wall fields will play a role in determining the profiles $f(t,w)$ and $u(t,w)$ of the localised scalars and fermions respectively. These localised fields will then contribute to the total stress-energy and this back-reaction will modify the metric components. However, here we shall ignore such back-reaction effects and consider the thin domain wall as a small perturbation to the fundamental-brane scenario presented in Section 7.1. In order for this perturbative approach to work, it is necessary that the brane

[6] If one were to pursue the numerical avenue, the methods described by Dzhunushaliev et al. [233, 234, 235] may be a good place to start.

localised sources be relatively small, meaning that $\epsilon \ll 1$.

To compute a_ϕ within this approximation scheme, we first normalise $f(t,w)$ such that $T=1$. This is done by defining

$$f(t,w) = \tau(t)\tilde{f}(t,w) \tag{7.53}$$

so that

$$T(t) = \tau(t)\,\tilde{F}^{-1/4}(t)\,\tilde{G}^{3/4}(t)\,, \qquad X(t) = \tau(t)\,\tilde{F}^{1/4}(t)\,\tilde{G}^{1/4}(t)\,, \tag{7.54}$$

where $\tilde{F}(t)$ and $\tilde{G}(t)$ are defined as in equation (7.23) but with $f(t,w)$ replaced by $\tilde{f}(t,w)$. Enforcing $T=1$ gives $\tau(t) = \tilde{F}^{1/4}(t)\,\tilde{G}^{-3/4}(t)$ so that $X(t) = \tilde{F}^{1/2}(t)\,\tilde{G}^{-1/2}(t)$. We may then compute $\tilde{F}(t)$ and $\tilde{G}(t)$ by substituting in for the bulk metric solutions (7.14) yielding, for example,

$$\tilde{G}(t) = \int \tilde{f}^2\, an\, dw \tag{7.55a}$$

$$= a_0 \int \tilde{f}^2 \left[e^{-2\mu|w|} - (\epsilon+\tilde{\epsilon})e^{-\mu|w|}\sinh(\mu|w|) + \epsilon\,\tilde{\epsilon}\,\sinh^2(\mu|w|) \right] dw\,. \tag{7.55b}$$

Requiring that the localisation profile $\tilde{f}(t,w)$ be sharply peaked at the centre of the domain wall ($w=0$) and fall off rapidly in the bulk translates to $\tilde{f}^2(t,w)\sinh^2(\mu|w|) \to 0$ as $w \to \pm\infty$. This condition is consistent with the sufficiently-thin domain-wall brane we are dealing with here. Thus, we may ignore the second order term $\mathcal{O}(\epsilon\,\tilde{\epsilon})$ and write

$$\tilde{G}(t) = a_0\left[I_1(t) - (\epsilon+\tilde{\epsilon})I_2(t)\right]\,, \tag{7.56}$$

where

$$I_1(t) = \int \tilde{f}^2(t,w)e^{-2\mu|w|}\,dw\,, \tag{7.57a}$$

$$I_2(t) = \int \tilde{f}^2(t,w)e^{-\mu|w|}\sinh(\mu|w|)\,dw\,. \tag{7.57b}$$

These integrals, $I_1(t)$ and $I_2(t)$, are dependent on the exact form of the extra-dimensional profile $\tilde{f}(t,w)$. However, if the profile is sufficiently peaked, as we are assuming, we have $I_2(t) \ll I_1(t)$ because $\sinh(\mu|w|) \sim 0$ close to the

centre of the domain wall. Under these assumptions, we may compute

$$\tilde{F}(t) = a_0^3 \left[I_1(t) - (3\epsilon - \tilde{\epsilon}) I_2(t) \right] , \tag{7.58}$$

so that the effective scale factor for the scalar field becomes

$$a_\phi(t) = X(t) = a_0(t) \left[1 - (\epsilon - \tilde{\epsilon}) \frac{I_2(t)}{I_1(t)} \right] \tag{7.59a}$$

$$= a_0(t) \left[1 + \frac{\dot{\epsilon}}{H_0} \frac{I_2(t)}{I_1(t)} \right] . \tag{7.59b}$$

This is one of the main results of this chapter — an explicit, quantitative computation of the corrections to the effective four-dimensional scale factor arising from considering a domain-wall brane, rather than a fundamental one. The corrections are proportional to the ratio between the rate of change of energy density on the brane and the brane tension, $\dot{\epsilon}$, and inversely proportional to the effective Hubble parameter. The corrections also depend in a non-trivial way on the specific localisation profile of the associated field, so that different fields are corrected differently.

The expression (7.59b) satisfies $a_\phi \to a_0$ for the independent limits of a Minkowski brane with no sources ($\epsilon \to 0$), and an infinitely-thin brane ($I_2 \to 0$). For a concrete example of this latter limit, consider the profile[7]

$$\tilde{f}^2(t, w) = \frac{\Gamma(\lambda + \frac{1}{2})}{\sqrt{\pi}\Gamma(\lambda)} \mu [\cosh(\mu w)]^{-2\lambda} , \tag{7.60}$$

which obeys $\tilde{f}^2 \to \delta(w)$ as $\lambda \to \infty$ (the thin domain-wall limit) and is a typical example of smooth localisation factors; see, for example, the KK modes obtained in Chapter 3. It is then straightforward to compute

$$\frac{I_2(t)}{I_1(t)} = \frac{2\Gamma(\lambda + \frac{1}{2}) - \sqrt{\pi}\Gamma(\lambda)}{2\sqrt{\pi}\Gamma(\lambda + 1) - 4\Gamma(\lambda + \frac{1}{2})} \quad \xrightarrow{\lambda \to \infty} \quad \frac{1}{\sqrt{\pi\lambda}} , \tag{7.61}$$

which vanishes in the infinitely-thin wall limit. A better approximation for this quantity can be found by solving the differential equation (7.34) for $\tilde{f}(t, w)$, using the background metric components $n(t, w)$ and $a(t, w)$.

For a fermion field the result for the effective scale factor is almost iden-

[7] The time dependence of this sample $\tilde{f}$ would arise from the time dependence of the parameter λ, corresponding to the brane thickness changing over time.

tical to the scalar case:

$$a_\psi(t) = a_0(t)\left[1 + \frac{\dot{\epsilon}}{H_0}\frac{J_2(t)}{J_1(t)}\right] , \tag{7.62}$$

where the relevant integrals are

$$J_1(t) = \int \tilde{u}^2(t,w) e^{-3\mu|w|}\, dw , \tag{7.63a}$$

$$J_2(t) = \int \tilde{u}^2(t,w) e^{-2\mu|w|} \sinh \mu|w|\, dw , \tag{7.63b}$$

and $\tilde{u}(t,w)$ is defined in a similar way to $\tilde{f}(t,w)$.

The results from this section, namely equations (7.59b) and (7.62), are concrete expressions for modifications to cosmology in a domain-wall brane construction, and are the starting point for an analysis of the constraints on such theories from observations. We expect that a species-dependent scale factor should have an impact on a vast array of cosmological observables, including the predictions of BBN, the era of recombination and the spectra of the microwave background and large scale structure. Acceptable cosmological behaviour should imply constraints on the brane tension σ, which appears in ϵ and μ, and the width of the domain wall, which enters implicitly through the localisation profiles $\tilde{f}$ and $\tilde{u}$.

7.4 Conclusion

In this chapter we have proposed a formalism for examining the cosmology associated with a five-dimensional domain-wall brane. The formalism is based on the requirement that the kinetic and gradient terms of the effective four-dimensional action be equivalent to their counterparts for a prototypical, four-dimensional FLRW metric. It is important to consider such things because one should be able to constraint certain aspects of domain-wall models, like the width of the wall, by comparing the theory's cosmological predictions with data.

The calculation of the effective Friedmann equation for the case of a fundamental brane was reviewed in Section 7.1, and Sections 7.2 and 7.3 considered the generalisation to a domain-wall brane. The main obstacle was the fact that the cosmological metric, equation (7.2), displays different behaviour for its temporal and spatial components. This makes it difficult

to perform the requisite dimensional reduction of the domain-wall model, which involves integrating over the extra-dimension in the five-dimensional action. In the case where the brane-metric is Minkowski spacetime, dimensional reduction is straightforward because the kinetic and gradient terms of a given field have equivalent structure. Their four-dimensional versions share a common pre-factor — the overlap integral — and they can thus be packaged together to form the usual, four-Lorentz-invariant kinetic term. Furthermore, all the fields in the four-dimensional Minkowski action can be normalised such that they share the same effective metric, and it is therefore sensible to say that the four-dimensional theory has a unique spacetime.

In contrast to the Minkowski case, the more general metric which allows for FLRW-like expansion on the brane treats the kinetic and gradient terms differently. During the normalisation of the kinetic and gradient terms, one must take into account the fact that *different fields may feel different spacetimes*. Thus, for domain-wall branes it is not sensible to ask the question "what is the effective scale factor on the brane?". Since the brane has non-trivial dependence on the extra-dimensional coordinate w, and since the metric components $n(t, w)$ and $a(t, w)$ are not proportional to each other in the bulk, each four-dimensional slice at constant w corresponds to a different spacetime. The effective four-dimensional spacetime for a localised field with a smooth profile in w will thus be an average over all the different slices. This produces a kind of "dimensional parallax" effect, since different fields have different averages, and thus a different "perspective" of the cosmological evolution of each slice.

Therefore, rather than seeking the effective scale factor on the domain-wall brane (which was possible in the fundamental brane case), we must be content with instead asking: "what is the effective four-dimensional spacetime in which a given localised field propagates?". For each low-energy four-dimensional field (each species and each mode of the KK tower), we may answer this question by determining the effective, four-dimensional line element ds_4^2. If this line element takes the form of an FLRW line element, then we may define an effective scale factor for the associated field. This is as close as we are able to come to answering our original question.

In the case of a localised scalar field, the effective scale factor is given in general by equations (7.27b) and (7.28), and for fermions one obtains equation (7.42b). For the case of a domain-wall brane which is thin enough

such that one can approximate the metric components $n(t,w)$, $a(t,w)$ and $b(t,w)$ with the solutions from the fundamental-brane scenario, the effective scale factors for scalars and fermions are (7.59b) and (7.62) respectively. All of these results reduce, in the infinitely-thin domain-wall limit, to the results obtained for fundamental-brane cosmology, where the effective scale factor is the bulk metric component $a(t,w)$ evaluated at $w=0$.

Aside from this basic difference between the fundamental-brane and the domain-wall case, there are a number of other interesting consequences that arise in the context of our formalism. In the cosmological scenario, the non-trivial averaging of the metric over w means that, just as different modes of a KK tower have different extra-dimensional profiles, it is also true that different *energies* of the same mass have different profiles. Thus, particles with different energies feel a different scale factor! Also, due to the association of γ^0 with the time coordinate, it is difficult to see how the localisation of fermion zero-modes can be recovered. It may be that the associated separation ansatz needs to treat each component of the Dirac spinor separately, leading to the physical interpretation that that different components of the spinor feel different spacetimes. This is in analogy with the fact that, since γ^5 is associated with the extra-dimension, left- and right-handed spinors couple differently to the kink background.

An outstanding problem is that of defining a unique Planck mass (if possible) at the four-dimensional level. We have provided some insight into the solution to this problem, in the form of the initial approximation (7.52). A more comprehensive treatment would begin by looking at how four-dimensional gravity perturbations couple to the effective, four-dimensional stress-energy tensor. It would also be of interest to look for solutions to the equations of motion which have the background scalar field, the kink, evolving in a self-consistent manner with the five-dimensional, time-dependent cosmological metric.

The novel features presented in this chapter — species-dependent scale factors and non-unique Planck masses — will lead to potentially observable cosmological phenomena. The next step, which shall not be attempted in the current thesis, would be to perform a detailed phenomenological analysis to determine how these effects constrain parameters such as the width and tension of the domain wall, and the extent to which they may allow new approaches to current, unsolved problems in cosmology.

Chapter 8

Conclusions and outlook

Throughout this thesis we have maintained the theme of domain-wall brane models of an infinite extra dimension, discussed all manner of techniques related to their construction and their properties, and provided a viable domain-wall brane-world extension of the standard model. The addition of extra spatial dimensions, be they compact or non-compact, to our current models of the universe certainly seems plausible, and we should work hard to understand the consequences. From our point of view, the case of a non-compact, infinite extra dimension is the more appealing path of study, as such a scenario places all spatial dimensions on an equal footing from the outset. Implementing this idea in the tried-and-tested language of field theory leads us naturally to domain-wall branes generated by a scalar field, and the ensuing studies have been the focus of this thesis.

The tools that we have presented here — stability analysis, mode decomposition, analysis of the thin-kink limit, fermion and Higgs localisation, the smooth version of the Randall-Sundrum warped metric, the Dvali-Shifman and clash-of-symmetries mechanisms, and domain-wall cosmology — form a set of building blocks for constructing and analysing domain-wall brane models of an infinite extra dimension. We have used these tools to piece together an SU(5) version of the standard model confined to a domain-wall, and we found that such a model is not only fairly minimal in its construction, but also has promising phenomenology. We have further explored the extension to an E_6 invariant action, which lead to the beginnings of an elegant realisation of a grand-unified-theory localised to a domain-wall brane. The next step would be to complete these models, and determine their precise phenomenology and resulting compatibility with current and future experi-

mental data.

In Chapter 2 we studied a simple model with two scalar fields charged under a $\mathrm{U}(1) \otimes \mathrm{U}(1)$ symmetry. The solutions to the Euler-Lagrange equations of motion were a pair of kinks which acted to semi-confine the gauge fields of the $\mathrm{U}(1) \otimes \mathrm{U}(1)$ symmetry. Our interest in this set-up lay in determining its perturbative stability. We looked at the normal modes of small fluctuations around the classical kink-gauge background, and found the modes to be oscillatory for a large range of parameters of the model, establishing the stability of the configuration. This model was then extended to include gravity and we gave analytic solutions for a smooth version of the Randall-Sundrum warped metric coupled to the kink background for the case where the gauge fields were set to zero. Our search for numerical solutions where the gauge fields assumed a non-zero configuration in the presence of gravity did not succeed, and we gave an argument which supported the non-existence of such solutions. Further work could look for a loophole in this argument and attempt to find kink-gauge-gravity solutions, but one must be careful to ensure the Randall-Sundrum fine-tuning condition is satisfied. The perturbative stability techniques presented in this chapter can be applied generally to determine if a given kink configuration is stable or not, which is of crucial importance if the background is to be used to confine the standard model.

A comprehensive study of the modes of the kink, and the modes of localised scalar and fermion fields, was undertaken in Chapter 3. Such a mode decomposition — a generalised Fourier transform — forms a necessary part of the analysis of domain-wall brane models, as it not only gives the properties of the ground state modes, but also elucidates the structure of the higher-mass modes, the Kaluza-Klein modes. A useful way of understanding how a kink localises four-dimensional fields is to consider one-dimensional quantum mechanics, with the kink setting up a potential well along the extra-dimension. For our case, the potential was found to have the form of a symmetric modified Pöschl-Teller potential. We then solved the resulting Schrödinger-like equation to determine the extra-dimensional profiles of the tower of Kaluza-Klein modes trapped to the domain-wall region. An important result was that the mass spectrum of the modes was directly related to the inverse-width of the domain-wall, implying a direct relationship between the structure of the wall and the particles that could be

produced in future collider experiments. Important for model building was the conclusion that chiral, massless, four-dimensional fermions can be localised to the kink, along with a four-dimensional scalar field with arbitrary quartic potential, which is necessary to implement the Higgs mechanism on the brane.

We also systematically studied the limiting behaviour of the kink, with a focus on the infinitely-thin kink limit. This is the phenomenologically important case because we have not measured any Kaluza-Klein modes, and so they must be very heavy — the kink must be very thin — if they exist at all. The thin kink limit also allows for a useful comparison with fundamental branes in string theory. During our analysis we discovered an interesting result: the four-dimensional zero mode corresponding to translations of the kink has its dynamics frozen out in the thin kink limit. Although the mass of this zero mode remains strictly zero, it is frozen out due to a divergent, quartic self-coupling term in the effective four-dimensional action. This is potentially at odds with the existence of Nambu-Goldstone bosons in theories with spontaneously broken symmetries, but we made the physical interpretation that our infinitely-thin kink corresponded to an infinitely-rigid one, and so the zero mode remains only as a constant shift of the entire wall, not as a dynamical field. As part of this study we considered the implicit collective coordinate approach, which we deemed to be an inadequate way of decomposing a given field in a general way. It is left for future studies to better understand this failure of implicit collective coordinates, and to determine the extent to which they are a useful way of characterising degrees of freedom associated with broken symmetries.

Chapter 4 was devoted to the extension of the previous mode analysis for the situation where gravity is included. We incorporated localised gravity via the generalisation of the Randall-Sundrum warped metric to the case where the brane is formed by a domain wall, and the metric becomes a smooth version of the original. The trapping of gravity was reviewed, and we discussed how the volcano potential induces a spectrum containing a massless graviton, which is followed directly (there is no mass gap) by a continuum of gravity modes. It was then shown that the trapping potentials for fermions and scalar fields coupled to a kink background become volcano-like when gravity is turned on. This effect induces a continuum of Kaluza-Klein states, starting at zero mass, in the spectra of four-dimensional fermions and

scalars. The resulting physics is not as drastically modified as one might think, because the extra-dimensional profiles of the continuum modes are highly suppressed near the centre of the domain wall. Furthermore, the chiral fermion zero modes remain in the spectrum, tachyonic scalar modes (the Higgs) remain tachyonic, and the massive bound Kaluza-Klein modes manifest as resonances in the continuum. We constructed a toy-model to analyse the interaction between the gravity-induced continuum modes and modes bound to the brane, and demonstrated that such an interaction is highly suppressed. This means that we can confidently incorporate the Randall-Sundrum warped metric into our domain-wall model, giving us a mechanism for trapping gravity.

Drawing on the techniques developed in the previous chapters, Chapter 5 proposed a domain-wall brane model of an infinite extra dimension, with an action that respected an SU(5) symmetry, and which reproduced at low energies a single generation version of the standard model. Our model also reproduced general relativity at low energies. For the localisation of gauge fields, we relied on the Dvali-Shifman mechanism, which required us to assume that SU(5) Yang-Mills is confining in five-dimensions. We gave a detailed discussion of this mechanism, and presented some lattice-gauge-theory results which suggest that Dvali-Shifman can be made to work in a five-dimensional setting. Apart from the gauge fields, the field content of our SU(5) model consists of two scalars η and χ which form the domain wall, two fermion fields Ψ_5 and Ψ_{10} whose localised zero modes provide one generation of fermions of the standard model, and a scalar Φ which yields the four-dimensional Higgs doublet.

Following the presentation of the SU(5) model, we gave a specific, analytic example for the kink background configuration, and determined the profiles of the zero mode fermions. This explicitly demonstrated how the split-fermion mechanism is inherent in our model. We also showed how the Higgs doublet and the coloured Higgs can be spilt in the extra dimension. The four-dimensional, effective electroweak sector was computed, and the fermion masses m_e, m_d and m_u were determined in terms of overlap integrals of extra-dimensional profiles. Because of the splitting of the fermion profiles, the usual tree-level mass relation of SU(5), namely $m_e = m_d$, is automatically absent in our model. Similarly, proton decay due the coloured Higgs can be suppressed by arranging to have the appropriate profiles well

separated. We discussed how the Randall-Sundrum warped metric has little impact on these general properties of our model, and we outlined the relationships among the various scales in the theory.

There are many avenues to take beyond this initial brane-world model. To start with, one needs to extend the fermion content to three generations and work out how to determine their extra-dimensional profiles, which may be complicated by the mixing induced by the Yukawa term that couples the three generations to the kink. A mechanism for obtaining massive neutrinos is also required. Following these model building problems, the parameters of the full theory must be fit to experimental data, and one would need to ensure that proton decay is well suppressed. Analysing the unification of the effective four-dimensional gauge coupling constants into the five-dimensional SU(5) coupling is an outstanding issue. The full spectrum of Kaluza-Klein modes, including the massive gauge bosons, is needed before proceeding with such an analysis. For this, one would also want to understand how the gauge boson spectrum is modified in the presence of the warped metric, as we know that for the case of matter fields a continuum is induced. This seems to be a non-trivial task, as the gauge sector is non-perturbative in the bulk. As we have previously emphasised, confinement of Yang-Mills in five-dimensions is crucial for Dvali-Shifman, and hence crucial to the success of our model. More work is needed — in the form of a dedicated lattice-gauge-theory calculation — to check the non-perturbative aspects of our model, and verify or debunk its validity. If Dvali-Shifman does work in five-dimensions, then our SU(5) model becomes a very promising candidate for a theory of an infinite extra dimension.

In Chapter 6 we considered extensions of our SU(5) model to larger gauge groups. The clash-of-symmetries mechanism played an important role here, and we gave an in-depth review of it, pointing out a natural connection with Dvali-Shifman. Utilising these two mechanisms, our first extension of the SU(5) model was to SO(10), but, unfortunately, there were problems with the localisation of the gauge bosons. In particular, the photon and neutral Z boson leak into the bulk on one side of the domain wall. The cure was to move to an E_6 invariant theory. We first performed a comprehensive analysis of the Casimir invariants associated with this group and found that there exist twenty-seven distinct embeddings of $SO(10) \otimes U(1)$ in E_6. Using these embeddings in a clash-of-symmetries context, we found that one could obtain

either $SO(8) \otimes U(1)^2$ or $SU(5) \otimes U(1)^2$ as the symmetry on the brane. The latter of these is the phenomenologically acceptable one, and we proceeded to construct a Higgs potential, and find the associated domain-wall solutions, which yielded localised SU(5) gauge bosons. Unfortunately, such a solution was found to have a greater energy density than the corresponding SO(8) theory, but there remains a lot of freedom in choosing the form of the Higgs potential, so it is certainly possible that the SU(5) model can be made energetically favourable.

Assuming that such a stable background configuration could be found, we looked at adding fermions to the model using the **27** of E_6. When coupled to the kink, this multiplet separated into individual SU(5) multiplets, in direct analogy with the splitting of the fermions in the SU(5) model of Chapter 5. Of these split multiplets, some were localised to the kink and some were not, depending on their hypercharges. Those that were localised consisted of one generation of standard model fermions plus two singlet neutrinos, which was a non-trivial outcome, and certainly provides motivation to consider a more realistic version of the E_6 model. Before working on a realistic model, it is important to understand the stability of the background kink configuration, and find, if possible, a Higgs potential that endows the SU(5)-inducing kink with the lowest energy density. Following this, one would need to incorporate gravity in the form of the Randall-Sundrum warped metric, and arrange to have the SU(5) symmetry on the brane break to the standard model, and ensure that the electroweak symmetry can be further broken. It would also be of interest to study the rearrangement conjecture regarding the twenty-seven different embeddings of $SO(10) \otimes U(1)$ in E_6.

Leaving particle physics behind, we studied the cosmology of domain-wall branes in Chapter 7. The fundamental brane case was first reviewed, and then we moved on to propose a formalism for analysing the cosmology of branes that are constructed from a scalar field. The key idea was to inspect the kinetic and gradient terms of the four-dimensional fields in the dimensionally reduced, effective action. These terms must be normalised in a specific way for an expanding spacetime, and we determined such normalisation by matching the effective action with a prototype action. This was done for both scalar and fermion fields. The general result is that different species, and different Kaluza-Klein modes of the same species, propagate in different effective, four-dimensional spacetimes. They thus experience a different scale factor, and we concluded that it is not sensible to define a

unique scale factor for the effective theory of a domain-wall brane model. It is also difficult to define a unique effective Newton's constant in the four-dimensional theory, although our analysis of this particular aspect was only preliminary and requires additional study.

Further to these results, we found that, for a cosmological spacetime, a particle associated with a given Kaluza-Klein mode has an extra-dimensional profile that depends on the four-dimensional energy of the particle. This implies that the effective scale factor also changes with energy. Localised fermions are also no longer chiral because the usual separation ansatz — that each component of the five-dimensional Dirac spinor has the same extra-dimensional profile — breaks down when the background spacetime is not exactly Minkowskian. It was left to future work to consider a more general ansatz for the separation, and to determine if it is possible to recover a localised fermion with proper spinor structure. We showed how these remarkable effects are suppressed in the thin domain-wall limit. To this end, we found expressions for corrections to the scale factor of the fundamental-brane case when the brane is considered as a domain-wall with relatively small width. These corrections are proportional to overlap integrals, and can be made small by decreasing the width of the wall. This analysis assumed that the metric for the domain-wall brane could be well approximated by the metric of the fundamental-brane case. It would be interesting to find solutions, possibly numerical ones, which have the kink background evolving consistently with the metric components. Then one could think about computing observable effects of the cosmology of domain walls, and possibly constrain the width of the wall by comparing such effects with data.

The idea of extra dimensions is both old and profound, and it may be that nature is hiding such dimensions from us, in reach only of high energy processes, processes that we may one day harness with our machines. The possibility of extra dimensions comes with the responsibility, for us, of working out if they do in fact exist. While there are many theoretical directions we can take to tackle this fascinating problem, this thesis attempted to stay on a more traditional path by considering an infinite extra dimension, in line with the spatial dimensions we already know of, and by utilising standard, field theoretic tools. The natural outcome of these basic tenets is the domain-wall brane model, of which our SU(5) model is but the beginning of what we hope shall be a faithful description of the extra-dimensional character of the world we live in.

List of publications

1. D.P. George, M. Trodden and R.R. Volkas,
   "Extra-dimensional cosmology from a domain-wall brane",
   JHEP **02** (2009) 035, [arXiv:0810.3746].

2. A. Davidson, D.P. George, A. Kobakhidze, R.R. Volkas and K.C. Wali,
   "SU(5) grand unification on a domain-wall brane from an E_6-invariant action",
   Phys. Rev. D **77** (2008) 085031, [arXiv:0710.3432].

3. R. Davies, D.P. George and R.R. Volkas,
   "The standard model on a domain-wall brane?",
   Phys. Rev. D **77** (2008) 124038, [arXiv:0705.1584].

4. R. Davies and D.P. George,
   "Fermions, scalars and Randall-Sundrum gravity on domain-wall branes",
   Phys. Rev. D **76** (2007) 104010, [arXiv:0705.1391].

5. D.P. George and R.R. Volkas,
   "Kink modes and effective four dimensional fermion and Higgs brane models",
   Phys. Rev. D **75** (2007) 105007, [arXiv:hep-ph/0612270].

6. E. Di Napoli, D. George, M. Hertzberg, F. Metzler and E. Siegel,
   "Dark Matter In Minimal Trinification",
   Proceedings of the LXXXVI Les Houches Summer School,
   pages 517–524 (2006), [arXiv:hep-ph/0611012].

7. D.P. George and R.R. Volkas,
   "Stability of domain walls coupled to Abelian gauge fields",
   Phys. Rev. D **72** (2005) 105011, [arXiv:hep-ph/0508206].

8. G. Dando, A. Davidson, D.P. George, R.R. Volkas and K.C. Wali, "Clash of symmetries in a Randall-Sundrum-like spacetime", Phys. Rev. D **72** (2005) 045016, [arXiv:hep-ph/0507097].

Bibliography

[1] F. Ravndal, "Scalar gravitation and extra dimensions." 2004. [gr-qc/0405030].

[2] G. Nordstrom, *On the possibility of unifying the electromagnetic and the gravitational fields*, *Phys. Zeit.* **15** (1914) 504–506, [physics/0702221].

[3] G. Nordstrom, *On a theory of electricity and gravitation*, *Öfversigt af Finska Vetenskaps-Societetens Förhandlingar* ((Helsingfors), Bd. LVII. 1914-1915. Afd. A. N:o 4, p. 1–15) [physics/0702222].

[4] G. Nordstrom, *On a possible foundation of a theory of matter*, *Översigt af Finska Vetenskaps-Societetens Förhandlingar* ((Helsingfors), Bd. LVII. 1914-1915. Afd. A. N:o 28, p. 1–21) [physics/0702223].

[5] T. Kaluza, *On the unification problem in physics*, in Lee [243], pp. 1–9. English translation by T. Muta.

[6] A. Pais, *The Genius of Science*. Oxford University Press Inc., 2000.

[7] O. Klein, *From my life of physics*, in Ekspong [244], pp. 103–117.

[8] O. Klein, *Quantum theory and five-dimensional relativity*, in Lee [243], pp. 10–22. English translation by T. Muta.

[9] G. Ekspong, ed., *The Oskar Klein Memorial Lectures*, p. 111. Vol. 1 of Ekspong [244], 1991.

[10] O. Klein, *The atomicity of electricity as a quantum theory law*, in Ekspong [244], pp. 81–83.

[11] E. Schrödinger, *An undulatory theory of the mechanics of atoms and molecules*, *Phys. Rev.* **28** (Dec, 1926) 1049–1070.

[12] F. Mandl and G. Shaw, *Quantum Field Theory*. John Wiley & Sons, 1984.

[13] M. E. Peskin and D. V. Schroeder, *An Introduction to Quantum Field Theory*. Westview Press, 1995.

[14] C.-N. Yang and R. L. Mills, *Conservation of isotopic spin and isotopic gauge invariance*, *Phys. Rev.* **96** (1954) 191–195.

[15] S. L. Glashow, *Partial Symmetries of Weak Interactions*, *Nucl. Phys.* **22** (1961) 579–588.

[16] A. Salam and J. C. Ward, *Electromagnetic and weak interactions*, *Phys. Lett.* **13** (1964) 168–171.

[17] J. Goldstone, *Field Theories with Superconductor Solutions*, *Nuovo Cim.* **19** (1961) 154–164.

[18] Y. Nambu and G. Jona-Lasinio, *Dynamical model of elementary particles based on an analogy with superconductivity. I*, *Phys. Rev.* **122** (1961) 345–358.

[19] Y. Nambu and G. Jona-Lasinio, *Dynamical model of elementary particles based on an analogy with superconductivity. II*, *Phys. Rev.* **124** (1961) 246–254.

[20] J. Goldstone, A. Salam, and S. Weinberg, *Broken Symmetries*, *Phys. Rev.* **127** (1962) 965–970.

[21] P. W. Higgs, *Broken symmetries, massless particles and gauge fields*, *Phys. Lett.* **12** (1964) 132–133.

[22] P. W. Higgs, *Broken Symmetries and the Masses of Gauge Bosons*, *Phys. Rev. Lett.* **13** (1964) 508–509.

[23] P. W. Higgs, *Spontaneous Symmetry Breakdown Without Massless Bosons*, *Phys. Rev.* **145** (1966) 1156–1163.

[24] S. Weinberg, *A Model of Leptons*, *Phys. Rev. Lett.* **19** (1967) 1264–1266.

[25] A. Salam, *Weak and electromagnetic interactions*, in *Elementary Particle Theory: proceedings of the Eighth Nobel Symposium* (N. Svartholm, ed.), pp. 367–377. Almqvist & Wiksell, 1968.

[26] M. Gell-Mann and Y. Ne'eman, eds., *The Eightfold Way: A Review — With A Collection of Reprints*. W. A. Benjamin, Inc., 1964.

[27] M. Gell-Mann, *A Schematic Model of Baryons and Mesons*, *Phys. Lett.* **8** (1964) 214–215.

[28] O. W. Greenberg, *Spin and Unitary Spin Independence in a Paraquark Model of Baryons and Mesons*, *Phys. Rev. Lett.* **13** (1964) 598–602.

[29] M. Y. Han and Y. Nambu, *Three-triplet model with double SU(3) symmetry*, *Phys. Rev.* **139** (1965) B1006–B1010.

[30] P. H. Frampton, *Dual resonance models*. W. A. Benjamin, Inc., 1974.

[31] J. H. Schwarz, *Superstring Theory*, *Phys. Rept.* **89** (1982) 223–322.

[32] M. B. Green, J. H. Schwarz, and E. Witten, *Superstring theory*, vol. 1. Cambridge University Press, 1987.

[33] J. Scherk and J. H. Schwarz, *Dual Field Theory of Quarks and Gluons*, *Phys. Lett.* **B57** (1975) 463–466.

[34] D. J. Gross and F. Wilczek, *Ultraviolet Behavior of Non-Abelian Gauge Theories*, *Phys. Rev. Lett.* **30** (1973) 1343–1346.

[35] H. D. Politzer, *Reliable Perturbative Results for Strong Interactions?*, *Phys. Rev. Lett.* **30** (1973) 1346–1349.

[36] H. Fritzsch, M. Gell-Mann, and H. Leutwyler, *Advantages of the Color Octet Gluon Picture*, *Phys. Lett.* **B47** (1973) 365–368.

[37] H. Georgi and S. L. Glashow, *Unity of All Elementary Particle Forces*, *Phys. Rev. Lett.* **32** (1974) 438–441.

[38] H. Georgi, *The State of the Art — Gauge Theories*, in *AIP Conference Proceedings No. 23: Particles and Fields Subseries No. 10* (C. Carlson, ed.), pp. 575–582, 1975.

[39] A. Davidson, B. F. Toner, R. R. Volkas, and K. C. Wali, *Clash of symmetries on the brane*, *Phys. Rev.* **D65** (2002) 125013, [hep-th/0202042].

[40] J. C. Pati and A. Salam, *Lepton Number as the Fourth Color*, *Phys. Rev.* **D10** (1974) 275–289.

[41] D. W. Joseph, *Coordinate Covariance and the Particle Spectrum*, *Phys. Rev.* **126** (1962) 319–323.

[42] I. Robinson and Y. Ne'eman, *Seminar on the embedding problem*, *Rev. Mod. Phys.* **37** (1965) 201–230. This is a collection of six articles by various authors.

[43] K. Akama, *An early proposal of 'brane world'*, *Lect. Notes Phys.* **176** (1982) 267–271, [hep-th/0001113].

[44] H. B. Nielsen and P. Olesen, *Vortex-line models for dual strings*, *Nucl. Phys.* **B61** (1973) 45–61.

[45] V. A. Rubakov and M. E. Shaposhnikov, *Do We Live Inside a Domain Wall?*, *Phys. Lett.* **B125** (1983) 136–138.

[46] R. Rajaraman, *Solitons and instantons : an introduction to solitons and instantons in quantum field theory*. North-Holland Pub. Co., 1982.

[47] M. Visser, *An Exotic Class of Kaluza-Klein Models*, *Phys. Lett.* **B159** (1985) 22, [hep-th/9910093].

[48] E. J. Squires, *Dimensional Reduction Caused by a Cosmological Constant*, *Phys. Lett.* **B167** (1986) 286.

[49] G. W. Gibbons and D. L. Wiltshire, *Space-Time as a Membrane in Higher Dimensions*, *Nucl. Phys.* **B287** (1987) 717, [hep-th/0109093].

[50] M. B. Green and J. H. Schwarz, *Anomaly Cancellation in Supersymmetric D=10 Gauge Theory and Superstring Theory*, *Phys. Lett.* **B149** (1984) 117–122.

[51] I. Antoniadis, *A Possible new dimension at a few TeV*, *Phys. Lett.* **B246** (1990) 377–384.

[52] J. Dai, R. G. Leigh, and J. Polchinski, *New Connections Between String Theories*, *Mod. Phys. Lett.* **A4** (1989) 2073–2083.

[53] J. Polchinski, *Dirichlet-Branes and Ramond-Ramond Charges*, *Phys. Rev. Lett.* **75** (1995) 4724–4727, [hep-th/9510017].

[54] P. Horava and E. Witten, *Heterotic and type I string dynamics from eleven dimensions*, *Nucl. Phys.* **B460** (1996) 506–524, [hep-th/9510209].

[55] P. Horava and E. Witten, *Eleven-Dimensional Supergravity on a Manifold with Boundary*, *Nucl. Phys.* **B475** (1996) 94–114, [hep-th/9603142].

[56] A. Lukas, B. A. Ovrut, K. S. Stelle, and D. Waldram, *The universe as a domain wall*, *Phys. Rev.* **D59** (1999) 086001, [hep-th/9803235].

[57] G. R. Dvali and M. A. Shifman, *Domain walls in strongly coupled theories*, *Phys. Lett.* **B396** (1997) 64–69, [hep-th/9612128].

[58] N. Arkani-Hamed and M. Schmaltz, *Field theoretic branes and tachyons of the QCD string*, *Phys. Lett.* **B450** (1999) 92–98, [hep-th/9812010].

[59] G. Dvali, H. B. Nielsen, and N. Tetradis, *Localization of Gauge Fields and Monopole Tunnelling*, *Phys. Rev.* **D77** (2008) 085005, [arXiv:0710.5051].

[60] S. L. Dubovsky and V. A. Rubakov, *On models of gauge field localization on a brane*, *Int. J. Mod. Phys.* **A16** (2001) 4331–4350, [hep-th/0105243].

[61] N. Arkani-Hamed, S. Dimopoulos, and G. R. Dvali, *The hierarchy problem and new dimensions at a millimeter*, *Phys. Lett.* **B429** (1998) 263–272, [hep-ph/9803315].

[62] I. Antoniadis, N. Arkani-Hamed, S. Dimopoulos, and G. R. Dvali, *New dimensions at a millimeter to a Fermi and superstrings at a TeV*, *Phys. Lett.* **B436** (1998) 257–263, [hep-ph/9804398].

[63] N. Arkani-Hamed, S. Dimopoulos, and G. R. Dvali, *Phenomenology, astrophysics and cosmology of theories with sub-millimeter dimensions and TeV scale quantum gravity*, *Phys. Rev.* **D59** (1999) 086004, [hep-ph/9807344].

[64] N. Arkani-Hamed and S. Dimopoulos, *New origin for approximate symmetries from distant breaking in extra dimensions*, *Phys. Rev.* **D65** (2002) 052003, [hep-ph/9811353].

[65] N. Arkani-Hamed, S. Dimopoulos, and J. March-Russell, *Stabilization of sub-millimeter dimensions: The new guise of the hierarchy problem*, *Phys. Rev.* **D63** (2001) 064020, [hep-th/9809124].

[66] N. Arkani-Hamed, S. Dimopoulos, G. R. Dvali, and J. March-Russell, *Neutrino masses from large extra dimensions*, *Phys. Rev.* **D65** (2002) 024032, [hep-ph/9811448].

[67] N. Arkani-Hamed and M. Schmaltz, *Hierarchies without symmetries from extra dimensions*, *Phys. Rev.* **D61** (2000) 033005, [hep-ph/9903417].

[68] M. Gogberashvili, *Hierarchy problem in the shell-universe model*, *Int. J. Mod. Phys.* **D11** (2002) 1635–1638, [hep-ph/9812296].

[69] M. Gogberashvili, *Our world as an expanding shell*, *Europhys. Lett.* **49** (2000) 396–399, [hep-ph/9812365].

[70] M. Gogberashvili, *Four dimensionality in non-compact Kaluza-Klein model*, *Mod. Phys. Lett.* **A14** (1999) 2025–2032, [hep-ph/9904383].

[71] M. Gogberashvili, *Gravitational trapping for extended extra dimension*, *Int. J. Mod. Phys.* **D11** (2002) 1639–1642, [hep-ph/9908347].

[72] A. Friedman, *Über die Krümmung des Raumes (On the curvature of space)*, *Phys. Zeit.* **10** (1922) 377–386.

[73] A. Friedmann, *Über die Möglichkeit einer Welt mit konstanter negativer Krümmung des Raumes (On the possibility of a world with constant negative curvature of space)*, *Phys. Zeit.* **21** (1924) 326–332.

[74] Lemaître, G., *Un univers homogène de masse constante et de rayon croissant rendant compte de la vitesse radiale des nébuleuses extra-galactiques (A homogeneous universe of constant mass and increasing radius accounting for the radial velocity of extra-galactic nebulæ)*, *Annales de la Société Scientifique de Bruxelles* **A47** (1927) 49–56.

[75] Lemaître, G., *l'Univers en expansion (Expansion of the universe)*, *Annales de la Société Scientifique de Bruxelles* **A53** (1933) 51–85.

[76] H. P. Robertson, *Kinematics and World-Structure*, *Astrophys. J.* **82** (1935) 284.

[77] H. P. Robertson, *Kinematics and World-Structure II*, *Astrophys. J.* **83** (1936) 187.

[78] H. P. Robertson, *Kinematics and World-Structure III*, *Astrophys. J.* **83** (1936) 257.

[79] A. G. Walker, *On Milne's Theory of World-Structure*, *Proc. London Math. Soc.* **s2-42** (1937), no. 1 90–127.

[80] **WMAP** Collaboration, E. Komatsu *et. al.*, *Five-Year Wilkinson Microwave Anisotropy Probe (WMAP) Observations: Cosmological Interpretation*, `arXiv:0803.0547`.

[81] Y. B. Zeldovich, I. Y. Kobzarev, and L. B. Okun, *Cosmological Consequences of the Spontaneous Breakdown of Discrete Symmetry*, *Zh. Eksp. Teor. Fiz.* **67** (1974) 3–11. (also in *Sov. Phys. JETP*, **40** (1974) pp. 1–5).

[82] T. W. B. Kibble, *Topology of Cosmic Domains and Strings*, *J. Phys.* **A9** (1976) 1387–1398.

[83] A. H. Guth, *The Inflationary Universe: A Possible Solution to the Horizon and Flatness Problems*, *Phys. Rev.* **D23** (1981) 347–356.

[84] A. D. Linde, *A New Inflationary Universe Scenario: A Possible Solution of the Horizon, Flatness, Homogeneity, Isotropy and Primordial Monopole Problems*, *Phys. Lett.* **B108** (1982) 389–393.

[85] A. D. Linde, *Phase Transitions in Gauge Theories and Cosmology*, *Rept. Prog. Phys.* **42** (1979) 389.

[86] A. Vilenkin, *Gravitational Field of Vacuum Domain Walls and Strings*, *Phys. Rev.* **D23** (1981) 852–857.

[87] A. Vilenkin, *Gravitational Field of Vacuum Domain Walls*, *Phys. Lett.* **B133** (1983) 177–179.

[88] A. Vilenkin, *Cosmic Strings and Domain Walls*, *Phys. Rept.* **121** (1985) 263.

[89] M. Cvetic, S. Griffies, and S.-J. Rey, *Static domain walls in N=1 supergravity*, *Nucl. Phys.* **B381** (1992) 301–328, [hep-th/9201007].

[90] M. Cvetic and H. H. Soleng, *Supergravity domain walls*, *Phys. Rept.* **282** (1997) 159–223, [hep-th/9604090].

[91] G. R. Dvali and S. H. H. Tye, *Brane inflation*, *Phys. Lett.* **B450** (1999) 72–82, [hep-ph/9812483].

[92] N. Arkani-Hamed, S. Dimopoulos, N. Kaloper, and J. March-Russell, *Rapid asymmetric inflation and early cosmology in theories with sub-millimeter dimensions*, *Nucl. Phys.* **B567** (2000) 189–228, [hep-ph/9903224].

[93] P. Binetruy, C. Deffayet, and D. Langlois, *Non-conventional cosmology from a brane-universe*, *Nucl. Phys.* **B565** (2000) 269–287, [hep-th/9905012].

[94] L. Randall and R. Sundrum, *A large mass hierarchy from a small extra dimension*, *Phys. Rev. Lett.* **83** (1999) 3370–3373, [hep-ph/9905221].

[95] L. Randall and R. Sundrum, *An alternative to compactification*, *Phys. Rev. Lett.* **83** (1999) 4690–4693, [hep-th/9906064].

[96] E. G. Adelberger *et. al.*, *Constraints on exotic interactions from a recent test of the gravitational inverse square law*, *Phys. Rev. Lett.* **98** (2007) 131104, [hep-ph/0611223].

[97] V. A. Rubakov, *Large and infinite extra dimensions: An introduction*, *Phys. Usp.* **44** (2001) 871–893, [hep-ph/0104152].

[98] C. Csaki, *TASI lectures on extra dimensions and branes*, in *Boulder 2002, Particle physics and cosmology*, pp. 605–698, 2002. [hep-ph/0404096].

[99] A. Pérez-Lorenzana, *An introduction to extra dimensions*, *J. Phys. Conf. Ser.* **18** (2005) 224–269, [hep-ph/0503177].

[100] E. Kiritsis, *D-branes in standard model building, gravity and cosmology*, *Fortsch. Phys.* **52** (2004) 200–263, [hep-th/0310001].

[101] C. Csaki, M. Graesser, C. F. Kolda, and J. Terning, *Cosmology of one extra dimension with localized gravity*, *Phys. Lett.* **B462** (1999) 34–40, [hep-ph/9906513].

[102] J. M. Cline, C. Grojean, and G. Servant, *Cosmological expansion in the presence of extra dimensions*, *Phys. Rev. Lett.* **83** (1999) 4245, [hep-ph/9906523].

[103] D. J. H. Chung and K. Freese, *Cosmological challenges in theories with extra dimensions and remarks on the horizon problem*, *Phys. Rev.* **D61** (2000) 023511, [hep-ph/9906542].

[104] P. Kanti, I. I. Kogan, K. A. Olive, and M. Pospelov, *Cosmological 3-brane solutions*, *Phys. Lett.* **B468** (1999) 31–39, [hep-ph/9909481].

[105] P. Binetruy, C. Deffayet, U. Ellwanger, and D. Langlois, *Brane cosmological evolution in a bulk with cosmological constant*, *Phys. Lett.* **B477** (2000) 285–291, [hep-th/9910219].

[106] E. E. Flanagan, S. H. H. Tye, and I. Wasserman, *Cosmological expansion in the Randall-Sundrum brane world scenario*, *Phys. Rev.* **D62** (2000) 044039, [hep-ph/9910498].

[107] J. M. Cline, *Braneworld cosmology*, *PoS* **STRINGSLHC** (2006) 011, [arXiv:0704.2198].

[108] N. Kaloper, *Bent domain walls as braneworlds*, *Phys. Rev.* **D60** (1999) 123506, [hep-th/9905210].

[109] K. Skenderis and P. K. Townsend, *Gravitational stability and renormalization-group flow*, *Phys. Lett.* **B468** (1999) 46–51, [hep-th/9909070].

[110] T. Shiromizu, K.-i. Maeda, and M. Sasaki, *The Einstein equations on the 3-brane world*, *Phys. Rev.* **D62** (2000) 024012, [gr-qc/9910076].

[111] M. Cvetic and J. Wang, *Vacuum domain walls in D-dimensions: Local and global space-time structure*, *Phys. Rev.* **D61** (2000) 124020, [hep-th/9912187].

[112] E. E. Flanagan, S. H. H. Tye, and I. Wasserman, *Brane world models with bulk scalar fields*, *Phys. Lett.* **B522** (2001) 155–165, [hep-th/0110070].

[113] J. M. Maldacena, *The large N limit of superconformal field theories and supergravity*, *Adv. Theor. Math. Phys.* **2** (1998) 231–252, [hep-th/9711200].

[114] H. L. Verlinde, *Holography and compactification*, *Nucl. Phys.* **B580** (2000) 264–274, [hep-th/9906182].

[115] M. J. Duff and J. T. Liu, *Complementarity of the Maldacena and Randall-Sundrum pictures*, *Class. Quant. Grav.* **18** (2001) 3207–3214, [hep-th/0003237].

[116] A. Hebecker and J. March-Russell, *Randall-Sundrum II cosmology, AdS/CFT, and the bulk black hole*, *Nucl. Phys.* **B608** (2001) 375–393, [hep-ph/0103214].

[117] J. D. Lykken and L. Randall, *The shape of gravity*, *JHEP* **06** (2000) 014, [hep-th/9908076].

[118] A. Karch and L. Randall, *Locally localized gravity*, *JHEP* **05** (2001) 008, [hep-th/0011156].

[119] W. D. Goldberger and M. B. Wise, *Bulk fields in the Randall-Sundrum compactification scenario*, *Phys. Rev.* **D60** (1999) 107505, [hep-ph/9907218].

[120] T. Gherghetta and A. Pomarol, *Bulk fields and supersymmetry in a slice of AdS*, *Nucl. Phys.* **B586** (2000) 141–162, [hep-ph/0003129].

[121] P. Mounaix and D. Langlois, *Cosmological equations for a thick brane*, *Phys. Rev.* **D65** (2002) 103523, [gr-qc/0202089].

[122] D. Langlois, *Brane cosmology: An introduction*, *Prog. Theor. Phys. Suppl.* **148** (2003) 181–212, [hep-th/0209261].

[123] P. Brax and C. van de Bruck, *Cosmology and brane worlds: A review*, *Class. Quant. Grav.* **20** (2003) R201–R232, [hep-th/0303095].

[124] P. Brax, C. van de Bruck, and A.-C. Davis, *Brane world cosmology*, *Rept. Prog. Phys.* **67** (2004) 2183–2232, [hep-th/0404011].

[125] R. Maartens, *Brane-world gravity*, *Living Rev. Rel.* **7** (2004) 7, [gr-qc/0312059].

[126] S. H. Henry Tye, *Brane inflation: String theory viewed from the cosmos*, *Lect. Notes Phys.* **737** (2008) 949–974, [hep-th/0610221].

[127] P. Kraus, *Dynamics of anti-de Sitter domain walls*, *JHEP* **12** (1999) 011, [hep-th/9910149].

[128] A. Kehagias and E. Kiritsis, *Mirage cosmology*, *JHEP* **11** (1999) 022, [hep-th/9910174].

[129] D. Ida, *Brane-world cosmology*, *JHEP* **09** (2000) 014, [gr-qc/9912002].

[130] S. Mukohyama, T. Shiromizu, and K.-i. Maeda, *Global structure of exact cosmological solutions in the brane world*, *Phys. Rev.* **D62** (2000) 024028, [hep-th/9912287].

[131] H. B. Kim and H. D. Kim, *Inflation and gauge hierarchy in Randall-Sundrum compactification*, *Phys. Rev.* **D61** (2000) 064003, [hep-th/9909053].

[132] D. N. Vollick, *Cosmology on a three-brane*, *Class. Quant. Grav.* **18** (2001) 1–10, [hep-th/9911181].

[133] R. Maartens, D. Wands, B. A. Bassett, and I. Heard, *Chaotic inflation on the brane*, *Phys. Rev.* **D62** (2000) 041301, [hep-ph/9912464].

[134] R. N. Mohapatra, A. Pérez-Lorenzana, and C. A. de Sousa Pires, *Inflation in models with large extra dimensions driven by a bulk scalar field*, *Phys. Rev.* **D62** (2000) 105030, [hep-ph/0003089].

[135] E. J. Copeland, A. R. Liddle, and J. E. Lidsey, *Steep inflation: Ending braneworld inflation by gravitational particle production*, *Phys. Rev.* **D64** (2001) 023509, [astro-ph/0006421].

[136] S. H. S. Alexander, *Inflation from D - anti-D brane annihilation*, *Phys. Rev.* **D65** (2002) 023507, [hep-th/0105032].

[137] G. R. Dvali, Q. Shafi, and S. Solganik, *D-brane inflation*, hep-th/0105203.

[138] D. Langlois, *Brane cosmological perturbations*, *Phys. Rev.* **D62** (2000) 126012, [hep-th/0005025].

[139] D. Langlois, R. Maartens, and D. Wands, *Gravitational waves from inflation on the brane*, *Phys. Lett.* **B489** (2000) 259–267, [hep-th/0006007].

[140] T. Hiramatsu, K. Koyama, and A. Taruya, *Evolution of gravitational waves from inflationary brane-world: Numerical study of high-energy effects*, *Phys. Lett.* **B578** (2004) 269–275, [hep-th/0308072].

[141] R. Easther, D. Langlois, R. Maartens, and D. Wands, *Evolution of gravitational waves in Randall-Sundrum cosmology*, *JCAP* **0310** (2003) 014, [hep-th/0308078].

[142] L. Randall and G. Servant, *Gravitational Waves from Warped Spacetime*, *JHEP* **05** (2007) 054, [hep-ph/0607158].

[143] R. H. Brandenberger and C. Vafa, *Superstrings in the Early Universe*, *Nucl. Phys.* **B316** (1989) 391.

[144] S. Alexander, R. H. Brandenberger, and D. Easson, *Brane gases in the early universe*, *Phys. Rev.* **D62** (2000) 103509, [hep-th/0005212].

[145] C. P. Burgess *et. al.*, *The Inflationary Brane-Antibrane Universe*, *JHEP* **07** (2001) 047, [hep-th/0105204].

[146] A. Karch and L. Randall, *Relaxing to three dimensions*, *Phys. Rev. Lett.* **95** (2005) 161601, [hep-th/0506053].

[147] N. Arkani-Hamed, S. Dimopoulos, G. R. Dvali, and N. Kaloper, *Infinitely large new dimensions*, *Phys. Rev. Lett.* **84** (2000) 586–589, [hep-th/9907209].

[148] C. Csaki and Y. Shirman, *Brane junctions in the Randall-Sundrum scenario*, *Phys. Rev.* **D61** (2000) 024008, [hep-th/9908186].

[149] A. E. Nelson, *A new angle on intersecting branes in infinite extra dimensions*, *Phys. Rev.* **D63** (2001) 087503, [hep-th/9909001].

[150] A. Chodos and E. Poppitz, *Warp factors and extended sources in two transverse dimensions*, *Phys. Lett.* **B471** (1999) 119–127, [hep-th/9909199].

[151] N. Kaloper, *Crystal manyfold universes in AdS space*, *Phys. Lett.* **B474** (2000) 269–281, [hep-th/9912125].

[152] T. Gherghetta and M. E. Shaposhnikov, *Localizing gravity on a string-like defect in six dimensions*, *Phys. Rev. Lett.* **85** (2000) 240–243, [hep-th/0004014].

[153] Y.-X. Liu, L. Zhao, and Y.-S. Duan, *Localization of Fermions on a String-like Defect*, *JHEP* **04** (2007) 097, [hep-th/0701010].

[154] T. Gherghetta, E. Roessl, and M. E. Shaposhnikov, *Living inside a hedgehog: Higher-dimensional solutions that localize gravity*, *Phys. Lett.* **B491** (2000) 353–361, [hep-th/0006251].

[155] S. M. Carroll, S. Hellerman, and M. Trodden, *BPS domain wall junctions in infinitely large extra dimensions*, *Phys. Rev.* **D62** (2000) 044049, [hep-th/9911083].

[156] S.-k. Nam, *Modeling a network of brane worlds*, *JHEP* **03** (2000) 005, [hep-th/9911104].

[157] D. Lust, *Intersecting brane worlds: A path to the standard model?*, *Class. Quant. Grav.* **21** (2004) S1399–1424, [hep-th/0401156].

[158] R. Blumenhagen, M. Cvetic, P. Langacker, and G. Shiu, *Toward realistic intersecting D-brane models*, *Ann. Rev. Nucl. Part. Sci.* **55** (2005) 71–139, [hep-th/0502005].

[159] N. Kaloper, J. March-Russell, G. D. Starkman, and M. Trodden, *Compact hyperbolic extra dimensions: Branes, Kaluza-Klein modes and cosmology*, *Phys. Rev. Lett.* **85** (2000) 928–931, [hep-ph/0002001].

[160] G. D. Starkman, D. Stojkovic, and M. Trodden, *Large extra dimensions and cosmological problems*, *Phys. Rev.* **D63** (2001) 103511, [hep-th/0012226].

[161] G. D. Starkman, D. Stojkovic, and M. Trodden, *Homogeneity, flatness and 'large' extra dimensions*, *Phys. Rev. Lett.* **87** (2001) 231303, [hep-th/0106143].

[162] S. Nasri, P. J. Silva, G. D. Starkman, and M. Trodden, *Radion stabilization in compact hyperbolic extra dimensions*, *Phys. Rev.* **D66** (2002) 045029, [hep-th/0201063].

[163] W. D. Goldberger and M. B. Wise, *Modulus stabilization with bulk fields*, *Phys. Rev. Lett.* **83** (1999) 4922–4925, [hep-ph/9907447].

[164] P. J. Steinhardt, *General considerations of the cosmological constant and the stabilization of moduli in the brane-world picture*, *Phys. Lett.* **B462** (1999) 41–47, [hep-th/9907080].

[165] O. DeWolfe, D. Z. Freedman, S. S. Gubser, and A. Karch, *Modeling the fifth dimension with scalars and gravity*, *Phys. Rev.* **D62** (2000) 046008, [hep-th/9909134].

[166] C. Csaki, M. Graesser, L. Randall, and J. Terning, *Cosmology of brane models with radion stabilization*, *Phys. Rev.* **D62** (2000) 045015, [hep-ph/9911406].

[167] W. D. Goldberger and M. B. Wise, *Phenomenology of a stabilized modulus*, *Phys. Lett.* **B475** (2000) 275–279, [hep-ph/9911457].

[168] Z. Chacko and A. E. Nelson, *A solution to the hierarchy problem with an infinitely large extra dimension and moduli stabilization*, *Phys. Rev.* **D62** (2000) 085006, [hep-th/9912186].

[169] C. Csaki, J. Erlich, C. Grojean, and T. J. Hollowood, *General properties of the self-tuning domain wall approach to the cosmological constant problem*, *Nucl. Phys.* **B584** (2000) 359–386, [hep-th/0004133].

[170] T. Boehm, R. Durrer, and C. van de Bruck, *Dynamical instabilities of the Randall-Sundrum model*, *Phys. Rev.* **D64** (2001) 063504, [hep-th/0102144].

[171] S. M. Carroll, J. Geddes, M. B. Hoffman, and R. M. Wald, *Classical stabilization of homogeneous extra dimensions*, *Phys. Rev.* **D66** (2002) 024036, [hep-th/0110149].

[172] A. Chamblin and G. W. Gibbons, *Nonlinear supergravity on a brane without compactification*, *Phys. Rev. Lett.* **84** (2000) 1090–1093, [hep-th/9909130].

[173] M. Gremm, *Four-dimensional gravity on a thick domain wall*, *Phys. Lett.* **B478** (2000) 434–438, [hep-th/9912060].

[174] C. Csaki, J. Erlich, T. J. Hollowood, and Y. Shirman, *Universal aspects of gravity localized on thick branes*, *Nucl. Phys.* **B581** (2000) 309–338, [hep-th/0001033].

[175] M. Gremm, *Thick domain walls and singular spaces*, *Phys. Rev.* **D62** (2000) 044017, [hep-th/0002040].

[176] F. Brito, M. Cvetic, and S. Yoon, *From a thick to a thin supergravity domain wall*, *Phys. Rev.* **D64** (2001) 064021, [hep-ph/0105010].

[177] R. Guerrero, A. Melfo, and N. Pantoja, *Self-gravitating domain walls and the thin-wall limit*, *Phys. Rev.* **D65** (2002) 125010, [gr-qc/0202011].

[178] R. P. Geroch and J. H. Traschen, *Strings and Other Distributional Sources in General Relativity*, *Phys. Rev.* **D36** (1987) 1017.

[179] M. Shaposhnikov, P. Tinyakov, and K. Zuleta, *The fate of the zero mode of the five-dimensional kink in the presence of gravity*, *JHEP* **09** (2005) 062, [hep-th/0508102].

[180] D. Stojkovic, *Fermionic zero modes on domain walls*, *Phys. Rev.* **D63** (2001) 025010, [hep-ph/0007343].

[181] A. Melfo, N. Pantoja, and J. D. Tempo, *Fermion localization on thick branes*, *Phys. Rev.* **D73** (2006) 044033, [hep-th/0601161].

[182] T. R. Slatyer and R. R. Volkas, *Cosmology and Fermion Confinement in a Scalar-Field-Generated Domain Wall Brane in Five Dimensions*, *JHEP* **04** (2007) 062, [hep-ph/0609003].

[183] F. Dahia and C. Romero, *Confinement and stability of the motion of test particles in thick branes*, *Phys. Lett.* **B651** (2007) 232–238, [gr-qc/0702011].

[184] Y.-Z. Chu and T. Vachaspati, *Fermions on one or fewer Kinks*, *Phys. Rev.* **D77** (2008) 025006, [arXiv:0709.3668].

[185] Y.-X. Liu, L.-D. Zhang, L.-J. Zhang, and Y.-S. Duan, *Fermions on Thick Branes in Background of Sine-Gordon Kinks*, arXiv:0804.4553.

[186] S. L. Dubovsky, V. A. Rubakov, and P. G. Tinyakov, *Brane world: Disappearing massive matter*, *Phys. Rev.* **D62** (2000) 105011, [hep-th/0006046].

[187] C. Ringeval, P. Peter, and J.-P. Uzan, *Localization of massive fermions on the brane*, *Phys. Rev.* **D65** (2002) 044016, [hep-th/0109194].

[188] A. Kehagias and K. Tamvakis, *Localized gravitons, gauge bosons and chiral fermions in smooth spaces generated by a bounce*, *Phys. Lett.* **B504** (2001) 38–46, [hep-th/0010112].

[189] D. Bazeia, A. R. Gomes, and L. Losano, *Gravity localization on thick branes: a numerical approach*, arXiv:0708.3530.

[190] M. Cvetic and M. Robnik, *Gravity Trapping on a Finite Thickness Domain Wall: An Analytic Study*, *Phys. Rev.* **D77** (2008) 124003, [arXiv:0801.0801].

[191] M. Minamitsuji, W. Naylor, and M. Sasaki, *Can thick braneworlds be self-consistent?*, *Phys. Lett.* **B633** (2006) 607, [hep-th/0510117].

[192] Y.-i. Takamizu and K.-i. Maeda, *Collision of domain walls and reheating of the brane universe*, *Phys. Rev.* **D70** (2004) 123514, [hep-th/0406235].

[193] G. Gibbons, K.-i. Maeda, and Y.-i. Takamizu, *Fermions on colliding branes*, *Phys. Lett.* **B647** (2007) 1–7, [hep-th/0610286].

[194] Y.-i. Takamizu, H. Kudoh, and K.-i. Maeda, *Dynamics of colliding branes and black brane production*, *Phys. Rev.* **D75** (2007) 061304, [gr-qc/0702138].

[195] P. M. Saffin and A. Tranberg, *Particle transfer in braneworld collisions*, *JHEP* **08** (2007) 072, [arXiv:0705.3606].

[196] P. M. Saffin and A. Tranberg, *The fermion spectrum in braneworld collisions*, *JHEP* **12** (2007) 053, [arXiv:0710.3272].

[197] G. A. Palma, *Gauge-Higgs unification on the brane*, *J. Phys. Conf. Ser.* **53** (2006) 621–634, [hep-th/0701174].

[198] C. Adam, N. Grandi, J. Sanchez-Guillen, and A. Wereszczynski, *K fields, compactons, and thick branes*, *J. Phys.* **A41** (2008) 212004, [arXiv:0711.3550].

[199] J. S. Rozowsky, R. R. Volkas, and K. C. Wali, *Domain wall solutions with Abelian gauge fields*, *Phys. Lett.* **B580** (2004) 249–256, [hep-th/0305232].

[200] E. M. Shin and R. R. Volkas, *O(10) kinks: Clash of symmetries on the brane and the gauge hierarchy problem*, *Phys. Rev.* **D69** (2004) 045010, [hep-ph/0309008].

[201] A. Demaria and R. R. Volkas, *Kink-induced symmetry breaking patterns in brane-world $SU(3)^3$ trinification models*, *Phys. Rev.* **D71** (2005) 105011, [hep-ph/0503224].

[202] G. Dando, A. Davidson, D. P. George, R. R. Volkas, and K. C. Wali, *The clash of symmetries in a Randall-Sundrum-like spacetime*, *Phys. Rev.* **D72** (2005) 045016, [hep-ph/0507097].

[203] L. Pogosian and T. Vachaspati, *Domain walls in SU(5)*, *Phys. Rev.* **D62** (2000) 123506, [hep-ph/0007045].

[204] T. Vachaspati, *A class of kinks in SU(N) x Z(2)*, *Phys. Rev.* **D63** (2001) 105010, [hep-th/0102047].

[205] L. Pogosian and T. Vachaspati, *Space of kink solutions in SU(N) x Z(2)*, *Phys. Rev.* **D64** (2001) 105023, [hep-th/0105128].

[206] W. H. Press, S. A. Teukolsky, W. T. Vetterling, and B. P. Flannery, *Numerical Recipes in C: The Art of Scientific Computing*. Cambridge University Press, 1992.

[207] Y. Burnier and K. Zuleta, "Effective action of a five-dimensional domain wall." 2008. [arXiv:0812.2227].

[208] J. R. Morris, *Domain defects in strings and walls*, *Phys. Rev.* **D51** (1995) 697–702.

[209] P. Q. Hung and N.-K. Tran, *Kaluza-Klein structure associated with fat brane*, *Phys. Rev.* **D69** (2004) 064003, [hep-ph/0309115].

[210] A. S. de Castro and M. B. Hott, *Trapping neutral fermions with kink-like potentials*, *Phys. Lett.* **A351** (2006) 379–383, [hep-th/0511129].

[211] A. Davidson and P. D. Mannheim, "Dynamical localization of gravity." 2000. [hep-th/0009064].

[212] B. Bajc and G. Gabadadze, *Localization of matter and cosmological constant on a brane in anti de Sitter space*, *Phys. Lett.* **B474** (2000) 282–291, [hep-th/9912232].

[213] S. Kobayashi, K. Koyama, and J. Soda, *Thick brane worlds and their stability*, *Phys. Rev.* **D65** (2002) 064014, [hep-th/0107025].

[214] E. Witten, *Superconducting Strings*, *Nucl. Phys.* **B249** (1985) 557–592.

[215] C. A. S. Almeida, J. Ferreira, M. M., A. R. Gomes, and R. Casana, *Fermion localization and resonances on two-field thick branes*, arXiv:0901.3543.

[216] G. 't Hooft, *Gauge Fields with Unified Weak, Electromagnetic, and Strong Interactions*, . Rapporteur's talk given at Int. Conf. on High Energy Physics, Palermo, Italy, Jun 23-28, 1975.

[217] S. Mandelstam, *Vortices and quark confinement in non-Abelian gauge theories*, *Phys. Rept.* **23** (1976) 245–249.

[218] M. Creutz, *Confinement and the Critical Dimensionality of Space-Time*, *Phys. Rev. Lett.* **43** (1979) 553–556.

[219] M. Laine, H. B. Meyer, K. Rummukainen, and M. Shaposhnikov, *Effective gauge theories on domain walls via bulk confinement?*, *JHEP* **04** (2004) 027, [hep-ph/0404058].

[220] A. Coulthurst, K. L. McDonald, and B. H. J. McKellar, *Suppressing Proton Decay By Separating Quarks And Leptons*, *Phys. Rev.* **D74** (2006) 127701, [hep-ph/0610345].

[221] E. B. Dynkin, *Semisimple subalgebras of semisimple Lie algebras*, *Mat. Sb. (N.S.)* **30(72)** (1952) 349–462.

[222] G. R. Dvali and M. A. Shifman, *Dynamical compactification as a mechanism of spontaneous supersymmetry breaking*, *Nucl. Phys.* **B504** (1997) 127–146, [hep-th/9611213].

[223] L.-F. Li, *Group Theory of the Spontaneously Broken Gauge Symmetries*, *Phys. Rev.* **D9** (1974) 1723–1739.

[224] O. Kaymakcalan, L. Michel, K. C. Wali, W. D. McGlinn, and L. O'Raifeartaigh, *Absolute minima of a SO(10) invariant Higgs potential*, *Nucl. Phys.* **B267** (1986) 203.

[225] G. Racah *Lincei. Rend. Sci. Fis. Mat. Nat.* **8** (1950) 108.

[226] J. A. Harvey, *Patterns of symmetry breaking in the exceptional groups*, *Nucl. Phys.* **B163** (1980) 254.

[227] M. Bando and T. Kugo, *Neutrino masses in E(6) unification*, *Prog. Theor. Phys.* **101** (1999) 1313–1333, [hep-ph/9902204].

[228] M. Bando, T. Kugo, and K. Yoshioka, *Mass Matrices in E6 Unification*, *Prog. Theor. Phys.* **104** (2000) 211–236, [hep-ph/0003220].

[229] G. W. Anderson and T. Blazek, *E(6) unification model building. I: Clebsch-Gordan coefficients of 27 x 27-bar*, *J. Math. Phys.* **41** (2000) 4808–4816, [hep-ph/9912365].

[230] N. Maekawa and T. Yamashita, *Flipped SO(10) model*, *Phys. Lett.* **B567** (2003) 330–338, [hep-ph/0304293].

[231] N. Chatillon, C. Macesanu, and M. Trodden, *Brane cosmology in an arbitrary number of dimensions*, *Phys. Rev.* **D74** (2006) 124004, [gr-qc/0609093].

[232] V. I. Afonso, D. Bazeia, and L. Losano, *First-order formalism for bent brane*, *Phys. Lett.* **B634** (2006) 526–530, [hep-th/0601069].

[233] V. Dzhunushaliev, V. Folomeev, D. Singleton, and S. Aguilar-Rudametkin, *Thick branes from scalar fields*, *Phys. Rev.* **D77** (2008) 044006, [hep-th/0703043].

[234] V. Dzhunushaliev, V. Folomeev, K. Myrzakulov, and R. Myrzakulov, *Thick brane in 7D and 8D spacetimes*, *Gen. Rel. Grav.* **41** (2009) 131–146, [arXiv:0705.4014].

[235] V. Dzhunushaliev, V. Folomeev, and M. Minamitsuji, *Thick de Sitter brane solutions in higher dimensions*, *Phys. Rev.* **D79** (2009) 024001, [arXiv:0809.4076].

[236] C. W. Misner, K. S. Thorne, and J. A. Wheeler, *Gravitation*. W. H. Freeman and Co., 1973.

[237] L. D. Landau and E. M. Lifshitz, *The Classical Theory of Fields*. Pergamon Press, Fourth revised English ed., 1975.

[238] S. Weinberg, *Gravitation and cosmology*. John Wiley & Sons, 1972.

[239] N. Rosen and P. M. Morse, *On the Vibrations of Polyatomic Molecules*, *Phys. Rev.* **42** (oct, 1932) 210–217.

[240] M. M. Nieto, *Exact wave-function normalization constants for the $B_0 \tanh z$-$U_0 \cosh^{-2} z$ and Pöschl-Teller potentials*, *Phys. Rev.* **A17** (1978) 1273.

[241] A. Gangopadhyaya and J. V. Mallow, *Ab Initio Method for Obtaining Exactly Solvable Quantum Mechanical Potentials*, arXiv:0708.2454.

[242] C.-L. Ho, "Simple unified derivation and solution of Coulomb, Eckart and Rosen-Morse potentials in prepotential approach." 2008. [arXiv:0809.5253].

[243] H. C. Lee, ed., *An introduction to Kaluza-Klein theories*. World Scientific Publishing Co Pte Ltd., 1984.

[244] G. Ekspong, ed., *The Oskar Klein Memorial Lectures*, vol. 1. World Scientific Publishing Co. Pte. Ltd., 1991.

Appendix A

Conventions, definitions and identities

Here we state the important conventions and definitions used throughout this thesis, including the sign choices we have made when working with general relativity, along with some useful identities and limits. The vielbein formalism is also briefly outlined. Our notation for the commutator of A and B is $[A, B] \equiv AB - BA$, and for the anti-commutator, $\{A, B\} \equiv AB + BA$.

A.1 Spinors

The Pauli matrices are

$$\sigma_1 = \begin{pmatrix} 0 & 1 \\ 1 & 0 \end{pmatrix}, \qquad \sigma_2 = \begin{pmatrix} 0 & -i \\ i & 0 \end{pmatrix}, \qquad \sigma_3 = \begin{pmatrix} 1 & 0 \\ 0 & -1 \end{pmatrix}, \tag{A.1}$$

and are normalised to $\{\sigma_i, \sigma_j\} = 2\delta_{ij}$, where $i, j \in \{1, 2, 3\}$. In the Dirac representation, the four Gamma matrices are

$$\gamma^0 = \begin{pmatrix} \mathbb{1} & 0 \\ 0 & -\mathbb{1} \end{pmatrix}, \qquad \gamma^i = \begin{pmatrix} 0 & \sigma_i \\ -\sigma_i & 0 \end{pmatrix}, \tag{A.2}$$

where $\mathbb{1}$ is the 2×2 identity matrix. These matrices satisfy $\{\gamma^\mu, \gamma^\nu\} = 2\eta^{\mu\nu}$, where $\mu \in \{0, 1, 2, 3\}$ and $\eta^{\mu\nu} = \mathrm{diag}(1, -1, -1, -1)$. The fifth, independent Gamma matrix is

$$\gamma^5 = i\gamma^0\gamma^1\gamma^2\gamma^3 = \begin{pmatrix} 0 & \mathbb{1} \\ \mathbb{1} & 0 \end{pmatrix}. \tag{A.3}$$

A four-dimensional spinor $\psi(x^\mu)$ in a Minkowski spacetime with metric $\eta_{\mu\nu} = (+1, -1, -1, -1)$ uses the Gamma matrices in equation (A.2). Its left- and right-chiral components are, respectively,

$$\psi_L = \frac{1}{2}(1 - \gamma^5)\psi \,, \tag{A.4a}$$

$$\psi_R = \frac{1}{2}(1 + \gamma^5)\psi \,, \tag{A.4b}$$

and its charge conjugate is

$$\psi^c = \gamma^2 \psi^* \,. \tag{A.5}$$

In five-dimensions, a fermion $\Psi(x^M)$, where $M \in \{0, 1, 2, 3, 5\}$, uses the Gamma matrices Γ^M defined by $\{\Gamma^M, \Gamma^N\} = 2\eta^{MN}$. There is a choice for the signature of the Minkowski metric, and an associated choice for the Gamma matrices:

$$\eta_{MN} = \mathrm{diag}(+1, -1, -1, -1, -1) \quad \text{has} \quad \Gamma^M = (\gamma^\mu, -i\gamma^5) \,, \tag{A.6a}$$

$$\eta_{MN} = \mathrm{diag}(-1, +1, +1, +1, +1) \quad \text{has} \quad \Gamma^M = (i\gamma^\mu, \gamma^5) \,. \tag{A.6b}$$

In both cases the five-dimensional charge conjugate is defined by

$$\Psi^c = \Gamma^2 \Gamma^5 \Psi^* \,. \tag{A.7}$$

A.2 Some useful integrals and limits

An integral which is often used when integrating out the extra-dimension to obtain an effective, four-dimensional action is:

$$\int_{-\infty}^{\infty} \cosh^{-2a}(z)\, dz = \frac{\sqrt{\pi}\,\Gamma(a)}{\Gamma(a + \frac{1}{2})} \qquad \text{if } \Re(a) > 0 \,. \tag{A.8}$$

Some relevant limits of the generalised factorial function $\Gamma(z)$ are:

$$\lim_{a \to 0} \frac{\Gamma(a + n)}{a\,\Gamma(a)} = \Gamma(n) \,, \tag{A.9a}$$

$$\lim_{a \to \infty} \frac{\Gamma(a + n)}{a^n\,\Gamma(a)} = 1 \,. \tag{A.9b}$$

The Dirac delta-distribution can be related by two limits to the hyperbolic-cosine function:

$$\delta(x) = \lim_{a\to\infty} \frac{\Gamma(a+\frac{1}{2})}{\sqrt{\pi}\,\Gamma(a)}\, b\cosh^{-2a}(bx)\,, \tag{A.10a}$$

$$\delta(x) = \lim_{b\to\infty} \frac{\Gamma(a+\frac{1}{2})}{\sqrt{\pi}\,\Gamma(a)}\, b\cosh^{-2a}(bx)\,. \tag{A.10b}$$

A.3 Sign conventions for general relativity

The metric is $g_{\mu\nu}$, and our conventions for the Christoffel symbols (connection coefficients), Riemann curvature tensor, Ricci tensor, Ricci scalar and Einstein tensor are, respectively,

$$\Gamma^{\sigma}_{\mu\nu} = \frac{1}{2} g^{\sigma\rho}\left(\partial_\nu g_{\rho\mu} + \partial_\mu g_{\rho\nu} - \partial_\rho g_{\mu\nu}\right)\,, \tag{A.11a}$$

$$R^{\mu}{}_{\nu\sigma\rho} = \partial_\sigma \Gamma^{\mu}_{\nu\rho} - \partial_\rho \Gamma^{\mu}_{\nu\sigma} + \Gamma^{\mu}_{\lambda\sigma}\Gamma^{\lambda}_{\nu\rho} - \Gamma^{\mu}_{\lambda\rho}\Gamma^{\lambda}_{\nu\sigma}\,, \tag{A.11b}$$

$$R_{\mu\nu} = R^{\sigma}{}_{\mu\sigma\nu}\,, \tag{A.11c}$$

$$R = g^{\mu\nu} R_{\mu\nu}\,, \tag{A.11d}$$

$$G_{\mu\nu} = R_{\mu\nu} - \frac{1}{2} g_{\mu\nu} R\,. \tag{A.11e}$$

The choices that we have made are for the signs of the Riemann tensor (A.11b) and the Ricci tensor (A.11c). This implies that the Einstein equation is $G_{\mu\nu} = 8\pi G_N T_{\mu\nu}$, where G_N is Newton's constant, and $T_{\mu\nu}$ is the stress-energy tensor. In terms of Misner, Thorne and Wheeler [236] (MTW), this choice corresponds to a + for column 3 and a + for column 4. And we also have $T_{00} \geq 0$. We then get a choice for the signature of the metric, either space-like or time-like, corresponding to column 2 of MTW. Such a choice constrains the sign for the kinetic terms in the action, such that, if A is some field, then the term $(\partial_t A)^2$ appears as a positive quantity. This is true for all fields, including the metric (see the end of §93 of Landau and Lifshitz [237], page 270).

Space-like metric

For a space-like metric, with signature $(-\,+\,+\,+)$, which corresponds to MTW's $+\,+\,+$, the Ricci scalar appears with a *positive* coefficient, but, for example, the kinetic term for a scalar field appears with a negative

coefficient. The action, Einstein's equations and the stress-energy tensor are

$$\mathcal{S} = \int d^4x\sqrt{-g}\left[M_{\rm Pl}^2(R-2\Lambda)+\mathcal{L}_{\rm matter}\right]\,, \tag{A.12a}$$

$$G_{\mu\nu} = \frac{1}{2M_{\rm Pl}^2}T_{\mu\nu} - g_{\mu\nu}\Lambda\,, \tag{A.12b}$$

$$T_{\mu\nu} = -2\frac{\partial\mathcal{L}_{\rm matter}}{\partial g^{\mu\nu}} + g_{\mu\nu}\mathcal{L}_{\rm matter}\,. \tag{A.12c}$$

Here, $M_{\rm Pl}^2 = 1/16\pi G_N$, the constant Λ is an optional bulk cosmological constant, and $\mathcal{L}_{\rm matter}$ includes any matter or gauge fields. For a real scalar field, the Lagrangian and stress-energy tensor are

$$\mathcal{L}_{\rm matter} = -\frac{1}{2}g^{\mu\nu}\partial_\mu\phi\partial_\nu\phi - \frac{1}{2}m^2\phi^2\,, \tag{A.13a}$$

$$T_{\mu\nu} = \partial_\mu\phi\partial_\nu\phi - \frac{1}{2}g_{\mu\nu}\left(g^{\sigma\rho}\partial_\sigma\phi\partial_\rho\phi + m^2\phi^2\right)\,. \tag{A.13b}$$

Time-like metric

For a time-like metric, with signature $(+---)$, which corresponds to MTW's $-+++$, the Ricci scalar must appear with a *negative* coefficient, while other fields have kinetic terms with their usual appearance. The action, Einstein's equations and the stress-energy tensor are

$$\mathcal{S} = \int d^4x\sqrt{-g}\left[M_{\rm Pl}^2(-R-2\Lambda)+\mathcal{L}_{\rm matter}\right]\,, \tag{A.14a}$$

$$G_{\mu\nu} = \frac{1}{2M_{\rm Pl}^2}T_{\mu\nu} + g_{\mu\nu}\Lambda\,, \tag{A.14b}$$

$$T_{\mu\nu} = +2\frac{\partial\mathcal{L}_{\rm matter}}{\partial g^{\mu\nu}} - g_{\mu\nu}\mathcal{L}_{\rm matter}\,. \tag{A.14c}$$

For a real scalar field, the Lagrangian and stress-energy tensor are

$$\mathcal{L}_{\rm matter} = \frac{1}{2}g^{\mu\nu}\partial_\mu\phi\partial_\nu\phi - \frac{1}{2}m^2\phi^2\,, \tag{A.15a}$$

$$T_{\mu\nu} = \partial_\mu\phi\partial_\nu\phi - \frac{1}{2}g_{\mu\nu}\left(g^{\sigma\rho}\partial_\sigma\phi\partial_\rho\phi - m^2\phi^2\right)\,. \tag{A.15b}$$

In flat space, for both choices of the signature, we have $T_{00} = \frac{1}{2}\dot{\phi}^2 + \frac{1}{2}|\vec{\nabla}\phi|^2 + \frac{1}{2}m^2\phi^2$.

A.4 The vielbein formalism

We know a lot about Minkowski spacetime, which is described by the metric $\eta_{\alpha\beta}$, and for which we build actions that are Lorentz scalars. In constructing an action which respects the general coordinate transformations of general relativity, we can use the vierbein $e^{\alpha}{}_{\mu}(x^{\rho})$ (or vielbein as we shall call it for a spacetime of arbitrary dimension) to turn a local Lorentz vector at point x^{ρ}, with index α, into a general coordinate vector, with index μ. The metric of the general spacetime is then

$$g_{\mu\nu} = e^{\alpha}{}_{\mu}\, e^{\beta}{}_{\nu}\, \eta_{\alpha\beta}\,. \tag{A.16a}$$

Note that $\eta_{\alpha\beta}$ is a constant diagonal metric, while $g_{\mu\nu}$ can depend on the spacetime coordinate. The vielbeins specify $g_{\mu\nu}$ up to a Lorentz transformation. The inverse vielbein $e_{\alpha}{}^{\mu}$ satisfies

$$e^{\alpha}{}_{\mu} e_{\alpha}{}^{\nu} = \delta^{\nu}_{\mu}\,, \tag{A.17a}$$

$$e^{\alpha}{}_{\mu} e_{\beta}{}^{\mu} = \delta^{\alpha}_{\beta}\,, \tag{A.17b}$$

and we use $\eta_{\alpha\beta}$ ($\eta^{\alpha\beta}$) to lower (raise) Lorentz indices, and $g_{\mu\nu}$ ($g^{\mu\nu}$) to lower (raise) coordinate indices.

Consider a Lorentz object ϕ that, under an infinitesimal Lorentz transformation $\Lambda^{\alpha}{}_{\beta} = \delta^{\alpha}_{\beta} + \epsilon^{\alpha}{}_{\beta}$, becomes ϕ'. We define the anti-symmetric object $\sigma^{\alpha\beta}$ by

$$\phi' = \left(1 + \frac{1}{2}\,\eta_{\alpha\gamma}\cdot\epsilon^{\gamma}{}_{\beta}\cdot\sigma^{\alpha\beta}\right)\phi\,. \tag{A.18}$$

For clarity, we use the operator '$\cdot$' to denote usual multiplication of numbers. A Lorentz vector V^{δ} transforms to $(V')^{\gamma}$ using

$$(\sigma^{\alpha\beta})^{\gamma}{}_{\delta} = \eta^{\gamma\alpha}\delta^{\beta}_{\delta} - \eta^{\gamma\beta}\delta^{\alpha}_{\delta}\,. \tag{A.19}$$

For a spinor ψ we have

$$\sigma^{\alpha\beta} = \frac{1}{4}[\gamma^{\alpha}, \gamma^{\beta}]\,, \tag{A.20}$$

where the γ^{α} are the flat space Gamma matrices defined by $\{\gamma^{\alpha}, \gamma^{\beta}\} = 2\eta^{\alpha\beta}$. The derivative which acts like a coordinate vector is then

$$\mathcal{D}_{\mu}\phi = \left(\partial_{\mu} + \frac{1}{2}\sigma^{\alpha\beta}\omega_{\mu\alpha\beta}\right)\phi\,. \tag{A.21}$$

This derivative is used to construct kinetic terms that transform as general coordinate scalars.

Of course, we have not yet specified the so-called spin connection $\omega_{\mu\alpha\beta}$. Recall that the connection coefficients $\Gamma^{\rho}_{\mu\nu}$ are used when computing derivatives of vectors and tensors in GR, and are defined by demanding that the covariant derivative of $g_{\mu\nu}$ vanishes. Similarly, we demand that the covariant derivative of the vielbein vanishes to determine the spin connection:

$$\mathcal{D}_\mu e^{\alpha}{}_{\nu} = \mathcal{D}_\mu e_{\alpha}{}^{\nu} = 0\,. \tag{A.22}$$

Since the vielbein has both Lorentz and coordinate indices, its covariant derivative has multiple components:

$$\mathcal{D}_\mu e^{\alpha}{}_{\nu} = \partial_\mu e^{\alpha}{}_{\nu} - \Gamma^{\rho}_{\mu\nu} e^{\alpha}{}_{\rho} + \frac{1}{2}(\sigma^{\gamma\delta})^{\alpha}{}_{\beta} \cdot \omega_{\mu\gamma\delta} \cdot e^{\beta}{}_{\nu}\,, \tag{A.23}$$

Substituting equation (A.19) into equation (A.23) and demanding that the latter vanishes yields

$$\omega_{\mu\alpha\beta} = e_{\alpha}{}^{\nu}\left(\partial_\mu e_{\beta\nu} - \Gamma^{\rho}_{\mu\nu} e_{\beta\rho}\right)\,. \tag{A.24}$$

This formula can be used to compute the explicit components of the spin connection. For a diagonal metric we have diagonal vielbeins, the inverse is $e_{\alpha}{}^{\mu} = (e^{\alpha}{}_{\mu})^{-1}$, and the spin connection simplifies to

$$\omega_{\mu\alpha\beta} = e_{\beta}{}^{\nu} \cdot \partial_\nu e_{\alpha\mu} - e_{\alpha}{}^{\nu} \cdot \partial_\nu e_{\beta\mu}\,, \tag{A.25}$$

which is manifestly anti-symmetric in α and β. See Weinberg [238] for a more detailed discussion of the vielbein formalism.

Appendix B

Numerical techniques

Given a function $y(x)$ that solves some differential equation, we want to use an appropriate numerical technique to find solutions for y. The technique that we use will depend on the type of differential equation, and whether we have initial conditions or boundary conditions. In this thesis, for the most part, we encounter ordinary, second order differential equations, which a lot of the time simplify to a Schrödinger-like equation. This makes the numerics much easier to handle.

For a second order differential equation with boundary conditions specified at the edges of the domain of x, the relaxation on a mesh technique provides a satisfactory way of solving for y. It can be slow if the domain is large and there are many coupled equations, as the technique requires many tens-of-thousands of iterations to converge to acceptable accuracy.

If the differential equation takes the form of a Schrödinger-like equation, we can do much better than the relaxation technique. The fourth order Runge-Kutta method is normally used to solve a first order differential equation, but it can be adapted to a second order equation with initial conditions. We can implement a version of the shooting method if we have boundary conditions rather than initial conditions.

The core equations for these two numerical techniques are given in the next two sections. Both techniques assume that the function y can be well approximated by evaluating it at evenly spaced positions along the domain of x (on a mesh). The domain of x is defined by

$$L_- \leq x \leq L_+ \,. \tag{B.1}$$

If the domain is infinite then it must be truncated. We now choose the number of divisions to split this domain into for numerical evaluation, the number being N. Equivalently, we can choose the step size between evaluation points, h. For good numerical accuracy, N should be large, meaning h should be small. It is good practice to always check a given solution with the solution computed with $2N$. Also, if the domain is symmetric about $x = 0$, it is a good idea to choose N to be even so that $x = 0$ is one of the evaluated points. Note that the number of evaluated points is $N + 1$, and we label these points with the index n, where $0 \leq n \leq N$. We then make the following definitions:

$$h = \frac{L_+ - L_-}{N} \,, \tag{B.2a}$$

$$x_n = hn + L_- \,, \tag{B.2b}$$

$$y_n = y(x_n) \,. \tag{B.2c}$$

This scheme transforms the continuous variable x into the discrete index n. In what follows, prime denotes a derivative with respect to x.

B.1 Relaxation on a mesh

Given the second order differential equation

$$y'' = R\left(y, y'\right) \,, \tag{B.3}$$

we can approximate the second derivative by a difference equation relating adjacent mesh points, and invert this equation to get

$$\overline{y}_n = \frac{1}{2}\left(y_{n+1} + y_{n-1} - h^2 R_n\right) \,. \tag{B.4}$$

The set of values $\overline{y}_n$ for all n provide an improved guess for the solution y, computed in terms of the previous guess. Equation (B.4) must be applied repeatedly for all points n until the difference between y_n's of successive iterations is sufficient small. In practice, one must take a weighted average of the old and new guesses to seed the next iteration:

$$\overline{\overline{y}}_n = \theta y_n + (1 - \theta)\overline{y}_n \,, \tag{B.5}$$

where θ is the relaxation damping parameter (we have found $\theta = 0.1$ to be a sensible choice), and $\overline{\overline{y}}_n$ are the values to use for y_n in the subsequent iteration. An initial guess must be made for y_n to begin the algorithm, which can most of the time be $y_n = 0$ for all n. The relaxation on a mesh technique can only accommodate boundary value problems, where the boundary conditions, which can be Neumann and/or Dirichlet, are used to determine y_0 and y_N. If the problem consists of multiple, coupled, second order differential equations, then one can just apply equations (B.4) and (B.5) to each function in succession, and repeat this for each iteration.

B.2 Twofold fourth-order Runge-Kutta

The fourth order Runge-Kutta technique is used to solve first order differential equations of the form

$$y' = F(x, y) \,, \tag{B.6}$$

with given initial condition $y(L_-)$. This technique is not iterative. Rather, it computes y at the next point in terms of y and F at previous points:

$$y_{n+1} = y_n + \frac{h}{6}\left(k_1 + 2k_2 + 2k_3 + k_4\right) + \mathcal{O}(h^5) \,, \tag{B.7}$$

where

$$k_1 = F(x_n, y_n) \,, \tag{B.8a}$$
$$k_2 = F(x_n + \tfrac{1}{2}h, y_n + \tfrac{1}{2}hk_1) \,, \tag{B.8b}$$
$$k_3 = F(x_n + \tfrac{1}{2}h, y_n + \tfrac{1}{2}hk_2) \,, \tag{B.8c}$$
$$k_4 = F(x_n + h, y_n + hk_3) \,. \tag{B.8d}$$

Note that the k's depend on n.

We can apply Runge-Kutta to the Schrödinger-like equation

$$-\psi'' + V\psi = E\psi \,, \tag{B.9}$$

where $\psi(x)$ is the function to solve for, $V(x)$ is an arbitrary function of x, and E is a constant (which can really just be absorbed in V). Let $\phi = \psi'$

to get the first order, matrix differential equation

$$-\begin{pmatrix}\phi\\ \psi\end{pmatrix}' + \begin{pmatrix}0 & V-E\\ 1 & 0\end{pmatrix}\begin{pmatrix}\phi\\ \psi\end{pmatrix} = 0\,. \tag{B.10}$$

For convenience, define

$$w_1 = V(x_n) - E\,, \tag{B.11a}$$
$$w_2 = V(x_n + \tfrac{1}{2}h) - E\,, \tag{B.11b}$$
$$w_3 = V(x_n + h) - E\,, \tag{B.11c}$$
$$w_4 = V(x_n + \tfrac{3}{2}h) - E\,, \tag{B.11d}$$

which depend on the point n. Given the value and derivative of ψ at a point, we can compute the next value via

$$\psi_{n+1} = \frac{1}{24}\left(a\psi_n + b\psi'_n\right) + \mathcal{O}(h^5)\,, \tag{B.12}$$

where

$$a = 24 + 4h^2(w_1 + 2w_2) + h^4 w_1 w_2\,, \tag{B.13a}$$
$$b = 24h + 4h^3 w_2\,. \tag{B.13b}$$

Given two adjacent values of ψ, we can compute the next value using

$$\psi_{n+2} = \frac{1}{c}\left(d\psi_{n+1} + e\psi_n\right) + \mathcal{O}(h^5)\,, \tag{B.14}$$

where

$$c = 72 + 12h^2 w_2\,, \tag{B.15a}$$
$$d = 144 + 12h^2(3w_2 + 2w_3 + 3w_4) + h^4(5w_2w_3 + 8w_2w_4 + 5w_3w_4)\,, \tag{B.15b}$$
$$e = -72 - 12h^2 w_4 + h^4(w_1w_2 - 2w_1w_3 + w_2w_3)\,. \tag{B.15c}$$

In practice, one specifies the initial conditions ψ_0 and ψ'_0, equation (B.12) is then used to compute ψ_1, and then equation (B.14) is used to compute the rest of the values $\psi_{2,\ldots,N}$. If boundary conditions are given instead of initial conditions, the shooting method can be used. In implementing the shooting

method, note that the equations are linear in ψ (assuming V is free of ψ), so taking $\psi_0 = 0$ or $\psi_0 = 1$ covers all possible solutions, and then only ψ'_0 needs to be scanned to find the solution that gives the correct boundary value ψ_N. Further note that if the solutions are known to have definite parity, then $\psi_0 = 1$, $\psi'_0 = 0$ finds the even solution, and $\psi_0 = 0$, $\psi'_0 = 1$ finds the odd solution. The resulting solutions can be normalised if necessary. For the definite parity case, if the eigenvalue E of the Schrödinger-like equation is not known, then the shooting method can again be applied to scan over E until, say, a bound solution is found (one that has $y_N = 0$, or at least has y very close to zero). This is a very effective technique, and is how the resonant peaks in Figures 4.4, 4.5 and 4.6 were found.

Appendix C

Symmetric modified Pöschl-Teller potential

In this appendix we give analytic solutions to the symmetric modified Pöschl-Teller potential. The non-symmetric potential was first studied by Rosen and Morse in the context of molecular dynamics [239]. They presented solutions in terms of hypergeometric functions. Later work by Nieto [240] computed explicit forms of the bound mode solutions, including normalisation coefficients, in terms of regular functions. Section 5.3 of Rajaraman [46] lists unnormalised solutions for the bound and continuum modes for a specific case of the potential, and the hypergeometric forms of the solutions are again explored by Hung and Tran [209]. Bound state solutions are also expressed in terms of Gegenbauer polynomials in the paper by de Castro and Hott [210]. More recently, there has been some work investigating ways to classify and generate potentials that are exactly solvable [241, 242], and these schemes include the Pöschl-Teller potential. We present here the exact closed form solutions for the continuum modes and their normalisation factors for the specific case of the symmetric modified Pöschl-Teller potential. This includes simple expressions for the bound states, simple recurrence relations for higher modes, normalisation coefficients, and the closure relation.

The time-independent Schrödinger equation with the symmetric version of the potential, and with wave-function $\psi_n(x)$ and energy E_n, takes the form

$$\left(-\frac{d^2}{dx^2} + l(l+1)\tanh^2 x - l\right)\psi_n = E_n\psi_n \,. \tag{C.1}$$

If $l = 0$ then the solutions are just plane waves. For $l > 0$ there are a set of

bound modes followed by continuum modes. The bound solutions are

$$E_0^l = 0 \qquad \psi_0^l(x) = A_0^l \cosh^{-l} x \,, \tag{C.2a}$$

$$E_1^l = 2l - 1 \qquad \psi_1^l(x) = A_1^l \sinh x \cosh^{-l} x \,, \tag{C.2b}$$

$$E_2^l = 4l - 4 \qquad \psi_2^l(x) = A_2^l \left(\frac{2l-2}{2l-1} \cosh^{-l+2} x - \cosh^{-l} x \right) , \tag{C.2c}$$

$$\vdots$$

$$E_n^l = 2nl - n^2 \qquad \psi_n^l(x) = \frac{1}{\sqrt{E_n^l}} \left(l \tanh x - \frac{d}{dx} \right) \psi_{n-1}^{l-1}(x) \,. \tag{C.2d}$$

The square integrable ortho-normalisation condition is

$$\int_{-\infty}^{\infty} \psi_n^l(x) \psi_{n'}^l(x) \, dx = \delta_{nn'} \,, \tag{C.3}$$

and the normalisation coefficients are

$$A_0^l = \sqrt{\frac{\Gamma(l + \frac{1}{2})}{\sqrt{\pi}\,\Gamma(l)}} \,, \tag{C.4a}$$

$$A_1^l = \sqrt{2l-2} A_0^l \,, \tag{C.4b}$$

$$A_2^l = \sqrt{(2l-1)(l-2)} A_0^l \,. \tag{C.4c}$$

These bound mode solutions are valid for for all positive real values of l. There are $\lceil l \rceil$ bound modes[1] and so the mode index takes the values $n = 0, 1, \ldots, \lceil l - 1 \rceil$. For the continuum we have found forms for the solutions in terms of regular functions for the case where l is a positive integer. Instead of the discrete bound mode index n, the continuum is indexed with a continuous label $p \in \mathbb{R}$. The solutions take the form

$$E_p^1 = p^2 + 1 \quad \psi_p^1(x) = A_p^1 e^{ipx} \left(\tanh x - ip \right) \,, \tag{C.5a}$$

$$E_p^2 = p^2 + 4 \quad \psi_p^2(x) = A_p^2 e^{ipx} \left(3 \tanh^2 x - (p^2 + 1) - 3ip \tanh x \right) \,, \tag{C.5b}$$

$$\vdots$$

$$E_p^l = p^2 + l^2 \quad \psi_p^l(x) = \frac{1}{\sqrt{E_p^l}} \left(l \tanh x - \frac{d}{dx} \right) \psi_p^{l-1}(x) \,. \tag{C.5c}$$

[1] We use the standard notation $\lceil . \rceil$ for the ceiling function.

The delta distribution ortho-normalisation condition is

$$\int_{-\infty}^{\infty} \psi_p^l(x)\psi_{p'}^l(x)^* \, dx = \delta(p-p') \,, \tag{C.6}$$

and the normalisation coefficients are

$$A_p^1 = \frac{1}{\sqrt{2\pi}} \frac{1}{\sqrt{p^2+1}} \,, \tag{C.7a}$$

$$A_p^2 = \frac{1}{\sqrt{p^2+4}} A_p^1 \,. \tag{C.7b}$$

These continuum modes are valid only for $l = 1, 2, 3, ...$; for other values of l one must resort to the hypergeometric form.

For a given l, the bound modes $\psi_n^l(x)$ and continuum modes $\psi_p^l(x)$ form a complete set. These two classes are orthogonal to each other,

$$\int_{-\infty}^{\infty} \psi_n^l(x)\psi_p^l(x) \, dx = \int_{-\infty}^{\infty} \psi_n^l(x)\psi_p^l(x)^* \, dx = 0 \,, \tag{C.8}$$

and the closure relation is

$$\sum_{n=0}^{\lceil l-1 \rceil} \psi_n^l(x)\psi_n^l(x') + \int_{-\infty}^{\infty} \psi_p^l(x)\psi_p^l(x')^* \, dp = \delta(x-x') \,. \tag{C.9}$$